FUNCTIONAL ANALYSES OF THE MOLECULAR MECHANISMS UNDERLYING TWO EQUINE RESPIRATORY DISEASES: RECURRENT AIRWAY OBSTRUCTION AND *RHODOCOCCUS EQUI* PNEUMONIA

A Dissertation

by

PRIYANKA KACHROO

Submitted to the Office of Graduate Studies of
Texas A&M University
in partial fulfillment of the requirements for the degree of

DOCTOR OF PHILOSOPHY

May 2012

Major Subject: Biomedical Sciences

Functional Analyses of the Molecular Mechanisms Underlying

Two Equine Respiratory Diseases: Recurrent Airway

Obstruction and *Rhodococcus equi* Pneumonia

FUNCTIONAL ANALYSES OF THE MOLECULAR MECHANISMS UNDERLYING TWO EQUINE RESPIRATORY DISEASES: RECURRENT AIRWAY OBSTRUCTION AND *RHODOCOCCUS EQUI* PNEUMONIA

A Dissertation

by

PRIYANKA KACHROO

Submitted to the Office of Graduate Studies of
Texas A&M University
in partial fulfillment of the requirements for the degree of

DOCTOR OF PHILOSOPHY

Approved by:

Chair of Committee,	Bhanu P. Chowdhary
Committee Members,	Christopher M. Seabury
	Huaijun Zhou
	Ivan Ivanov
Head of Department,	Evelyn Tiffany-Castiglioni

May 2012

Major Subject: Biomedical Sciences

ABSTRACT

Functional Analyses of the Molecular Mechanisms Underlying
Two Equine Respiratory Diseases: Recurrent Airway
Obstruction and *Rhodococcus equi* Pneumonia. (May 2012)
Priyanka Kachroo, B.E., PES Institute of Technology
Chair of Advisory Committee: Dr. Bhanu P. Chowdhary

Recurrent airway obstruction (RAO) and *Rhodococcus equi* (*R. equi*) pneumonia are two equine respiratory diseases. RAO is an allergic asthma like disease of the middle-aged horses while the *R. equi* pneumonia affects only young foals. Respiratory disease is considered among the major causes of economic loss to the equine industry and tops the priority list for research that will focus on preventative and diagnostic facets of such disease. The objective of this research was to investigate the effect of antigen exposure and remission (via allergen avoidance and/or drug) on chronically affected RAO horses. Additionally, we also wanted to understand the changes in equine neonatal immune system due to *R. equi* exposure and identify molecular biomarkers for early disease screening. Various biological samples (lung tissue for the RAO study and blood leukocytes and nasal epithelial cells for the *R. equi* study) were used to extract ribonucleic acid (RNA). Complimentary deoxyribonucleic acid (cDNA) obtained from RNA was used to perform microarray hybridization experiments.

Our findings suggest that compared to control horses allergen exposure leads to an elevated protein synthesis and inflammation that contributes to aggravation of symptoms and airway changes. We found that allergen avoidance controls inflammation and causes an improvement in lung function and other chronic features of RAO. The drug administration led to an accelerated remission in the chronic RAO features; a complete remission could however not be achieved. Hence it appears that although not a complete resolution, but allergen avoidance and drugs will help in a better management of chronic RAO symptoms.

Our results suggest that the neonatal immune system is capable of initiating a protective immune response through birth up to 8 weeks of age. However there are also processes present that may be counter-productive to the host. Induction of such suppressive mechanisms may be a result of bacterial modulation of the host immune response or a result of immature host immune system. We also identified molecular biomarkers that will have the potential to screen foals for *R. equi* pneumonia soon after birth and before the onset of clinical symptoms. The research findings of this study will improve the current understanding of the two equine diseases.

DEDICATION

I would like to dedicate this work to my parents, Mrs. Asha Kachroo and Mr K. L. Kachroo , my sister Prerna Kachroo and my fiancé Arun Rao . Their love and support throughout this period has made it possible to accomplish this goal. Soon after completing college, pursuing a doctoral degree was nowhere in my plans and it just happened. When I did decide to start a Ph.D., my parents were highly supportive of my decision. I have troubled them with late night calls and nervous breakdowns during dissertation writing and defense. They gave me strength to overcome all hurdles and tackle every situation head on. My Dad is my role model and I always look up to him. His achievements and dedication towards work have taught me that everything is possible once you put your mind to it. My mother is a friend and guardian. I derive my strength from her and thank her for her unconditional love. I continue to learn from my parents and I truly dedicate this achievement to them.

My heartfelt gratitude to my fiancé Arun Rao for being my rock. His love and belief in my abilities made it easier to sail through this period. He believed in my capabilities and stood by me no matter what. He made sure nothing led me astray from my goal, no matter how difficult the circumstance. I feel lucky to have him in my life. I owe this degree to him and my family. Finally I thank the almighty god for the blessings and showing me the way.

ACKNOWLEDGEMENTS

I would like to thank my advisor Dr. Bhanu Chowdhary for his guidance and support. His suggestions, comments and critiques have helped me immensely in improving as a researcher. I thank him for believing in me and giving me an opportunity to pursue a Ph.D. under his supervision.

I am sincerely thankful to my committee members for their immense help throughout the course of my research. I would like to thank Dr. Ivan Ivanov for always being there whenever I have needed any help with my research or when I just needed to talk. I am, and continue to be, grateful for his help, support and belief in me. I have learnt a lot from him and always look up to him for any advice. I would also like to thank Dr. Christopher Seabury for being ever so helpful and kind. He has proactively shown interest in my research and my progress. I am really thankful for his guidance during this period. I thank Dr. Huaijun Zhou for always taking time to discuss my research and helping me with various technical difficulties. I feel lucky to have great professionals on board as my committee members and feel I have learnt a lot from them.

I would like to acknowledge all the collaborators in my research projects. To begin with, I would like to thank Dr. Jean-Pierre Lavoie and Ms. Josiane Lavoie from University of Montreal, for kindly providing us with samples for the RAO related projects. I also thank Dr. Noah Cohen for his valuable help with foal pneumonia related projects. He has

been very instrumental in all stages of our research projects and continues to provide guidance and support. I would also like to thank Dr. Glenn Blodgett and Ms. Cassie DeFiori from Ranch 6666, Guthrie, Texas, for their assistance in sample collection in the foal pneumonia project.

I would like to thank other faculty members for their help with various research related questions. Dr. Michael Criscitiello took his precious time to read and critique one of my manuscripts. He provided valuable insights and significant suggests towards improving the manuscript. I thank Dr. Terje Raudepp for supervising and teaching me various laboratory techniques when I was new in the lab.

I would also like to thank the office staff of Veterinary Integrative Biological Sciences department -Ms. Dana Parks, Ms. Deborah Daniels, Ms. Sandra Reyes, Ms. Gay Perry and the rest. Their valuable service and help towards managing several administrative tasks has smoothened my graduate career.

I would finally like to thank all my lab colleagues. I would like to thank Dr. Jan Janecka for being very instrumental with revisions of all my manuscripts. He has been very kind and understanding and I truly appreciate his help. He has been there whenever I needed any kind of help or guidance. I would like to thank Dr. Samantha Steelman and Dr. Pranab Jyoti Das for teaching me various lab techniques and for providing valuable suggestions regarding the manuscripts. I would like to thank Sharmila Ghosh, Felipe

Avila and Jana Caldwell for all their help and for simply being wonderful people. I would like to thank Dr. Ashley Seabury for mentoring me when I first joined the lab. She is a wonderful person and had been immensely helpful. I would also like to thank Dr. Nandina Paria for being a great colleague and an ever so wonderful friend. I feel grateful for all the things I learnt from her and for making the lab a wonderful place to work.

TABLE OF CONTENTS

CHAPTER Page

Page

LIST OF FIGURES

Page

LIST OF TABLES

CHAPTER I

INTRODUCTION AND LITERATURE REVIEW

INTRODUCTION TO RESPIRATORY DISEASES IN THE HORSE

The respiratory system of a horse begins at the nostrils and continues via the airway passages to the nasopharynx then through the larynx to the trachea. The trachea then leads to the bronchi and bronchioles, and finally culminates at the alveoli of the lungs. The alveolus is the place where the exchange of oxygen and carbon dioxide occurs between inspired air and circulating blood. The interplay between the respiratory and other body systems confers the horse with a considerable proportion of its athletic ability. Dysfunction in the respiratory system is one of the factors that is known to seriously limit the athletic potential of horses Clarke (1987). Early detection of respiratory ailments is hence a priority to minimize the treatment and management cost associated with the disease and improve the horses' fitness and performance potential. In the United States, the equine industry has an annual impact of $112 billion on the national economy (Chowdhary and Bailey, 2003). Respiratory disease is considered among the major causes of economic loss to the equine industry and therefore necessitates immediate research attention.

This dissertation follows the style of *Veterinary Immunology and Immunopathology*.

Diseases of the respiratory system can be broadly categorized according to the specific anatomical locations in the respiratory tract: i) diseases affecting the upper respiratory tract and ii) diseases affecting the lower respiratory tract. Disease in both categories can then be further classified as infectious or non-infectious. Pleuropneumonia and *Rhodococcus equi* pneumonia are examples of infectious diseases of the lower respiratory tract. Summer pasture associated obstructive pulmonary disorder (SPAOPD), inflammatory airway disease (IAD) and recurrent airway obstruction (RAO) are examples of the non-infection diseases of the lower respiratory tract. Equine influenza and strangles are examples of the infectious, and recurrent sinus empyema and laryngeal hemiplegia are examples of non-infectious upper respiratory tract diseases. This doctoral research will focuses on recurrent airway obstruction (RAO or Heaves) and *Rhodococcus equi* (*R. equi*) pneumonia: diseases of the lower respiratory tract. While RAO is a non-infectious disease affecting adult horses, *R. equi* pneumonia is an infectious disease of the foals.

RECURRENT AIRWAY OBSTRUCTION (RAO)

Equine RAO, also known as heaves, is a performance limiting allergic respiratory disease caused by exposure to organic dust. This disease becomes clinically evident in middle-aged horses and commonly develops in horses stabled during winter months. It is a multifactorial condition caused individually by environmental, infectious and genetic factors or a combination of these factors (Robinson et al., 1993b; Couetil and Ward, 2003). The pathological features of RAO include reversible airway obstruction,

inflammation of lower airways, and bronchial hyperresponsiveness. Similar to RAO, a syndrome named summer pasture-associated obstructive pulmonary disease (SPAOPD) occurs in horses that are kept on pasture during warm weather (Robinson et al., 1993a). RAO shares many pathological features with human asthma; therefore, research in equine RAO will increase the understanding in this field and contribute to the existing knowledge of various features of causes, pathogenesis and treatment of asthma in humans as one of the large animal models for the disease.

Clinical signs

RAO horses show early signs of respiratory distress including cough, wheezing and difficulty in breathing (Robinson, 2001). If left unmanaged, mild clinical symptoms will progress and become severe. Clinical signs can be assessed during a physical exam; in severe cases, these signs include nasal discharge, exercise intolerance, flared nostrils and heaves line (caused by severe respiratory distress) (Robinson, 2001). The hypertrophy and forceful contraction of smooth muscles to assist in breathing leads to the development of heaves line, which is visible as a groove in the external abdominal oblique muscles (Lowell, 1964). Depending on the severity of the disease, wheezing and varying levels of lung sounds (crackles) can also be heard due to obstructed airways (Gerber, 1973; Robinson, 2001). Clinical symptoms are pronounced when horses are stabled whereby they get exposed to allergens. Environmental management of RAO susceptible horses (e.g. moving them to pasture) help in resolving the severity of clinical symptoms.

Diagnosis

Diagnosis of RAO is mainly based on history and physical exams. The likelihood of other lung diseases can be ruled out by radiography. If the horses with seven years of age and older have been stabled and fed hay for most of their life, they begin to cough while stabled and begin to display exercise intolerance. Knowing these important facts while assessing the history of such horses is important in diagnosis. Further diagnosis can be evaluated by bronchoalveolar lavage fluid (BALF) and tracheal aspirates, lung function tests, thoracic radiography and ultrasound (Leguillette, 2003). While tracheal mucus or tracheal lavage is not as reliable for evaluating lung inflammation, BALF can be used for a more accurate assessment (Hoffman, 1999). Cytology of BALF in affected horses displays elevated levels of neutrophils (Gerber, 1973; Robinson, 2001). Lung function tests provide an assessment of the degree of airway obstruction, but the variability in results make them less reliable (Robinson, 2001). Techniques like forced oscillation (van Erck et al., 2003), forced expiration, volume capnography (Herholz et al., 2003) and respiratory induced plethysmography (Hoffman et al., 2001) are considered more sensitive and less invasive (Lavoie, 2007) for the measurement of airway function in order to assess airway obstruction. Following bronchodilator administration, the measurement of the degree of reversibility in airway obstruction can assist the evaluation of obstructive pulmonary diseases (Richter et al., 2008).

Pathology and Pathophysiology

Pathological changes of the disease constitute inflammation of lower airways that are infiltrated mainly with lymphocytes and monocytes along with neutrophils and mucus in lumen (Leguillette, 2003). Persistent airway inflammation due to the presence of immune cells and the inflammatory mediators in the lower airways, combined with poor management of RAO horses (maintaining horses in dusty stables and feeding hay) lead to structural changes of the airways termed as "remodeling". The latter is an aberrant repair processes to airway injuries following constant inflammation (Elias et al., 1999; Sumi and Hamid, 2007; Halwani et al., 2010). Features of airway remodeling include epithelial damage, subepithelial fibrosis, thickening of the airway wall, increase in smooth muscle mass, goblet cell hyperplasia and hypertrophy and also vascular changes (Elias et al., 1999; Vignola et al., 2000; Vignola et al., 2001; Sumi and Hamid, 2007; Halwani et al., 2010).

Similar to observations in human asthma, elevated airway smooth muscle mass is an important component of airway remodeling in RAO too. A study by (Herszberg et al., 2006) was the first to show that horses with heaves also display an increased airway smooth muscle mass (ASM) like asthmatic patients and that the ASM increase is associated with elevated myocyte proliferation (Herszberg et al., 2006). Similarly, Leclere et al. (2011a) reported smooth muscle hyperplasia due to in-situ proliferation of myocytes (2 fold increase compared to control) without reduced apoptosis. Airway remodeling contributes to airway hyperresponsiveness and eventual loss of lung

function. Hence it is important to understand the molecular mechanism underlying remodeling and develop treatment to reverse it (Herszberg et al., 2006).

Pathogenesis

Environmental factors

RAO is caused by inhalation of organic dust containing allergens, endotoxins, mold and particulate matter in the stabling environment of horses. Bacterial products like endotoxins and peptidoglycans, plant debris, dust and noxious gases like ammonia or methane can initiate the inflammatory response (Lavoie, 2007). Environmental management and drugs have been known to alleviate disease severity; hence any management strategy for RAO should encompass reduction in aero-allergens. Since main sources of allergens are feed hay and straw bedding, maintaining an allergen free environment would be one such step in the management of horses, for example, keeping the horses on green pasture (Woods et al., 1993; Vandenput et al., 1997; Robinson, 2001). Instead of dry hay that generates air-borne dust and allergens, moistened hay, silage or pelleted diet are considered more beneficial and shown to improve lung function (Robinson, 2001; Art et al., 2002).

Immunity and Immunologic factors

Immunological basis of RAO is still not completely understood and the underlying immune mechanism is believed to be a hypersensitivity reaction to inhaled allergens. Mediated by immunoglobulin E (IgE), type I hypersensitivity/ immediate type

hypersensitivity eventually leads to production of inflammatory mediators initiating the early phase reaction (within 0.5-1hr of exposure), which is followed by late phase reactions (Kunzle et al., 2007). Type III hypersensitivity (3-10 hrs. post exposure) also known as late type reaction is initiated due to deposition of immune complex causing activation of complement system (Lavoie et al., 2001). While type IV hypersensitivity (within 24-48 hrs. post exposure) is also known as delayed type reaction where CD8+ and CD4+ cell types recognize antigen presented by type 1 or 2 major histocompatibility complex (MHC) and initiate cell mediate immune response (Averbeck et al., 2007).

It was believed that RAO develops in two phases: first phase is an IgE mediated type I hypersensitivity reaction, while the second phase is a type III or type IV reaction (Lavoie et al., 2001; Robinson, 2001; Pietra et al., 2007; Tahon et al., 2009). However, the role of Type I hypersensitivity in RAO pathogenesis is controversial (Tahon et al., 2009). It is due to the contradictory results supporting an IgE-mediated type-I hypersensitivity reaction, that its role in RAO pathogenesis is considered debatable.

Type I hypersensitivity has been supported by researchers due to findings like: release of histamine following allergen exposure (Gerber et al., 1982; Dirscherl et al., 1993; McGorum et al., 1993), elevated degranulation of mast cells after allergen exposure in RAO affected horses (Hare et al., 1999) and presence of elevated allergen specific IgE in serum (Eder et al., 2000; Kunzle et al., 2007). However, some studies did not find any difference in the serum levels of IgE against molds (Halliwell et al., 1993). Also a poor

correlation between intradermal testing and clinical diagnosis was observed in RAO horses (McGorum et al., 1993; Lorch et al., 2001). Again, some of the recent research findings do not support the role of IgE mediated reactions in RAO (Tahon et al., 2009; Wagner, 2009). Tahon et al. (2009) used an in-vitro allergy test and intradermal tests to find if type-I hypersensitivity reaction is associated with RAO. Although they found slightly elevated IgE levels in RAO animals compared to controls, these values were below the acceptable test threshold and hence their results do not support a type-I reaction (Tahon et al., 2009). A more recent study in 2010 hypothesized involvement of type-I hypersensitivity in RAO with a role of IgE and some IgG subclass of antibodies. Using an in-vitro assay for such antibodies but they found that only 30% of horses tested positive (Moran et al., 2010).

Further disfavor for early phase reaction in RAO comes from the observation that immediate onset of airway obstruction which is typical of type I reaction and presence of eosinophil in BALF after allergen exposure is rarely observed in RAO and also because hours or days of stabling eventually leads to obstruction (Lavoie, 2007). Hence, until consistent results do not confirm the role of type-I hypersensitivity in RAO pathogenesis its association with the disease will not be certain.

Some of the recent studies suggest a role of late or delayed type reaction contributing to the pathogenesis of RAO (Tahon et al., 2009; Wagner, 2009; Moran et al., 2010). There are studies that support type III hypersensitivity reaction associated with RAO (Halliwell

et al., 1979; Robinson, 2001). Lavoie et al. (2001) reported neutrophil release after 3-5 hours of allergen exposure that is a feature of type III reactions. There is also growing support for involvement of type IV reaction in RAO (Halliwell et al., 1979; McGorum et al., 1993; Tahon et al., 2009). For example, occurring of reactivity to allergic response 24 hours after exposure supports a delayed type response (Jose-Cunilleras et al., 2001; Wong et al., 2005). Hence, due to inconclusive proof to support any single type of hypersensitivity reaction underlying this disease, further research will be needed to conclusively associate type-I, type III or/and Type IV reactions with RAO pathogenesis.

In addition to the immunologic reactions that mediate the host immune factors in response to allergenic stimuli, it is also important to discuss the role of innate and adaptive immunity in RAO pathogenesis.

Innate immunity is the first line of defense against various antigens via recognition molecules like toll like receptors and immune cells like neutrophils and macrophages (Moran and Folch, 2011). Toll like receptors (TLR) are important for recognition of fungal and bacterial allergens (Shizuo, 2003). However, it has been shown that stabling does not increase the expression of TLR2 because it is the cellular localization of this protein that influences its function and not the transcript abundance (Berndt et al., 2009). TLR4 are important for recognition of lipopolysaccharide and expressed in various cell types within lungs and elevated mRNA levels of TLR4 were observed after allergen challenge in bronchial epithelium of RAO-affected horses (Berndt et al., 2007).

Neutrophils are key contributors to innate immunity and their influx into airways occurs within 3-5 hours post exposure (Fairbairn et al., 1993). Neutrophils exert their effect by producing pro-inflammatory mediators and cytokines (Franchini et al., 2000; Giguere et al., 2002). Elevated expression of various cytokines produced by equine neutrophils from RAO affected horses: interleukins 8, 13, 17 (IL-8, IL-13, IL-17) and tumor necrosis factor-alpha (TNF-α) further enhance inflammation (Franchini et al., 2000; Giguere et al., 2002; Debrue et al., 2005; Ainsworth et al., 2006). Cytokines and chemokines involved in migration and recruitment of neutrophils have also been elevated in RAO affected horses highlighting the important of neutrophils in pulmonary inflammation (Lavoie, 2007). In addition to neutrophils, macrophages also contribute to the airway inflammation, tissue damage and repair. Upon allergen challenge alveolar macrophages up regulate the expression of TNF-α, IL-1β and IL-8 (Laan et al., 2006). These cytokines contribute to the inflammatory reaction and initiate adaptive immunity.

Modulation of immune response via T-lymphocytes is a component of adaptive immunity and critical for RAO pathogenesis. It is believed that T-helper cells (both Th1 and Th2) play an important role in the T-cell mediated immune response in RAO (Leclere et al., 2011b; Moran and Folch, 2011). A common immunological basis has been suggested for RAO and asthma due to shared similarities between the two diseases. In asthma T-helper 2 (Th2) cells and cytokines IL-4, IL-5 and IL-13 have been linked to allergen inhalation response (Bowles et al., 2002). Hence a similar immune response was implicated in equine RAO and suggested that Th2 cells and associated cytokines may

contribute to the pathogenesis (Lavoie et al., 2001). Initial evidence pointing towards a Th-2 immune response was provided by various studies that reported production of IgE to inhaled allergens (Dirscherl et al., 1993; Eder et al., 2000), degranulation of basophils and mast caused due to allergenic stimulus (Dirscherl et al., 1993; Hare et al., 1998), infiltration of T cells into the lungs of RAO horses (Watson et al., 1997) and elevated levels of IL-4 and IL-5 positive BALF cells (Lavoie et al., 2001).

In contrast, other data suggests role of Th1 or a mixed Th1/Th2 cellular response in RAO (Beadle et al., 2002; Giguere et al., 2002; Ainsworth et al., 2003). Involvement of Th-1 type cytokines has been reported by many studies, which may suggest role of this type of immune response in RAO pathogenesis (Giguere et al., 2002; Ainsworth et al., 2003; Debrue et al., 2005). Another important study in 2003 documented elevation expression of IFN-γ in chronically affected horses (5 weeks exposure), indicating that disease is not a polarized Th2 response. Furthermore, at no stage (pre-exposure, acute or chronic), IL-4 and IL-13 expression was increased in RAO affected horses (Ainsworth et al., 2003). Study by Giguere et al. (2002) support these results since they did not detect significant increases in IL-4 expression in BALF cells While a study by Ainsworth et al. (2003) observed an increase in mRNA expression of only IFN-γ in RAO affected horses while the Th2 type cytokines remained unaltered suggesting a polarized Th1 response in affected horses. And finally, apart from evidence that supports a polarized Th1 or Th2 response, increase in mRNA levels of both IL-4 and IFN-γ by some studies suggest a

mixed Th1/Th2 response (Beadle et al., 2002; Giguere et al., 2002; Ainsworth et al., 2003).

Hence based on the literature, it can be hypothesized that RAO affected horses produce both Type 1 and 2 cytokines based on the stage of their disease. Hence, no consensus has been reached towards whether RAO condition is mediated by a polarized T-cell response or a mixed response. This may be due to complexity of the factors that determine heaves phenotype, and suggest that multiple pathways and mechanism may lead to this disease.

Mucus production

It has been long established that goblet cell hyperplasia and mucus hyper-secretion are associated with RAO affected horses (Gerber, 1973; Robinson et al., 1996). Excessive mucus production and accumulation (compared to healthy animals) is one of the factors leading to airway obstruction and is hence considered a key feature of RAO (Gerber et al., 2004b). Exposure to allergen and dust increases mucus accumulation in RAO horses compared to control (Gerber et al., 2004b). It has been reported that RAO phenotype is associated with qualitative and/or quantitative alterations of mucin side chains leading to persistent increased secretion of mucin in airways of affected individuals (Jefcoat et al., 2001). In a similar study increased viscoelasticity of mucus was observed as a consequence of disease exacerbation, and hence it was suggested that change in mucus rheology might also contribute to its accumulation in the airways (Gerber et al., 2004a).

Since accumulation of mucus in RAO can only partly be explained by decrease in mucus clearability (Gerber et al., 2003), it was suggested that the hypersecretion (and accumulation) of mucus might be explained by overexpression of mucin genes. It was found that MUC5AC gene was up regulated in RAO affected horses (Gerber et al., 2003), and later by Rousseau et al. (2007) suggested that mucus in equine airways is a mixture of MUC5B and MUC5AC. Calcium-activated chloride channel (CLCA) proteins are considered important targets in respiratory disorders like asthma and COPD and an elevated expression of human and murine CLCA gene has been reported to cause overproduction of mucus and disease exacerbation (Nakanishi et al., 2001; Hoshino et al., 2002). An up-regulation of chloride channel accessory 1 (CLCA1) protein was observed in RAO affected horses by Anton et al. (2005). A strong correlation between CLCA1 and MUC5AC mRNA levels further supported the role of CLCA1 signaling in mucus regulation in RAO affected horses (Gerber et al., 2009b). However during chronic stages of RAO, CLCA1 was not differentially expressed between RAO affected and healthy controls (Ryhner et al., 2008). Hence different genes and signaling pathways seem to be involved in mucus production in acute and chronic phases of RAO. A thorough understanding of genes involved with mucus production at various stages of the disease might help resolve mucus hypersecretion. Since mucus hypersecretion is associated with airway inflammation, it is suggested that a therapy or drug targeted towards airway inflammation should in theory resolve mucus hypersecretion too (Lugo et al., 2006).

Host genes and genetic factors

Some studies have proposed RAO to have a genetic basis and an inheritance mode that is considered to be complex (Marti et al., 1991; Ramseyer et al., 2007; Swinburne et al., 2009). A familial predisposition for RAO was first reported by (Schaeper, 1939) and later supported by the findings of (Koch, 1957), (Gerber, 1989) and Jost et al. (2007). Study by Gerber et al. (2008) reported a genetic basis for the disease with high heritability. They suggest that offsprings with one parent affected with RAO are at a 3-fold increased risk of developing the disease while a higher risk (5-fold) is observed when both parents are affected with RAO Research findings by Gerber et al. (2009a) and Swinburne et al. (2009) once again proposed genetic basis for RAO and suggested a role of locus heterogeneity. In a sample of swiss warmblood horses (obtained from two RAO-affected stallions), autosomal dominant mode of inheritance was observed in one family while an autosomal recessive mode was evident in the second family suggesting a mixed mode of inheritance in RAO affected horses (Gerber et al., 2009a).

There have been three studies that have hinted at association of genomic regions with RAO (Jost et al., 2007; Gerber et al., 2009a; Swinburne et al., 2009). Jost et al. (2007) employed linkage analysis and observed significant association of a region on chromosome 13 in only one of the two families considered in their study, implying locus heterogeneity associated with RAO. They studied the association of microsatellite markers in two warmblood families and obtained a region on equine chromosome 13 that showed signs of statistical association, and also reported gene IL4RA (within the

candidate region) as a candidate gene for further research. Gerber et al. 2009 also suggested association of miscrosatellite markers with equine chromosome 13 and found mixed mode of inheritance in RAO-affected animals Gerber et al. (2009a). A more recent study in 2009 implicated regions on chromosome 13 and 15 having a strong statistical association with RAO, while region on chromosome 11 showing modest association (Swinburne et al., 2009). Swinburne et al. 2009 used 250 microsatellite markers for genotyping 239 warmblood horses belonging to two half-sib families and report significant and modest association of few genetic loci with RAO. They found regions significantly associated with QTL's from their study: 6-28MB on chromosomes 13, 40-62MB on chromosome 15 and 6-44MB on chromosome 21. Within these regions they found many biologically relevant genes liked IL21R, CCL24, IL27, IL4R and SOCS5. Variants of IL4R gene have been associated with asthma risk and in RAO studies, a SNP in this gene due to locus heterogeneity was only associated with one of the two families studies by Jost et al. 2007. IL4R and other genes reported by Swinburne et al. 2009, due to their positional significance (presence within regions statistically associated with RAO) are good candidates for future research.

In addition to the studies focused on identifying the genetic association with the disease, research during recent years has been focused on evaluating the role of various candidate genes in RAO pathogenesis while very few attempts have been made in understanding the transcriptional profile associated with the lung tissue in RAO affected horses.

To date, there has been only a single attempt at using microarrays to understand the transcriptome profile of blood and BALF in RAO affected animals (Ramery et al., 2008a). However, the limitation of this study was the use of a cross-species microarray, which has limited sensitivity due to sequence divergence between species and is prone to reduced hybridizations and cross hybridization, reducing the reliability of results. Recently another study reported transcriptional changes associated with SPAOPD-RAO horse and found 18 differentially expressed genes via differential display PCR (DD-PCR) mainly involved in defense, inflammation and oxidative stress (Venugopal et al., 2010a). There are very few studies that have focused on genome wide transcriptome analysis and hence the tools of expression analysis like microarrays to understand the pathogenesis of RAO are largely unexplored and offer great research potential.

In addition to the whole genome approaches that have only recently been utilized, researchers have mainly been using candidate gene approach to understand the role of biologically relevant gene/genes in RAO pathogenesis. Selection of these candidate genes have been done on the premise of their potential role in RAO disease pathology due to their biological functional relevance, while many candidates have also been chosen due to their relevance with other respiratory diseases like asthma or COPD etc. For example, Pentraxin 3 (PTX3) gene plays a role in host defense and its elevated expression is observed in airway injury. Overexpression of PTX3 in cells like bronchial epithelium, macrophages and neutrophils derived from BALF has been observed in RAO affected horses (Ramery et al., 2010).

Neurokinins are neuropeptides that function via their receptors and mediate various airway functions, neurogenic inflammation and lung function (Bochner et al., 1994; Cohen et al., 2005a; Ramalho et al., 2011). Venugopal et al. 2009, evaluated the expression of neurokinins: NK-A, NK-B and neurokinin receptor NK-2 in RAO affected horses and reported that NK-A to be a more potent contractile agent than NK-B (Venugopal et al., 2009). According to their study, bronchial samples from RAO-affected horses showed increased hyperresponsiveness towards NK-A than control horses, and this was attributed to overexpression of NK-2 receptors in smooth muscle cells and epithelium of bronchi. NK-A activates NK-2 receptor and causes contraction of the airway smooth muscle leading to airway constriction. Their study proposes that antagonists to this receptor may be of therapeutic efficacy in RAO affected horses as some studies in asthma have already reported (Gao and Peet, 1999; Joos et al., 2004; Schelfhout et al., 2009)

Clara cell secretory protein (CCSP) possesses anti-inflammatory activity and it has been suggested based on studies in human asthma patients that this protein may have a vital role in airway inflammation. A reduced level of this protein is suggested to increase the inflammatory response in asthma (Van Vyve et al., 1995; Luo et al., 2003). Based on the hypothesis that CCSP has anti-inflammatory properties and important for airway response against allergens, Katavolos et al. 2009 reported a decrease in number of clara cells (non-ciliated CCSP producing epithelial cells of distal airways) containing fewer secretory granules (storing CCSP) and also a reduced CCSP content in BALF of RAO-

affected horses (Katavolos et al., 2009). In a more recent study by the same group, it was suggested that CCSP directly interacts with neutrophils and reduces the oxidative burst capacity and increases phagocytosis (Katavolos et al., 2011). During the lung inflammation in RAO with neutrophils as predominant inflammatory cells, CCSP enters and alters the functions of blood neutrophils. Hence based on their findings, authors propose that a reduced CCSP (observed in RAO-affected animals) will allow uncontrolled respiratory burst and release of inflammatory mediators by neutrophils that may lead to structural changes in airways.

Endothelin-1 is a potent bronchoconstrictive peptide that mediates its response through type A and B receptors. These receptors have been implicated to have a role in asthma and RAO pathogenesis (Benamou et al., 1998; Granstrom et al., 2004; Venugopal et al., 2006; Kassuya et al., 2008). Endothelin-1 is involved in airway smooth muscle contraction, obstruction of bronchi, airway remodeling and up regulation of cytokines like IL-1, IL-4, TNF-α and IL-8 causing a pro-inflammatory environment in the airways (Polikepahad et al., 2006; Kassuya et al., 2008).

An elevated ET-1 concentration was first reported in blood and BALF of RAO-affected horses compared to control horses by Benamou et al. (1998). Later the same group tried to evaluate the effect of ET-1 on airways and blood vessels, and found that ET-1 causes contraction of third generation bronchus via both ET-A and ET-B receptor while modulation of vasoconstriction was mediated via ET-A receptor only (Benamou et al.,

2003). Later, Venugopal et al. 2006 found that ET-1 causes potent contraction in equine airways and in SPAOPD affected horses, they proposed that ET-1 is involved in hyperresponsiveness due to alteration of ET-B receptors(Venugopal et al., 2006). The latest study in this area reported that ET-1 exerts its role via enhanced expression of both ET-A and ET-B receptors in bronchial smooth muscle of SPAOPD-affected horses compared to healthy horses (Polikepahad et al., 2006). Hence, it appears that ET-1 may have a role in RAO pathophysiology due to its role in bronchoconstriction and airway hyperresponsiveness, and therefore developing antagonists for ET-1 receptors maybe of therapeutic value.

Parallels with human Asthma

Equine RAO is very similar to human asthma and hence it is easy to draw parallels between the two diseases. In both cases the severity of the disease increases by inhalation of aero-allergens, while reducing or eliminating the inciting factors lead to clinical remission. Pathological features like reversible airway obstruction, bronchospasm, airway hyperreactivity and airway remodeling are similar in both the diseases. However there are few differences between the equine and human forms of the disease: primary influx of the airways in human asthma is eosinophils; contrary to this, the cell population released in the equine airway in RAO is predominantly neutrophils (Art et al., 2008). Although there have been few studies that have reported neutrophils in airways of non-atopic and atopic human asthmatics (Leclere et al., 2011b), majority of the literature still supports that predominant inflammatory cell type in asthma is

eosinophil. Compared to this, allergenic reaction in asthma is proposed to be two phased, with an early type I hypersensitivity reaction (modulated by mast cells and IgE) followed by a type IV hypersensitivity reaction. Early phase response has not been found to be associated with RAO (Deaton et al., 2007; Lavoie, 2007; Tahon et al., 2009). It is believed that type I hypersensitivity reactions are not important for RAO pathogenesis (Marti et al., 2008; Wagner, 2009) while late (Type-III) and delayed reactions (Type-IV) may be important (Halliwell et al., 1979; Tahon et al., 2009).

However, recent publications show a closer correlation between asthma and RAO, due to similarities in various pathological features like bronchoconstriction, hyperresponsiveness, chronic inflammation and features of airway remodeling, hence supporting that horse can a good large animal model (Herszberg et al., 2006; Leclere et al., 2011a; Leclere et al., 2011b). Horse as an animal model has various advantages; to start with, RAO is a naturally occurring disease unlike rodents where asthma needs to be induced. Features of ASM remodeling are same in asthma and RAO (Herszberg et al., 2006; Leclere et al., 2011a) and hence it would be easier to study chronic asthma with remodeling in horses and extend those findings in humans. It is easier to design controlled experiments in horses (e.g. repeated allergen exposure or time course experiments) compared to humans where stringent ethical concerns prevent conducting similar work. Also large size of airways in the horse makes it easier to repeatedly sample biopsies (Leclere et al., 2011b) that can be very useful in understanding temporal changes leading to progression of the disease. However, genetic heterogeneity of the

RAO affected horses and cost prohibitiveness (animal related cost and other facilities) have been suggested as some of the limitations of using RAO horses as a model for human asthma, because genetic heterogeneity will make it difficult to obtain statistical significance for small effects measured in genetic studies with a small sample size (Leclere et al., 2011b).

Summary

RAO is an allergic, obstructive, pulmonary equine disease. This disease causes exercise intolerance and severely affects the athletic potential of horses. Equine industry suffers economic loss due to expensive management practices, decreased athletic potential of horses and treatment costs associated with RAO and hence this equine disease necessitates research attention.

Presently RAO research suffers from various limitations that need to be addressed in the near future in order to gain a more comprehensive understanding of this disease. One of the limitations is our inadequate understanding of the genes and genetic mechanisms orchestrating RAO pathogenesis. Very little is known about the molecular interactions and signaling that triggers the early reaction in the epithelial layer of the lower airway which is the primary site of allergen-host interactions. There is also limited knowledge about mechanisms contributing to airway inflammation, neutrophilic influx, mucus hyper-secretion and airway remodeling. Moreover, interplay of innate and adaptive immune responses in causing RAO are not yet fully elucidated. It is still not clear if

RAO is a polarized Th1/Th2 or a mixed immune response and hence targeted therapies cannot be tailored if a clear understanding of immune response underlying this disease is not achieved.

Complex diseases with an immunologic basis need to be studied using high throughput techniques to capture interplay between various immune components. Only one study has used a high throughput method to study RAO thus far (Ramery et al., 2008b). Therefore genome wide identification of signature gene profile associated with various stages of the disease will add tremendously to the present knowledge base by providing extensive information at transcriptional level. Additionally, there are many potential susceptibility genes implicated in human asthma and only a handful of those genes have been characterized in RAO thus far. Hence, utilizing an equine specific microarray will expedite the process of identifying genes involved in RAO.

My study on recurrent airway obstruction strives to address two key issues. Firstly, to understand the change in gene expression profile of RAO affected horses compared to their control counterparts before and after a short-term allergen exposure. The RAO susceptible horses are asymptomatic when in remission (without any allergen exposure) and become became symptomatic after being exposed to allergens. Secondly, to identify gene expression profile of RAO affected animals after a long-term (3 months) allergen challenge and also obtain the transcriptional profile when allergen are eliminated from their environment. This study also attempts to identify the effect of fluticasone

propionate (a corticosteroid) on the airway remodeling by observing the changes in the pattern of gene expression profile at the two time points (6 and 12 months).

The objectives of the first study (Chapter II)

1. Obtain the gene expression profile for peripheral lung biopsies from asymptomatic and symptomatic RAO affected horses and similarly for control horses before and after the allergen exposure using the whole genome 70-mer equine oligoarray.
2. Obtain DE genes for asymptomatic RAO horses compared to control horses before allergen exposure and similarly identify DE genes between symptomatic horses compared to control horses.
3. Perform pathway and network analysis of the obtained differentially expressed genes (p-value <0.05) to identify key molecular and cellular processes and networks involved in RAO pathogenesis.

The objectives of the second study (Chapter III)

1. Perform a time course study (baseline, 6 months and 12 months as time points) to understand gene expression changes associated with prolonged allergen cessation and fluticasone propionate treatment of horses with chronic allergen exposure (3 months).

2. Perform pathway and network analysis of the obtained differentially expressed genes (p-value <0.05) to identify key molecular and cellular processes and networks associated with chronic RAO due to allergen exposure.
3. Identify pathways and processes associated with the transcription profile after allergen cessation and corticosteroid treatment in the horses with chronic RAO.

RHODOCOCCUS EQUI PNEUMONIA

Rhodococcus equi (*R. equi*) is recognized globally as a leading causes pneumonia in foals up to 6 months of age, while adult horses do not develop the disease unless they are immune deficient (Prescott, 1991; Takai et al., 2001; von Bargen et al., 2009). There are also non-equine species susceptible to *R. equi* pneumonia, like pigs (Karlson et al., 1940), cattle (Woolcock and Rudduck, 1973), cats (Elliott et al., 1986), goats (Addo and Dennis, 1977), dogs (Takai et al., 2003), and even humans, in which it affects only HIV-infected or immune-comprised individuals (Linder, 1997; Kedlaya et al., 2001). The course of *R. equi* infection in foals is insidious, and disease is often progressed by the time diagnosis is made (Cohen et al., 2005b). The mortality rate due to foal pneumonia is estimated to be around 2-13% (Mousel et al., 2003). Hence, this disease has serious implications on the equine industry and requires research attention. A comprehensive understanding of the genetic factors, pathogenesis, and host immunity will help in developing early and accurate screening and diagnostic tools and improved treatment. In the sections that follow, the ecology, epidemiology, pathogenesis, and immunity to *R. equi* are discussed.

Ecology

R. equi is a gram-positive intracellular bacterium belonging to the Actinomycetales order (Barton and Hughes, 1984). It is a soil-dwelling organism also present in the fecal matter of herbivores (Barton and Hughes, 1984; Takai, 1997). Once ingested, the pathogen survives and proliferates in the gastrointestinal tract and enters the environment via feces (Takai et al., 1986; Takai et al., 1991). Proliferation of *R. equi* in soil depends on temperature, concentration of horse feces, and soil pH (Takai et al., 1996; Muscatello et al., 2006). Acidic conditions and high temperatures are believed to assist in the expression of virulence genes (Muscatello et al., 2006), and the optimal growth of bacteria is observed at 38°C and at pH 6.5 (Takai et al., 1996). *R. equi* has simple nutritional requirements and hence can survive in the manure of herbivores and in summer temperatures (Chaffin et al., 2003b). It is a ubiquitous organism and is detectable in most equine farms (Muscatello et al., 2007).

Epidemiology

In addition to gaining knowledge about the pathogenesis and virulence, understanding the epidemiology of *R. equi* will help in the prevention and control of foal pneumonia (Narren, 2007). The natural route of entry of the pathogen is via inhalation or ingestion (Takai et al., 1991; Giguere and Prescott, 1997), and the clinical signs appear in infected foals around 30-90 days after birth (Giguere and Prescott, 1997). Though foals are exposed early in life, the actual onset of infection is not well established. Some researchers believe infection may coincide with waning of maternal antibodies (Wichtel

et al., 1991; Hines et al., 1997; Heidmann et al., 2006; Jacks et al., 2007). However, an increasing body of evidence now points toward a greater likelihood of early infection in foals (Horowitz et al., 2001; Cohen et al., 2002; Chaffin et al., 2008; Kuskie et al., 2011). Thus, future research should provide further evidence for determining the precise time after birth when foals are exposed to the pathogen and whether this exposure is variable from foal to foal.

Rhodococcus equi pneumonia of foals is prevalent around the world. A study by Muscatello et al. in 2006 found that up to 10% of foals in Australia were infected with *R. equi* (Muscatello et al., 2006), while in the United States, a study of 138 farms found a disease incidence rate of 13% and mortality rate of 8% (Cohen et al., 2005c). A study by Chaffin et al. (2003) conducted at two Texas equine breeding farms using 220 foals found that 15% were affected by pneumonia and the mortality rate was 13% (Chaffin et al., 2003b). The same study reported that factors like large farms and high foal and/or mare-foal pair density increased the risk of pneumonia (Chaffin et al., 2003a). Recently, Kuskie et al. 2011 performed a study on a single *R. equi* endemic farm in Kentucky. The study results support the hypothesis that foals get infected early in life by reporting that airborne virulent *R. equi* may increase the risk of foals developing the disease if they are exposed during their first week of life. This study also found a significantly increased association of virulent *R. equi* concentrations in the presence of mares and foals during sampling (Kuskie et al., 2011).

On farms where the *R. equi* infection is endemic, foals are exposed to increased levels of virulent *R. equi* (von Bargen and Haas, 2009). Since only virulent strains of *R. equi* cause the disease (Takai et al., 1991; Takai et al., 1993), characterizing virulent *R. equi* is important in epidemiological studies. The proportion of foals with *R. equi* pneumonia at endemic farms has been reported to be around 10-20%, or at times more (Cohen et al., 2008). Hence, evaluating the factors that contribute to the environmental burden of *R. equi* and understanding their association with the disease is important. It is believed by some that the feces of mares potentially contributes to the environmental burden of *R. equi* (Debey and Bailie, 1987; Takai et al., 1987); however, a study by Grimm et al. (2007) reported that although increased fecal shedding by mares is a contributing source of *R. equi* into the environment, it is not related to disease incidence in foals (Grimm et al., 2007). Some research studies have suggested a correlation between soil contaminated with virulent *R. equi* and disease incidence in foals (Takai et al., 1991; Takai, 1997), but recent research does not support this finding and has instead found a strong association between the prevalence of foal pneumonia and aerosolized virulent strains (Takai et al., 2001; Muscatello et al., 2006; Kuskie et al., 2011).

Pathogenesis

R. equi is an intracellular bacterium that infects only cells of the monocyte/macrophage lineage (Giguere and Prescott, 2000). An organism's pathogenicity depends on its ability to proliferate and eventually kill macrophages (Giguere and Prescott, 2000). Virulent strains of *R. equi* can survive and replicate in alveolar macrophages, and this capacity is

conferred by the presence of virulence plasmid (Hines, 2006). Hence, defining the mechanism by which *R. equi* survives and proliferates within macrophages, the role of virulence plasmid, and the host factors will increase understanding of the pathogenesis of the disease.

A pathogen's ability to thrive in the macrophage relies on the lack of phagosomal-lysosomal fusion (Hietala and Ardans, 1987). *R. equi* interferes with endosomal maturation and prevents vacuole acidification (Fernandez-Mora et al., 2005). The intra-macrophage proliferation kills the host cell and also causes damage to the lung tissue (formation of granuloma) (Meijer and Prescott, 2004). It has been proposed that the means by which *R. equi* enters into macrophages dictates the fate of the pathogen (Giguere and Prescott, 2000). Entry of the microorganism via binding of the complement receptor into macrophages can avoid microbial killing caused by oxidative burst, while opsonization of *R. equi* with antibodies enhances phagosome-lysosome fusion and hence killing of the microbe (Hietala and Ardans, 1987).

R. equi is widespread in the environment, and foal pneumonia is caused by virulent strains containing an 85-90 Kb plasmid (Takai et al., 1991; Takai et al., 1993). It has been shown that plasmid is important for virulence because plasmid-cured strains do not survive and replicate in macrophages and fail to induce pneumonia (Giguere and Prescott, 1997; Wada et al., 1997). Therefore, it appears that the pathogenesis of virulent *R. equi* depends on extrachromosomal DNA: an 85-90 Kb plasmid. Plasmid harbors a

27.5 Kb region called pathogencity island (PI) that contains genes critical for virulence (Takai et al., 2000). It has been reported that the PI contains nine virulence-associated (Vap) genes (Muscatello et al., 2007), and these virulence genes are overexpressed during growth of *R. equi* inside macrophages (Ren and Prescott, 2003). Other factors contributing to the pathogenesis of pneumonia are the polysaccharide capsule of the pathogen, iron acquisition, and glycolipids of the bacterial cell wall (Hondalus, 1997; Hines, 2006)). The polysaccharide capsule may affect virulence because it hinders the process of leukocytes binding and phagocytosing the bacterium (Prescott, 1991). Also, the length of the mycolic acid chains of glycoplipids constituting the cell wall influence virulence since longer chains have more capacity to induce granulomas than shorter chains (Gotoh et al., 1991). Finally, *R. equi*'s mechanisms of sequestering iron may also represent virulence factors since iron is important for its growth and survival (Jordan et al., 2003).

Immunity

While adult horses do not develop *R. equi* pneumonia, all newborn foals get exposed to it as some point early in life. Though most do not develop pneumonia, subsets of foals do get sick (Heidmann et al., 2006). The role of immunity seems critical in understanding the disease pathogenesis of foal pneumonia because unlike susceptible foals, most foals can mount a protective immune response. It appears that both innate immunity and adaptive immunity are important factors in fighting *R. equi* pneumonia infection (Takai et al., 1995b; Hines et al., 1997; Giguere and Prescott, 2000).

Innate immunity

Cells like neutrophils and macrophages are important components of an innate immune system, and a deficiency in radical generating mechanisms or reduced toll-like receptor (TLR) response of these cells may contribute to disease susceptibility (Hines, 2006). Neutrophils are key components of host immunity against bacterial pathogens and have been found to play a protective role against microbial infections in neonates (McTaggart et al., 2001; Martens et al., 2005). Although the phagocytic capability of foal neutrophils is comparable to that of adults (Takai et al., 1985; Hietala and Ardans, 1987; Martens et al., 1988), foal serum has limited opsonic capability (McTaggart et al., 2001). Demmers et al. (2001) suggested that the low killing capacity of neutrophils in foals up to 3 months of age could be a contributing factor toward foal susceptibility. Also, a significantly reduced concentration of neutrophils in the blood of foals for 2 to 4 weeks after birth has been observed in foals that developed pneumonia (Chaffin et al., 2004). Even in mice, a deficiency of neutrophils was found in *R. equi*-infected subjects; hence, it appears that neutrophils exert a protective immune response in the *R. equi* infected mice (Martens et al., 2005). Cytokines like IFN-γ and TNF-α are important for neutrophil and macrophage activation to start microbial killing (Meijer and Prescott, 2004); however, reduced expression of IFN-γ has been reported in young foals (Breathnach et al., 2006; Ryan et al., 2010). Additionally, in mice, it has been observed that IFN-γ and TNF-α are produced in response to virulent *R. equi* and play a role in restricting the proliferation of the pathogen. Also, IFN-γ is important for clearing the

infection since it a component of the T-helper 1 (Th1) immune response (Kasuga-Aoki et al., 1999).

TLRs are important components of innate immunity for pathogen recognition and also initiate adaptive immunity (Schnare et al., 2001; Pasare and Medzhitov, 2004). The *R. equi* surface antigen Vap-A activates TLRs on macrophages; however, a reduced TLR signaling in neonates has been observed that further contributes to the deficiency in innate immunity. TLR2, but not TLR4, has been associated with the macrophage response to *R. equi* where it was shown that a macrophage devoid of TLR2 was not able to generate a strong cytokine response to the pathogen (Darrah et al., 2004). In addition to factors discussed so far, dendritic cells (DCs) form a critical constituent of innate immunity. DCs, also known as professional antigen-presenting cells, are critical for innate immune response to infection. Dendritic cell function is reportedly reduced in foals (Chen et al., 2006), and although foal and adult DCs appear similar in many aspects (Flaminio et al., 2009), foal DCs do not have a robust MHC-II expression, which may compromise efficient priming of the effector cells (Prescott et al., 2010). Thus, reduced expression of class-II MHC by antigen-presenting cells may also contribute to the enhanced susceptibility of foals (Pargass et al., 2009; Dawson et al., 2010).

Adaptive immunity

Humoral immunity

Immunoglobulins like IgA, IgM, IgG, and IgE are expressed in horses (Wagner et al., 2004), and IgGa, IgA, and IgG(T) are the constituents of the early immunoglobulins in neonatal foals (Sheoran et al., 2000). Opsonization via IgG has been reported to enhance phagocytosis of *R. equi* and microbial killing via phagosomal-lysosomal fusion (Cauchard et al., 2004; Dawson et al., 2010). After the waning of maternal antibodies, synthesis of immunoglobulins persists for up to 5-8 weeks of life (Holznagel et al., 2003); however, a delayed synthesis of IgGb and lower level of this immunoglobulin is observed in foals (Sheoran et al., 2000; Holznagel et al., 2003). Given the role of IgGb in bacterial resistance, this immunoglobulin may contribute to foal susceptibility (Holznagel et al., 2003). Sheoran et al. (2000) reported that nasal secretions are devoid of IgA during the first month of life, which may also contribute to susceptibility (Sheoran et al., 2000).

Cell-mediated immunity

Due to the intracellular nature of survival and replication of *R. equi*, an efficient cell-mediated immune response is a critical form of immunity against infection (Hines et al., 1997; Meijer and Prescott, 2004). It is known that CD4+ and CD8+ lymphocytes contribute to immunity toward *R. equi* infection (Nordmann et al., 1992; Kanaly et al., 1993; Ross et al., 1996). CD4+ lymphocytes have subtypes like T helper 1 (Th1) and T helper 2 (Th2) cells. Th1 cells produce IFN-γ and hence contribute to the killing of *R.*

equi via macrophage activation, while Th2 cells initiate the humoral response (Weinstock and Brown, 2002). Th1 immune responses contribute to protective immunity against *R. equi*, while Th2 immune responses are believed to be detrimental (Dawson et al., 2010). The protective role of Th1 immune responses has been elucidated by various studies in mice. One such study showed that the transfer of *R. equi*-specific CD4+ Th1 cells in nude mice cleared the bacteria, while nude mice receiving Th2 cell lines developed pulmonary lesions (Giguere et al., 1999). The role of CD4+ and CD8+ in producing IFN-γ and clearing *R. equi* infection has been studied in mice and adult horses (Kanaly et al., 1993; Hines et al., 2001; Hines et al., 2003). It was shown in mice that CD4+ and CD8+ lymphocytes are involved in the clearance of virulent strains of *R. equi* by producing IFN-γ (Hines et al., 2003). IFN-γ in turn activates macrophages to cause phagolysosomal fusion killing the bacteria (Hines et al., 1997; Darrah et al., 2000).

Infection with *R. equi* can have immunomodulatory effects. Giguere et al. (1999) found that foals that received in-vitro stimulation of CD4+ lymphocytes with a virulent *R. equi* strain showed a significant decline in the production of IFN-γ compared to foals that were infected with strains made devoid of the plasmid (Giguere et al., 1999). This immunomodulatory effect initiates a Th2-like response instead of the protective Th1 response. Hines et al. (2003) showed that adult horses' infection cleared with enhanced production of IFN-γ via CD4+ and CD8+ lymphocytes, highlighting the differences between the adult and neonatal immune responses. Modulation of immune response

could also be due to the PI on virulence plasmid or the dose of bacteria (Hines et al., 2003).

The immature immune system of young foals makes them more susceptible to microbial infections than adults. Furthermore, additional deficiencies of some foals may predispose them to *R. equi* infection. Young foals are deficient in IFN-γ production (Boyd et al., 2003; Breathnach et al., 2006) and cytotoxic T-cell activity (Patton et al., 2005). Liu et al. 2009 demonstrated selective impairment of specific cytokines in neonatal foals, like IL-6 and IFN-γ in peripheral blood mononuclear cells (PBMCs), in response to *R. equi* stimulation (Liu et al., 2009). Pargass et al. (2009) also found that *R. equi*-infected, monocyte-derived macrophage cells expressed less of the Cd1b molecule compared to uninfected cells (Pargass et al., 2009). Cd1b is important for the presentation of lipid antigens, and reduced expression can be just another predisposing factor (Dawson et al., 2010).

In addition, there are age-related deficiencies in antigen-presenting molecules and cytokines important for effective cell-mediated immunity that, in response to pathogen exposure, further result in an ineffective immune response (Prescott et al., 2010).

Clinical Manifestations

The lung infection in *R. equi* pneumonia progresses slowly; thus, diagnosing the disease early is challenging. Early clinical signs include a mild fever and slightly elevated

respiratory rate that if missed will often progress in severity (Prescott, 1991; Giguere and Prescott, 1997). Disease progression causes clinical symptoms like reduced appetite, fever, lethargy, and increased breathing effort (Giguere and Prescott, 1997; Wada et al., 1997). There are three types of *R. equi* pneumonia. The first is the pneumonia type with suppurative bronchopneumonia (i.e., lung infection with abcessation); the second is the enteritis type with ulcerative enteritis (ulcers and inflammation of the mucosal lining of intestines due to bacterial infection) and abdominal abscesses; and the third is the mixed type with features from both types one and two (Takai et al., 1995b). Foals most commonly have chronic suppurative bronchopneumonia (Zink et al., 1986). A small percentage of foals develop intestinal manifestations or abdominal forms of the disease with symptoms like fever, colic, and diarrhea (Giguere and Prescott, 1997).

Diagnosis

The course of infection in foal pneumonia is insidious because the early signs of the disease are difficult to diagnose (Horowitz et al., 2001). Initial signs are often mild and could be detected by physical exams, but some foals succumb to infection without any previous signs of sickness (Heidmann et al., 2006). Recommended screening of foals for possible *R. equi* pneumonia involves monitoring the respiratory rate and, if it increases, taking the rectal temperature. If the rectal temperature is more than 39.2°C opting for a complete blood count is advised. If the blood count (>13,000/ul) and fibrinogen (>600mg/dL) levels are elevated, then advanced diagnostic tools should be employed (Heidmann et al., 2006).

Currently, there is no vaccination for *R. equi* pneumonia, and administration of hyperimmune plasma is commonly used; however, it is expensive and labor intensive (Martens et al., 2002; Chaffin et al., 2011). Hence, reliable, cost-effective, and accurate diagnostic tools to detect early infection are needed.

A variety of serological assays have been developed, e.g., ELISA, agar-gel immunodiffusion (AGID), and synergistic hemolysis inhibitor (SHI) assays. A study by Martens et al. (2002) evaluated five assays (three ELISA types, AGID, and SHI) and found them to be unreliable because of occurrences of high false positives and false negatives (Martens et al., 2002). Another study evaluated the concentration of white blood cells (WBCs) and fibrinogen and an AGID test for the purpose of early diagnosis and found that monitoring WBC count can be an effective diagnostic tool (Giguere et al., 2003). Monitoring hemotologic and immunophenotypic features of peripheral blood, like concentration of WBC, fibrinogen, neutrophils, CD4+ and CD8+ T-lymphocytes, and B lymphocytes, has also been found to be an unreliable screening tool (Chaffin et al., 2004). Recently, Sonmez et al. (2011) evaluated the efficacy of the immunocytochemical procedure on tracheal wash fluid. Their results do not show significant improvement in sensitivity (87.7%) and suffered from poor specificity (59.5%). It was believed that concentration of Serum Amyloid A (SAA) could be a helpful marker for foal pneumonia infection (Hulten and Demmers, 2002); however, the study evaluating the efficacy of this marker as a diagnostic or screening tool found that

concentration of SAA was variable among the diseased foals and hence not a useful tool (Cohen et al., 2005b).

PCR-based diagnostic methods have been regarded as superior to bacteriologic cultures (Heidmann et al., 2006). Bacterial culture methods yield false negative results and do not differentiate between virulent and avirulent strains of the pathogen (Pusterla et al., 2007). To circumvent this limitation, PCR-based methods can be employed (Takai et al., 1995a; Sellon et al., 2001; Ladron et al., 2003; Halbert et al., 2005; Harrington et al., 2005; Rodriguez-Lazaro et al., 2006). Using multiplex PCR assays for simultaneous confirmation of the pathogen (*R. equi*) and strains (virulent vs. avirulent) has been found to be an effective diagnostic tool and superior to traditional morphologic and biochemical tests that have limited specificity for pathogen discrimination (Halbert et al., 2005). Recently, repetitive sequence-based PCR (rep-PCR) was used by Bolton et al. (2010) to discriminate the genotypic variants of *R. equi* since genotyping variations were observed among individual *R. equi*-infected foals. Hence, there is evidence suggesting the superiority of PCR-based diagnostic assays over bacteriological or serological assays; however, PCR-based tests rely solely on detection of pathogenic factors to determine disease status and can lead to false positives.

Based upon the limitations of the present screening and diagnostic tools, using molecular biomarkers will be a superior method for early identification of infected foals. This information will reveal genetic signatures and statistically significant gene biomarkers of

the susceptible foal's immune response, which can then lead to the development of better therapies, more effective vaccines, and improved screening and diagnostic tests.

Host genes and genetic factors

Susceptibility to infection is a complex mechanism initiated by multiple genes, pathways, and proteins (Heller et al., 2010). Therefore, genetic studies that identify causative loci associated with the disease or genomic studies encompassing expression analysis are an important component as well. While genetic studies identify genetic loci associated with the affected foals and help to ascertain foals at greater risk, expression studies provide information about gene signatures that may contribute to foal susceptibility and influence the immune responses.

There have been few studies that have examined the association of certain genes and loci with *R. equi* pneumonia. In one such study, Horin et al. (2004) tested immune-related gene markers and microsatellite loci for association with *Rhodococcus equi* infection and found genes on equine chromosomes 5, 10, and 15 to be associated with clearance of the infection. Another study by the same group reported a single nucleotide polymorphism (SNP) within the caspase 1 (Casp1) gene was found to be associated with high bacterial burden (Horin et al., 2008) in foals. In a more recent study, the same group tested various functional and positional candidate genes, but none of them had a statistical relevance with the infection, with the exception of IL17R, for which a statistically

significant association was found between an SNP in IL17R and the *R. equi* burden (Horin et al., 2010).

In addition to the genetic studies, there have also been reports based on the candidate gene approach to test the role of a gene/gene product contributing to *R. equi* susceptibility. Cohen et al. (2004) suggested that the deletion of solute carrier 11 member 1 (SLC11A1/NRAMP1) does not contribute to susceptibility to *R. equi* in mice, while Halbert et al. (2006) reported an association between SLC11A1 and susceptibility to *R. equi* (Cohen et al., 2004; Halbert et al., 2006). The NRAMP1 gene promotes resistance against various intracellular bacteria because it is likely involved in restricting pathogen survival and proliferation by inhibiting pahgosome-lysosome fusion or by affecting iron availability, thereby creating an iron-restricted environment that is hostile and hinders bacterial survival (Halbert et al., 2006). Another study based on the knowledge that iron is critical for intracellular persistence and replication of *R. equi* evaluated the role of transferrin in *R. equi* infection by typing the transferrin from paraffin-embedded tissues from 34 thoroughbred foals (Jordan et al., 2003). Transferrin is a bacteriostatic iron-binding protein, and its biochemical polymorphism has been seen in many species including horses. A study by Mousel et al. (2003) found an association between foal death due to *R. equi* and transferrin type (Mousel et al., 2003).

In a separate study, association of a functionally relevant candidate gene, Galectin 3, with foal pneumonia was tested; this gene is considered to have a key role in innate and

adaptive immunities, which assist in clearance on microorganisms by macrophages via phagocytosis (Sano et al., 2003). The study reported that the knockout of this gene increased resistance to *R. equi* in mice because this gene regulated immune response by reducing the production of IL-1β by macrophages (Ferraz et al., 2008). The role of IL-1 was shown to regulate immune response by suppressing Th2 response, in turn affecting the susceptibility because the mice were resistant to bacterial infection.

Heller et al. (2010) studied the role of indoeamine 2,3-dioxygenase (IDO), which is involved in breakdown of tryptophan and whose role in immune response is to induce tolerance. Neonatal foals are IFN-γ deficient, and this deficiency may decrease IDO expression. In Heller et al.'s study, the IDO enzyme in mice was found to have an immunoregulatory role in the pathogenesis of *R. equi* infection (Heller et al., 2010). In another study, the same group used the suppression subtractive hybridization (SSH) technique to obtain differentially expressed genes from *R. equi*-infected, monocyte-derived dendritic cells from foals. The differentially expressed genes were mainly involved in biological functions including T-cell regulation, immune and inflammatory response, cellular migration, and vesicular transport and were suggested as topics for further research to understand host immunity and susceptibility to infection (Heller et al., 2010).

The aforementioned studies have provided valuable information on genes and proteins that may be involved in *R. equi* infection in foals. However, none of the studies so far

have focused on understanding the role of the *R. equi* molecular mechanism at a genome-wide level. A study at the transcriptome level will reveal expression signatures that may validate previously reported findings and yield novel foci for future research. It will also enable researchers to understand the molecular mechanism underlying *R. equi* infection in a more comprehensive manner.

Summary

Rhodococcus equi is the leading cause of pneumonia in foals. Expenses related to the foal management, treatment costs, and loss due to death negatively impact the equine industry. *R. equi* pneumonia is caused by interaction of the bacterial pathogen, host, and environment. Hence, all these critical factors need to be extensively understood to design effective and early courses of treatment.

Present research on *R. equi* pneumonia has made great attempts to understand the mechanism of bacterial pathogenesis. However, there is still a great need to understand the role of various genes and genetic factors that contribute to the susceptibility of foals. It is known that critical deficiencies like reduced IFN-γ production, reduced recognition of the pathogen, reduced function of antigen-presenting cells, and delayed synthesis of certain key immunoglobulins contribute to susceptibility of the foals. However, since these factors individually or in concert do not completely account for the susceptibility, there are additional undiscovered components that need to be identified in order to

explain what causes some foals to succumb to the infection while others clear it and remain resistant throughout their lives.

R. equi pneumonia research to date has focused on selected genes or proteins and limited cell types. Disease processes involve coordinated interaction of several pathways, processes, and proteins, which in turn are reflected in expression and interactions of several genes. Also, candidate gene approach is biased and has a limited scope because a single gene or few genes are evaluated in the context of the condition.

Therefore, detailed knowledge of the key genes modulating the disease pathogenesis is limited, and the interactions of genes or gene environments are sparsely known. Transcriptional profiling can be a useful tool in identifying signature genes associated with the disease. Microarrays explore genes in an unbiased manner and assess thousands of genes in parallel for a time point, disease state, or treatment type; hence, not only are genes with known functions obtained but also the ones with a novel function are revealed. The differential expression of genes obtained from microarrays may be due to host, pathogen, and environmental interactions. However, they still provide preliminary information about the genes associated with a condition, and the role of these genes can be dissected subsequently. Microarrays have some inherent limitations that will be discussed in detail in the final chapter, and alternate techniques that can be employed in the future for related studies will be examined.

This study on foal pneumonia strives to address two key issues: (1) develop an understanding of the changes in equine neonatal immune response upon foal in-vitro *R. equi* exposure of blood leukocytes during the first 3 months of life; (2) identify the candidate molecular markers for predicting *R. equi* pneumonia development from leukocytes and nasal epithelial cells at birth, week 2, and week 4 in foals.

The objectives of the first study (Chapter IV) are

1. Establish the temporal changes in gene expression profiles for equine peripheral blood leukocytes in response to in-vitro virulent *R. equi* exposure during the first 3 months of life (day 1, week 2, week 4, and week 8).
2. Compare the gene expression profile between *R. equi* stimulated and un-stimulated peripheral blood leukocytes at day 1, week 2, week 4, and week 8.
3. Perform functional analysis to identify key pathways and networks involved in foal immune responsiveness.

The objectives of the second study (Chapter V) are

1. Compare the gene expression profiles of *R. equi* pneumonia affected and unaffected foals from leukocytes and nasal epithelial cells at birth, week 2, and week 4.
2. Perform classification of differentially expressed genes using linear discriminant analysis (LDA) to discover strong and robust classifiers for the affected and unaffected foals.

CHAPTER II

TRANSCRIPTOME PROFILING OF EQUINE PERIPHERAL LUNG TISSUE TO UNDERSTAND THE EFFECTS OF ANTIGEN EXPOSURE IN RECURRENT AIRWAY OBSTRUCTION

SYNOPSIS

Recent studies in RAO have focused on airway remodeling and effect of antigen exposure on the structural changes. However, the molecular mechanisms associated with allergen exposure on already established remodeling in RAO-susceptible horses is still not fully understood. The purpose of this study is to determine the expression profile associated with asymptomatic (without allergen exposure) and symptomatic (after 30-day allergen exposure) RAO-susceptible horses and to compare it with control horses. Six RAO-susceptible horses and five control horses were maintained in low antigen environment (pasture) after which they were exposed to allergen for 30 days and peripheral lung biopsies were collected before (baseline) and after exposure. RNA was extracted and generated cDNA was labeled with fluorescent dyes for microarray hybridizations using equine whole genome oligoarray. Our results suggest that the 30-day allergen exposure causes minimal perturbation of the expression profile of the RAO-susceptible horses and the genes were mainly involved in cellular turnover. We found biologically relevant processes including cellular proliferation, cytoskeleton organization and apoptosis involved at both time points when RAO horses were compared to control.

Certain processes were also significantly enriched at either baseline (regulation of blood vessel size, immune system development etc.) or after 30-day allergen exposure (translation and translation elongation process). 30-day allergen exposure in RAO-susceptible horses does not cause a significant perturbation of the expression profile. We report novel biomarkers of RAO at remission and exacerbation and molecular processes governing disease pathogenesis with and without the allergenic stimulus.

INTRODUCTION

Recurrent airway obstruction (RAO) also known as heaves, is an equine lower airway respiratory disease that is caused by exposure to dust from moldy hay and straw. Horses affected by RAO are generally 7 years of age or older and display increased repiratory effort, exercise intolerance, neutrophilic influx into the airways and mucus accumulation (Robinson, 2001). Presently there are very few epidemiological studies regarding the prevalence of RAO in different parts of the world including careful evaluation based on breed, age, sex environment and other factors. The current limited data estimated prevalence of RAO to be around 14% in a selected horse population in Great Britain (Hotchkiss et al., 2007). Similar to RAO, a syndrome named summer pasture-associated obstructive pulmonary disease (SPAOPD) also occurs in horses that are kept on pasture in warm humid weather (Robinson, 2001). The clinical signs of RAO begin soon after exposure to aeroallergens, which cause airway inflammation, bronchoconstriction, and hypersecretion of mucus. Persistent airway inflammation and poor management of RAO lead to structural changes of the airways termed as “remodeling”, which includes a

distinct increase in airway smooth muscle (ASM) mass among other observed changes (Herszberg et al., 2006). The molecular mechanisms underlying pathogenesis of chronic RAO, and the associated inflammatory and remodeling processes, are not completely understood; therefore identification of genes and biological processes involved in RAO will help in improved understanding of this disease.

Some studies have proposed RAO to have a genetic basis and an inheritance mode that is considered to be complex (Marti et al., 1991; Ramseyer et al., 2007; Swinburne et al., 2009). A familial predisposition for RAO was first reported by (Schaeper, 1939) and later supported by the findings of (Koch, 1957), (Gerber, 1989) and Jost et al. (2007). Based on these initial studies it appears that RAO is a polygenic disease.

However, irrespective of whether or not RAO is an inherited disease, one of the key limitations of present research is our inadequate understanding of the genes and genetic mechanisms orchestrating RAO pathogenesis. The primary focus in developing this understanding has been restricted to either specific cell types or few candidate genes chosen for analysis based on their likely involvement in modulating pathogenesis (Franchini et al., 2000; Laan et al., 2005; Polikepahad et al., 2008; Ainsworth et al., 2009; Reyner et al., 2009; Venugopal et al., 2009; Ramery et al., 2010; Katavolos et al., 2011). Complex diseases involve coordinated interaction of several genes and genetic pathways that are associated with disease progression. Therefore, there is an acute need for expanding the investigations to several or possibly all genes, eventually facilitating

an improved understanding of this important disease. The comparison of the global transcriptional profile of lung tissues at the disease state compared to the profile of corresponding tissue in the control animals will reveal differences in expression pattern of genes that can play an important role in the modulation of RAO and may contribute to the susceptibility of horses to a range of allergens.

Microarrays have been extensively used as a high-throughput tool to identify differentially expressed genes in human asthma (Brutsche et al., 2001; Laprise et al., 2004; Syed et al., 2005; Hansel and Diette, 2007) and other animal models of asthma (Zou et al., 2002; Zimmermann et al., 2003; Heidenfelder et al., 2009). To date, there has been only a single attempt at using microarrays to understand the transcriptome profile of RAO-susceptible animals (Ramery et al., 2009). However, the limitation of this study was the use of a cross-species microarray, which has restricted sensitivity due to sequence divergence between species that leads to reduced hybridizations and/or cross hybridization, thus reducing the accuracy of results.

Hence, the aim of this study was to utilize for the first time a whole genome equine 70-mer oligoarray to investigate the transcriptome profile associated with chronic RAO including airway remodeling. The findings will provide global insight into the genes and biological processes associated with this disease, and will be of value in adding to current quest for understanding the basis of asthma in humans.

MATERIALS AND METHODS

Study Animals and Experimental Design

Animals, procedures and experimental design used for this study have been descripted previously (Relave et al., 2008; Leclere et al., 2010). In brief, six horses affected with RAO and 5 age-matched controls were used in this study. For RAO-susceptible horses the median age was 16 years while the range was 15–20 years; for control horses the median age was 14 years and the range was 11–17 years. RAO horses had a well-documented 3 to 10-year history of reversible inflammation and airway obstruction upon hay exposure. Control horses had never previously developed RAO. Both groups were otherwise healthy based on physical examination and blood count. All Animal procedures outlined below were performed in accordance with the Canadian Council for Animal Care guidelines as described by Leclere et al. (2010). RAO-susceptible and Control horses were maintained on a pasture for three months (baseline) to precondition all the horses in a low-allergen environment. Both groups (RAO and Control) were then stabled and continuously exposed to a 30-day allergen challenge to poorly cured moldy hay (allergen exposure).

Lung Biopsies and RNA extraction

The peripheral lung biopsies were obtained via thoracoscopy wherein peripheral lung tissue was harvested from the caudo-dorsal region of the lung in sedated horses (Relave et al., 2008). Tissue samples were frozen in liquid nitrogen and stored at -80C for a maximum of 5 months. The RNA was isolated using the cesium chloride technique as

describe previously (Bedard et al., 2003). The extracted RNA quality was evaluated using bioanalyzer (Agilent, CA) and only samples with RNA integrity number (RIN) >7 were considered suitable for the microarray analysis.

Experimental Design

We co-hybridized cDNA obtained from peripheral lung biopsies at baseline with cDNA obtained from biopsies after allergen exposure for the six RAO animals. Similarly, cDNA from 30-day allergen exposure samples were co-hybridized to baseline for the five control horses. We used a balanced block design for cDNA hybridization in which dye-swaps are embedded within the biological replicates (Dobbin et al., 2003; Simon and Dobbin, 2003).

Labeling and Microarray Hybridization

For each sample, cDNA was generated from total RNA using Superscript II Reverse Transcription kit (Invitrogen) and labeled with Cy3 or Cy5 dye via an indirect labeling method utilizing dendrimer technology (Stears et al., 2000). Labeling was carried out with the 3DNA Array 900 MPX Expression Array Detection kit (Genisphere, PA). Hybridizations were performed in a SureHyb hybridization chamber (Agilent, CA) at 55°C. Following post-hybridization washes, arrays were scanned with a GenePix 4000B scanner at 5-micron resolution (Molecular Devices, CA). GenePix Pro 6.1 software was utilized for raw data acquisition, spot-finding, and quantification of array images.

Equine 21K oligonucleotide microarray

We used an whole genome equine oligonucleotide expression array with 21,351 elements designed at Texas A&M University (Bright et al., 2009). This 70-mer oligoarray is the most comprehensive expression array available for expressed equine sequences. Probes were synthesized (Invitrogen, Carlsbad, CA) and printed onto amino-silane coated slides (Corning Incorporated, Corning, NY).

Expression Analysis

Differential expression analysis of microarray data was conducted using Bioconductor's LIMMA package running in the R statistical software environment (Smyth, 2004). Background correction of raw intensities was performed using the normexp correction method (Ritchie et al., 2007). Subsequently, the background corrected intensities were normalized using printip-loess normalization (within array normalization), and aquantile method was used to perform across array normalization (Smyth and Speed, 2003a). Linear modeling using moderated t-tests was performed to identify differentially expressed genes (Smyth, 2004). To account for the multiple comparisons, the false discovery rate correction method of Benjamini and Hochberg was used (Benjamini and Hochberg, 1995). Linear models were used to assess the differentially expressed (DE) genes in RAO-susceptible animals after 30-day allergen challenge compared to baseline (RAO T30/T0); similarly, linear models were fit to obtain DE genes in the control group of animals after 30-day allergen challenge compared to the baseline (CON T30/T0). Genes were considered significantly differentially expressed if they had a p value < 0.05

and fold change > 1.5. In order to compare the expression profile of RAO animals with the control group at baseline and after 30-day allergen challenge, we conducted individual channel analysis of the two-channel microarray data (Smyth, 2005), since no direct co-hybridizations of RAO and control group were performed due to limited availability of RNA. For this analysis the array information is converted to separate single channel data and two additional contrasts were set up: expression profile for symptomatic RAO horses compared to healthy after 30-day allergen exposure (RAO/CON T30) and also expression profile for asymptomatic RAO horses compared to healthy horses at baseline (RAO/CON T0) to obtain the list of differentially expressed genes.

Functional Gene Ontology analysis

The Database for Annotation, Visualization and Integrated Discovery (DAVID**)** v6.7 and GO Term Mapper online free software were used for the purpose of functional annotation. For any given gene list, DAVID functional annotation tools provide gene–term enrichment analysis to identify the most relevant statistically significant ($p<0.05$) biological GO terms associated with a given gene list (Huang et al., 2009b, a). For a more comprehensive functional analysis to understand the overall biological meaning of the differentially expressed genes we used GO Term Mapper (http://go.princeton.edu/cgi-bin/GOTermMapper). GO Term Mapper maps Gene Ontology (GO) annotations of genes to GO slim terms to provide a higher-level view of functions (http://www.geneontology.org/GO.slims.shtml). GO slims terms are especially

valuable for summarizing the GO annotation results of microarray data for a broad classification of gene product function (Onsongo et al., 2008).

Linear Discriminant Analysis

Linear Discriminant Analysis (LDA) is a statistical classification technique to find a linear combination of features to classify and discriminate two or more classes and perform dimensionality reduction (Ye and Ji, 2009). In our analysis, the features were differentially expressed genes and the two classes were RAO and control groups. We employed LDA to identify molecular classifiers based on 1, 2 and 3 DE genes that discriminate RAO-susceptible horses from controls. These classifiers, when ranked using their misclassification error, provide potential biomarkers for differentiating the asymptomatic and symptomatic horses from healthy horses. Thus, LDA can be used to obtain gene sets that can classify/distinguish two or more groups of experimental conditions or phenotypes. While performing classification it is vital to estimate the classification error when potential feature sets are large in number, particularly in cases where several hundred/thousand genes are simultaneously analyzed. When the sample size in terms of the number of animals tested is limited, the estimator of the classification error may have a large variance. This can produce many feature sets composed of several DE genes and classifiers based on those feature sets with low error estimates (Zhao et al., 2009). This problem was mitigated by applying bolstered error estimation (Zhao et al., 2009), which produces more conservative error estimates by injecting Gaussian noise in the real data. In our study DE genes ($p<0.05$) from the two

comparisons RAO/CON T0 and RAO/CON T30 were used as features for the subsequent LDA. The number of genes for each classifier was tested for three or less, which permitted to circumvent problems associated with the small-sample sized experimental designs. Thus, the classifiers based on feature/gene sets of sizes 1, 2, and 3 were used to discriminate between the RAO and Control groups at the two time points. In order to estimate the improvements in the classification, quantities like $\boldsymbol{\varepsilon_{bolstered}}$ and $\boldsymbol{\Delta\varepsilon_{bolstered}}$ have been used for each gene-set**.** $\boldsymbol{\varepsilon_{bolstered}}$ represents bolstered resubstitution error of the discriminant classifier, and $\boldsymbol{\Delta\varepsilon_{bolstered}}$ represents the reduction in error relative to the highest ranked of its subsets of genes (Braga-Neto and Dougherty, 2004). The gene sets were ranked based on the value of $\boldsymbol{\varepsilon_{bolstered}}$.

Quantitative Real-Time PCR

Quantitative real-time PCR was performed on genes significantly differentially expressed (Log fold change >0.58 or < -0.58 and p-value<0.05) and also biologically relevant to RAO (as determined from the function of the DE gene in relation to the disease). This technique was used to validate results obtained from the statistical analysis of the microarray data. Each gene was tested in duplicate along with 18s rRNA as the housekeeping gene. The fold change was calculated using the Pfaffl method (Pfaffl, 2001). The total RNA was directly reverse transcribed to cDNA using the TaqMan® Reverse Transcriptase reagents (Applied Biosystems, CA) and subsequently amplified using gene specific primers and master mix by qPCR in a single step reaction as described.

When possible, primers were designed to span intron-exon boundaries to represent a region of the mRNA corresponding to the location of the cDNA sequence present on the arrays. Serial dilutions of RNA from the reference sample were used to generate relative standard curves and test the amplification efficiency of each primer set. For each qPCR assay, ~100 ng of total RNA was used in a 25 µl reaction with 1x Universal SYBR® Green Master Mix (Applied Biosytems, CA) and 300 nM primers, and amplified on a LightCycler 480 (Roche Diagnostics, IN).

RESULTS

Differentially expressed Genes

Comparison of the lung tissue of the control animals at time points T0 and T30 showed that 25 genes were differentially expressed between them, of which 14 were up-regulated and 11 down-regulated **(Table 2-1)**. These genes are mainly involved in active cell recruitment and inflammation. A similar comparison between RAO-susceptible animals at the two time points led to the identification of only 7 DE genes that are mainly involved in translation. In contrast to these observations, when comparisons were made between RAO-susceptible and control animals at time point T0, we found 154 DE genes (61 up-regulated and 93 down-regulated) suggesting that there are intrinsic differences between the two groups of animals at this time point. Next, following a 30-day allergen exposure (T30), 104 DE genes were found across the two groups, of which 70 were up-regulated and 34 were down-regulated. A closer examination of the genes that were differentially expressed between the RAO-susceptible and control animals

irrespective of their exposure to allergens or not (i.e. at T0 as well as T30) showed only 30 of the total DE genes (154+104=258) were common to both time point comparisons, indicating that the majority of the DE genes at the two time-points were different. Predominant functions of the 30 common genes are signal transduction, response to stress, cell differentiation and death. A summary of these genes is presented in **figure 2-1**. Of these 30 genes, 19 remained up-regulated and 11 remained down-regulated. Detection of only a small proportion of common DE genes between the two groups suggests that the impact of allergen exposure on the expression profile at the two time points, as assessed by the different set of DE genes at T0 and T30, is clearly different in the RAO-susceptible versus control comparisons.

Table 2-1: Differentially expressed genes. List of differentially expressed genes for each comparison is shown in the table. Genes were considered differentially expressed with pvalue<0.05 and fold change >1.5. [T30 represents 30-day allergen exposure time point and T0 represents baseline].

Comparison	Differentially expressed genes
RAO T30 versus Control T30	Up: 70 Down: 34
RAO T0 versus Control T0	Up: 61 Down: 93
RAO T30 versus RAO T0	Up: 3 Down: 4
Control T30 versus Control T0	Up: 14 Down: 11

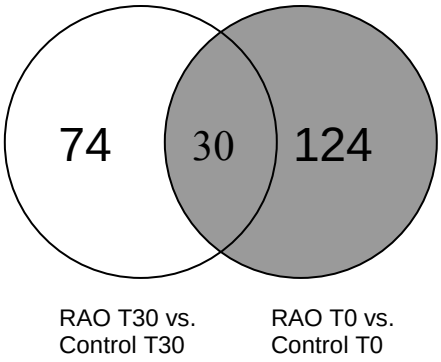

Figure 2-1: Overlap analysis. The venn diagram represents overlap of the DE genes at baseline and 30 days after allergen exposure in RAO versus Control comparison. 30 genes were found to be common between RAO-control comparison at 30 days (104 DE genes) and RAO-control comparison at baseline (154 DE genes).

Quantitative real-time PCR validation

Real-time PCR (qPCR) was used to validate findings of select genes that were significantly differentially expressed from the four comparisons in this study. Because limited amount of RNA was available from each peripheral lung tissue sample, we could choose only 6 genes for the validation purposes. Of the 6 genes selected for validation, we could confirm the differential expression for 5 genes in relation to the microarray data: NLRP1 (CON T30/T0), HCK (RAO/CON T30), ELAVL1 (RAO/CON T0), PIK3R1 (RAO/CON T0) and KIF2A (RAO T30/T0). Based on microarray results, genes ELAVL1 and NLRP1 were up-regulated and HCK, KIF2A and PIK3R1 were down-regulated **(figure 2-2).**

Although qPCR results were not as pronounced as the microarray results, the trend (up- and down-regulation) essentially matched. Variation in correlation between microarray

based fold change values and lack of repeatability of the results in qPCR could be attributed to various factors. Small sample size increases the probability of obtaining false positives that pose challenge in qPCR validation. Additionally, various factors like data normalization, fold change and p-value stringency also effect confirmation of correlation between microarray and qPCR results (Dallas et al., 2005; Morey et al., 2006). Greater correlation is observed between the two results when genes exhibit at least 1.4 fold change, and stringent p-value limits of 0.0001 or less are imposed in microarray data analysis (Morey et al., 2006).

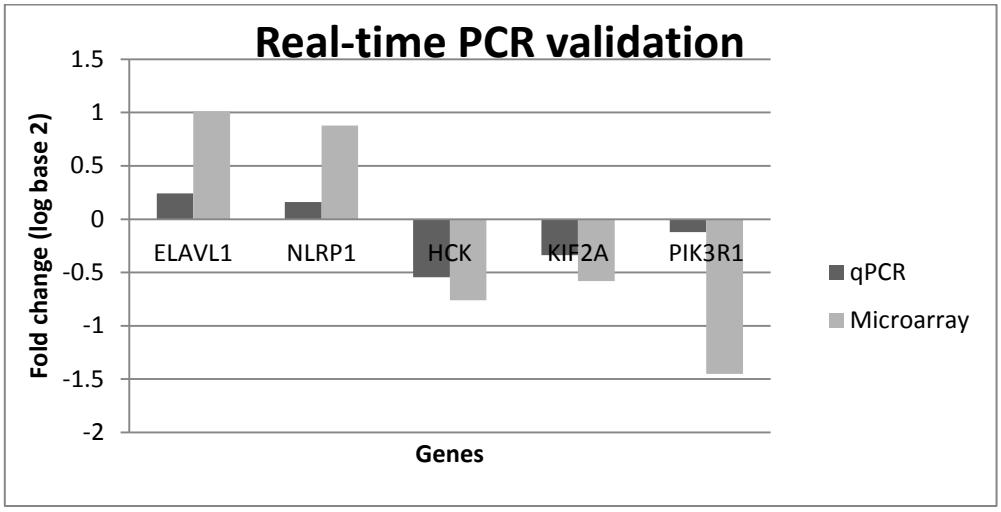

Figure 2-2: Real-time PCR validation. Fold changes (log base 2) of five genes were validated using qPCR. The genes were differentially expressed ($p<0.05$ and fold change>1.5) EVAVL1 (RAO/CON T0), NLRP1 (CON T30/T0), HCK (RAO/CON T30), KIF2A (RAO T30/T0), PIK3R1 (RAO/CON T0).

Gene Ontology Analysis

Gene ontology analysis was performed using the list of DE genes (both up- and down-regulated). Biological processes, cellular components and molecular functions associated with the DE genes were obtained in each of the four comparisons.

RAO-susceptible horses at 30-day exposure versus baseline (RAO T30/T0)

Comparison of gene expression in the lung tissue among RAO-susceptible animals at time points T0 and T30 revealed the involvement of biological process of translation elongation, with a central role of ribosomal protein S3A (RPS3A) and ribosomal protein S15a (RPS15A) genes (**table A-1).** The table shows that both genes are predominantly present at all the levels of gene ontology highlighting their importance.

Control horses at 30-day exposure versus baseline (CON T30/T0)

The GO analysis for DE genes in this comparison is detailed in **table A-2**. Some of the relevant GO biological processes that emerged from this comparison include a) regulation of cell adhesion involving genes like protein phosphatase 2, catalytic subunit, alpha isoform (PPP2CA), adenosine deaminase (ADA), and phosphoinositide-3-kinase, regulatory subunit 1 alpha (PIK3R1) b) purine base metabolic process involving genes like ADA and adenosine monophosphate deaminase 1 (AMPD1) and, c) B-cell differentiation, with genes like ADA and PIK3R1. Genes ADA and AMPD1 appear to be predominantly associated with majority of biological processes in this comparison listed in the table (**table A-2**.**).**

RAO-susceptible versus control horses at baseline (RAO/CON T0)

The GO analysis of the DE gene for this comparison is presented in **table A-3**. Key biological processes associated with these genes include a) regulation of blood pressure and blood vessel size b) regulation of protein kinase cascade, and c) immune system development **(figure 2-3)**. Regulation of blood pressure includes genes like actin alpha 2, smooth muscle, aorta (ACTA2), angiotensinogen (AGT) and hemoglobin beta (HBB). Regulation of protein kinase cascade includes genes like ubiquitin-conjugating enzyme E2N (UBE2N), cardiotrophin-like cytokine factor 1 (CLCF1), erythroblastic leukemia viral oncogene homolog 2 (ERBB2), angiotensinogen (AGT) and cystathionine-beta-synthase (CBS). Key genes involved in the immune system development process included tumor necrosis factor receptor superfamily, member 11a, NFKB activator (TNFRSF11A), cardiotrophin-like cytokine factor 1 (CLCF1), sialomucin (CD164) and phosphoinositide-3-kinase, regulatory subunit 1 alpha (PIK3R1).

RAO-susceptible versus control horses after 30-day allergen exposure (RAO/CON T30)

After 30-day allergen exposure of horses in the two groups, GO analysis yielded enriched biological process, molecular function and cellular component terms associated with the DE genes **(table A-4).** The most significant GO biological processes were translation and translation elongation **(figure 2-3)**. The translation process was associated with genes like eukaryotic elongation factor 1A1 (EEF1A1), MRPL21, ribosomal protein S3A (RPS3A), ribosomal protein L13a (RPL13A) and ribosomal

protein, large, P1 (RPLP1). In the translation elongation category we found genes such as EEF1A1, RPS3A, RPL13A and RPLP1 as significant players. The overall results of the GO analysis suggest that at baseline (T0), difference between RAO and control animals were mainly related to vasculature and immune response. However, at the 30-day time point (post allergen exposure), difference between the RAO-susceptible and control horses is largely related to triggering of the protein synthetic machinery.

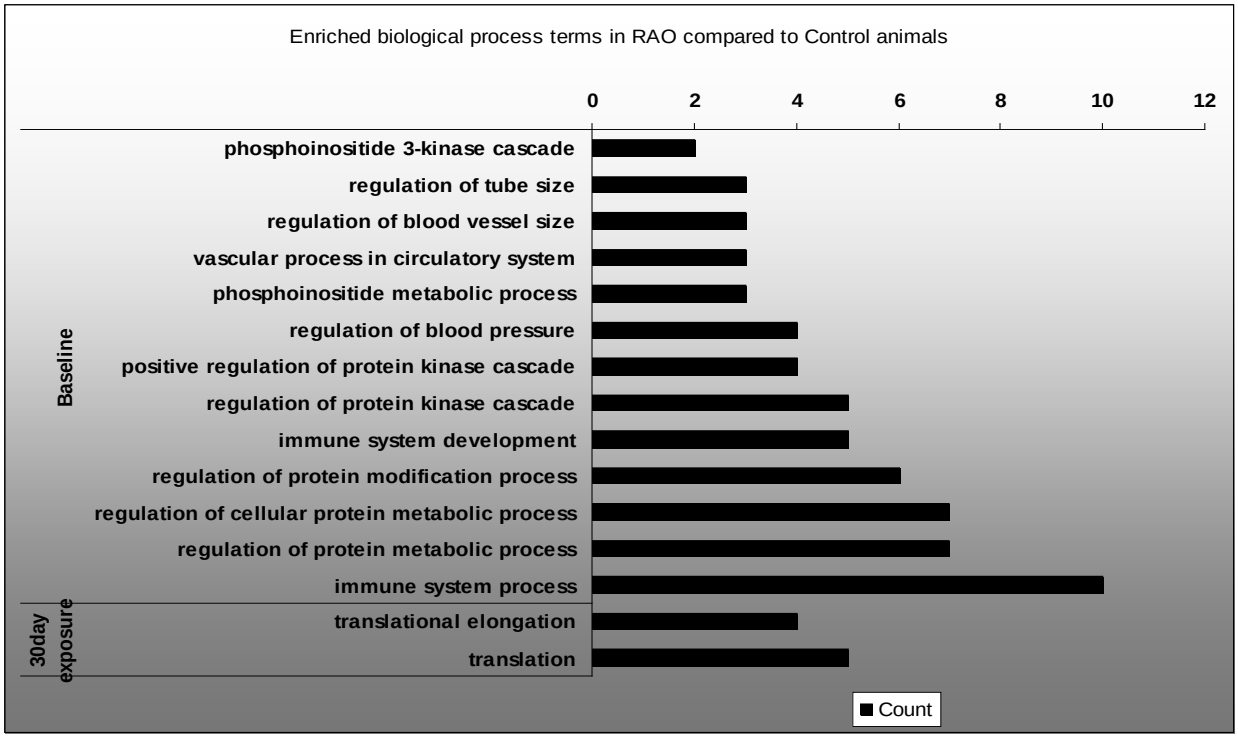

Figure 2-3: Enriched biological process terms in RAO animals compared to control. The enriched biological process terms were obtained via DAVID. Count represents the number of genes belonging to each process.

GO slim analysis of differentially expressed genes

DAVID analysis of DE genes yields only statistically significant GO terms. Hence, in order to get a broader overview of biological processes associated with expression profile comparisons carried out in this study between animals at different time points, we conducted additional analysis of the DE genes using GO Term Mapper that conducts GO-slim analysis and provides the GO-slim terms. GO-slim terms thus obtained give an overview of the ontology content, and hence are useful in summarizing results of GO annotation of microarray results. The analysis led to the identification of additional (compared to DAVID analysis only) biologically meaningful processes associated with the DE genes including cellular component organization, response to stress, signal transduction, death, cell differentiation, cell communication and cell proliferation (**figure 2-4**). Although broadly these GO categories were common to both RAO/CON at T0 and RAO/CON at T30 comparisons, the DE genes present in each of the categories were largely different (the degree of differentiation i.e. the difference between the genes in the two categories, ranged between 90-100%). For example, in the GO term "death", only 1 gene was common for the comparison at time point T0 (total 10 genes) and T30 (total 6 genes), due to which the difference in the genes involved between the groups is around 93.75%.

GO Term Mapper results also provide differences in GO term usage in the DE gene list versus their usage across the genome. All the over-represented GO terms associated with DE genes in RAO-susceptible versus control horses at T0 and after T30 time points are

listed in **table A5**. For both the comparisons at T0 and T30, we observed that certain GO terms were highly enriched in the list of DE genes compared to 18410 annotated genes present in human gene database. Comparisons indicate that the genome levels most of the above mentioned biological process i.e. percentage of genes belonging to each process from the list of DE genes were higher than percentage of genes involved in that process at the genomic level. For example, we observed that 22 out of 90 (24.44%) DE genes at T0 were involved in cellular component organization (GO term), while only 3370 of 18410 (18.31%) of annotated genes in human database were associated with that GO term **(table A-5).** Hence, over-representation of certain GO terms with the list of DE genes suggests that these processes may potentially explain the molecular mechanisms underlying the transcriptional changes occurring at two time points (T0 and T30).

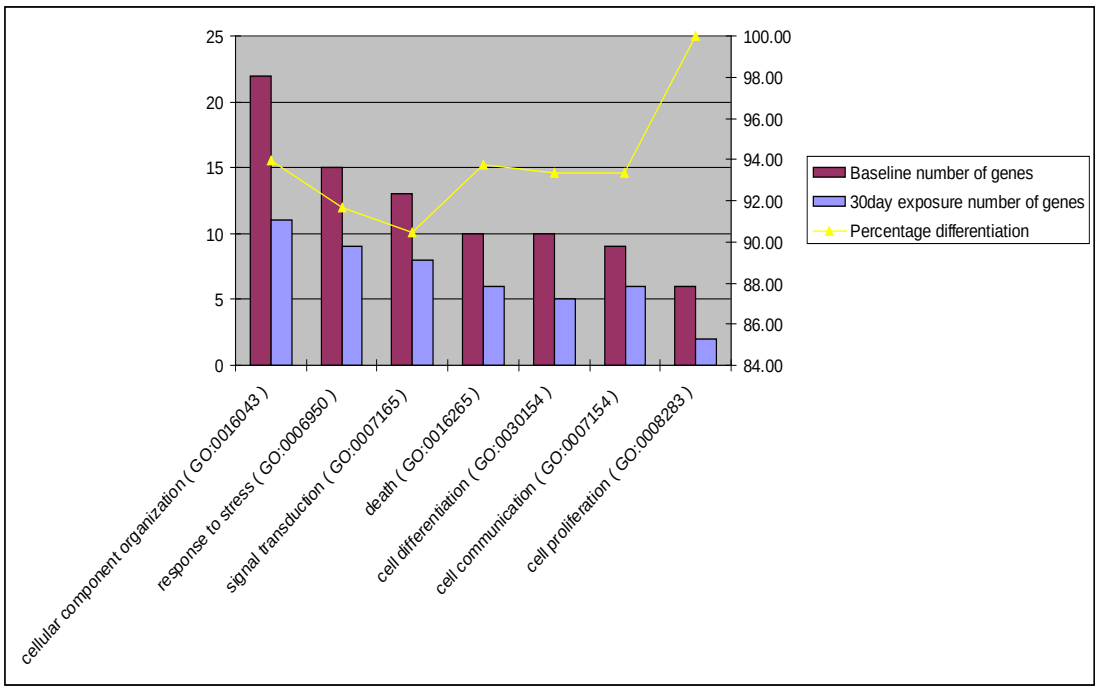

Figure 2-4: GO Term Mapper result. Bar graph represents certain biologically relevant processes associated with RAO versus Control comparison. Plum bars represent number of genes associated with each process at baseline. Blue bars represent number of genes associated with each process after 30-day allergen exposure. Yellow line denotes percentage of differentiation (in terms of number of genes different for each process) between the baseline and exposure group.

Linear Discriminant Analysis

In order to explain the effect of allergen exposure in RAO-susceptible horses compared to control horses, we utilized the LDA classification technique to identify the best single-gene and combinations of two- to three- genes classifiers that are key discriminators between the transcription profiles of RAO-susceptible and control animals. The classifiers were ranked based on their misclassification error ($\varepsilon_{bolstered}$), with the understanding that the best classifiers have lower misclassification error. We

identified the top ten 1-, 2- and 3-gene classifiers with the lowest misclassification error ($\boldsymbol{\varepsilon_{bolstered}}$**)** that distinguish RAO-susceptible and control animals at time points T0 **(table 2-2)** and T30 **(table 2-3).** The classification results demonstrate that there are noteworthy instances where a single gene can adequately distinguish the RAO-susceptible animals from the control with a low error estimate. Furthermore, when these single-gene features were considered as part of the 2 or 3-gene classifiers, a significant decrease in the classification error was observed as evident from the percent decrease in the error depicted by $\boldsymbol{\Delta\varepsilon_{bolstered}}$ shown in **table 2-2 and 2-3**. The specific results for discriminating the expression profiles of RAO from control horses at T0 and T30 are detailed below.

Classification of expression profile of RAO-susceptible from control horses at baseline

At time-point T0, the top single-gene classifier discriminating RAO-susceptible animals from the controls was found to be CT02034A1G04 (top in the list of single-gene classifiers; **table 2-2**), with an estimated classification error of 0.0877**.** Among the 2-gene classifiers, a combination of MYLIP and PTGS2 ranked high in the ability to distinguish between the two groups of animals ($\varepsilon_{bolstered=}$ 0.0368). Moreover, together the two genes were better discriminators (lower error estimate) compared to either of them individually, as evidenced by around 7% ($\Delta\varepsilon_{bolstered}$ =0.0749) reduction in misclassification error. While, programmed cell death 5 (PDCD5), CX602251, and C17orf63 formed the top 3-gene classifier set distinguishing the two groups of animals with an error estimate of 0.0107, it was also interesting to note that none of these genes were among the top ten single gene classifiers. There was an improvement of around 3%

($\Delta\varepsilon_{bolstered}$ =0.0365) in the classification when PDCD5 was used in combination with CX602251 and C12orf63 over the 2-gene classifier with the two genes. Among the top 1-, 2- and 3-gene classifiers, the latter not only had the lowest classification error but also showed sizable decrease in the error when compared to the single- and two-gene classifiers. Thus, the top three-gene classifiers appear to be better discriminators between the RAO-susceptible and control group of horses at time point T0 **(table 2-2).** A clear separation of RAO-susceptible and control animals at time point T0 by the three dimensional LDA hyperplane based on the top triplet classifier is presented on **figure 2-5**. The figure illustrates how the separating plane (LDA hyperplane) defined by the classifiers based on genes PDCD5, CX602251, and C17orf63 (representing the three axes) clearly separates the RAO (represented by circles in the figure) and control (represented by triangles in the figure) horses on the two sides of the plane without any overlap.

Table 2-2: Linear discriminant analysis of RAO versus control animals at baseline. The top ten one-, two-, and three-gene LDA classifiers are shown in the table below. $\varepsilon_{bolstered}$ represents the bolstered resubstitution error for the respective gene classifier and $\Delta\varepsilon_{bolstered}$ represents the decrease in error for each feature set relative to its highest ranked subset of genes.

1 feature	2 feature	3 feature	$\varepsilon_{bolstered}$	$\Delta\varepsilon_{bolstered}$
CT02034A1G04.f1.ab1			0.0877	
MYLIP			0.1117	
CT020018B20G01.ab1			0.1272	
TLOC1			0.1469	
PTGS2			0.1475	
SERPINB7			0.149	
RPS15A			0.1539	
PLT23-F13-M13R.ab1			0.1595	
CT020024A20C11.ab1			0.1615	
TMPO			0.165	
MYLIP	PTGS2		0.0368	0.0749
RPL13A	gnl|UG|Eca#S36639312		0.0401	0.1396
MYLIP	CT02034A1G04.f1.ab1		0.043	0.0447
PTGS2	OR6C2		0.0431	0.1044
CT020018B20G01.ab1	gnl|UG|Eca#S36639312		0.0457	0.0815
TLOC1	RPL13A		0.0463	0.1006
CT020024A20C11.ab1	C17orf63		0.0466	0.1149
gnl|UG|Eca#S36644801	C17orf63		0.0472	0.178
RPL13A	WDR36		0.0505	0.1292
CT02034A1G04.f1.ab1	gnl|UG|Eca#S36644799		0.0515	0.0362
PDCD5	CX602251	C17orf63	0.0107	0.0365
RPL13A	WDR36	OR6C2	0.0131	0.0374
RPL13A	ACCN5	gnl|UG|Eca#S36639312	0.0151	0.025
RPL13A	WDR36	gnl|UG|Eca#S36639312	0.0169	0.0232
MYLIP	gnl|UG|Eca#S36644801	C17orf63	0.0207	0.0265
MYLIP	PIGW	PTGS2	0.0222	0.0146
PIGW	gnl|UG|Eca#S36644801	C17orf63	0.0236	0.0236
TLOC1	RPL13A	PIGW	0.0238	0.0225
CT02034A1G04.f1.ab1	TP53BP2	CLCF1	0.0241	0.0292
TP53BP2	CT020018B20G01.ab1	gnl|UG|Eca#S36639312	0.0251	0.0206

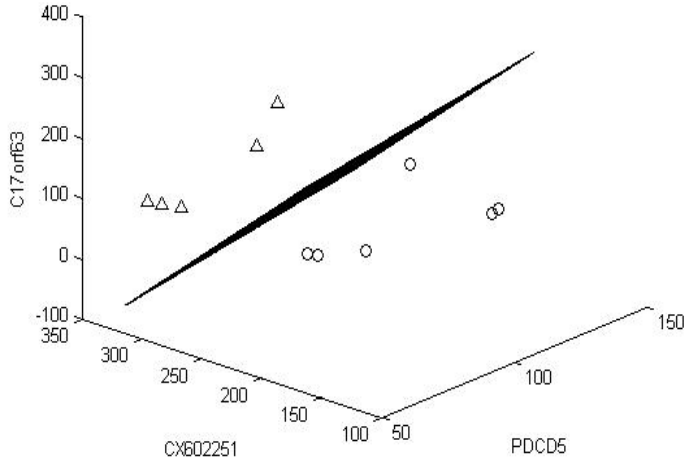

Figure 2-5: Linear discriminant analysis using three-gene classification model for RAO versus control at baseline. C17orf, CX602251 and PDCD5 provided the best-performing three-gene feature set. The three dimensional LDA hyperplane discriminates between control (circles) and RAO-susceptible (triangles). Normalized intensity values of the corresponding genes are represented on the axes.

Classification of expression profile of RAO-susceptible from control horses after 30-day allergen exposure

At time-pint T30, the top 1-gene classifier discriminating RAO-susceptible animals from the controls was found to be GRHL2 (top in the list of single-gene classifiers), with an estimated classification error of 0.0788 (**table 2-3).** Among the 2-gene classifiers, a combination of GRHL2 and CT020008B20C03.ab1 ranked high in the ability to distinguish between the two groups of animals ($\varepsilon_{bolstered=}$ 0.035). Jointly, the two genes were better discriminators (lower error estimate) compared to either of them

individually, as evidenced by around 4% ($\Delta\varepsilon_{bolstered}$ =0.0463) reduction in misclassification error. Next, gnl|UG|Eca#S36625350, GRHL2 and CT020008B20C03.ab1 formed the top 3-gene classifier distinguishing the two groups of animals with an error estimate of 0.0141. This classifier showed an improvement of 1.8% ($\Delta\varepsilon_{bolstered}$ =0.0184) in the classification over the 2-gene classifier based on GRHL2 and CT020008B20C03.ab1 only. A clear separation of RAO and control group at time point T30 by the respective LDA plane is presented on **figure 2-6**. The figure illustrates the separation plane (LDA hyperplane) obtained by classifiers based on genes gnl|UG|Eca#S36625350, GRHL2 and CT020008B20C03.ab1 (representing the three axes) clearly separates the RAO (represented by circles in the figure) and control (represented by triangles in the figure) horses on the two sides of the plane without any overlap.

Overall, it is noteworthy that GRHL2, in addition to being the best 1-feature classifier was a part of combinations of genes for the best 2- and 3-feature classifiers. Another notable feature was that GRHL2 appears frequently with other lower ranked 2- and 3-feature classifiers highlighting the potential significance of this gene as a discriminating feature between the RAO and control groups.

Table 2-3: Linear discriminant analysis of RAO from control animals after allergen exposure. The top ten one-, two-, and three-gene LDA classifiers are shown in the table below. $\varepsilon_{bolstered}$ represents the bolstered resubstitution error for the respective gene classifier and $\Delta\varepsilon_{bolstered}$ represents the decrease in error for each feature set relative to its highest ranked subset of genes.

1 feature	2 feature	3 feature	$\varepsilon_{bolstered}$	$\Delta\varepsilon_{bolstered}$
GRHL2			0.0788	
GENE:17761			0.0999	
COPS3			0.1186	
C9orf23			0.1303	
CT020013B10D12.ab1			0.1355	
gnl|UG|Eca#S36626276			0.1421	
C17orf49			0.1432	
ACTR2			0.1434	
CT020003A10_PLT_B08_58_064.ab1			0.1445	
TYRP1			0.1517	
GRHL2	CT020008B20C03.ab1		0.0325	0.0463
C9orf23	GENE:17761		0.0358	0.0641
GRHL2	CT020003A10_PLT_B08_58_064.ab1		0.0396	0.0392
GRHL2	gnl|UG|Eca#S38809095-5		0.0401	0.0387
GRHL2	CT02040B1E07.f1.ab1		0.047	0.0318
gnl|UG|Eca#S36625350	GRHL2		0.0474	0.0314
SH2D1A	GRHL2		0.0483	0.0305
CT020013B10D12.ab1	GRHL2		0.0507	0.0281
CT020013B10D12.ab1	HCK		0.0532	0.0823
NENF	GRHL2		0.055	0.0238
gnl|UG|Eca#S36625350	GRHL2	CT020008B20C03.ab1	0.0141	0.0184
SH2D1A	GRHL2	CT020008B20C03.ab1	0.0183	0.0142
GRHL2	CT020022B10E09.ab1	CT020003A10_PLT_B08_58_064.ab1	0.0184	0.0212
GRHL2	CT020008B20C03.ab1	CT020003A10_PLT_B08_58_064.ab1	0.0189	0.0136
CT010001000_PLT_G09_71_068.ab1	GRHL2	CT020008B20C03.ab1	0.0205	0.012
GRHL2	CT020008B20C03.ab1	TYRP1	0.0207	0.0118
CT010001000_PLT_G09_71_068.ab1	GRHL2	gnl|UG|Eca#S38809095-5	0.021	0.0191
HCK	GRHL2	gnl|UG|Eca#S38809095-5	0.0211	0.019
TMEM165	GRHL2	CT020008B20C03.ab1	0.0215	0.011

Table 2-3 Continued

1 feature	2 feature	3 feature	$\varepsilon_{bolstered}$	$\Delta\varepsilon_{bolstered}$
GRHL2	GENE:17761	gnl|UG|Eca#S38809095-5	0.0215	0.0186

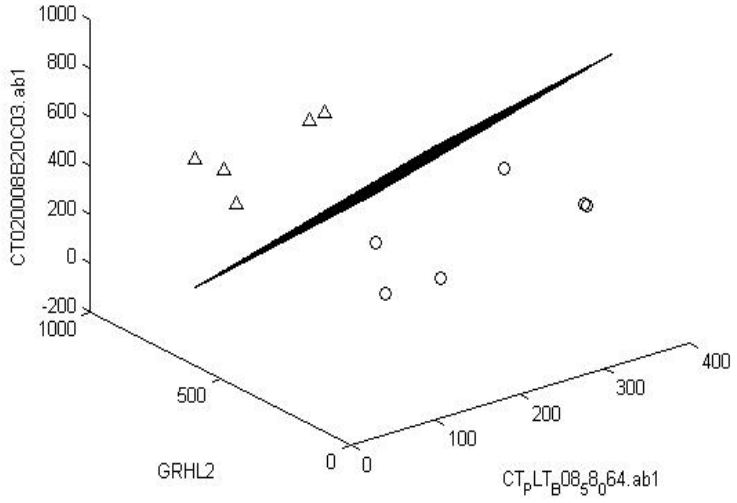

Figure 2-6: Linear discriminant analysis using three-gene classification model for RAO versus control after allergen exposure. CT_PLT_B08_58_064.ab1, GRHL2, CT020008B20C03.ab1 provided the best-performing three-gene feature set. The three dimensional LDA hyperplane discriminates between RAO (circles) and Control (triangles). Axes represent normalized intensity values of the corresponding genes.

DISCUSSION

Expression profiles associated with peripheral lung tissue in asymptomatic (without allergen exposure: T0) and symptomatic (after 30-day allergen exposure: T30) RAO-susceptible horses were compared with the expression profiles of control horses at the two time points. Our findings suggest that allergen exposure in RAO-susceptible horses (compared to baseline) modulates processes related to protein synthesis, immune response and inflammation. While RAO-susceptible horses show a lingering impact of airway remodeling from prior exposure (and subsequent remission) compared to the controls before being exposed to allergens for 30 days, it is apparent that allergen exposure led to elevated protein synthesis and inflammation that contributes to aggravation of symptoms and airway changes.

Differentially expressed genes

We observed dozens of differentially expressed genes while comparing expression profiles of RAO-susceptible and control animals both at time-points T0 and T30. In contrast, only a few genes (7) were differentially expressed between asymptomatic (T0) and symptomatic (T30) RAO-susceptible animals. A similar trend was observed for comparison involving the control group before and after allergen exposure, where only a limited number of DE genes (25) were identified. In essence, changes in gene expression profile are greater in the RAO-susceptible horses vs. the controls following allergen exposure, while the changes were limited within the susceptible/diseased group for the before and after allergen exposure comparison. Further, detection of largely different

sets DE genes between the RAO vs. CON at T0 and RAO vs. CON at T30 comparisons point to marked differences in the transcription profile between the two groups that could be attributed to allergen exposure.

Functional analysis

RAO-susceptible horses at 30-day exposure versus baseline (RAO T30/T0)

In the asymptomatic RAO-susceptible animals, 30-day allergen exposure resulted in differential expression of genes involved in translation elongation, among which ribosomal protein S3A (RPS3A) and S15a (RPS15A) are prominent. Collectively, ribosomal proteins are involved in protein synthesis, however, various components of protein machinery like ribosomal proteins, translation initiation and elongation factors have been reported to be involved in the regulation of cell growth, regulation of apoptosis, DNA repair and RNA splicing (Naora et al., 1998; Lai and Xu, 2007). RPS3A, which was found to be down-regulated in symptomatic RAO horses, is reported to play a key role in translation initiation and regulation of cellular apoptosis (Naora, 1999). Suppression of RPS3A expression has been proposed to induce apoptosis, hence reduced expression of this gene after allergen exposure may contribute to an increase in the apoptosis of smooth muscle cells (Naora et al., 1998). Study by Leclere et al. (2010)., suggested that increase in airway smooth muscle mass in chronically affected RAO horses is maintained by an elevated cellular proliferation and apoptosis (cellular turnover). They suggested that the allergen exposure in such horses does not lead to further increase in muscle mass. RPS3A could be contributing to myocyte apoptosis and

thus maintenance of an increased muscle mass in the RAO-susceptible horses compared to control horses.

Since, limited number of DE genes were obtained for the RAO T30/T0 comparison, we expanded the list of the DE genes by relaxing the threshold to p-value <0.05 with no fold change restriction to obtain a broader overview of genes impacted at/during this time point. The DE genes thus obtained were associated with biologically processes like induction and regulation of apoptosis (RPS3A, UBC, TP53, MAL, TRAF6, UNC13B, RPS27A), immune response (HLA-DRB1, PLUNC, ANXA11, CD1A, TRAF6, S100A9, TP53) and antigen processing and presentation (HLA-DRB1, CD1A, TRAF6). Genes like TP53, RPS3A and RPS27A are known to be associated with induction and regulation of apoptosis. Further, S100A9, one of the central genes in the immune response process in our results, has a role in neutrophil migration to the sites of inflammation (Ryckman et al., 2003; Vandal et al., 2003; Gebhardt et al., 2006). Interestingly a heteromeric complex of S100A8 and S100A9 has been reported to play a role in human asthma pathogenesis and is also proposed to be involved in airway remodeling (Halayko and Ghavami, 2009). Likewise PLUNC (down-regulated in our findings), another immune response gene, is involved in an inflammatory response to irritants in upper airways (Bingle and Craven, 2002) and has been found to be down-regulated in murine model of allergic asthma (Follettie et al., 2006). Further, human leukocyte antigen (HLA) class II genes that are part of both immune response and antigen presentation processes, are present on antigen presenting cells (APC's) like DC,

macrophages, B-lymphocytes(Brown et al., 1993). DRB1 alleles have been implicated in atopic asthma (Lara-Marquez et al., 1999; Cho et al., 2000; Spinetti et al., 2003) and are proposed to modulate total serum IgE concentration and IgE response to allergens (Moffatt et al., 2001).

Next, gene TRAF6 was associated with all the three biological processes: apoptosis, immune response and antigen presentation in our results. TRAF6 has been reported to play a role in innate immunity, maintaining immune homeostasis and critical for maturation and function of dendritic cells (DC's) (Kobayashi et al., 2003a). Since DC's cells are known to play an important role in Th2 immune response and allergic inflammation (Lambrecht, 2005; Lambrecht and Hammad, 2010) involvement of this gene in maturation and functioning of DC's can be of significance as a biomarker of inflammation during RAO.

Hence, it is plausible that the allergenic stimulus to the RAO-susceptible horses initiates inflammatory reaction (with migration of neutrophils for example due to genes like S100A9), activates innate immunity, and by presentation of antigens via APC's (HLA-DRB1 and TRAF6 gene), recruits components of adaptive immunity. Thus, the 30-day allergen exposure in RAO-susceptible animals potentially causes increased protein synthesis (possibly to account for slightly increased smooth muscle cellular turnover due to increased apoptosis), increased apoptosis, antigen recognition and inflammation.

Control horses at 30-day exposure versus baseline (CON T30/T0)

In the control horses, allergen exposure for 30 days (compared to T0) caused differential expression of genes involved in processes like cell adhesion (PPP2CA, ADA, PIK3R1), B-cell differentiation (ADA, PIK3R1) and purine base metabolic process (ADA, AMPD1).

Adenosine deaminase (ADA) metabolizes adenosine and its deficiency in mice causes respiratory distress and lung inflammation due to accumulation of adenosine (Blackburn and Kellems, 2005). Adenosine levels increase during acute and chronic inflammation (asthma) and its exogenous administration is known to cause bronchoconstriction in asthmatics and not in healthy subjects (Mann et al., 1985). Down-regulation of ADA in the control horses could thus primarily be contributing to inflammation in response to the allergen exposure without any concomitant development of airway obstruction. A similar observation was also reported by, Leclere et al. 2010 who found that 30-day allergen exposure in healthy horses (controls) resulted in a transiently increased inflammation as evidenced by an elevated neutrophil count in bronchoalveolar lavage but no evidence of bronchoconstriction in the control horses (Leclere et al., 2010).

Phosphoinositide-3-kinase, regulatory subunit 1 (PIK3R1) is associated with biological processes including cell activation, regulation of cell-matrix adhesion, immune system development and leukocyte differentiation. Since PIK3R1 gene is involved in signaling

events that mediate various biological processes, it will be difficult to comment on its exact functional role in control horses.

To summarize, we found a small number of DE genes (25) associated with the control horses. In line with this observation, we found very few distinct biological processes associated with the DE genes. Genes ADA and AMPD associated with purine nucleoside synthesis and metabolism related processes were predominantly present in the list of statistically significant processes.

In essence, indications are that although the control horses are inherently not susceptible to allergen exposure, underlying molecular mechanisms do get underway in this group of horses as evidenced by the DE genes. However, it appears that the impact of these genes either does not reach a threshold necessary for manifestation of clinical signs, or it is contained by other genes that potentially render resistance to visible reaction to allergen exposure.

RAO-susceptible versus control horses at baseline (RAO/CON T0)

The DE genes between RAO-susceptible and control animals before allergen exposure (at T0 time-point) were related to biological processes including regulation of blood pressure (PTGS2, ACTA2, AGT, HBB), regulation of blood vessel size (ACTA2, AGT, HBB), protein kinase signaling (UBE2N, CLCF1, ERBB2, AGT, CBS), and immune system development (POLL, TNFRSF11A, CLCF1, CD164, PIK3R1) as deduced from

GO biological terms using DAVID, and response to stress (AGT, AP1G1, ATG3, ERBB2, HFE, HSPE1, LAT, MARK2, PIK3R1, POLL, PSMA1, PTGS2, SLC7A7, TNFRS11A, UBE2N) , cellular proliferation (AGT, CD164, ERBB2, PTGS2, RPS15A, TNFRS11A) and apoptosis (AGT, ATG3, CLCF1, ERBB2, HSPE1, PDCD5, PEO1, PSMA1, PTGS2, TP53BP2) as indicated by GO-slim terms.

Airway remodeling is associated with features like angiogenesis and elevated smooth muscle mass (Chu et al., 2001; Herszberg et al., 2006; Ribatti et al., 2009; Leclere et al., 2010). It is known that blood pressure regulation and size of blood vessels are features of angiogenesis (Charan et al., 1997; Chu et al., 2001; Nissim Ben Efraim and Levi-Schaffer, 2008; Simcock et al., 2008), and increased cellular proliferation and apoptosis are considered as factors that contribute to increased smooth muscle mass (Herszberg et al., 2006; Leclere et al., 2010). For example, angiotensinogen (AGT) gene associated with blood pressure and blood vessel size in our study is a member of renin-angiotensin system, and is known to regulate angiogenesis (formation of blood vessels) that underlies pathogenesis of variety of disorders including asthma (Corvol et al., 2003; Clapp et al., 2009). Angiotensinogen has anti-angiogenic properties (Clapp et al., 2009) and reduced mRNA levels are known to promote angiogenesis (Chang and Perlman, 1988). Hence we speculate that down-regulated of AGT in RAO-susceptible horses at T0 possibly contributes to the vascular remodeling component of lower airways. Response to stress was another process associated with the DE genes at T0, and among those genes was heat shock protein 1 (HSPE1) that was found to be up-regulated in

RAO-affected horses. HSPE1 acts as a chaperonin by enhancing protein folding and also protects cell against stress induced by inflammation (Johnson et al., 2005; Jia et al., 2011). Gene CD164 (sialomucin; up-regulated in asymptomatic RAO animals compared to controls) is a component of both immune system development and cellular proliferation process. The up-regulation of CD164 is known to cause cell growth dysregulation (Kurosawa et al., 1999; Chan et al., 2001), And the gene has been reported to be up-regulated in patients with seasonal allergic rhinitis caused by grass pollens (Wolanczyk-Medrala et al., 2010), in response to pollen exposure. Up-regulation of this gene in asymptomatic RAO-susceptible horses at T0 (in absence of any allergen stimulus) suggests remnant effects of the gene in response to previous allergen exposure, and it is plausible that the gene mediates hyperplasia/hypertrophy of smooth muscle cells of lower airways in these animals.

It is noteworthy that comparing asymptomatic RAO-susceptible horses and their healthy counterparts at time-point T0 (no allergen exposure) yielded a number of DE genes even though both group of horses are expected to be almost in the same ‘stage of health and no-exposure. A possible explanation for this difference could partly be attributed to inherent differences between the RAO susceptible and control animals, but partly also because of past allergen exposures of RAO-susceptible horses that established remodeling and thus have a lingering impact of genes and processes associated with it in the observed DE genes even at time-point T0 when animals have not been exposed to allergens. Since majority of the identified processes contribute to airway remodeling,

further investigation of the significance of the genes involved in these processes can potentially shed light on molecular mechanisms associated with airway smooth muscle remodeling.

RAO-susceptible versus control after 30-day allergen exposure (RAO/CON T30)

The 30-day allergen exposure in RAO-susceptible horses compared to control at time-point T30 mainly highlighted genes that were associated with biological processes like translation (EEF1A1, MRPL21, RPS3A, RPL13A, RPLP1) and translation elongation (EEF1A1, RPS3A, RPL13A, RPLP1). GO-slim terms associated with the DE genes revealed processes like response to stress (ALDOB, CCL5, EYA4, HCK, HSPE1, SH2D1A, SPHK1, TFPI2, UBE2N), proliferation (IGFBP6, SPHK1), and apoptosis (DNASE1L3, HSPE1, RPS3A, SH2D1A, SPHK1). Elongation factor 1 alpha (EEF1A) gene from our results is a part of both translation and translation elongation processes. The EEF1A1 transcript was up-regulated in symptomatic RAO horses compared to the controls. Recently, Venugopal et al. 2010 also found this gene to be up-regulated in RAO animals compared to the controls (Venugopal et al., 2010b). Although no direct role of EEF1A1 has been reported so far in RAO or human asthma studies, its overexpression may contribute to cellular proliferation and apoptosis, that are histological features of asthma and RAO (Johnson et al., 2001; Huang et al., 2005; Herszberg et al., 2006; Leclere et al., 2010). High mRNA levels of this gene are observed in rapidly proliferating cultured cells, embryos, and various human tumors (Condeelis, 1995); however its overexpression has also been reported to play a role in

increased apoptosis by increasing protein synthesis of pro-apoptotic factors (Duttaroy et al., 1998).

Some of the DE genes in our results were not a part of any of the identified statistically significant biological processes in the symptomatic RAO/CON comparison at the time-point T30. However, we found few such genes up-regulated in symptomatic RAO-susceptible horses (compared to controls). We found some immune response and inflammation related genes in this comparison that are worthy of discussion. These genes include signaling lymphocytic activation molecule-associated protein (SH2D1A), hemopoietic cell kinase (HCK), chemokine ligand 5 (CCL5)/RANTES, CCL8 and CCL11.

HCK gene is essential in the signaling pathway resulting in polymorphonuclear leukocyte (PMN) degranulation. PMNs synthesize pro-inflammatory cytokines and chemokines that cause inflammation. Elevated mRNA levels of HCK gene has been shown to cause increased PMN degranulation leading to severe inflammation in COPD patients (Zhang et al., 2007). HCK gene is known to influence neutrophilic degranulation that can contribute in inflammation and tissue injury (Mocsai et al., 1999; Lacy, 2006). Allergen induced inflammation in RAO-affected animals is known to be predominantly neutrophilic (Lavoie et al., 2001). Up-regulation of HCK gene in RAO-affected horses at T30 maybe contributing to inflammation compared to control horses. Expression of SH2D1A (up-regulated in RAO-affected horses at T30) is reported to be

increased post allergen exposure and its role is considered to be involved in Th2 activation (Mobini et al., 2009).

Chemokines like CCL5, CCL11 and CCL8 release pro-inflammatory mediators and activate Th2 cells (Romagnani, 2002). In mouse model of asthma it was shown that neutralizing CCL5 reduces the features of allergic asthma (Schuh et al., 2001). Th2 cells promote allergic airway inflammation (Lloyd and Hessel, 2010) and underlie pathogenesis of asthma and RAO. Targeting chemokine ligands (due to their role in Th2 immune response) or their receptors are considered promising therapeutic strategies for asthma (Caramori et al., 2008). These chemokines and genes HCK and SH2D1A should hence be targeted for their therapeutic potential in RAO research.

To summarize, our results suggest that allergen exposure increases protein synthesis, possibly to meet needs due to elevated cellular proliferation and apoptosis in RAO horses compared to control horses. Since allergen exposure is causing a modulation in the components of the protein synthesis machinery, it will be interesting to investigate whether targeting these components affects cellular turnover of smooth muscle cells that could indirectly affect ASM and hence remodeling. There is also evidence of increased inflammation caused by allergens in the RAO-affected horses compared to controls since we identified genes that release pro-inflammatory mediators and activate Th2 cells. Our study identifies genes that influence cellular turnover (feature of airway remodeling) and

inflammation and can hence be promising targets for therapeutic strategies that reduce remodeling and inflammation component of the disease pathology.

GO slim analysis of differentially expressed genes

An interesting observation with respect to GO-slim analysis was that many shared GO biological categories for RAO/CON T0 and RAO/CON T30 comparison had a high level of differentiation in terms of genes associated with each category. The allergenic stimulus could be the factor that induces the same molecular pathways via induction of different genes (very different genes associated with biological GO slim terms). Biological processes like cellular proliferation and apoptosis were found common in both comparisons, but they were associated with different genes at the two time points. Both these processes have been shown to be important for airway remodeling in horses(Leclere et al., 2011a). Because of their presence at both time points, it appears that both proliferative and apoptotic pathways are important for maintenance of RAO phenotype, however different genes are contributing to the asymptomatic and symptomatic phase of the disease.

Positional relevance of DE genes

A study by Swinburne et al. 2009 identified two positional candidate regions on equine chromosome 13 and 15 as significantly associated with RAO via a genome-wide scan using microsatellite markers to genotype two half-sib families (Swinburne et al., 2009). Some of the DE genes obtained by us (RAO T30/T0,

RAO/CON T0, RAO/CON T30 comparison) are interesting candidates for future investigation because of their chromosomal location. Ribosomal protein S15 (RPS15A) gene is located on chromosome 13 adjoining the positional candidates region (6-28 Mb) identified by Swinburne et al. 2009 while zinc finger, HIT type 1 (ZNHIT1) is within the candidate region of chromosome 13. ARP2 actin-related protein 2 (ACTR2) gene was adjoining the positional candidate region (40-62 Mb) on chromosome 15. Genes, kinesin heavy chain member 2A (KIF2A) and v-erb-b2 erythroblastic leukemia viral oncogene homolog 2 (ERBB2) were also found to be within 6-44 Mb region on chromosome 21. Due to the proximity of these genes to the candidate regions defined in the family based genetic association study, we hypothesize that such genes could possibly be associated with RAO phenotype. At the mRNA level, we observed a differential expression of the transcript abundance of these genes; it will be interesting to probe if a polymorphism at DNA level is causing this alteration. These genes could hence be contributing to the susceptibility of the RAO-affected horses and hence can be good targets for further investigation into the role they play in RAO pathogenesis.

Linear discriminant analysis

LDA classification found the best one, two or three-feature classifiers for discriminating the asymptomatic RAO animals from control. Since the classifiers can discriminate the two groups of horses, such classifiers will have the potential to be used as the markers of the disease state (remission or clinical exacerbation) from the normal healthy state. Such discrimination will hence enable diagnosis of animals even when no clinical symptoms

are present. At remission, the differences between RAO-affected and control horses should primarily be governed by genetic factors. Our findings can thus be extended to screen animals for RAO susceptibility from the animals that will not develop the disease under similar environmental conditions. We observed that classifiers including programmed cell death 5 (PDCD5), CX602251, and C17orf63 (three-feature classifier with the lowest error estimate) were the best triplet set to classify the two groups of horses. No functional annotation is currently available for CX602251 and C17orf63 and therefore although they are a part of the best three-gene classifier, it is difficult to comment on their functional relevance. PDCD5 (third member of the three-gene classifier set) is a positive regulator in classic apoptotic and paraptotic programmed cell death. PDCD5 mRNA and protein levels are up-regulated in response to various apoptotic signals (Li et al., 2000; Liu et al., 2003). The expression of this protein has been shown to be elevated in cells undergoing apoptosis and is considered an early apoptotic marker (Chen et al., 2001). Increased apoptosis is a hallmark of asthma and along with increased cell proliferation it is known to contribute in airway remodeling as well. Hence, this classifier maybe acting as a discriminatory biomarker since RAO-affected horses have an elevated rate of apoptosis of smooth muscle cells compared to the control animals.

Grainyhead-like 2 (GRHL2), CT020008B20C03 and CT020003A10_PLT_B08_58_064 were the best triplet classifiers with the ability to discriminate the symptomatic RAO animals from the control animals. These classifiers will help in discriminating horses

that develop airway obstruction and other clinical symptoms of RAO after an allergen exposure from the animals that do not. Additionally, these classifiers can be potential targets for developing therapeutics to resolve severity of disease in RAO-affected horses. Currently, there is no functional annotation available for CT020008B20C03 and CT020003A10_PLT_B08_58_064 and hence it is beyond the scope of this study to rationalize their functional relevance to the disease. It has been proposed that grhl2 (pat of the three-gene classifier set) transcription factor has a role in morphogenesis of alveolar epithelial cells and are involved in maintaining cuboidal shape of the distal alveolar epithelial cells and help in epithelial differentiation (S. Varma, 2009; Werth et al., 2010). This gene appears to have role in formation, structural integrity and differentiation of alveolar epithelial cells. Allergenic reactions cause injury to airway epithelium; one of the ways to repair this damage involves migration of progenitor cells that proliferate and differentiate in order to assist in functioning and integrity of epithelium (Crosby and Waters, 2010). Epithelium injury and mechanistic changes of epithelium are observed during RAO/asthma and gene GRHL2 may contribute to this impairment.

LDA results suggest that the three-gene classifiers can provide a good separation of asymptomatic and symptomatic RAO animals from control. LDA has been used to obtain discriminatory molecular signature for various studies (Kim et al., 2002; Kobayashi et al., 2003b; Morikawa et al., 2003). However, to our knowledge this technique is relatively novel in the field of large animal disease genetics. We therefore

provide a preliminary evidence for the potential of this technique in high-throughput genomic studies utilizing microarrays or next-generation sequencing. Our study provides the first line of evidence for their potential role as a disease biomarker and these genes should be further investigated for their role in disease pathogenesis and as possible therapeutic targets. For our future studies, we will extend our present research findings to understand the role of some of the molecular biomarkers and processes for their direct relevance to the disease.

Summary

This study reports many biologically relevant differentially expressed genes that may have a role in disease pathogenesis and contribute to airway remodeling. We also present significant GO categories and enriched GO terms associated with the list of DE genes. These data contributes to information about important processes associated with RAO. Based on our results it also appears that airway remodeling is maintained in RAO horses via processes of cell proliferation, apoptosis and cellular component organization.

The classifiers obtained from this study are potential biomarkers of the disease and may play important role in disease pathogenesis. The findings from our study contributes to the field of equine RAO, however more research investigation is needed to validate these findings. Given the parallels between human asthma and equine RAO, our study reports several novel genes that can be of importance to asthma research. Hence, this study supports that equine RAO is an appropriate animal model for the study of asthma. We

propose potential new targets that are discriminatory molecular biomarkers obtained from LDA classification: programmed cell death 5 (PDCD5) and grainyhead-like 2 (GRHL2).

CONCLUSION

The results obtained from this study will contribute to the advancement of understanding of molecular mechanisms involved in RAO and asthma. There were some limitations in our study that should be taken into consideration while interpreting the results, which include small sample size and inadequate amount of RNA from biopsies. These shortcomings prevented us from doing direct hybridizations between RAO and control horses at the two time points and validating more genes via qPCR. Small sample size did not allow us to perform false discovery rate correction of the microarray results. For our future studies, we will be using larger sample size to understand the process of airway remodeling in horses affected with RAO. Also with next generation tools becoming more affordable, application of RNA-Seq will provide more accurate and extensive data and also reveal different isoforms, single nucleotide polymorphisms (SNP's) and structural variations (Hurd and Nelson, 2009; Wang et al., 2009). These tools have greater sensitivity and accuracy and overcome many limitations inherent to microarray platforms. Hence application of such tools in RAO research will expedite the process of understanding molecular causes underlying the disease or identify associated susceptibility loci.

CHAPTER III

EFFECT OF ALLERGEN CESSATION AND FLUTICASONE PROPIONATE ON AIRWAY REMODELING IN RECURRENT AIRWAY OBSTRUCTION AFFECTED HORSES

SYNOPSIS

Recurrent airway obstruction (RAO) is an obstructive, pulmonary, equine respiratory disease characterized by airway inflammation and morphological changes (termed as remodeling) in the airways of affected horses. Airway remodeling leads to increased airway obstruction, hyper-responsiveness and a decline in lung function. Understanding the molecular mechanisms underlying airway remodeling and its reversal is essential for developing therapeutic treatments. The aim of this study was to understand the effect of prolonged allergen avoidance and the corticosteroid treatment (fluticasone propionate) of established airway remodeling. Eleven horses affected with RAO were exposed to allergens for 3 months. During this time, they developed airway obstruction and inflammation (considered baseline). Out of eleven, five horses were placed in the allergen-avoidance group and the remaining six horses were placed in the treatment group. The allergen avoidance group was maintained in a low-antigen environment (pasture) for 12 months. The treatment group received the drug for 12 months; for the first six months, the horses were maintained in a stable, and for the next 6 months, they were moved to the pasture. Peripheral lung biopsies were obtained for both the groups at

baseline, 6 months and 12 months. RNA was extracted and converted to cDNA that was labeled with fluorescent dyes for microarray hybridizations using equine whole genome oligoarray**.** Allergen avoidance for 6 months did not resolve inflammation and features of airway remodeling. After 12 months of prolonged allergen avoidance, the environmental management led to less pronounced features of remodeling. The fluticasone propionate treatment concurrently with the allergen challenge (first six months) predominantly did not diminish the inflammatory response. Administration of the drug during allergen avoidance (last six months) appeared to reduce inflammation and features of remodeling. Environmental management (like allergen avoidance) is a critical component in the reversal of chronic features of RAO. However allergen avoidance alone is not sufficient to result in an early reversal of the airway remodeling. Since the concurrent administration of fluticasone propionate and allergen avoidance helped in achieving a relatively early recovery, an early introduction of the drug together with environmental management will be a beneficial strategy to reduce airway remodeling in RAO affected horses.

INTRODUCTION

Recurrent airway obstruction (RAO) is an asthma-like is a naturally lower airway respiratory disease in horses that is caused by exposure to dust from moldy hay and straw. Horses affected by RAO are generally 7 years of age or older and display an increased breathing effort and exercise intolerance when stabled during cold weather (Robinson, 2001). 10-20% of horses are estimated to be affected by RAO (Leclere et al.,

2011b) and an epidemiological study has reported the disease prevalence to be around 14% in a selected horse population in Great Britain (Hotchkiss et al., 2007). The clinical signs of RAO begin soon after exposure to aeroallergens, which cause airway inflammation, bronchoconstriction, and hypersecretion of mucus. Persistent airway inflammation and poor management of RAO leads to structural changes of the airways termed as "remodeling," which includes an increase in airway smooth muscle (ASM) mass (Herszberg et al., 2006). The molecular mechanisms underlying pathogenesis of chronic RAO, and the associated inflammatory and remodeling processes, are not completely understood; therefore, identification of genes and biological processes involved in RAO will help to improve the understanding of this disease.

The remodeling response in the airways consists of structural alterations that are considered manifestations of chronic allergic inflammation or a consequence of an aberrant process of wound repair (Elias, 2000; Jeffery, 2001; Homer and Elias, 2005; Zuyderduyn et al., 2008). Features of airway remodeling include the thickening of airways due to abnormal epithelium, an increased sub-basement membrane size, an increased vascularization and an enhanced mucus production (Chakir et al., 2003; Vignola et al., 2003; Postma and Timens, 2006; Doherty and Broide, 2007). An increase of airway smooth muscle mass and alterations in extracellular matrix also contribute to airway remodeling (Jeffery, 2001; Vignola et al., 2003; Lazaar and Panettieri, 2005). Airway remodeling can lead to an increased airway hyperresponsiveness and obstruction and can eventually lead to a decline in lung function (Pascual and Peters, 2005).

Prevention or reversing of airway remodeling is hence considered an important therapeutic target. However, exact pathophysiological and molecular mechanisms underlying remodeling are not fully understood.

Studies in RAO and asthma have highlighted the significance of environmental management, for example reducing allergens in the environment (Custovic et al., 1998; Vandenput et al., 1998; Platts-Mills, 2003; Simpson and Custovic, 2004) and drugs for the treatment of the disease (Jackson et al., 2000; Nelson et al., 2000; Robinson et al., 2002; Picandet et al., 2003; Harrison et al., 2004; Couetil et al., 2006; Woodcock et al., 2011). Currently, the focus of the treatment revolves around beta-agonists and corticosteroids to reduce inflammation and allergic reactions (Barnes, 2006).

There have been several studies conducted in the field of RAO and asthma that focus on the evaluation of the effect of allergen avoidance and corticosteroid therapy on affected individuals. A study in 2005 by Couetil at al. highlighted the importance of combining environmental management and early corticosteroid therapy (Couetil et al., 2005). Another study by Giguere et al. 2002 reported that inhaled fluticasone propionate (a potent corticosteroid) during severe disease exacerbation causes resolution of clinical signs and pulmonary function tests (Giguere et al., 2002).

The aim of our study was to perform transcriptome profiling using equine whole genome expression array to understand the effect of allergen avoidance and fluticosone

propionate on structural alterations of the airways in RAO-affected horses. Allergen avoidance and a corticosteroid drug like fluticasone propionate can aid in treatment of allergic respiratory diseases like asthma and RAO. Transcriptome profiling will enable the understanding of the genes/processes/pathways that are being modulated by each disease management strategy (allergen avoidance and/or fluticasone propionate). These genes/pathways can then be targeted to achieve improved resolution of chronic RAO symptoms. Even though a complete resolution of symptoms may not be achieved by either treatment strategy alone or in combination, knowledge of the molecular mechanisms underlying their therapeutic action will enhance the understanding of each strategy's effect on RAO.

MATERIALS AND METHODS

Study Animals and Experimental Design

Eleven horses affected with RAO were exposed to allergen (poorly cured moldy hay) for 3 months during which they developed airway obstruction and inflammation (considered baseline time period). During this time, they developed airway obstruction and inflammation (considered baseline). Out of eleven, five horses were placed in the allergen-avoidance group and the remaining six horses were placed in the treatment group. The allergen avoidance group was maintained in a low-antigen environment (pasture) for 12 months. Peripheral lung biopsies were obtained from these five horses at the end of the 3-month allergen challenge (baseline) and the end of 6 and 12 months.

The treatment group received the drug for 12 months; for the first six months, the horses were maintained in a stable (with naturally occurring antigens present in the environment). For the next 6 months, the six horses were moved to the pasture. Out of these, five horses were then maintained in a low-antigen environment (Pasture) for 12 months. Peripheral lung biopsies were obtained for the treatment group of horses at baseline, 6 months and 12 months.

Treatments

Antigen avoidance consisted in keeping horses on pasture and supplementing them with a pelleted diet. In the ICS group, fluticasone propionate (Flovent HFA, GlaxoSmithKline, Montreal, Canada) was administered at a dosage of 2000 µg q12h for a month, then dosages were adjusted to control clinical signs (2000 to 3000 µg q12 to 24h). Two horses received 2000 µg q24h from month 1, the other ones requiring higher or more frequent administration during the first 6 months.

Lung Biopsies and RNA extraction

The peripheral lung biopsies were obtained via thoracoscopy wherein peripheral lung tissue was harvested from the caudo-dorsal region of the lung in sedated horses (Relave et al., 2008). Tissue samples were frozen in liquid nitrogen and stored at -80C. The RNA was isolated using the cesium chloride technique as describe previously (Bedard et al., 2003). The extracted RNA quality was evaluated using bioanalyzer (Agilent, CA) and only samples with RNA integrity number (RIN) >7 were considered suitable for the microarray analysis.

Experimental Design

We co-hybridized cDNA obtained from the 5 horses at baseline with cDNA obtained from biopsies after 6 and 12 months of allergen avoidance. Similarly for the treatment group, cDNA from the 6 horses at baseline were hybridized with cDNA obtained from biopsies extracted at the 6 and 12-month time point. We used a balanced block design (BBD) for microarray hybridizations because for class comparison studies, BBD is considered optimal (Dobbin and Simon, 2002). The dye swap was embedded within the biological replicates to overcome any bias associated with the fluorescent dyes (Dobbin et al., 2003; Simon and Dobbin, 2003)

Labeling and Microarray Hybridization

For each sample, cDNA was generated from total RNA using Superscript II Reverse Transcription kit (Invitrogen) and labeled with Cy3 or Cy5 dye via an indirect labeling method utilizing dendrimer technology (Stears et al., 2000). Labeling was carried out with the 3DNA Array 900 MPX Expression Array Detection kit (Genisphere, PA). Hybridizations were performed in a SureHyb hybridization chamber (Agilent, CA) at 55°C. Following post-hybridization washes, arrays were scanned with a GenePix 4000B scanner at 5-micron resolution (Molecular Devices, CA). GenePix Pro 6.1 software was utilized for raw data acquisition, spot-finding, and quantification of array images.

Equine 21K oligonucleotide microarray

We used an whole genome equine oligonucleotide expression array with 21,351 elements designed at Texas A&M University (Bright et al., 2009). This 70-mer oligoarray is the most comprehensive expression array available for expressed equine sequences. Probes were synthesized (Invitrogen, Carlsbad, CA) and printed onto amino-silane coated slides (Corning Incorporated, Corning, NY).

Expression Analysis

Differential expression analysis of microarray data was conducted using Bioconductor's LIMMA package running in the R statistical software environment (Smyth, 2004). Background correction of raw intensities was performed using the normexp correction method (Ritchie et al., 2007). Subsequently, the background corrected intensities were normalized using printip-loess normalization (within array normalization), and aquantile method was used to perform across array normalization (Smyth and Speed, 2003a). Linear modeling using moderated t-tests was performed to identify differentially expressed genes (Smyth, 2004). To account for the multiple comparisons, the false discovery rate correction method of Benjamini and Hochberg was used (Benjamini and Hochberg, 1995). Linear models were used to assess the differentially expressed (DE) genes in RAO-affected animals after 6-month (R-t6/t0) and 12-month (R-t12/t0) of allergen avoidance compared to baseline (t0). Linear models were fit to obtain DE genes in the treatment group of animals for the first 6-months of treatment concomitant with allergen exposure compared to baseline (T-t6/t0). Similarly, DE genes were obtained for

the treatment group of animals for the next six months of continued treatment and allergen avoidance (T-t12/t0). Genes were considered significantly differentially expressed if they had a p value < 0.05 and fold change > 1.2.

Quantitative Real-Time PCR

Quantitative real-time PCR was performed on a subset of genes that were significantly differentially expressed (Fold change > 1.5 and p-value<0.05). Each gene was tested in duplicate along with a housekeeping gene control peptidylprolyl isomerase A (PPIA). This technique was used to validate results obtained from the statistical analysis of the microarray data. The total RNA was directly reverse transcribed to cDNA using the SuperScript® VILO™ cDNA Synthesis Kit (Invitrogen, Carlsbad, CA) and subsequently amplified using gene specific primers and master mix by qPCR in a single step reaction. When possible, primers were designed to span intron-exon boundaries to represent a region of the mRNA corresponding to the location of the cDNA sequence located on the arrays. Serial dilutions of RNA from the reference sample were used to generate relative standard curves and test the amplification efficiency of each primer set. For each qPCR assay, ~100 ng of total RNA was used in a 25 µl reaction with 1x Universal SYBR® Green Master Mix (Applied Biosytems, CA) and 300 nM primers and amplified on a LightCycler 480 (Roche Diagnostics, IN).

RESULTS

Differentially expressed genes

The genes were considered DE with the pvalue <0.05 fold change restriction of 1.2 **(table 3-1).** Comparing the lung tissue from the RAO-affected animals (allergen avoidance group) at the 6-month time point (R-t6/t0) to baseline yielded 86 DE genes, of which 23 genes were up-regulated and 63 down-regulated. We found 157 DE genes (43 up-regulated and 114 down-regulated) by comparing the RAO-affected animals (allergen avoidance group) at the 12-month time point to baseline. In contrast to these observations, for the treatment group of animals, RAO-affected horses at the 6-month time point (T-t6/t0) compared to baseline yielded 31 DE genes (6 up-regulated and 25 down-regulated). 65 genes were DE (49 up-regulated and 26 down-regulated) at the 12-month time point (T-t12/t0) when RAO-affected horses in the treatment group were compared to the baseline. The list of DE genes for all four comparisons is presented in **table B-1** (R-t6/t0), **table B-2** (R-t12/t0), **table B-3** (T-t6/t0) and **table B-4** (T-t12/t0).

Table 3-1: List of differentially expressed genes. The genes are listed in the table according to fold regulation and total number in each comparison: Allergen avoidance group at 6-month time point (R-t6/t0), allergen avoidance group at 12-month time point (R-t12/t0), treatment group at 6-month time point (T-t6/t0), treatment group at 12-month time point (T-t12/t0). DE genes for each comparison were calculated by comparing the expression values at each time point with respect to baseline (t0). Genes were considered DE if the pvalue<0.05 with fold change cut off of 1.2.

Comparisons	**Up-regulated genes**	**Down-regulated genes**	**Total DEG**
R-t6/t0	63	23	86
R-t12/t0	43	114	157
T-t6/t0	6	25	31
T-t12/t0	49	26	65

In the allergen avoidance group, out of the 374 DE genes at the 6-month time point and 553 DE genes at the 12-month time point, only 25 genes (common fraction) remained differentially expressed between the two time points (**figure 3-1**). In the treatment group, out of the 269 DE genes at the 6-month time point and 572 DE genes at the 12-month time point, 18 genes (common fraction) remained differentially expressed between the two time points (**figure 3-1**). Obtaining only a few DE genes common across the two-time points in the allergen avoidance and the treatment group suggests that the interventions (allergen cessation or/and corticosteroid treatment) indeed had an impact on the expression profile at the two time points.

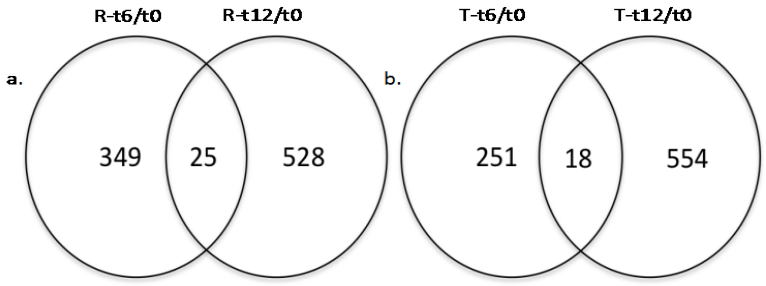

Figure 3-1: Overlap analysis. a) Overlap of gene expression profile of the allergen avoidance group at the 6-month and 12-month time point**.**
In total 374 (349+25) genes were differentially expressed for R-t6/t0 (6-month time point) and 553 (528+25) genes were differentially expressed for R-t12/t0 (12-month time point). Out of these, 25 genes were found to be common across the two time points.
b. Overlap of gene expression profile of the treatment group at the 6-month and 12-month time point.
In total 269 (251+18) genes were differentially expressed for T-t6/t0 (6-month time point) and 572 (554+18) genes for T-t12/t0 (12-month time point). Out of these, 18 genes were found to be common across the two points.

Real-time PCR

Real-time PCR was used to validate the regulation of expression of 11 DE genes from the four comparisons in this study. The fold regulation for these genes was calculated using the Pfaffl method (Pfaffl, 2001). The following 11 genes were considered for the real-time analysis: RASGEF1, CX603642, B4GALT3, NAGK, ITGA9, LOC651, RHOG, PES, ACSM5, WHSC2 and UQCRB (**figure 3-2).** We validated the direction of regulation of all 12 genes, however, ITGA9, RHOG and PES fold change did not correlate well with the microarray results.

Real-time PCR was used to validate findings of select genes that were significantly differentially expressed from the four comparisons in this study. Because limited amount of RNA was available from each peripheral lung tissue sample, we chose only 11 genes for the validation purposes. We could confirm the differential expression of all 11 genes in relation to the microarray data: UQCRB (R-t6/t0), WHSC2 (R-t6/t0), LOC651 (R-t6/t0), RASGEF1 (R-t12/t0), CX603642 (R-t12/t0), B4GALT3 (R-t12/t0), NAGK (R-t12/t0), PES (R-t12/t0), ITGA9 (T-t6/t0), ACSM5 (T-t6/t0) and ITGA9 (T-t12/t0).

Based on the microarray results, genes LOC651, RASGEF1, B4GALT3, ITGA9 were down-regulated AND UQCRB**,** WHSC2**,** CX60364, NAGK, PES, ACSM5 were up-regulated **(figure 3-2).** Though the real-time PCR results were not as pronounced as the microarray results for some of the genes, the trend (up and down regulation) essentially matched. Variation in correlation between the microarray based fold change values and lack of repeatability of the results in real-time PCR could be attributed to various factors. Small sample size increases the probability of obtaining false positives that pose challenge in qPCR validation. Literature also suggests that various factors like data normalization, fold change and p-value stringency also effect correlation between microarray and qPCR results (Dallas et al., 2005; Morey et al., 2006). Greater correlation is observed between the two results when genes exhibit at least 1.4 fold change and stringent p-value limits of 0.0001 or less are imposed in microarray data analysis (Morey et al., 2006).

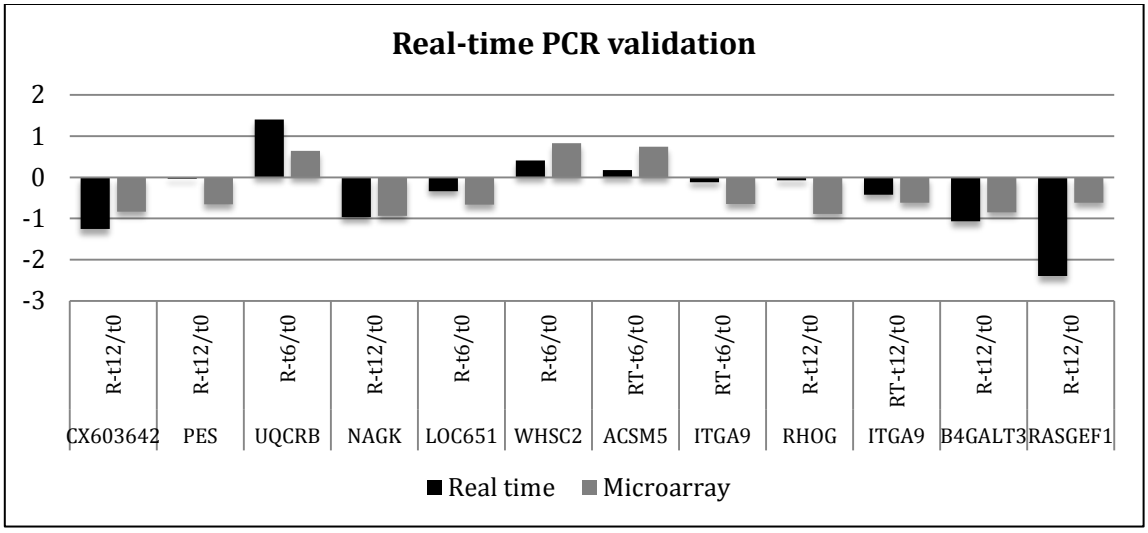

Figure 3-2: Real-time PCR validation of the microarray results. The y-axis represents fold change value of the genes selected for real-time validation. The Y-axis depicts the genes from each of the experimental comparisons.

DISCUSSION

Allergen avoidance for 6 months led to a reduction in the inflammation and improvement in lung function. At the end of 12 months, allergen avoidance caused a further reduction in the bronchial inflammation and a marked improvement in ASM reduction. Compared to the allergen avoidance group, in the treatment group during the first six months a marked reduction in ASM mass was observed and was comparable to results achieved after 12-months of allergen avoidance. During the next six months, when the treatment groups of horse were maintained on a pasture, a better resolution of inflammation was achieved.

Allergen avoidance group at the end of 6-months on pasture

We observed decreased expression of genes related to inflammatory processes at this time point. This supports the clinical findings of reduced perivascular inflammation and decreased numbers of neutrophils in brochoalveolar lavage fluid (Leclere 2012 unpublished data). Specifically, down-regulation of genes MHC class I polypeptide-related sequence B (MICB) and Interferon alpha 5 (IFNA5) suggest that the signals required to activate cytolytic response of NK and CD8 cells maybe diminished. NK cells have been reported to have a role in the development of allergenic inflammation, but the exact mechanism of its role is not established. However high number of NK, CD4+ and CD8+ cells have been observed after allergen challenge in broncho-alveolar lavage fluid (BAL) and lung parenchyma (Korsgren, 2002).

Cytochrome P450, family 26, subfamily A, polypeptide 1 (CYP26A1) metabolizes retinoic acid (RA), where overexpression of CYP26A1 reduced RA levels (Chang et al., 2008). Retinoic acid directly influences T-cells to suppress the production of IFN-g production and augments IL-4, IL-5 synthesis, thus promoting Th2 response (Iwata et al., 2004). It is well established that Th2 immune response underlies the pathophysiology of allergic disease like asthma (Barnes, 2001a). Since RA is known to exacerbate the allergic immune response, up-regulation of CYP26A1 could be contributing to the reduction in pulmonary inflammation by suppressing T-cell recruitment. Hence modulation of these genes could underlie the observed reduction in pulmonary inflammation and clinical indices of disease severity. There is no direct association

between the anti-inflammatory role of CYP26A1 in allergic diseases, and further studies will be needed to evaluate this observation.

However, the up-regulation of CCR8, which is a receptor for the T-cell chemokine CCL1 (Spinetti et al., 2003), indicates that lymphocytes are still trafficking to the lung at this time point. Our data suggest that, during the initial months of allergen avoidance, therapies aimed at prevention of T-cell migration to the lung might be of some use, although treatments targeting the innate branch of the immune system would probably not provide any further benefit.

We also observed reduced expression levels of collagen (COL1A1, COL5A1) and other extracellular matrix (CH13L1) related genes that could contribute to the process of reducing airway remodeling. Clinically, allergen avoidance alone resulted in a decrease in pulmonary elastance and resistance at 6-months. Our results suggest that allergen avoidance for a duration of 6 months may improve pulmonary function and reduce airway remodeling by down-regulating genes encoding collagen types I and V. Collagen I and V are the predominant sub-types of collagen genes that, in addition to other extracellular components, contribute to structural alteration of the airways in pulmonary diseases like asthma and RAO (Takizawa, 2007). Since structural alterations of the airway lead to functional changes, alteration in ECM composition and excessive collagen deposition will increase airway elastance and resistance (Xisto et al., 2005;

Lancas et al., 2006). Since allergen avoidance led to a decrease in collagen genes, it might contribute to the reduced elastance and resistance observed in the clinical data.

CH13L1 may also contribute to reduction in fibrosis since it can interact with type I collagen to regulate collagen fibril formation (Bigg et al., 2006). It is still not clear if the role of this gene in tissue remodeling and angiogenesis is limited to its capacity to interact with collagen (Coffman, 2008). However, preliminary studies in asthma have shown increased expression of CH13L1 to correlate positively with thickening of the sub-epithelial basement membrane and disease severity and negatively with pulmonary function (Ober et al., 2008). Hence the down-regulation of CH13L1 and the above mentioned collagen genes could be a response to the environmental intervention and lead to the structural reversibility in chronic RAO.

Allergen avoidance group at the end of 12-months on pasture

At the end of 12-months we observed down-regulation of genes involved in inflammatory process (CD99, ULBP3/NKG2DL3 and C5AR1). This observation lends support to the clinical observation of further reduction in BALF inflammation and biopsy inflammation as measured by neutrophil count (Leclere 2012, in press). Our data suggest that prolonged allergen avoidance (12 months) led to a decline in inflammation via modulation of genes involved in activation and migration of immune cells. We observed down-regulation of genes that would lead to a decline in neutrophilic influx into the site of inflammation (CD99 gene), activation of NK cells (ULBP3) and

migration of leukocytes (C5AR1) (Eleme et al., 2004; Lou et al., 2007; Gonzalez et al., 2008). Since RAO is characterized by neutrophilic inflammation, reduced activity of CD99 and C5AR1 (a potent neutrophil chemoattractant) could be a factor in reduction of the pulmonary inflammation.

A complete resolution of inflammation was not achieved due to mechanisms that sustain residual inflammation, for example, via up-regulation of TNFSF4 gene. The expressed protein of TNFSF4 is present on airway smooth muscle cells (ASMC) and antigen presenting cells (APC). Also known as OX40L, it is highly expressed on ASMC and their engagement with OX40 on CD4+ T-cells leads to a Th2 biased cytokine production (Lane, 2000). The OX40L-OX40 interaction causes proliferation and long-term survival of CD4+ cells and generates memory T-cells (Krimmer et al., 2009). Hence elevated OX40L would suggest its role in inflammation by promoting Th2 environment that underlie pathology of chronic allergic disease like asthma. Also OX40L activation could have a role in sustained inflammation because of its role in proliferation of antigen-specific CD4+ T cells and memory T cells.

We also observed down-regulation of various genes involved in the regulation of cell cycle and proliferation (TMEM97, RPL29, PAPPA2, PES1, FOXJ3, HES7, PPM1A) which could be involved in reducing airway smooth muscle (ASM) cell number and thereby reducing ASM mass. At this time point, clinical data showed a reduction in ASM mass but no significant difference in the myocyte proliferation or apoptosis (as

measured by PCNA and TUNEL assays). Reduction in ASM could be initiated as a consequence of decrease in ECM matrix as observed during first 6 months of allergen avoidance. Although during the next 6-months of allergen avoidance, we did not observe modulation of genes influencing ECM matrix but we did notice down-regulation of certain genes that regulate cell cycle that could lead to modest reduction in myocyte proliferation (since a significant different was not found clinically). Since there was not a significant reduction in myocyte proliferation at this time point, anti-inflammatory factors active at 12-months could also drive a reduction in myocyte size.

However we speculate that reduction in ASM could also be a consequence of reduced ECM deposition observed during the first six months. ECM proteins can also influence various features like survival, proliferation and contraction of ASM cells (Schwartz and Assoian, 2001). In addition to the ability of ECM components to affect the proliferative potential of myocytes, it can influence its phenotype. For example in a study it was shown that fibronectin and collagen type I enhanced the proliferation of myocytes and promotes a less contractile phenotype (Hirst et al., 2000).

Treatment group at the end of 6-months in stable

At this time point, clinical data suggested that the inhaled corticosteroid (ICS) caused an accelerated reduction in ASM mass when compared to the allergen avoidance group (Lecelre 2012, in press). However, the ICS was not able to reduce inflammation in the face of continuous allergen exposure. In our study we did not observe differential

expression of any gene involved in inflammation at this time point compared to baseline. This possibly suggests that the induction of pro-inflammatory genes due to the three-month allergen challenge at baseline was not altered by the ICS administration due to continued allergen exposure during the 6-month time period.

In line with the clinical observation that ICS administration led to a decrease in ASM mass, we observed modulation of genes that could contribute to this reduction. We observed the down-regulation of genes involved in the ECM receptor pathway (ITGA9, RHOG) and cellular proliferation (ITGA9, RHOG, ATAD2, ZNF423). ITGA9 is involved in collagen, laminin binding and fibronectin assembly (Bazigou et al., 2009). Integrins are signaling molecules involved in cell-cell and cell-matrix interactions (Dekkers et al., 2009). During remodeling altered ECM deposition occurs not only under the basement membrane but also surrounding bundles of smooth muscle. ECM proteins can also influence various features like survival, proliferation and contraction of ASM cells (Schwartz and Assoian, 2001). Since integrins have a key role in ECM-cell signaling blocking them offers a target to reduce alterations in ECM as well as ASM proliferation. In an animal model of allergic asthma, blocking integrin with a peptide having motif specificity for fibronectin, collagen and laminin decreased the ASM proliferation (Dekkers et al., 2009). Direct involvement of ITGA9 in ECM signaling and its role in ASM proliferation has not been explored and it therefore provides an exciting target for further research in remission of airway remodeling by blocking this integrin activity.

The clinical data suggested a significant decrease in myocyte proliferation due to ICS administration at this time point. Down-regulation of genes like ITGA9 and RHOG that are involved in cytoskeleton rearrangement could decrease the muscle thickness caused by ECM deposition. RHOG is involved in cytoskeleton rearrangement and contributes to negative regulation of immune response (Vigorito et al., 2003; Vigorito et al., 2004). RHOG is hypothesized to regulate cellular growth of vascular smooth muscle cells, specifically G1-S transition in the cell cycle (Vincent et al., 1992). Down-regulation of genes like ATAD2 that is involved in progression of cell cycle could influence the proliferative potential of myocytes (Muller et al., 2011).

Treatment group at the end of 6-months on pasture

After 6-months of concurrent administration of the drug while the horses were maintained on a pasture, clinical data suggested that the inflammation had resolved at this time point. Twelve months of treatment with fluticasone resulted in a similar reduction in ASM as did the 12-month allergen avoidance protocol. However, compared to the 12-month allergen avoidance group, in the treatment group we observed down-regulation of genes TNFSF4 and ITGA9. Down-regulation of ITGA9 compared to baseline is seen only in the treatment group at both time points. The ICS could be modulating the reduction in its expression thereby causing a decrease in extracellular matrix although there is no published evidence of this observation so far. Down-regulation of TNFSF4 probably represents one of the anti-inflammatory mechanisms of ICS on chronic RAO pathology, which could lead to a reduction in sustained Th2

inflammation via reducing CD4+ T-cells and memory cell expansion (Hoshino et al., 2003; Wang and Liu, 2007).

The sustained low-grade inflammation and generation of antigen specific memory cells will generate stronger effector response every time there is an antigenic re-exposure (Wang and Liu, 2007). Down-regulation of TNFSF4 due to ICS could therefore be contributing to reduced Th2 immune response and memory T-cell expansion thereby alleviating inflammation and reducing a future allergic response. Clinical data showed a residual low-grade airway obstruction even after the ICS treatment (12-month time point), inadequate anti-inflammatory actions of ICS could be one of the factors responsible for it. Incomplete reduction in ASM mass (only 30%) could be another factor contributing to bronchoconstriction. Abnormal cholinergic signaling (neural transmission) of airways may be another contributor of the residual airway obstruction (Barnes, 2001b). ICS are able to control airway inflammation and hyperresponsiveness, adding long-acting β_2-agonist (LABA) to the treatment should yield better control of chronic RAO symptoms because LABA assist in bronchodilation by inhibiting release of mast cell mediators and reducing nervous stimulation of airways (Barnes, 2002). However, ICS and LABA therapy combined with allergen avoidance should be tested early for safety and efficacy prior to use in horses suffering from chronic RAO.

One such mechanism could be via importin 13 (IPO13), where this gene regulates the nuclear import of glucocorticoid receptor (GR) thus affecting the anti-inflammatory

effect of glucocorticoid (GC) (Tao et al., 2006). Most of the effects of GC's are exerted by its interaction with glucocorticoid receptor, where the receptor after GC binding enters nucleus where it regulated transcription of the steroid-responsive DNA elements (Tao et al., 2006). Function of GC depends in the translocation of GR from cytoplasm to nucleus and IPO13 mediates this transport. Inhibiting IPO13 prevents the entry of GR and abolishes the anti-inflammatory effects of GC (Raby et al., 2009) for e.g. inhibit the synthesis of pro-inflammatory cytokines. We found IPO13 to be down-regulated at this time point, which could reduce the anti-inflammatory potential of the drug, preventing it from achieving a complete resolution of inflammation.

Clinical data showed that all of the reversibility in airway remodeling occurred only within the first 6-months of study with ICS administration with no addition improvement during the next 6-months. The lack of complete reversibility of the airway remodeling could be due to certain additional unresponsive molecular mechanisms that prevent the complete remission of chronic features. For example, EGF-like repeats and discoidin I-like domains 3 (EDIL3) that encodes an angiogenic ECM protein was found to be up-regulated. This protein initiates angiogenesis and promotes vessel wall remodeling (Sun et al., 2010)**.** Up-regulation of this gene could therefore be inhibiting resolution of vascular remodeling component of the structural alterations of the airways. We did not measure changes in vascular remodeling during the clinical study. Hence we can only speculate that certain factors promoting angiogenesis might reduce the efficacy of the drug in reversal of airway structural alterations.

CONCLUSION

This study assessed the effects of allergen avoidance and ICS drug (fluticasone propionate) administration on the transcriptome profile RAO affected horses. Our goal was to identify the mechanisms in which both allergen avoidance and drug treatment achieved reduced airway remodeling and inflammation. Allergen avoidance for 6 months led to a reduction in the inflammation and an improvement in the lung function. At the molecular level, the decrease in the inflammatory response could be due to reduced activation of cytotoxic cells. In addition, diminished synthesis of metabolic intermediate that promotes a Th2 environment could also contribute to reduction in inflammation. Regulation of genes that affect extracellular matrix deposition were also observed at this time point. However this modulation did not lead to a significant reduction in ASM mass at this time point. At the end of 12 months, allergen avoidance caused a further reduction in the bronchial inflammation and a marked improvement in ASM reduction. A decrease in neutrophil chemotaxis could be have contributed to the improvement in inflammation at this time point, since neutrophils are the predominant immune cells involved in pathology of RAO.

Compared to the allergen avoidance group, in the treatment group during the first six months a marked reduction in ASM mass was observed and was comparable to results achieved after 12-months of allergen avoidance. The reduction in muscle mass are due to mechanisms that reduce cellular proliferation and ECM deposition and signaling. During the next six months, when the treatment groups of horse were maintained on a pasture, a

better resolution of inflammation was achieved. A better control of inflammation at this time point compared to allergen avoidance alone is due to various anti-inflammatory actions of the drug including its ability to reduce expansion of primed CD4+ T-cells and memory cells. However, the presence of factors that limit the effects of the drug and the inherent shortcoming of ICS as standalone treatment strategy were evident at this time point. First, it did not cause an additional decrease in ASM mass compared to what was observed during that first six months. Second, it did not to completely resolve bronchoconstriction. We propose that adding LABA to ICS may achieve better results for remission of chronic RAO symptoms.

Despite the insights obtained from this study, the results need to be interpreted with caution. For example, this study has a small sample size and, the treatment group lacked internal controls. When the treatment group of horses were maintained on pasture, there were no horses that were administered a placebo to better resolve the drug versus environment effects. Finally, the same set of horses was used in the treatment group. After they were exposed to allergen for first six months they were maintained on pasture for the next six; hence the two time-points in the treatment group were not entirely independent.

CHAPTER IV

GENE EXPRESSION PROFILING TO ESTABLISH TEMPORAL CHANGES IN PERIPHERAL BLOOD LEUKOCYTES OF HEALTHY FOALS AND FOALS AFFECTED WITH *RHODOCOCCUS EQUI* PNEUMONIA

SYNOPSIS

Rhodococcus equi (*R. equi*) is an intracellular bacterium that is primarily known as an equine pathogen that infects young foals causing a pyogranulomatuous pneumonia. The molecular mechanism mediating the foal immunity in response to *R. equi* is not fully elucidated. Hence global genomic high throughput tools like expression microarray analysis will elucidate genetic signatures and molecular pathways that modulate the immune system of young foals in response to *R. equi* infection. Identifying such genes will therefore help in disease control and design of drugs and vaccines. The objectives of this study were two-fold a) to determine the age-dependent changes in the expression profile associated with blood leukocytes stimulated with virulent *R. equi* compared to the un-stimulated ones. b) to obtain the temporal changes in the gene expression profile associated with blood leukocytes in response to the virulent *R. equi* stimulation. Peripheral blood leukocytes from six foals a day after birth and two, four and eight weeks after birth were obtained. The blood was grouped in two, where the first half was stimulated with the pathogen and second half served as un-stimulated control. RNA was extracted and generated cDNA was labeled with fluorescent dyes for microarray

hybridizations using equine whole genome oligoarray. Our findings suggest that the stimulated leukocytes appear capable of initiating a protective immune response through birth and up to 8 weeks of age. Concurrently, we also observed modulation of processes that may be detrimental to the host. Temporally it appeared that the across all the time points, the bacterial stimulation led to induction of pathogen recognition and mounting of immune response.

INTRODUCTION

Rhodococcus equi (*R. equi)* is recognized globally as a leading source of pneumonia in young foals up to six months of age while adult horses do not develop the disease unless they are immune-deficient (Heller et al., 2010). There are also non-equine species susceptible to *R. equi* pneumonia like pigs, cattle, cats, goats, dogs and humans (Muscatello et al., 2007). In humans, it affects only HIV-infected or immune-comprised individuals (Linder, 1997; Kedlaya et al., 2001). Mortality rate due to foal pneumonia is estimated to be 2-13% (Mousel et al., 2003) and hence this disease has serious implications on the equine industry. The course of *R. equi* infection in foals is insidious and disease is often progressed by the time diagnosis is made (Horowitz et al., 2001).

In addition to being one of the major equine pathogens, *R. equi* is evolving as a human pathogen (Weinstock and Brown, 2002). Till date the knowledge about the foal immune response against the *R. equi* infection has mainly been garnered by studying differences between foal and adult horse response to the pathogen. The ability of the foal to fight *R.*

equi infection heavily depends on its immunity. Young foals have immature immune system and leukocytes are critical in defense of the host against a plethora of infectious/ foreign agents. There is limited knowledge about the development of immune system in equine neonates. Additionally, knowledge about the changes in the gene expression of leukocytes during the first few months of foal life will help in understanding the development of its immune responses.

Hence the objective of this study is to identify the age-related expression profile of peripheral blood leukocytes after an in-vitro stimulation with virulent *R. equi* and compare it with the un-stimulated leukocytes. We also aimed to identify genes that are being modulated temporally in the stimulated blood leukocytes. We propose that this study will help in identifying genes and processes that modulate the immune system of the young foals in response to virulent *R. equi*. Additionally, we will also determine the age-related differences in the transcriptome of the stimulated peripheral blood leukocytes from healthy foals.

MATERIALS AND METHODS

Sample collection

Approximately 60 mL of blood was collected in 10 mL EDTA vacutainers via jugular venipuncture from each foal at day 1 (within first 24 hours) and weeks 2, 4, and 8. All blood was immediately processed in the laboratory following collection. The blood was divided into two aliquots (30 ml each) that was further divided into six portions and

added to a 6 well cell culture plate. For one plate the blood was subjected to the stimulation of live, virulent *R.equi* at an approximate multiplicity of infection (MOI) of 10, and another 6 well culture plate with the other 30 mL of blood served as the un-stimulated control. The plates were incubated for 3 hours (37°C, 5% CO_2) with slow rotation. After incubation, the blood of each treatment type was combined, and the leukocytes were isolated and stabilized using the LeukoLOCK Total RNA Isolation System (Ambion, CA).

RNA extraction

Total RNA was extracted from whole blood (both un-stimulated and stimulated with *R.equi*) using the LeukoLOCK Total RNA Isolation System (Ambion, CA) per the manufacturer's instructions. A DNase I treatment was also performed as a part of the RNA extraction protocol to remove any contaminating genomic DNA. Extracted RNA was quantified with a spectrophotometer (NanoDrop) while the RNA quality was then evaluated with the Agilent 2100 Bioanalyzer.

Experimental design

In order to obtain the temporal expression changes in the in-vitro *R. equi* stimulated leukocytes, we utilized the common reference design for microarray hybridizations (reference). Hybridizations were performed with 6 biological replicates at each experimental time-point: day-1 (D-1) and weeks 2 (W-2), 4 (W-4) and 8 (W-8). The D-1 sample served as the reference for each foal and all other experimental samples from

that foal were co-hybridized to it. Additionally, in order to compare the stimulated blood leukocytes with the un-stimulated ones, we performed perform direct co-hybridization of un-stimulated and the stimulated samples at each experimental time-point.

RNA amplification

Due to low quantity of RNA obtained from some of the samples, we had to amplify the RNA samples. Not all the samples needed amplification but to ensure uniformity across all the samples RNA was amplified for every sample (for both nasal epithelial cells and blood leukocytes). 500ng of RNA was used for each amplification reaction using the sensation kit (Genisphere) as per the manufacturer's protocol.

Labeling and Microarray Hybridization

For each sample, cDNA was generated from total RNA using Superscript II Reverse Transcription kit (Invitrogen, Carlsbad, CA) and labeled with Cy3 or Cy5 dye via an indirect labeling method utilizing dendrimer technology (Stears et al., 2000). Labeling was carried out with the 3DNA Array 900 MPX Expression Array Detection kit (Genisphere, PA). Hybridizations were performed in a SureHyb hybridization chamber (Agilent, CA) at 55°C. Following post-hybridization washes, arrays were scanned with a GenePix 4000B scanner at 5-micron resolution (Molecular Devices, CA). GenePix Pro 6.1 software was utilized for raw data acquisition, spot-finding, and quantification of array images.

Equine 21K oligonucleotide microarray

We used an equine whole genome oligonucleotide array with 21,351 elements developed at Texas A&M University (Bright et al., 2009). This 70-mer equine oligoarray is one of the most exhaustive gene arrays currently present for expression analyses. Probes were synthesized (Invitrogen, Carlsbad, CA) and printed onto amino-silane coated slides (Corning Incorporated, Corning, NY).

Expression Analysis

Differential expression analysis of microarray data was conducted using Bioconductor's LIMMA package running in the R statistical software environment (Smyth, 2004). Background correction of raw intensities was performed using the normexp correction method with offset 50 (ref). Subsequently, the background corrected intensities were normalized using printip-loess normalization (within array normalization) but no across array normalization was performed (Smyth and Speed, 2003b). Linear modeling using moderated t-tests was performed to identify differentially expressed genes (Smyth, 2004). To account for the multiple comparisons, the false discovery rate correction method of Benjamini and Hochberg was used (Benjamini and Hochberg, 1995). Linear models were used to assess the age-related differentially expressed (DE) genes in the stimulated leukocytes (temporal expression) for the three comparisons: a) day1 versus week2 (C1) b) day1 versus week4 (C2) and c) day1 versus week8 (C3). Similarly, linear models were fit to obtain DE genes between the stimulated and the un-stimulated

leukocytes at each time point (D-1, W-2, W-4, W-8). Genes were considered significantly differentially expressed if they had a p value < 0.05 and fold change > 1.5.

Functional analysis

Functional gene ontology analysis was performed using a web-based tool WebGestalt : **WEB**-based **GE**ne **S**e**T** **A**na**L**ysis **T**oolkit (Zhang et al., 2005; Duncan et al., 2010). Gene ontology analysis was performed using the list of differentially expressed genes to obtain statistically significant biological processes. In order to calculate the statistical significance, DE genes for each comparison were compared to all the genes present on our equine microarray. Benjamini Hochberg method was used for multiple test adjustment with significance level < 0.1.

RESULTS

Differentially expressed genes (table 4-1)

Comparison of the stimulated versus un-stimulated peripheral blood leukocytes at day-1 showed that 125 genes were differentially expressed between them, of which 89 were up-regulated and 36 down-regulated (D-1). A similar comparison at week-2 time point led to the identification of 127 DE with 92 up-regulated and 35 down-regulated genes (W-2). At week-4 time point, 73 genes were differentially expressed with 35 up-regulated and 38 down-regulated genes (W-4). Finally at week-8 time point, there were 135 genes that were differentially expressed, of which 92 were up-regulated and 43 down-regulated (W-8).

Likewise, when the first time point was compared to the remaining three time points (week-2, week-4 and week-8) for the stimulated peripheral blood leukocytes, differentially expressed genes were obtained for each comparison due to temporal changes in gene expression profile. There were 102 DE genes for the comparison C1, with the highest number of DE genes was comparison C2 (192 genes) and finally C3 with 148 genes.

Table 4-1: Differentially expressed (DE) genes. List of differentially expressed genes for each comparison is shown in the table. Genes were considered differentially expressed with pvalue<0.05 and fold change >1.5. C1: comparison 1, C2: comparison 2, C3: comparison 3.

Comparison type	Time point	DE genes	Total DE genes
Stimulated versus unstimulated leukocytes	Day1 (D1)	Up: 89 Down: 36	125
	Week-2 (W2)	Up: 92 Down: 35	127
	Week-4 (W4)	Up: 35 Down: 38	73
	Week-8 (W8)	Up: 92 Down: 43	135
Temporal changes in stimulated leukocytes	Day1 vs. week-2 (C1)	Up: 30 Down: 72	102
	Day1 vs. week-4 (C2)	Up: 83 Down: 109	192
	Day1 vs. week8 (C3)	Up: 75 Down: 73	148

Functional analysis

Stimulated versus un-stimulated blood leukocytes

We performed functional analysis of the DE genes associated with each time point for each comparison type. The top ten biological processes (**figure 4-1**) associated with the up-regulated genes at the earliest time point (day1), appeared to be involved in variety of roles ranging from adiponectin secretion, defense response to endocrine process. Strikingly different, the biological processes associated with the down-regulated genes were mainly involved in wound healing and blood coagulation. Interestingly among the down-regulated genes, mainly PLSCR1, SELP and SCUBE1 were involved with all the statistically significant biological process.

For the W-2 time point, we did not find association of any statistically significant biological process with the down-regulated genes. For the up-regulated genes, the top ten biological processes (**figure 4-1c**) were associated with regulation of temperature (fever) and immune response (leukocyte migration, neutrophil chemotaxis, immune system process). Similarly for the W-4 time point, we did not find any statistically significant biological process associated with the down-regulated genes. For the up-regulated genes, the top ten biological processes (**figure 4-1d**) very closely resembled the ones obtained for W-2 time point (e.g. fever, immune response).

Uniqueness of the expression profile

In order to identify the genes that were unique for each experimental time point, we compared the list of DE genes across all four time-points and obtained the intersection and union of the gene sets (**figure 4-2**). The expression profile at each time point appeared to be largely distinct with very few common genes as depicted in the figure 3. Out of the 88 (D-1), 88 (W-2), 51 (W-4) and 87 (W-8) DE genes for each time point, only 11 genes were present in all the four. IL1A, IL1B and IL1RA were among the genes differentially expressed (up-regulated) across all four time-points.

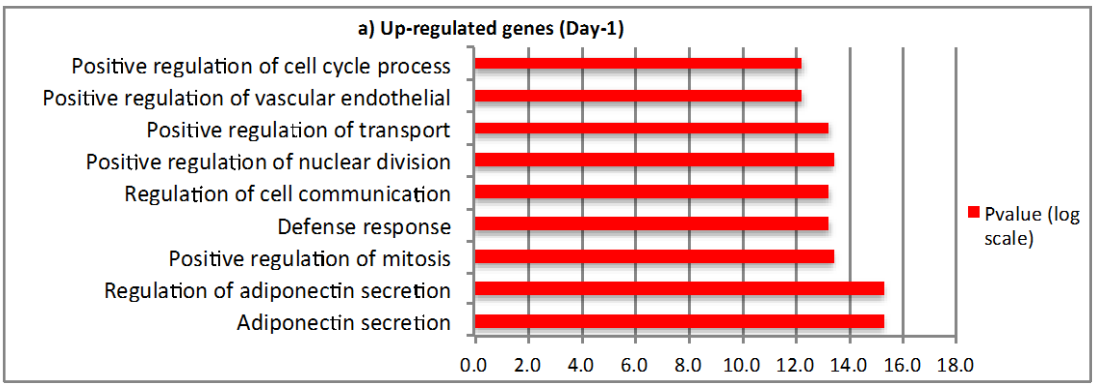

Figure 4-1: Biological processes associated with DE genes in leukocytes stimulated with *R. equi* compared to the un-stimulated leukocytes. Graphical representation of top fifteen statistically significant processes associated with the DE genes a) up-regulated (colored red bars) at day 1(D-1) and b) down-regulated genes (colored green bars) at day 1(D-1), c) up-regulated genes after two weeks (W-2) d) up-regulated genes after four weeks (W-4). The Y-axis represents the biological processes and the X-axis represents the pvalue displayed as $-\log_2$(pvalue).

Figure 4-1 Continued

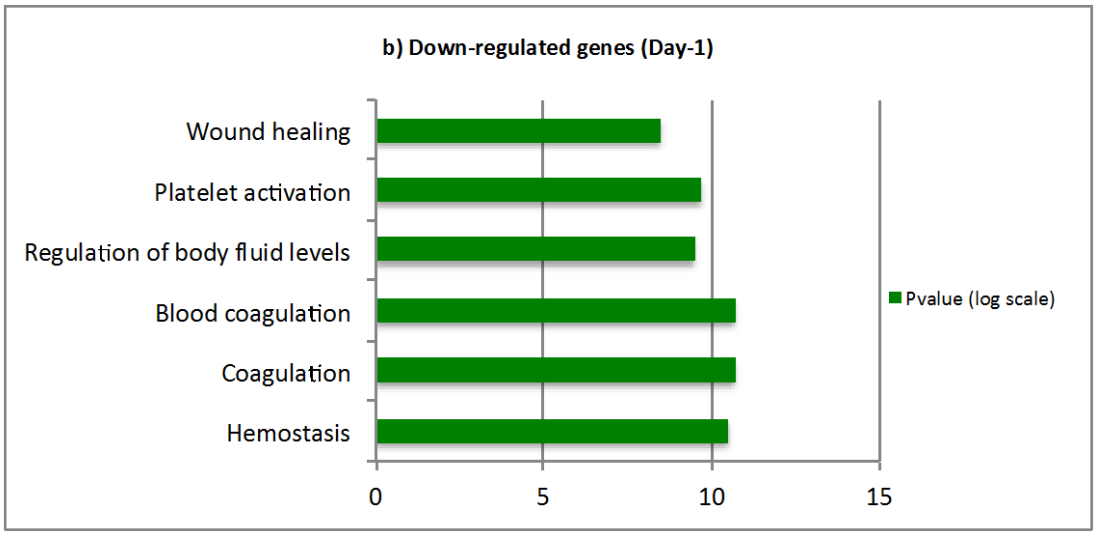

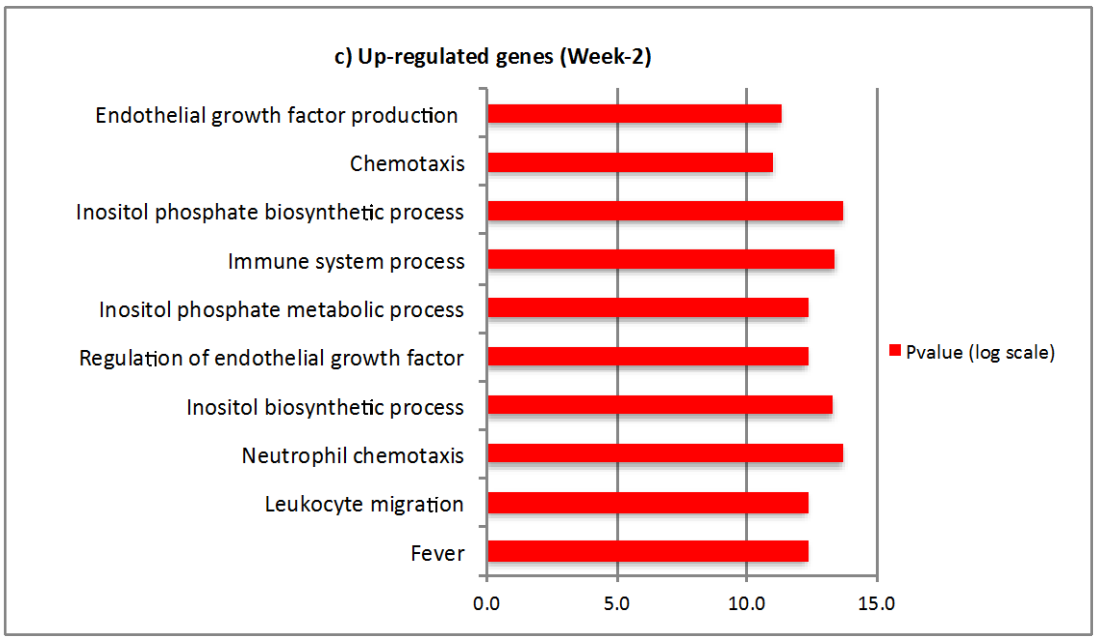

Figure 4-1 Continued

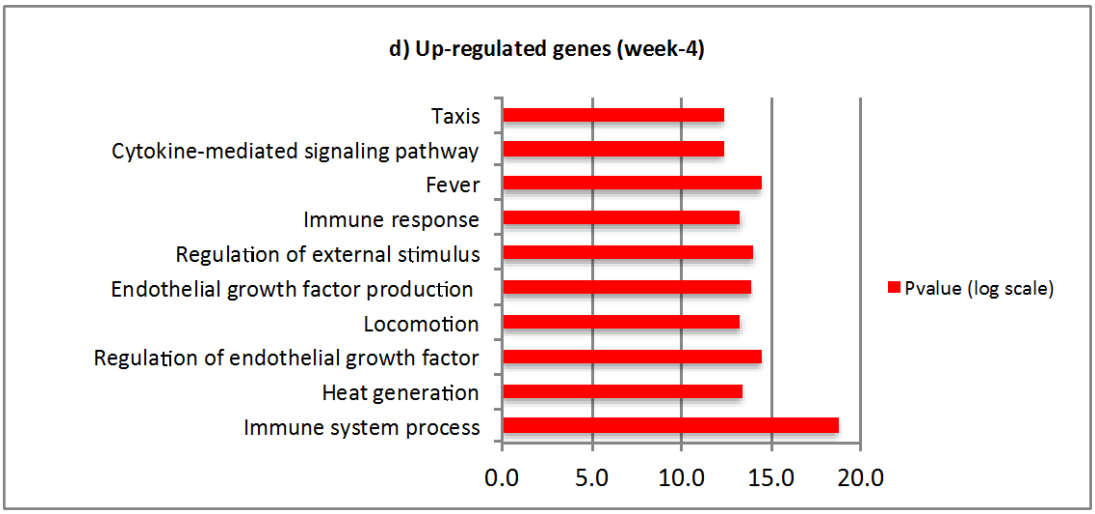

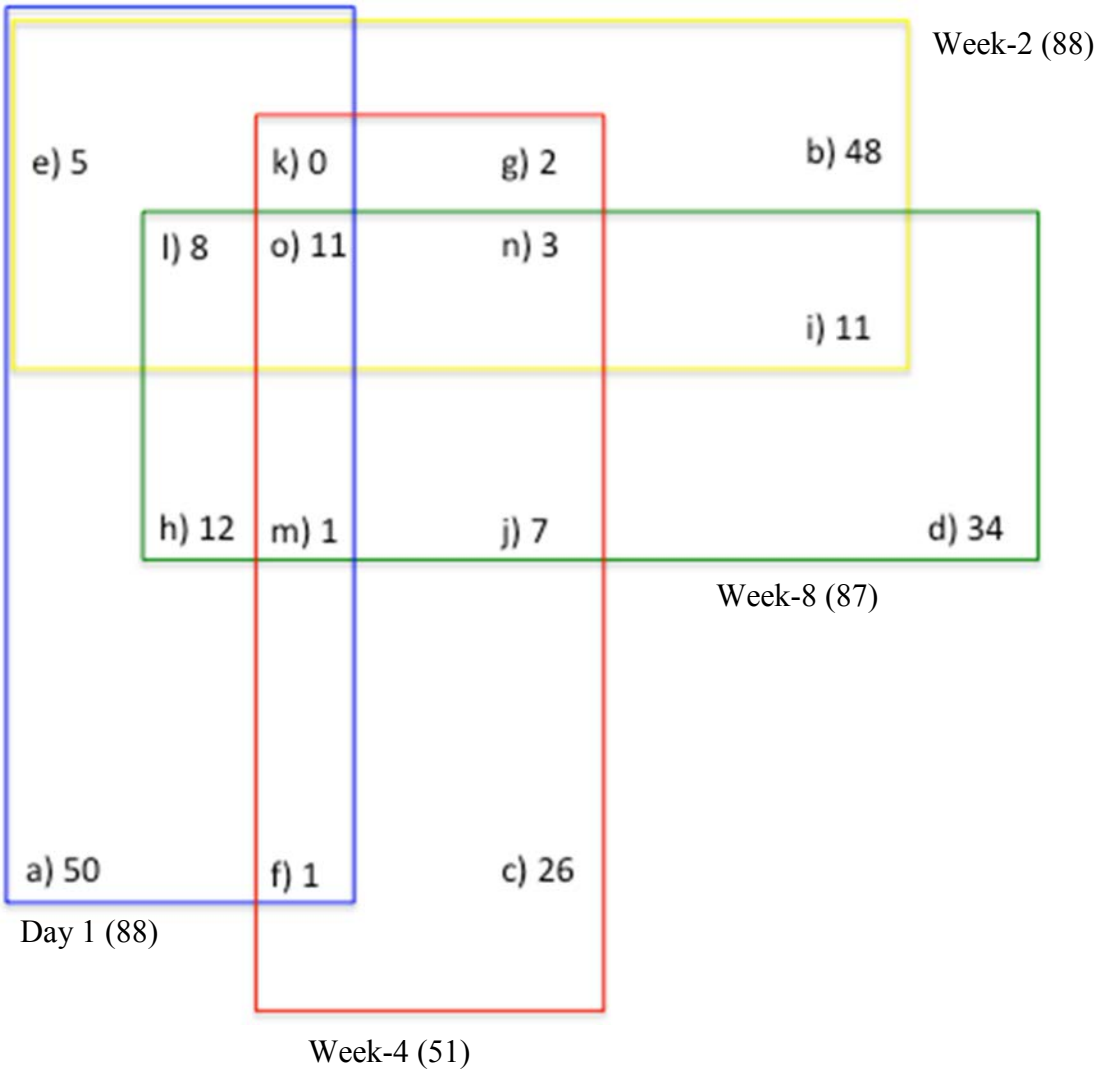

Figure 4-2: Venn diagram for pairwise comparison of the gene expression profile of stimulated versus un-stimulated leukocytes. The four time points are designated in the diagram as 1: day1, 2: week-2, 3: week-4, 4: week-8. In the figure below the letters represent: a-genes found in 1 only, b-genes found in 2 only, c-genes found in 3 only, d-genes found in 4 only, e-genes in 1&2 only, f-genes in 1&3 only, g-genes in 2&3 only, h-genes in 1&4 only, i-genes in 2&4 only, j-genes in 3&4 only, k-genes in 1,2,3 only, l-genes in 1,2,4 only, m-genes in 1,3,4 only, n-genes in 2,3,4 only, o-genes in 1,2,3,4.

Temporal changes in stimulated blood leukocytes

We also performed functional analysis for the DE genes obtained for the three comparisons (C1, C2, C3) when the expression profile obtained at day1 was compared to the remaining three time points individually. For comparison C1 (day1 vs. week-2) the top ten biological processes associated with the up-regulated genes were primarily involved in immune response (antigen processing and presentation and immune related process like antigen processing and presentation, immune response and hypoxia (**figure 4-3**). The top ten processes associated with the up-regulated genes appeared to be involved in synthesis and catabolism of various organic compounds (sulfur amino acid biosynthetic process, cellular nitrogen compound biosynthetic process). Similar to our observations for W-2 and W-4 functional analysis (stimulated versus unstimulated comparison), for the C2 (day1 vs. week2) and C3 (day1 vs. week4) comparisons there were no statistically significant processes associated with the down-regulated genes. The down-regulated genes for the C2 comparison were associated with few processes (five), which were involved lipid transport and macrophage chemotaxis (**figure 4-3c**). The top ten processes associated with the up-regulated genes for the C3 comparison were involved in protein translation (e.g. translation, translation elongation), protein folding (e.g. Chaperone mediated protein folding requiring cofactor, de -novo protein folding) are depicted in **figure 4-3d**.

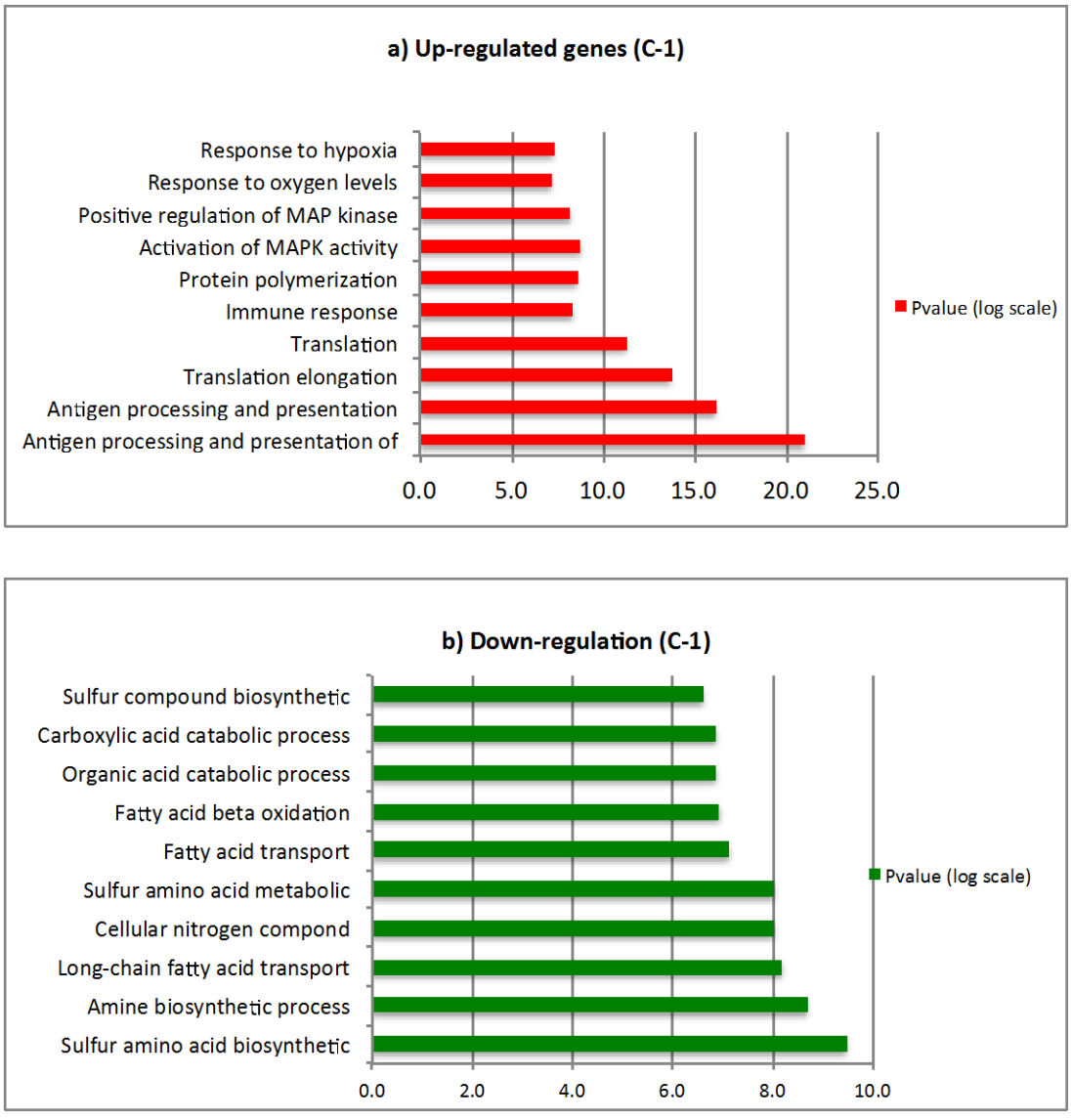

Figure 4-3: Biological processes associated with temporal expression of genes in leukocytes stimulated with *R. equi*. Graphical representation of top fifteen statistically significant processes associated with the DE genes a) down-regulated (colored green bars) for comparison C-1 (day1 vs. week2) b) up-regulated genes (colored red bars) at for comparison C-1 (day1 vs. week2), c) down-regulated genes for comparison C-2 (day1 vs. week4) and d) up-regulated genes for comparison C-3 (day1 vs. week8).The Y-axis represents the biological processes and the X-axis represents the pvalue displayed as $-\log_2(\text{pvalue})$.

Figure 4-3 Continued

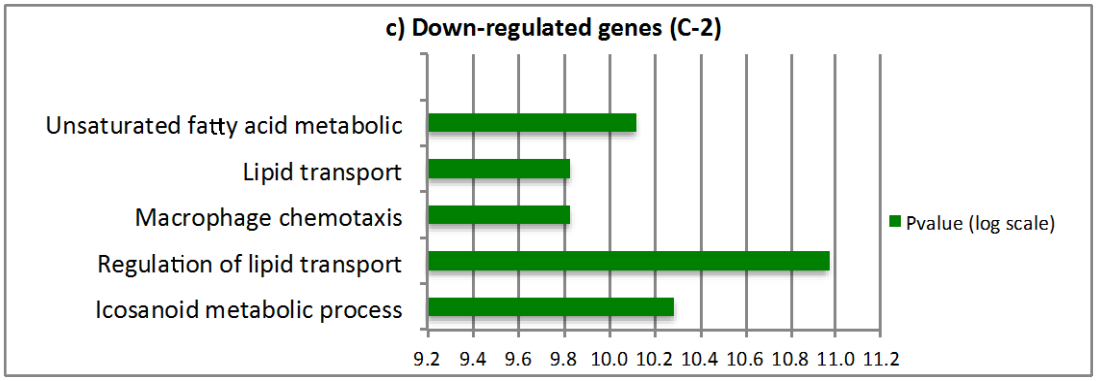

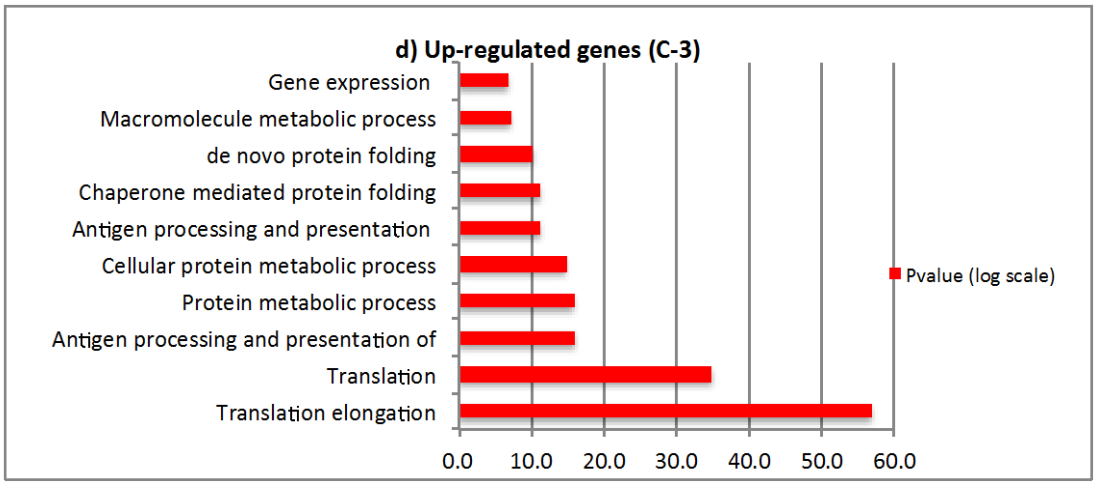

Uniqueness of the expression profile

We compared the list of DE genes obtained for each temporal comparison and obtained the intersection (**figure 4-4**). The expression profiles of the three comparisons (C1, C2, C3) were largely distinct, with the largest overlap between C1 and C2 (30 genes). None of the genes were present in all three comparisons once again highlighting the uniqueness of the expression profile.

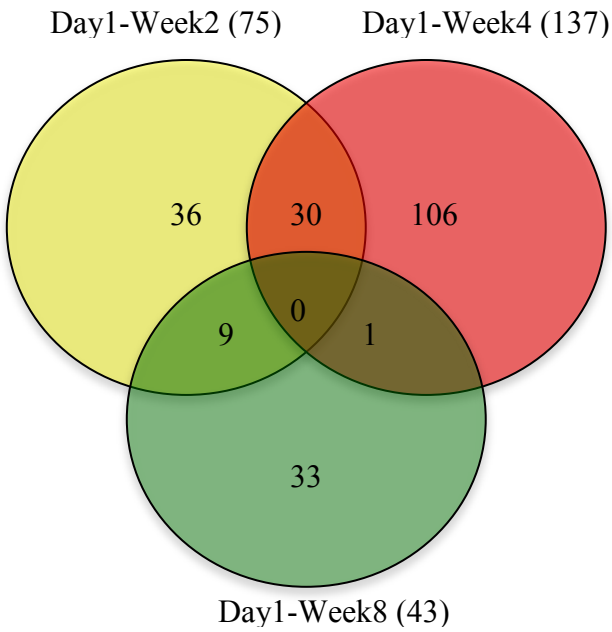

Figure 4-4: Venn diagram for temporal gene expression changes. This venn diagram depcts DE genes unique to each comparison: day1-week2 (C1), day1-week4 (C2) and day1-week8 (C3).

DISCUSSION

The gene expression profile of the stimulated leukocytes compared to the un-stimulated ones appears to be largely unique for each time point. However, after the functional analysis some patterns emerged that stayed common across the four time points. Our results suggest that the bacterial stimulation up-regulated many genes involved in fighting and clearance of the infection. However, there was also modulation of genes that could be detrimental for the host and lead to bacterial survival and proliferation.

Stimulated versus un-stimulated blood leukocytes

When the expression profiles of the stimulated leukocytes were compared to the un-stimulated ones, a pattern emerged between that was consistent across all the four time-points. For example, across all four time-points, we observed induction of processes involved in host protection/bacterial clearance as well as processes contributing to immune suppression. The pathogen seems to be stimulating a tug of war between the protective immune response and the suppressive factors that promote susceptibility to infection.

Soon after birth (D-1), the stimulated cells appear to modulate genes towards a protective immune response against the bacterium e.g. processes like defense response, fever, immune system process and immune response. However modulation of various other genes/processes could attenuate such protective response, preventing effective pathogen clearance by the host. It appears that across all the time points the genes (IL1A, IL1B) involved in fever were induced. Fever is a natural response to elevate the body temperature to create hostile environment for the pathogen. IL1A is a pyrogen (Hartung et al., 1998) that may be induced to assist host response against *R. equi*. We also observed induction of various pro-inflammatory mediators like CCL20, IL1A, IL1B, IFNA5 at this time point that recruit immune related cells to fight off the infectious agent.

CCL20, IL1A, IL1B and IFNA5 are pro-inflammatory cytokines whose induction by leukocytes (from a day old foal) due to bacterial stimulation leads to protective response by recruiting immune cells in order to contain the bacteria and fight the infection. Over expression of CCL20 is thought to be involved in development and maintenance of pulmonary granulomas (foci of infection) by causing migration of meutrophils, macrophages and lymphocytes to these sites (Lee et al., 2008). Such an elevated expression of this cytokine has been observed in human peripheral blood mononuclear cells (PBMC) and macrophages in response to *mycobacterium tuberculosis (Lee et al., 2008)*. IL1A and IL1B involved in recruitment of early inflammatory cells to the sites of infection (Burger et al., 2006). Early during the course of infection, host needs inflammatory agents to curtail pathogen spread to stop the infection, and such pro-ifnalmmatory factors will have a protective role against *R. equi*.

In addition to the protective immune response discussed so far, various other processes may diminish migration of immune cells (anti-inflammatory) and promote spread of infection (coagulation). For example at day-1, we observed down-regulation of genes involved in blood coagulation and platelet activation (SCUBE1, SELP, PLSCR1) in the stimulated cells. In mycobacterial infection of lungs, platelets have a protective role where the aggregation of platelets obstructs blood vessels around the foci of infection preventing the spread of the bacteria (Buyukasik et al., 1998). Elevated platelet count is seen as one of the clinical symptoms of the foal pneumonia. If the platelets are performing a similar action in foals then an elevated platelet count should have a

protective role in the pathology of the infection. However just a day after birth, reduced expression of genes associated with platelet activation possibly points towards a weak immune system unable to activate platelets soon after bacterial infection. As the disease progresses in severity the platelet count increases and can be detected as one of the clinical symptoms during the first three months of life. Elevated expression of genes involved in blood coagulation and platelet activation are observed at the later time points: W-2 (PLEK, PTAFR) and W-4 (PLEK, PLAU).

Adiponectic secretion could be another unfavorable factor that could be antagonizing the effect of protective immune response at D-1. Adiponectin is an anti-inflammatory adipokine. It suppresses the activity of NF-kB and pro-inflammatory cytokine like TNF-α in macrophages. Adiponectin also induces expression of various anti-inflammatory cytokines like IL-10 and IL1RN (Wolf et al., 2004). From our results at D-1, various anti-inflammatory factors seem to be induced by pathogenic stimulation like: IL1RN, NFKBIA, adiponectin (via GPR109A). Their anti-inflammatory action can dampen the protective immune response at this time point.

As the foals aged and their immunity matured, we observed up-regulation of a variety of chemokines: CCL20 (D-1); CXCL10, CXCL3 (W-2); CXCL2 (W-4), CXCL2, CCL20, CXCL10 (W-8). Activation of variety of chemokines and their increased expression only in the stimulated leukocytes may be helping in fighting *R. equi* infection. Neutrophils are the first responders to the site of infection and critical for mounting innate immunity.

Neutrophils in mice with *R. equi* infection can reduce the bacterial burden (Martens et al., 2005) and are important in controlling early infection. Induction of CCL20 after one day of birth, CXCL3 after two weeks and CXCL2 after four weeks of birth cause neutrophil chemotaxis and leukocyte migration to the site of infection (Kobayashi, 2008; Ha et al., 2010). Hence these chemokines at the various time points are invoking neutrophil response to control the early infection due to *R. equi* and also limit their spread. Eight weeks after birth chemokines involved in neutrophil recruitment are present. Induction of CXCL10 is involved in activation and recruitment of CD4+ and CD8+ T-cells (Lande et al., 2003). CD4+ T-cells are critical in effective clearance of *R. equi* (Kanaly et al., 1993), making induction of CXCL10 a key factor in host immune response. It is interesting to observe that at the earlier time points, chemokine profile is mainly supportive of the neutrophil recruitment to tackle the pathogen, however at week-8 the host appears capable of invoking CD4+ and CD8+ T-cells in addition to neutrophils.

Due to bacterial stimulation, the host is able to induce protective immune response, but the pathogen via modulation of host immune system is able to induce processes favoring its survival and proliferation. It appears that the immune related deficiencies of the foal allow the pathogen to regulate host immune response. Similar to D-1, at later time points we observed processes that maybe favorable to pathogen. For example, we observed up-regulation of superoxide dismutase 2 (SOD2) at W-2, W-4 and W-8. Up-regulation of SOD2 (superoxide dismutase) enables pathogen survival due to its ability to catalyze the

superoxide radicals and evade the damage from the reactive oxygen radicals within phagocytes (Roberts and Hirst, 1996).

Temporal changes

Compared to baseline, two weeks after birth, the expression profile from stimulated leukocytes showed elevated protein synthesis (ribosomal proteins) and antigen processing and presentation. High protein turnover could be a host response against bacteria (anti-microbial), or a consequence of pathogen modulating host machinery for its survival and replication. Genes involved in protein synthesis (translation and processing) was also reported to be elevated in the human macrophages stimulated by virulent *Mycobacterium tuberculosis* (Wang et al., 2003). It appears from our results that two weeks after birth, there is an improvement in the host immune response evident by up-regulation of genes expressing MHC class II antigens. A reduced expression of MHC class II by APC's like macrophages or dendritic cells is seen in young foals (Dawson et al., 2010). Reduced antigen presentation of such molecules can lead to diminished activation of class II restricted CD4+ T-cells. Since CD4+ cells are critical in pathogen clearance, effective antigen presentation is critical part of host immunity. For C-1, the down-regulated genes predominantly performed lipid transport and metabolism. Lipid metabolism is a major source of energy for mycobacterium and if a similar mechanism exists in *R. equi* then down-regulation of lipid transport and metabolism genes are probably modulated a reduction in pathogen survival. For the other two comparisons (C-2 and C-3), similar functional profile was revealed were processes contributing to

immune response and antigen processing and presentation were up-regulated and lipid metabolism was down-regulated.

CONCLUSION

We obtained the age-related gene expression profile associated with the stimulated leukocytes compared to the un-stimulated ones. We also identified genes that are modulated temporally when the blood leukocytes were stimulated with virulent *R. equi*. Our findings suggest that the stimulated cells seem capable of initiating a protective immune response through birth and up to 8 weeks of age, however there also were present genes/processes that may be counter-productive to the host. It is not clear from this study if such suppressive responses favoring the pathogen are indeed caused due to the immune-modulation by the pathogen or a host response due to immature immune system. Temporally it appeared that the across all the time points, the bacterial stimulation led to induction of pathogen recognition and mounting of immune response.

CHAPTER V

POTENTIAL MOLECULAR BIOMARKERS OF DISEASE SUSCEPTIBILITY FOR *RHODOCOCCUS EQUI* PNEUMONIA IN FOALS BY TRANSCRIPTOME PROFILING

SYNOPSIS

Rhodococcus equi (*R. equi*) is a gram-positive intracellular bacterium. It is an equine pathogen, which infects young foals causing pyogranulomatuous pneumonia. The host molecular mechanisms contributing to disease susceptibility are not fully understood. Current research to understand the host immunity has only targeted selected cytokines, candidate genes, and certain cell types. Global genomic high throughput tools such as expression microarrays may provide host genetic signatures and identify molecular pathways that contribute to disease susceptibility. Identifying the genes involved in disease susceptibility/resistance will help in disease control. The purpose of this study is to obtain molecular biomarkers discriminating infection-susceptible foals from healthy ones by examining expression profiles in blood leukocytes and nasal epithelial cells in *R. equi* affected and healthy foals. Peripheral blood leukocytes and nasal epithelial cells were obtained from six affected and six unaffected foals at birth, and at two and four weeks of age. RNA was extracted and the generated fluorescent-tagged cDNA was used for microarray hybridization, using an equine whole genome oligoarray. Profiles from infected blood leukocytes and nasal epithelial cells collected at birth indicate up-

regulation of genes involved in reduced immunity and increased susceptibility to infection. Samples collected at four weeks of age showed microarray profiles, which indicate up-regulation of cellular defense and immune-related genes. Results suggest that the most susceptible time point is at birth. Differences in expression profiles between infected and uninfected foals at birth suggest that disease susceptibility could be due to early exposure to *R. equi*, which could result in the different gene expression patterns observed between the two groups. These results may lead to the identification of specific cellular processes that contribute to foal susceptibility and disease progression. Identification of specific biomarkers will help to determine early foal susceptibility, and could provide for better drug design to treat infections.

INTRODUCTION

Rhodococcus equi (*R. equi)* is recognized globally as a primary cause of pneumonia in young foals (up to six months after birth). Adult horses do not develop the disease unless they are immune-deficient (Heller et al., 2010). *R. equi* can also cause pneumonia in pigs, cattle, cats, goats, dogs, and humans (Muscatello et al., 2007). However, in humans, only HIV infected or immune comprised individuals are infected (Linder, 1997; Kedlaya et al., 2001).

Mortality rates due to foal pneumonia are estimated to be 2-13% (Mousel et al., 2003) making this disease a serious economic problem for the equine industry. It is difficult to make an early diagnosis of foal pneumonia since clinical signs do not appear till the

disease has progressed in severity (Horowitz et al., 2001). Thus a lack of early and definitive diagnosis makes prevention and control of the disease difficult. There is a need to screen foals at a very early age to identify early infections and to determine which animals are more likely to have the disease. Early and accurate screening methods for foals, before the onset of clinical symptoms, are not available. Currently available screening methods are expensive, have low sensitivity, and are unreliable (Cohen et al., 2002). Gene microarrays from infected foals could identify target biomarkers for this disease. Compared to existing screening methods, identifying biomarkers at the molecular level will provide an early and more reliable screening of the disease status of the foals.

Although all foals on endemic farms are exposed to *R. equi*, some foals develop pneumonia while others do not (Chaffin et al., 2004). Clearly, the cause of resistance to *R. equi*-related pneumonia is a key to detection and treatment. The pathogen multiplies in alveolar macrophages, inside membrane-enclosed vacuoles. Survival of the bacteria may be due to impaired phagosomal maturation or lack of fusion with the lysosome (Fernandez-Mora et al., 2005; Rahman et al., 2005; Flaminio et al., 2009). In addition to the pathogen's subversion of the immune system host factors also contribute to susceptibility for *R. equi* related pneumonia. The mechanism by which this occurs remains unknown. Biomarkers identified by use of microarrays could help determine the mechanism by which the *R. equi* provides susceptibility to pneumonia.

Components of both innate and adaptive immunity are critical in prevention and clearance of the infection (Muscatello et al., 2007). In foals less than three months of age, reduced dendritic cell (DC) function and low killing capacity of neutrophils is observed (Demmers et al., 2001; Chen et al., 2006). Mounting a Th1 driven immune response against the *R. equi* infection is beneficial since it favors recruitment of IFN-γ, producing CD4+ and cytotoxic CD8+ cells (Dawson et al., 2010). It is the activation of macrophages by IFN-γ that assists in pathogen killing through stimulating the fusion of phagolysosomes, and increasing the synthesis of reactive oxygen species (von Bargen and Haas, 2009). Young foals have a reduced capacity to produce IFN-γ (Giguere et al., 1999). Thus, they may be more susceptible to pneumonia.

Information about the foal immune response against *R. equi* infection comes from studies of differences between foal and adult horse responses to the pathogen. Studying the differences in the transcriptome, using microarray analyses of infected and uninfected foals prior to onset of the clinical symptoms, will reveal the molecular mechanisms underlying susceptibility of some foals, while others remain unaffected.

We hypothesized that there are differences between foals susceptible to *R. equi* infection and the ones that remain healthy even after the pathogen exposure and that such differences can be captured at the transcriptome level. Additionally, the expression profile will provide us with biomarkers that could potentially be used to screen foals for early detection of infection/disease prior to the onset of clinical symptoms

MATERIALS AND METHODS

Study design

Peripheral blood leukocytes and nasal epithelial cells were collected from 100 foals at three time points: at birth, two weeks, and four weeks of age. Samples were taken from foals on a farm with a previously established high incidence of *R. equi* related pneumonia. We anticipated that about 20% of the foals would develop the disease. Soon after birth, every foal was closely monitored for cough, runny nose, lethargia, and diarrhea. Once any of these early symptoms were observed in a foal, they were evaluated for elevated body temperature, complete blood cell count (CBC), and fibrinogen levels. Ultrasound examination of foals was performed to evaluate lung abscesses. Based on the diagnosis, diseased foals were started on an antibiotic treatment regimen. During the treatment, CBC's and lung ultrasounds were performed every two weeks, while temperature was monitored 2-3 times per day.

Once the clinical diagnosis of pneumonia was made, the samples retrieved from all the foals (nasal epithelial cells and blood leukocytes) were assigned to either the *R. equi* pneumonia affected group or unaffected group. All foals on the farm could have been exposed to *R. equi*, however only foals that displayed the clinical symptoms were considered affected and the rest grouped as unaffected. No serological test was performed on the foals to definitively know the infection status of unaffected foals, since they did not display signs of pneumonia they were considered to be unaffected.

Of the samples collected from 100 foals, 45 foals were diagnosed with *R. equi* infection, and the remaining 55 healthy foals were uninfected. Out of the two groups of foals (infected and healthy), 10 foals were used in each group. Samples were typed (blood leukocyte and nasal epithelial) and saved for future experiments. In this study, we encountered various limitations that restricted the sample size to six. In addition, we could not extract enough RNA from nasal epithelial samples for further analyses. In specific cases, samples were of low quantity or quality of RNA, rendering that sample unusable.

Sample types and sampling time points

For the present study two sample types: peripheral blood leukocytes and nasal epithelium were considered. Since leukocytes defend the body against foreign/infectious agents and are mediators of innate and adaptive immunity, knowledge about the age-related response of leukocytes will provide a snapshot of the foal's immunity. We chose peripheral blood leukocytes under the premise that the systemic immunity will efficiently correlate with the host pulmonary immunity. Also leukocytes are easily accessible. Nasal epithelial cells were chosen to represent a component of the pulmonary system and also because nasal epithelium is the first to encounter the pathogen. Moreover, if the signatures from nasal epithelium can efficiently reflect the disease status before the clinical onset, than this could be developed as a non-invasive way to screen the foals.

R. equi pneumonia is rare in adult horses therefore the disease appears to be age-dependent. Young foals have immature immune system compared to adult horses, and are most susceptible to infection up to 3-months of age. The time points were therefore chosen starting from birth (T-0) and weeks 2 (T-2) and 4 (T-4). The foals in were diagnosed as clinically sick in the 5-6th week, after which we grouped the samples into affected and unaffected group. The three time-points in the affected group therefore reflect stages of susceptibility before foals show any clinical symptoms. Therefore if from any of the above time points (before clinical onset of disease), we can obtain discriminative biomarkers they will help in early screening of the foals that will most likely become sick in the near future.

Sample collection

Ten mL peripheral blood was collected via jugular venipuncture from each foal and stored in an EDTA-containing Vacutainer (Becton Dickinson Co., Franklin Lakes, NJ, USA). The leukocytes were isolated and stabilized using LeukoLOCK Total RNA Isolation System (Ambion, Grand Island, NY, USA). Nasal epithelial cells were retrieved from inferior turbinate using an interdental brush. Samples were collected from foals at birth, two weeks, and four weeks of age (Ramalho et al., 2004). The epithelial cells were collected by gently rubbing the brush head inside the nostrils of the foals. The brush head was then placed in a 1.5 mL tube containing RNAlater (Qiagen, Valencia, CA, USA). The interdental brush assembly had an ultrafine cylindrical brush head to

minimize any discomfort (Proxabrush, model #422, with a Proxabrush snap-on handle, model #625, Sunstar/GUM, Chicago, IL, USA).

RNA extraction

Total RNA was extracted from whole blood using the LeukoLOCK Total RNA Isolation System (Ambion, Grand Island, NY, USA) and from nasal epithelial cells using the RNeasy mini kit (Qiagen, Valencia, CA, USA) per the manufacturer's instructions. A DNase I treatment was also performed as part of the RNA extraction protocol to remove any contaminating genomic DNA as per the instructions in RNeasy mini kit. Extracted RNA was quantified with a spectrophotometer (NanoDrop, Thermo Scientific, Wilmington, DE, USA) and the RNA quality was evaluated with the Agilent 2100 Bioanalyzer (Agilent Technologies, Santa Clara, CA, USA). RNA extraction for nasal epithelial cells was performed by a modified protocol as described by Beck et al. (1999) and Ramalho et al. (2002) (Section D-3).

RNA amplification

Due to low quantity of some RNA samples, all RNA samples were amplified to ensure uniformity of procedure, both for nasal epithelial cells and blood leukocytes. Five hundred nanograms of RNA was used for each amplification reaction, using the Sensation Kit (Genisphere, Hatfield, PA, USA) as per the manufacturer's protocol.

Experimental design

The cDNA obtained at birth, two, or four weeks of age from nasal epithelium and blood leukocytes were co-hybridized between the six affected foals and six unaffected foals. We used a balanced block design (BBD) for microarray hybridizations because for class comparison studies, BBD is considered optimal (Dobbin and Simon, 2002). The dye swap was embedded within the biological replicates to overcome any bias associated with the fluorescent dyes. The same animals were used for extracting leukocytes and nasal epithelial cells at all three time points.

Labeling and microarray hybridization

For each sample, cDNA was generated from total RNA using Superscript II Reverse Transcription kit (Invitrogen, Carlsbad, CA, USA) and labeled with Cy3 or Cy5 dye via an indirect labeling method utilizing dendrimer technology (Stears et al., 2000). Labeling was carried out with the 3DNA Array 900 MPX Expression Array Detection kit (Genisphere, Hatfield, PA, USA). Hybridizations were performed in a SureHyb hybridization chamber (Agilent Technologies, Santa Clara, CA, USA) at 55°C. Following post-hybridization washes, arrays were scanned with a GenePix 4000B scanner at 5 micron resolution (Molecular Devices, Sunnyvale, CA, USA). GenePix Pro 6.1 software (Molecular Devices) was utilized for raw data acquisition, spot-finding, and quantification of array images.

Equine 21K oligonucleotide microarray

We used an whole genome equine oligonucleotide array with 21,351 elements designed at Texas A&M University (Bright et al., 2009). This 70-mer equine oligoarray is one of the most exhaustive gene arrays currently present for expression analyses. Probes were synthesized (Invitrogen, Carlsbad, CA) and printed onto amino-silane coated slides (Corning Incorporated, Corning, NY).

Expression analyses

Differential expression analyses of microarray data were conducted using the freely available Bioconductor Limma package running in the R statistical software environment (Smyth, 2004). Background corrections of raw intensities were performed using the "normexp" correction method (Ritchie et al., 2007). Subsequently, the background corrected intensities were normalized using printip-loess normalization (within array normalization), but no across array normalization was performed (Smyth and Speed, 2003a). Linear modeling using moderated *t*-tests was performed to identify differentially expressed genes (Smyth, 2004). To account for the multiple comparisons, the false discovery rate correction method of Benjamini and Hochberg was used (Benjamini and Hochberg, 1995). Linear models were used to assess the differentially expressed (DE) genes from blood leukocytes at birth (B-T0), two weeks (B-T2), and four weeks of age (B-T4). Similarly, linear models were fit to obtain DE genes from nasal epithelium of animals at birth (N-T0), two weeks (N-T2), and four weeks of age

(N-T4). Genes were considered significantly differentially expressed if they had a *p* value of $p < 0.05$ and fold change > 1.5.

Functional analyses

Functional gene ontological analyses were performed using a web-based tool WebGestalt: **WEB**-based **GE**ne **S**e**T** **A**na**L**ysis **T**oolkit (Zhang et al., 2005). Gene ontological analyses were performed using the list of differentially expressed genes to obtain statistically significant biological processes. In order to calculate the statistical significance, DE genes for each comparison were compared to all the genes present on our equine microarray. The method of Benjamini and Hochberg [24] was used for multiple test adjustments with significance level of $p < 0.1$.

Quantitative real-time PCR

Quantitative real-time PCR was performed on a subset of genes that were significantly differentially expressed (fold change > 1.5, and $p<0.05$). Each gene was tested in duplicate, with a housekeeping gene control. This technique was used to validate results obtained from the statistical analysis of the microarray data. The total RNA was directly reverse transcribed to cDNA using the SuperScript® VILO™ cDNA Synthesis Kit (Invitrogen) and subsequently amplified using gene-specific primers and master mix by qPCR, in a single-step reaction.

When possible, primers were designed to span intron-exon boundaries, to represent a region of the mRNA corresponding to the location of the cDNA sequence located on the

arrays. Serial dilutions of RNA from the reference samples were used to generate relative standard curves and to test the amplification efficiency of each primer set. For each qPCR assay, ~100 ng of total RNA was used in a 25 µl reaction with 1x Universal SYBR® Green Master Mix (Applied Biosystems, Carlsbad CA, USA) and 300 nM primers, and amplified on a LightCycler 480 (Roche Diagnostics, Indianapolis, IN, USA).

RESULTS

Differentially expressed genes

We obtained 268 DE genes (119 up-regulated and 149 down-regulated) for blood leukocytes samples at birth (B-T0) from infected foals compared to the controls (**table D-1**). There were 180 DE genes (93 up-regulated and 87 down-regulated) for blood leukocyte samples when infected foals were compared to control foals at two weeks (B-T2) and 319 DE genes (191 up-regulated and 128 down-regulated) for blood leukocyte samples from infected foals compared to controls at four weeks (B-T4).

Similarly, for nasal epithelial samples at birth (N-T0), we obtained 501 DE genes (360 up-regulated and 141 down-regulated) when infected foals were compared to control foals. There were 348 DE genes (228 up-regulated and 348 down-regulated) for nasal epithelial samples at two weeks (N-T2) when infected foals were compared to control foals while 267 genes were differentially expressed (108 up-regulated and 159 down-

regulated) for nasal epithelial samples at four weeks (N-T4), when infected foals were compared to control foals.

Functional analysis

Blood leukocytes

Functional analyses were performed to obtain statistically significant biological processes associated with the DE genes (for both up- and down-regulated genes) at the three time points for each biological sample type (leukocytes and nasal epithelium). The top 15 statistically significant biological processes associated with the down- and up-regulated DE genes for B-T0 comparison are presented in **figure 5-1a and figure 5-1b**, respectively. Various immunologically relevant processes that could be modulating the development of disease pathology were found to be associated with the down-regulated genes (e.g. endosome to lysosome transport, lysosome transport, negative regulation of immune functions) compared to those associated with the up-regulated genes (e.g., regulation of IL-6 biosynthetic processes). The list of all significant biological processes is presented in **table D-6a and table D-6b**.

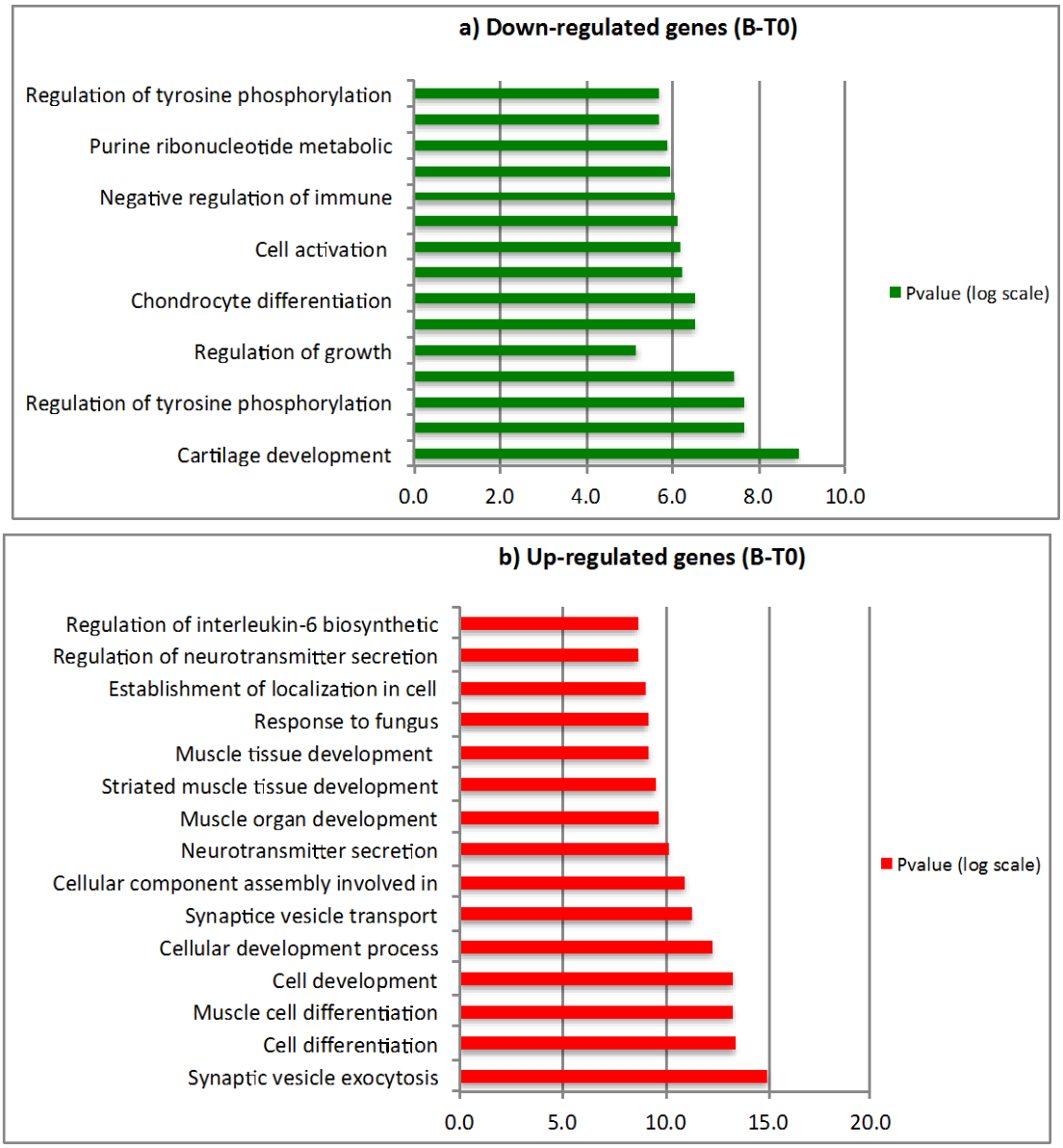

Figure 5-1: Biological processes associated with differentially expressed genes in blood leukocytes at birth. Graphical representation of top fifteen statistically significant processes associated with the DE genes in blood leukocytes at birth a) represents biological processes at birth (T0) associated with down-regulated (colored green bars) and b) up-regulated genes (colored red bars). The Y-axis represents the biological processes and the X-axis represents the *value* displayed as $-\log_2$ (*p* value).

The B-T2 comparison (**figure D-7a and D-7b**) found a majority of down-regulated genes associated with cellular growth and division-related processes (e.g., RNA splicing, mRNA processing, DNA packaging, nuclear division), while the up-regulated genes were predominantly associated with lipid synthesis and metabolism (e.g., steroid metabolic process, lipid biosynthesis, lipid metabolism).

The biological processes identified as down-regulated genes in B-T4 comparisons (**figure D-8a and D-8b**) were involved in neurogenesis (e.g., oligodendrocyte development, oligodendrocyte differentiation, neural fate commitment). The up-regulated genes for this comparison were associated with processes involved in respiratory system development (e.g., lung development, respiratory tube development) and immunologically relevant iron homeostasis.

Nasal epithelial cells

Similarly for nasal epithelial cells, functional analyses of the DE genes revealed various biological processes associated with the expression profiles at the three time points. For N-T0 comparisons (**figure 5-2**), the top 15 processes associated with the down-regulated genes were involved in synthesis and metabolism of biomolecules (e.g. alcohol biosynthetic processes, amino sugar metabolic processes, and oxoacid metabolic processes) and pathogen recognition and responses (e.g. response to polysaccharide, response to molecule of bacterial origin, response to cytokine stimulus). The biological

processes associated with up-regulated genes were predominantly associated with muscle cell growth and development.

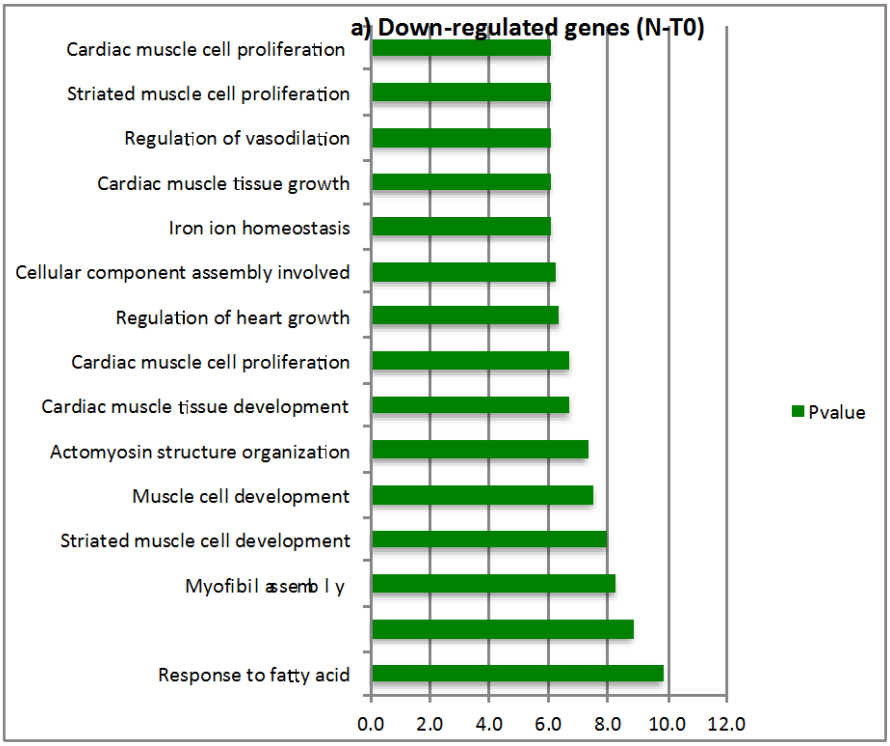

Figure 5-2: Biological processes associated with differentially expressed genes in nasal epithelium at birth. Graphical representation of top fifteen statistically significant processes associated with the DE genes in nasal epithelium at birth a) represents biological processes at birth (T0) associated with down-regulated (colored green bars) and b) up-regulated genes (colored red bars). The Y-axis represents the biological processes and the X-axis represents the *p* value displayed as $-\log_2$ (*p* value).

Figure 5-2 Continued

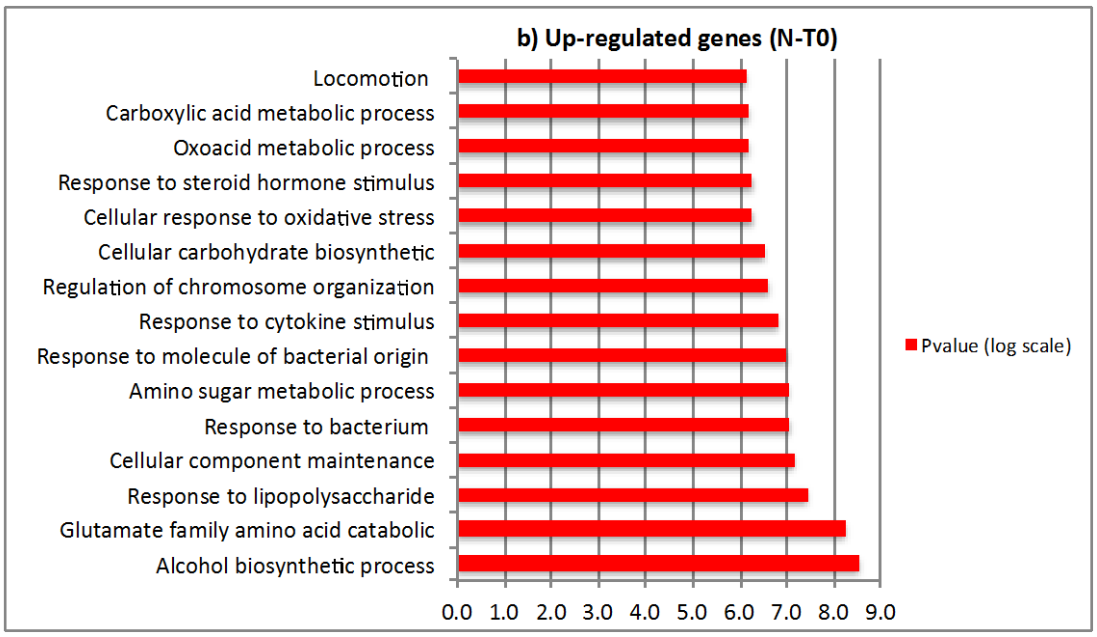

For the N-T2 comparison, the top 15 processes associated with the down-regulated genes were involved in early developmental processes (e.g., anterior/posterior pattern formation) and regulation of ligase activity. The top 15 processes associated with the up-regulated genes were involved in neuronal differentiation (e.g., neuron fate commitment, neuron fate specification) and biosynthetic processes (e.g., macromolecule biosynthetic processes, regulation of nucleobase, nucleoside, nucleotide, and nucleic acid metabolic processes). Finally, for the N-T4 comparison, the top 15 biological processes were involved in heme biosynthesis and metabolism (e.g. tetrapyrrole biosynthetic processes, porphyrin biosynthetic processes, heme metabolic processes). The biological processes

associated with the up-regulated genes were involved in carbohydrate biosynthesis and metabolism (e.g. glycogen metabolic processes and glucan metabolic processes).

Real-time PCR validation

Real-time PCR was used to validate findings of selected genes that were significantly differentially expressed from the two sample types at three time points (**figure 5-3**). We chose 15 genes for the validation purposes and confirmed their differential expression in relation to the microarray data. Two genes were selected from B-T0 (IQCF1, STX11), four genes from B-T2 (DNAH2, HRH1, KIAA0460, WDR90) and two genes from B-T4 (BBS5, CEP55). Similarly, three genes were selected for N-T0 (CNTROB, SLMAP, VAMP7), two genes from N-T2 (GNDPA1, SLC6A12) and two genes from N-T4 (HCCS, SYVN1). We could validate the direction of regulation (up/down) for all fifteen genes using real-time PCR

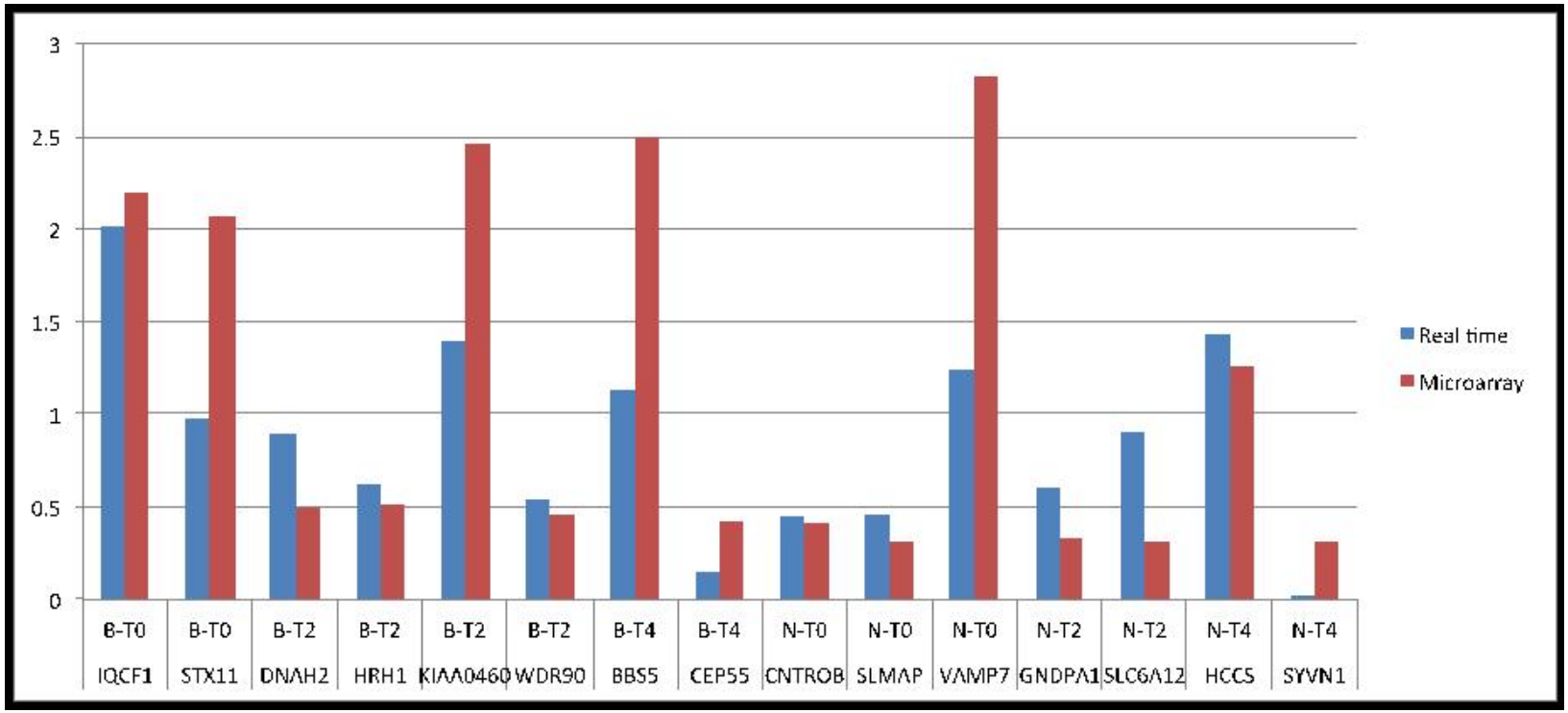

Figure 5-3: Real-time PCR validation. Differentially expression (pvalue<0.05 and fold change cutoff of 1.5) of fifteen genes was validated using real-time PCR

Linear discriminant analyses (LDA)

In order to obtain discriminatory molecular biomarkers, we utilized the LDA classification technique to identify the best single gene and two to three combinations of genes, generating classifiers which discriminate between the transcription profiles of *R. equi* affected *vs.* unaffected foals. The classifiers were ranked based on their misclassification errors ($\boldsymbol{\varepsilon_{bolstered}}$), i.e. the higher a classifier was ranked the lower its misclassification error. We identified the top ten single, two, and three gene classifiers with the lowest $\boldsymbol{\varepsilon_{bolstered}}$ to distinguish *R. equi* infected from control foals, using blood leukocytes and nasal epithelial cell samples at each time point. The classification results demonstrate that there are several cases where single genes can separate the *R. equi* infected foals from control foals with a low error estimate. Furthermore, when considering these features as part of two or three gene classifiers, we observed a significant decrease in the classification error as evident from the percent decrease in error ($\boldsymbol{\Delta\varepsilon_{bolstered}}$).

It has been suggested that multivariate feature sets (i.e. those containing two or more genes) are better discriminators when the phenotype is complex (Chapkin, 2010). For example, a two-feature classifier would be considered a better discriminator than a one-feature classifier, if the pair of genes performs better than either of the genes individually, as evident from the improvement in classification (Chapkin 2010, Chen Zhao 2009). The specific results for discriminating the expression profiles of *R. equi* infected from control foals at T0, T2, and T4 are detailed below.

Classification of expression profiles of R. equi infected foals from control foals using blood leukocytes

At birth (T0), the top single-gene classifier discriminating *R. equi* infected foals from the controls was found to be CARD9 (top in the list of single-gene classifiers), with an estimated classification error of 0.0719 (**table 5-1).** Among the 2-gene classifiers, the combination of CDKN2AIP and CARD9 ranked high in the ability to distinguish between the two groups of animals ($\boldsymbol{\varepsilon_{bolstered=}}$ 0.0278), and together they were better discriminators (lower error estimate) when compared to either of them individually. Around 9% ($\boldsymbol{\Delta\varepsilon_{bolstered}}$ =0.0926) improvement in classification can be observed when CDKNZAIP is combined with CARD9 as a two-feature classifier. From the table it is evident that of the top five three-feature classifiers listed, GLRA2, CARD9, and PHOX2A constituted the best three-gene classifier set with an error estimate of 0.0142. There was an improvement of around 2.8% ($\boldsymbol{\Delta\varepsilon_{bolstered}}$ =0.028) in classification when CARD9 was used in combination with GLRA2 and SRR over the 2-gene classifier based on GLRA2 and PHOX2A. Among the top one, two, and three gene classifiers, triplet classifiers not only had the lowest error but also showed sizable decrease in the classification error when compared to the single- and two-gene classifiers. Thus, the top triplet classifiers are better discriminators between the *R. equi* infected and control group at birth.

Table 5-1: Linear discriminant analysis of infected versus control foals at birth (blood leukocytes). The top five one-, two-, and three-gene LDA classifiers are shown in the table below. $\varepsilon_{bolstered}$ represents the bolstered resubstitution error for the respective gene classifier and $\Delta\varepsilon_{bolstered}$ represents the decrease in error for each feature set relative to its highest ranked subset of genes.

1 feature	2 feature	3 feature	$\varepsilon_{bolstered}$	$\Delta\varepsilon_{bolstered}$
CARD9			0.0719	
CDKN2AIP			0.1204	
PLT3-M24-M13.rgy.ab1			0.1543	
SRR			0.1644	
GLRA2			0.1656	
CDKN2AIP	CARD9		0.0278	0.0926
CDKN2AIP	ARF3		0.0401	0.0803
GLRA2	SRR		0.0422	0.1234
CT02031B1C07.f1.ab1	SDPR		0.0449	0.1195
SRR	CARD9		0.0453	0.0266
GLRA2	CARD9	PHOX2A	0.0142	0.028
CDKN2AIP	ARF3	CARD9	0.0151	0.0127
ARF3	CARD9	XM_001490209.1	0.0171	0.0377
CDKN2AIP	CARD9	gnl|UG|Eca#S38808416-m70	0.0182	0.0096
CDKN2AIP	AMZ1	ARF3	0.0196	0.0205

Similar results were obtained at T2, where PLEK2, DDX47, and HSPD1 were the best triplet classifiers, with an error estimate of 0.026 **(table D-2).** The modest improvement in error by using these triplet sets was 0.53% relative to the highest ranked subset of features (PLEK2 and HSPD1, with error estimate of 0.0313). At T4, best triplet

classifiers with lowest error were ZNF420, KRT4, and PROCR, with an error estimate of 0.0046 **(table D-3).** The improvement in error by using these triplet sets was around 3% relative to the highest ranked subset of features (ZNF420 and KRT4, with error estimate of 0.0361). A clear separation of *R. equi* infected *vs* control animals was observed at the three time points by the three dimensional LDA hyperplane, based on the top triplet classifier (**figure 5-4)**.

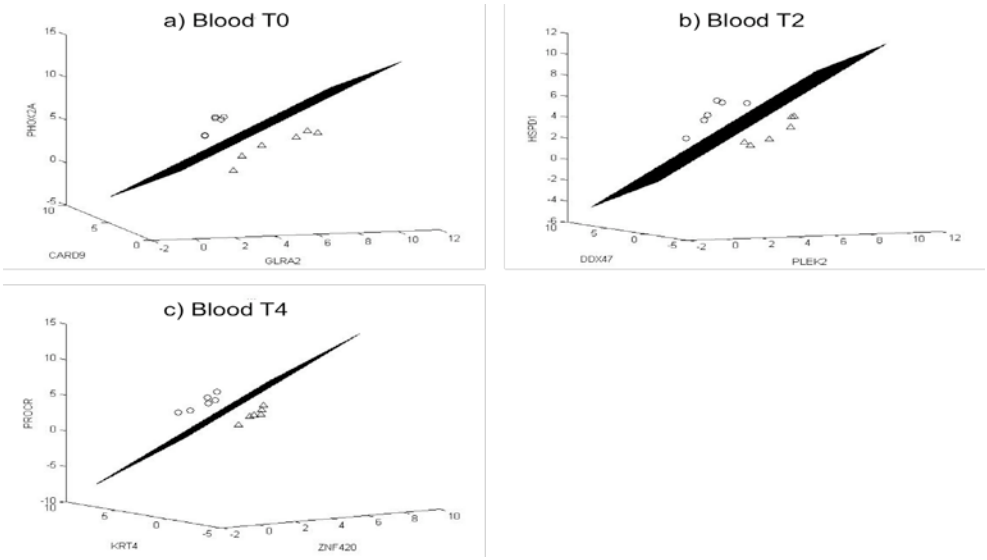

Figure 5-4: Linear discriminant analysis using three-gene classification model for infected versus control foals at birth (blood leukocytes). The best performing three-gene feature sets that classify infected foals from control foals at are; a) birth (T0) b) week2 (T2), and c) week4 (T4). The three dimensional LDA hyperplane discriminates between *R. equi* infected (circles) and control (triangles) foals. Axes represent normalized intensity values of the corresponding genes.

Classification of expression profile of R. equi infected foals from control foals using nasal epithelial cells

At birth (T0), the top single-gene classifier discriminating *R. equi* infected foals from the controls was found to be GNG12 (top in the list of single-gene classifiers), with an estimated classification error of 0.0185 (**table 5-2).** Among the 2-gene classifiers, a combination of GNG12 and RGS19 ranked high in the ability to distinguish between the two groups of animals ($\boldsymbol{\varepsilon_{bolstered=}}$ 0.0234), and together they were better discriminators (lower error estimate) when compared to either of them individually. While GNG12, COL9A2, and RGS19 formed the top three gene classifier set, with an error estimate of 0.0177, it was also important to note that these genes were also among the top ten single and two-gene classifiers. There was a very modest improvement ($\boldsymbol{\Delta\varepsilon_{bolstered}}$ =0.0057) in classification when COL9A2 was used in combination with GNG12 and RGS19 over the 2-gene classifier based on GNG12 and RGS19. Among the top one, two, and three gene classifiers, triplet classifiers not only have the lowest error but also show sizable decreases in the classification error when compared to the single- and two-gene classifiers. Thus, the top triplet classifiers are better discriminators between the infected and control group at birth.

Table 5-2: Linear discriminant analysis of infected versus control foals at birth (nasal epithelial cells). The top five one-, two-, and three-gene LDA classifiers are shown in the table below. $\varepsilon_{bolstered}$ represents the bolstered resubstitution error for the respective gene classifier and $\Delta\varepsilon_{bolstered}$ represents the decrease in error for each feature set relative to its highest ranked subset of genes.

1 feature	2 feature	3 feature	$\varepsilon_{bolstered}$	$\Delta\varepsilon_{bolstered}$
GNG12			0.0185	
BOC			0.118	
GENE 16246			0.1226	
CLDN3			0.1309	
LOC124220			0.1347	
GNG12	RGS19		0.0234	-0.0049
GNG12	COL9A2		0.0339	-0.0154
C1orf216	MRPS18A		0.0343	0.1543
GNG12	MRPS18A		0.0369	-0.0184
GNG12	FICD		0.0414	-0.0229
GNG12	COL9A2	RGS19	0.0177	0.0057
LOC100052930	ZNF709	PSCD4	0.0224	0.0549
TFDP1	HDAC8	GJA5	0.0232	0.0688
OR4F16	TFDP1	FANCI	0.0235	0.0265
GENE:16246	GNG12	COL9A2	0.0239	0.01

Similar results were obtained at T2, when CX604514, AHSA1, and GORASP2 were the best triplet classifiers with an error estimate of 0.013 (**table D-4**). The improvement in error by using these triplet sets was 1.87% ($\Delta\varepsilon_{bolstered}$ =0.0187) relative to its highest ranked subset of features (CX604514 and AHSA1, with error estimate of 0.0317). At T4,

the best triplet classifiers with lowest error were OR2L2, COL28A1, and DN508139, with an error estimate of 0.0397 (**table D-5**). The improvement in error by using these triplet sets was around 4% ($\Delta\varepsilon_{bolstered}$ =0.0397) relative to the highest ranked subset of features (OR2L2 and DN50139, with error estimate of 0.0794). A clear separation of *R. equi* infected and control animals at the three time points as shown by the three dimensional LDA hyperplane based on the top triplet classifier is shown in **figure 5-5**.

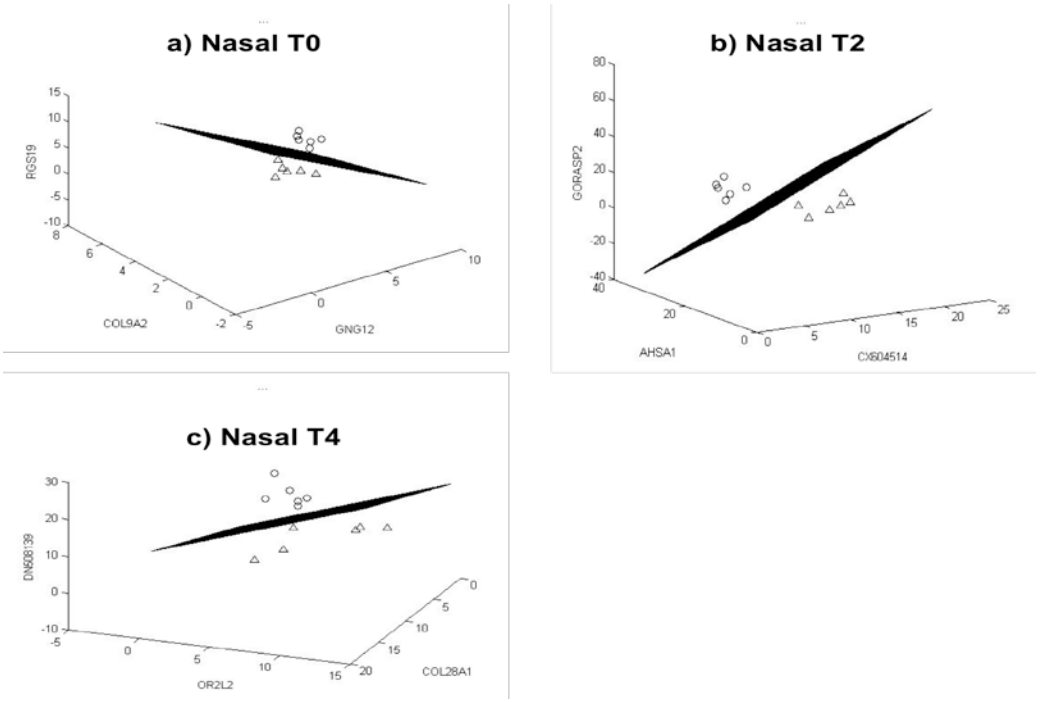

Figure 5-5: Linear discriminant analysis using three-gene classification model for infected versus control foals at birth (nasal epithelial cells). The best performing three-gene feature sets that classify infected foals from control foals are; at a) birth (T0) b) week2 (T2) and c) week4 (T4). The three dimensional LDA hyperplane discriminates between *R. equi* infected (circles) and control (triangles) foals. Axes represent normalized intensity values of the corresponding genes.

DISCUSSION

We hypothesized that the transcriptome profiling of peripheral blood leukocytes and nasal epithelial cells will yield key genes and biological processes that will contribute to the foal susceptibility to infection. Using the expression profile we will be able to identify biomarkers for early screening of foals that are likely to develop pneumonia. Obtaining hundreds of DE genes at each time point shows that there are differences between the two groups of foal at the transcriptional level. Using these DE genes we obtained sets of genes (triplets) that can classify the two groups with low error rate.

Although all neonatal foals have immature immune systems, our results suggest that there are additional molecular pathways that predispose some foals to contract *R. equi* pneumonia. Our findings suggest that the differences in the transcriptome profile between the susceptible foals (foals that later develop pneumonia) and the healthy foals early in life (soon after birth) contribute to the reduced immunity and increased susceptibility to infection. In blood leukocytes at birth, our findings suggest that at birth gene expression is supportive of a Th2 immune response. Similar to these observations, in the nasal epithelial cells at birth, we observed reduced expression of genes involved in mucosal immunity and intracellular pathogen killing. At the later time points (in both sample types) protective immune responses against the pathogen were observed. The molecular biomarkers identified in this study may allow early detection of at-risk foals. We discuss each group below.

Expression of genes from blood leukocytes of affected vs. unaffected foals

At birth, expression profiles from blood leukocytes of susceptible foals suggest that modulation of genes involved in phagocytosis, IFN-γ signaling, immune activation via dendritic cells, and IL-6 biosynthesis could promote susceptibility to intracellular pathogens by influencing their ability to eliminate the pathogen. In order to support our hypothesis that deficiencies at the molecular level (in addition to the immature neonatal immune system) predispose certain foals to develop *R. equi* infection and pneumonia, we identified the biological processes, which would be associated with the differentially expressed genes at birth.

Vesicle-associated membrane protein 7 (VAMP7) and sorting nexin 1 (SNX1) genes (associated with endosome to lysosome transport processes) play a role in phagosomal fusion, and are down-regulated in susceptible foals at birth. It is known that VAMP7 assists in completing membrane coalescence to facilitate phagosomal fusion by bringing organelles, such as endosomes and lysosomes, into close proximity (Flannagan et al., 2009). VAMP7 plays a crucial role in the onset of phagocytosis in macrophages while syntaxin 1(SNX1) is involved in fusion with endocytic compartments during maturation of phagosomes (Braun et al., 2004). Normally, immune responses prevent entry of a foreign body through phagocytosis by macrophages, dendritic cells, and neutrophils (Braun et al., 2004). However, lack of phagosomal-lysosome fusion or an altered phagocyte maturation process would allow *R. equi* to survive and replicate in macrophages (Fernandez-Mora et al., 2005). Reduced expression of genes associated

with phagocytosis in susceptible foals, as observed in our study, may predispose them to infection with *R. equi*.

Interleukin 27 receptor, alpha (IL27RA/ WSX1) associated with negative regulation of immune response processes are known to be important for normal IFN-γ production by CD4+ cells, and is therefore essential for mounting a T_h1 response (Takeda et al., 2003). In addition, it has been reported that mice deficient in WSX1 display increased susceptibility to infection with the intracellular pathogen, *Listeria* due to reduced IFN-γ production (Chen et al., 2000). JAK-STAT signaling was also down-regulated at birth in affected foals. The JAK2 gene associated with JAK-STAT signaling is important for development and functionality of dendritic cells (DCs) and IFN-γ signaling (Campbell et al., 1994). In mice, loss of JAK2 is reported to impair the capacity of DCs to initiate innate immune responses due to reduced expression of TNF-α and IL-12 (Zhong et al., 2010). IFN-γ and TNF-α are involved in clearance of *Rhodococcus equi* by activating macrophages to kill the intracellular pathogen (Darrah et al., 2004). Neonatal foals have reduced capacity to produce IFN-γ and mount Th1 responses, and down-regulation of IL27RA and JAK2 could contribute towards reduced ability of susceptible foals to mount sufficient protective responses when compared to healthy foals.

Among the processes associated with up-regulated genes, regulation of IL-6 biosynthesis appeared most relevant. IL-6 produced by antigen presenting cells is known to modulate differentiation of CD4+ T-cells into effector Th1 or Th2 cells, and has been found to

shift the T-cell helper type one and two balance towards a type two response by inhibiting IFN-γ production (Diehl and Rincon, 2002). Elevated expression of IL-6 has been reported in *R. equi* infected foals (Giguere et al., 1999; Ferraz et al., 2008; Nerren et al., 2009), and increased expression in neutrophils stimulated by *R. equi* is greater in newborn foals than two, four, and eight week old foals (Nerren et al., 2009). Hence, it appears that elevated IL-6 could be responsible for promoting a Th2-driven immune response, especially at birth in the infected group of foals, making foals highly susceptible to exposure early in life. Although, we did not observe an upregulation of IL-6 in susceptible foals, we found overexpression of genes that modulate IL-6 production (CARD9 and CEBPB).

The CCAAT/enhancer binding protein (C/EBP), beta (CEBPB/ NF-IL6) gene modulates IL6 biosynthesis and is a key element in IL-6 signaling as well as in transcriptional regulation of IL-6 (Lu et al., 2009). In addition to regulating IL-6, CEBPB is responsible for regulation of genes encoding many acute phase proteins and cytokines critical for bacterial killing by macrophages (Tanaka et al., 1995). The caspase recruitment domain family, member 9 (CARD9) gene (also associated with IL-6 biosynthetic processes) is required for cytokine production in response to intracellular bacterial and viral infections. Deficiency or aberrant activation of CARD9 is associated with susceptibility to infection or immune diseases, respectively (Ruland, 2008). Both CEBPB and CARD9 could be favoring Th2 immune responses via influencing IL-6 production and increasing susceptibility to infection.

Two weeks after birth we observed, in blood leukocytes, upregulation of genes involved in antimicrobial actions involved in fighting *R. equi* infection. At week four, up-regulated genes were associated with biological processes that could help fight against infection, including genes involved in development of lymphocytes, defense, and iron homeostasis. The details for these time-points are presented in Appendix D (**section D-1 and D-2**).

Linear discriminant analysis

The objective of this study was to identify biomarkers for early screening of foals. Since we identified biomarkers that could discriminate the two groups of foal at birth with minimum misclassification error rate, the remaineder of the discussion will focus only on those.

Using discriminant analyses, triplet classifiers like genes, glycine receptor, alpha 2 (GLRA2), paired-like homeobox 2a (PHOX2A), and caspase recruitment domain family, member 9 (CARD9) were found to discriminate the *R. equi* infected group of foals from the healthy foals at birth with a low misclassification error. Protein encoded by PHOX2A gene is involved in the development of autonomous nervous system. In neonatal mice expression of this genes is considered critical in development of normal respiratory rhythm (neuronal impulse muscle that control inspiration an expiration) (Viemari et al., 2004; Wrobel et al., 2007). GLRA2 are ligand-gated chloride channels and is proposed to have a role in neuronal development (Young-Pearse et al., 2006). The caspase recruitment domain family member-9 (CARD9) gene is proposed to have a role

in innate immune responses against certain intracellular bacterium. Alterations in CARD9 expressions are thought to influence susceptibility to infections (Ruland, 2008). Hence, it appears that the biological role of these genes in concert could influence the susceptibility of foals towards *R. equi* pneumonia and discriminate such foals from the unaffected ones.

We propose that these biomarkers can be developed as a qPCR based screening test to identify foals at a high risk of infection. Once this screening test is validated experimentally, it should be possible to screen foals soon after birth for earlier disease detection and lowering the disease incidence by starting the foals on appropriate treatment regimen.

Expression of nasal epithelial cell genes in affected vs. unaffected foals

Nasal epithelium is the first host tissue to encounter the *R. equi* bacterium and provides the first line of defense against this pathogen. Down-regulation of genes involved in mucosal immunity and intracellular pathogen killing may lead to the pathogen evading immune responses at the epithelium and entering the lower airways. In spite of these deficiencies, the mucosal barrier appears to be responding and limiting the *R. equi* growth by recognizing the bacterial lipids and creating a hostile environment by reducing iron bioavailability.

From our results one significant biological process was response to bacterium associated with genes, FOS, CCL20, SNCA, and NOS3. Mucosal surfaces are key portals of antigen/ pathogen/ foreign particle entry into the body and gene chemokine (C-C motif) ligand 20 (CCL20) is involved in mucosal immunity (Williams, 2006) and is up-regulated under inflammatory conditions (Schutyser et al., 2003). CCL20 stimulates migration of immature DC, B-cells, and a subset of memory T-cells to mucosal epithelium, providing antimicrobial properties (Starner et al., 2003). Reduced expression of CCL20 and eNOS3 is involved in mucosal immunity and may contribute towards immune incompetency of *R. equi* susceptible foals at birth.

Cell mediated immunity is essential against *R. equi* infection, and CD4+ and CD8+ T-lymphocytes are of critical importance in *R. equi* clearance. Hence down-regulation of IL-7 and IL-17F could contribute to lower T cell proliferation in susceptible foals. IL17F shares homology with IL-17 and is hence thought to stimulate T cell proliferation and regulate inflammatory responses (Chang and Dong, 2007). IL-7 has a role in maintenance and growth of T lymphocytes, regulation of naïve and memory T cells, stimulation of CD8+ T cell proliferation, and other antimicrobial properties (Vranjkovic et al., 2007). Low serum levels of IL-7 cause impaired T cell function (Holm et al., 2005; O'Connor et al., 2010). In mice, IL-7 enhanced the ability of murine macrophages to kill *Lishmania major* infected cells, and *in vivo* administration stimulated protective immunity against *Toxoplasma gondii* by increasing IFN-γ production and CD8+ CTL responsiveness (Pierrete Appaswamy 1998). Since both *Lishmania major* and

T*oxoplasma gondii* are intracellular pathogens like *R. equi*, reduced IL-7 could contribute to susceptibility towards *R. equi* infection as well.

Up-regulated genes at N-T0 are involved in responses to fatty acid metabolism, vesicle fusion, leukocyte degranulation, and iron homeostasis. Presence of fatty acids may be a response reaction to the *R. equi* cell envelope. *R. equi* belongs to *Mycolata*, and members of this bacterial group have a characteristic cell envelope composed of branched fatty acids (mycolic acid). It has been recently suggested that recognition of lipids in bacterial cell walls is an important part of host defense responses to *R. equi* (Harris et al., 2010).

Genes involved in iron homeostasis (HPX, HMOX1, HAMP) are also up-regulated in foals at birth. Availability and acquisition of iron is crucial for survival and growth of most bacterial pathogens. Prophylactic and therapeutic strategies designed to interfere with acquisition and use of iron have proven to be effective in the management of other bacterial diseases and may help in control of pneumonia attributable to *R. equi* in foals (Jordan et al., 2003). The HPX gene encodes a glycoprotein with high heme binding affinity, which protects the cell from oxidative stress. Heme oxygenase (HMOX1) catalyzes the degradation of heme. Up-regulation of genes involved in heme homeostasis could be a response to *R. equi* infection and may represent host defenses to limit iron mediated survival and replication of the pathogen.

At two weeks of age, the gene expression profiles of nasal epithelial cells suggest upregulation of genes involved in wound healing, negative regulation of T-cell proliferation, and regulation of IFN-γ production. Four weeks after birth, expression profiles of nasal epithelial cells suggested that genes are being modulated (up or down) to initiate protective immune responses to restrict bacterial growth for e.g. by limiting iron pathogen's iron supply.

Linear discriminant analysis

We found biomarkers from nasal epithelial cells at birth with the potential to screen foals for pneumonia before the onset on clinical symptoms. The advantage of using nasal epithelium (over blood) for screening purposes is that this method is less invasive and can be stored and shipped easily.

Linear discriminant analysis of nasal epithelium produced three-gene classifiers, guanine nucleotide binding protein (G protein), gamma 12 (GNG12), regulator of G-protein signaling 19 (RGS19), and collagen, type IX, alpha 2 (COL9A2), that could discriminate *R. equi* infected foals from healthy foals at birth with the lowest misclassification error. The GNG12 gene is involved in signal transduction and G-protein coupled receptor signaling. GNG12 is believed to be involved in inflammatory pathways and is thought to be involved in negative regulation of inflammation (Larson et al., 2010). It may also play a role in signal transduction on phagosomal membranes (Lee et al., 2010). RGS19 is also involved in signal transduction and is found in germinal centers of B cells, suggesting a

possible role in germinal center formation and maintenance (H. Chok 2004). These classifiers can discriminate the two groups of foals at birth using nasal epithelial cells, and could potentially be utilized to screen foals that will develop *R. equi* from resistant foals.

Finally, we observed that all the time points the misclassification error was <2% for blood leukocytes and <4% for nasal epithelial cells. Since detecting an early susceptibility to infection is ideal, based on our results biomarkers obtained at birth from leukocytes and nasal epithelium with 98.58% (due to error rate 0.0142) and 98.23% (due to error rate of 0.0177) accuracy, respectively, can be used for discriminating affected group from the unaffected. The accuracy and reliability of the discriminatory genes can only be assessed after validation on new samples from various farms to avoid any bias. However, since the handling of nasal epithelial cells is easier, not temperature sensitive and less invasive; this may be the choice of screening tools for some equine farms.

CONCLUSION

In summary, data from samples of blood leukocytes and nasal epithelial cells taken at three time points demonstrate that genes involved in maintaining the balance of Th1/Th2 immune response, T cell proliferation, and antimicrobial actions are up-regulated. This could contribute to susceptibility/resistance to infection in foals. While temporal changes improving host defense (antimicrobial action and protective immunity) against the pathogen may be developing as the foal ages, there are biological processes or gene

functions that lead to impaired/less efficient defense responses compared to healthy control counterparts. This study provides novel biomarkers of *R. equi* susceptibility with potential to be developed into qPCR-based screening tests. Future research should focus on extending this study at various equine farms across the country to validate the reproducibility and usefulness of the molecular biomarkers for screening purposes.

CHAPTER VI

CONCLUSION

This research represents one of the first attempts to perform the transcriptome profiling to uncover the molecular mechanism underlying the two equine respiratory diseases (RAO and *R. equi* pneumonia).

One of the limitations of present research in recurrent airway obstruction is our inadequate understanding of the molecular mechanisms orchestrating RAO pathogenesis. Research till date has focused on specific cell types or selected genes only (Franchini et al., 2000; Laan et al., 2006; Polikepahad et al., 2006; Ainsworth et al., 2009; Katavolos et al., 2009; Venugopal et al., 2009). Complex diseases involve coordinated interaction of several pathways and hence needs investigation of hundreds and thousands of genes simultaneously. Therefore a complete understanding of this disease requires a global genomic approach. Such an approach will ensure that all the genes are investigated at the same time in the disease state. The transcriptional profiling of disease state compared to control animals will reveal informative expression pattern of genes that can play important role in RAO and may contribute to the susceptibility.

Microarrays have been extensively used as a high-throughput tool to identify differentially expressed genes in human asthma (Brutsche et al., 2001; Laprise et al.,

2004; Syed et al., 2005; Hansel and Diette, 2007) and other animal models of asthma (Zou et al., 2002; Zimmermann et al., 2003; Heidenfelder et al., 2009). To date, there has been only a single attempt at using microarrays to understand the transcriptome profile of RAO affected animas (Ramery et al., 2009).

We aimed at understanding the effect of allergen exposure on RAO-susceptible horses with airway remodeling and obtained the biological processes and pathways associated with the gene profiles. We found that allergen exposure in susceptible horses only causes an increase in inflammation without any further increase in the airway smooth muscle mass. We also identified biomarkers that were able to discriminate/ classify the affected group of animals from the control group.

Our findings also suggest that allergen avoidance is a key factor in the resolution of inflammation. We found that an inhaled corticosteroid alone is not sufficient and together with allergen avoidance it should be introduced early in disease management. It appeared from the clinical reports that corticosteroid administration along with allergen avoidance could not resolve the airway obstruction completely. Hence we propose exploring the efficacy of adding long acting beta-agonists (LABA) to the inhaled corticosteroid (ICS) treatment protocol. LABA's are bronchodilators that together with ICS act synergistically in reducing the airway inflammation (Barnes, 2002). Finally, from our studies on RAO-susceptible horses, we report association of a variety of genes with different aspects of the RAO pathology like inflammation and remodeling. These

genes can likely be used as candidates for developing new research hypotheses to examine their direct role in disease progression or remission.

Next, from our research on *R. equi* pneumonia, we attempted to understand the age-related immune response of foals exposed to the pathogen. In order to achieve this goal we in-vitro stimulated blood leukocytes and examined the changes in gene expression profile during the first few weeks of life. The results suggested that immune cells are capable of Our findings suggest that the stimulated immune cells are capable of initiating a protective immune response through birth and up to 8 weeks of age, however there also were present genes/processes that could be counter-productive to the host. It was beyond the scope of this study to identify if such suppressive responses are caused due to the pathogen modulation host response, or a consequence of the immature immune system of the host. Therefore, future studies can be designed to understand the role of these suppressive mechanisms (and associated genes) in the pathogenicity of *R. equi*. If found directly implicated, these genes can be targeted to improve the host immune response against the pathogen.

We also report genes and molecular mechanisms associated with the susceptibility to *R. equi* pneumonia using blood leukocytes and nasal epithelial cells. This susceptibility can be attributes to modulation of genes involved in phagosome maturation, IFN-γ signaling, dendritic cell activation, IL-6 biosynthesis and T-cell proliferation. This study also identified biomarkers that can be used for screening foals that have a likelihood of developing pneumonia.

Early screening using such molecular biomarkers will allow appropriate management of foals and starting them timely antibiotic treatments, thus reducing disease incidence and foal mortality. For the future studies in *R. equi* pneumonia, understanding the host-pathogen interactome will be of utmost importance. The interactome studies will capture the host and pathogen gene expression overlay it with protein and metabolome level. It is the complex interaction between components of host and pathogen that can determine the outcome of an infection. Investigating such interaction networks will elucidate the complex interplay of the host and pathogen factors, and hence improve the understanding of the disease pathogenesis (Raman et al., 2009). Identifying such extensive host-pathogen networks will help in designing novel drugs and developing of targeted immunotherapeutics.

To summarize, the knowledge garnered from the RAO research will have a cross species impact. RAO shares many pathological features with human asthma and hence research in equine RAO will contribute to the existing knowledge of pathogenesis and treatment of asthma in humans. *R. equi* is an opportunistic pathogen that also affects other species like cats, dogs, pigs and cattle and immunocompromised human subjects like HIV affected patients. The outcomes from my research can hence be extended to other species. The classification technique used in this study is a relatively novel tool in animal research and can therefore be extended to accelerate biomarker discovery in other animal diseases.

REFERENCES

Addo, P.B., Dennis, S.M., 1977. Ovine pneumonia caused by Corynebacterium equi. Vet. Rec. 101, 80.

Ainsworth, D.M., Grunig, G., Matychak, M.B., Young, J., Wagner, B., Erb, H.N., Antczak, D.F., 2003. Recurrent airway obstruction (RAO) in horses is characterized by IFN-gamma and IL-8 production in bronchoalveolar lavage cells. Vet. Immunol. Immunopathol. 96, 83-91.

Ainsworth, D.M., Matychak, M., Reyner, C.L., Erb, H.N., Young, J.C., 2009. Effects of in vitro exposure to hay dust on the gene expression of chemokines and cell-surface receptors in primary bronchial epithelial cell cultures established from horses with chronic recurrent airway obstruction. Am. J. Vet. Res. 70, 365-372.

Ainsworth, D.M., Wagner, B., Franchini, M., Grunig, G., Erb, H.N., Tan, J.Y., 2006. Time-dependent alterations in gene expression of interleukin-8 in the bronchial epithelium of horses with recurrent airway obstruction. Am. J. Vet. Res. 67, 669-677.

Anton, F., Leverkoehne, I., Mundhenk, L., Thoreson, W.B., Gruber, A.D., 2005. Overexpression of eCLCA1 in small airways of horses with recurrent airway obstruction. J. Histochem. Cytochem. 53, 1011-1021.

Art, T., Bayly, W., Lekeux, P. 2002. Pulmonary function in the exercising horse, In: Lekeux, P. (Ed.) Equine Respiratory Diseases.

Art, T., Bureau, F., Robinson, N.E., 2008. Hunting for a key to the enigma of heaves in the black box of the white cells. Vet. J. 177, 307-308.

Averbeck, M., Gebhardt, C., Emmrich, F., Treudler, R., Simon, J.C., 2007. Immunologic Principles of Allergic Disease. JDDG: Journal der Deutschen Dermatologischen Gesellschaft 5, 1015-1027.

Barnes, P.J., 2001a. Cytokine modulators for allergic diseases. Curr Opin Allergy Clin Immunol 1, 555-560.

Barnes, P.J., 2001b. Neurogenic inflammation in the airways. Respir. Physiol. 125, 145-154.

Barnes, P.J., 2002. Scientific rationale for inhaled combination therapy with long-acting beta2-agonists and corticosteroids. Eur. Respir. J. 19, 182-191.

Barnes, P.J., 2006. Drugs for asthma. Br. J. Pharmacol. 147, S297-S303.

Barton, M.D., Hughes, K.L., 1984. Ecology of Rhodococcus equi. Vet. Microbiol. 9, 65-76.

Bazigou, E., Xie, S., Chen, C., Weston, A., Miura, N., Sorokin, L., Adams, R., Muro, A.F., Sheppard, D., Makinen, T., 2009. Integrin-alpha9 is required for fibronectin matrix assembly during lymphatic valve morphogenesis. Dev Cell 17, 175-186.

Beadle, R.E., Horohov, D.W., Gaunt, S.D., 2002. Interleukin-4 and interferon-gamma gene expression in summer pasture-associated obstructive pulmonary disease affected horses. Equine Vet. J. 34, 389-394.

Bedard, J., Brule, S., Price, C.A., Silversides, D.W., Lussier, J.G., 2003. Serine protease inhibitor-E2 (SERPINE2) is differentially expressed in granulosa cells of dominant follicle in cattle. Mol. Reprod. Dev. 64, 152-165.

Benamou, A.E., Art, T., Marlin, D.J., Roberts, C.A., Lekeux, P., 1998. Variations in systemic and pulmonary endothelin-1 in horses with recurrent airway obstruction (heaves). Pulm. Pharmacol. Ther. 11, 231-235.

Benamou, A.E., Marlin, D.J., Callingham, B.C., Hiley, R.C., Lekeux, R., 2003. Spasmogenic action of endothelin-1 on isolated equine pulmonary artery and bronchus. Equine Vet. J. 35, 190-196.

Benjamini, Y., Hochberg, Y., 1995. Controlling the False Discovery Rate: A Practical and Powerful Approach to Multiple Testing. Journal of the Royal Statistical Society. Series B (Methodological) 57, 289-300.

Berndt, A., Derksen, F.J., Venta, P.J., Ewart, S., Yuzbasiyan-Gurkan, V., Robinson, N.E., 2007. Elevated amount of Toll-like receptor 4 mRNA in bronchial epithelial cells is associated with airway inflammation in horses with recurrent airway obstruction. Am J Physiol Lung Cell Mol Physiol 292, L936-943.

Berndt, A., Derksen, F.J., Venta, P.J., Karmaus, W., Ewart, S., Yuzbasiyan-Gurkan, V., Robinson, N.E., 2009. Expression of toll-like receptor 2 mRNA in bronchial epithelial cells is not induced in RAO-affected horses. Equine Vet. J. 41, 76-81.

Bigg, H.F., Wait, R., Rowan, A.D., Cawston, T.E., 2006. The mammalian chitinase-like lectin, YKL-40, binds specifically to type I collagen and modulates the rate of type I collagen fibril formation. J. Biol. Chem. 281, 21082-21095.

Bingle, C.D., Craven, C.J., 2002. PLUNC: a novel family of candidate host defence proteins expressed in the upper airways and nasopharynx. Hum. Mol. Genet. 11, 937-943.

Blackburn, M.R., Kellems, R.E. 2005. Adenosine Deaminase Deficiency: Metabolic Basis of Immune Deficiency and Pulmonary Inflammation, In: Frderick, W.A. (Ed.) Advances in Immunology. Academic Press, 1-41.

Bochner, B.S., Undem, B.J., Lichtenstein, L.M., 1994. Immunological aspects of allergic asthma. Annu. Rev. Immunol. 12, 295-335.

Bowles, K.S., Beadle, R.E., Mouch, S., Pourciau, S.S., Littlefield-Chabaud, M.A., Le Blanc, C., Mistric, L., Fermaglich, D., Horohov, D.W., 2002. A novel model for equine recurrent airway obstruction. Vet. Immunol. Immunopathol. 87, 385-389.

Boyd, N.K., Cohen, N.D., Lim, W.S., Martens, R.J., Chaffin, M.K., Ball, J.M., 2003. Temporal changes in cytokine expression of foals during the first month of life. Vet. Immunol. Immunopathol. 92, 75-85.

Braga-Neto, U., Dougherty, E., 2004. Bolstered error estimation. Pattern Recognition 37, 1267-1281.

Braun, V., Fraisier, V., Raposo, G., Hurbain, I., Sibarita, J.B., Chavrier, P., Galli, T., Niedergang, F., 2004. TI-VAMP/VAMP7 is required for optimal phagocytosis of opsonised particles in macrophages. EMBO J. 23, 4166-4176.

Breathnach, C.C., Sturgill-Wright, T., Stiltner, J.L., Adams, A.A., Lunn, D.P., Horohov, D.W., 2006. Foals are interferon gamma-deficient at birth. Vet. Immunol. Immunopathol. 112, 199-209.

Bright, L.A., Burgess, S.C., Chowdhary, B., Swiderski, C.E., McCarthy, F.M., 2009. Structural and functional-annotation of an equine whole genome oligoarray. BMC Bioinformatics 10 Suppl 11.

Brown, J.H., Jardetzky, T.S., Gorga, J.C., Stern, L.J., Urban, R.G., Strominger, J.L., Wiley, D.C., 1993. Three-dimensional structure of the human class II histocompatibility antigen HLA-DR1. Nature 364, 33-39.

Brumell, J.H., Scidmore, M.A., 2007. Manipulation of rab GTPase function by intracellular bacterial pathogens. Microbiol. Mol. Biol. Rev. 71, 636-652.

Brutsche, M.H., Brutsche, I.C., Wood, P., Brass, A., Morrison, N., Rattay, M., Mogulkoc, N., Simler, N., Craven, M., Custovic, A., Egan, J.J.G., Woodcock, A., 2001. Apoptosis signals in atopy and asthma measured with cDNA arrays. Clin. Exp. Immunol. 123, 181-187.

Burger, D., Dayer, J.M., Palmer, G., Gabay, C., 2006. Is IL-1 a good therapeutic target in the treatment of arthritis? Best Pract Res Clin Rheumatol 20, 879-896.

Buyukasik, Y., Soylu, B., Soylu, A.R., Ozcebe, O.I., Canbakan, S., Haznedaroglu, I.C., Kirazli, S., Baser, Y., Dundar, S.V., 1998. In vivo platelet and T-lymphocyte activities during pulmonary tuberculosis. Eur. Respir. J. 12, 1375-1379.

Campbell, G.S., Argetsinger, L.S., Ihle, J.N., Kelly, P.A., Rillema, J.A., Carter-Su, C., 1994. Activation of JAK2 tyrosine kinase by prolactin receptors in Nb2 cells and mouse mammary gland explants. Proc. Natl. Acad. Sci. U. S. A. 91, 5232-5236.

Caramori, G., Groneberg, D., Ito, K., Casolari, P., Adcock, I.M., Papi, A., 2008. New drugs targeting Th2 lymphocytes in asthma. J Occup Med Toxicol 3 Suppl 1, S6.

Cauchard, J., Sevin, C., Ballet, J.J., Taouji, S., 2004. Foal IgG and opsonizing anti-Rhodococcus equi antibodies after immunization of pregnant mares with a protective VapA candidate vaccine. Vet. Microbiol. 104, 73-81.

Chaffin, M.K., Cohen, N.D., Martens, R.J., 2003a. Evaluation of equine breeding farm characteristics as risk factors for development of Rhodococcus equi pneumonia in foals. J Am Vet Med Assoc 222, 467-475.

Chaffin, M.K., Cohen, N.D., Martens, R.J., 2008. Chemoprophylactic effects of azithromycin against Rhodococcus equi-induced pneumonia among foals at equine breeding farms with endemic infections. J Am Vet Med Assoc 232, 1035-1047.

Chaffin, M.K., Cohen, N.D., Martens, R.J., Edwards, R.F., Nevill, M., 2003b. Foal-related risk factors associated with development of Rhodococcus equi pneumonia on farms with endemic infection. J Am Vet Med Assoc 223, 1791-1799.

Chaffin, M.K., Cohen, N.D., Martens, R.J., Edwards, R.F., Nevill, M., Smith, R., 3rd, 2004. Hematologic and immunophenotypic factors associated with development of Rhodococcus equi pneumonia of foals at equine breeding farms with endemic infection. Vet. Immunol. Immunopathol. 100, 33-48.

Chaffin, M.K., Cohen, N.D., Martens, R.J., O'Conor, M., Bernstein, L.R., 2011. Evaluation of the efficacy of gallium maltolate for chemoprophylaxis against pneumonia caused by Rhodococcus equi infection in foals. Am. J. Vet. Res. 72, 945-957.

Chakir, J., Shannon, J., Molet, S., Fukakusa, M., Elias, J., Laviolette, M., Boulet, L.P., Hamid, Q., 2003. Airway remodeling-associated mediators in moderate to severe asthma: effect of steroids on TGF-beta, IL-11, IL-17, and type I and type III collagen expression. J. Allergy Clin. Immunol. 111, 1293-1298.

Chan, J.Y., Lee-Prudhoe, J.E., Jorgensen, B., Ihrke, G., Doyonnas, R., Zannettino, A.C., Buckle, V.J., Ward, C.J., Simmons, P.J., Watt, S.M., 2001. Relationship between novel isoforms, functionally important domains, and subcellular distribution of CD164/endolyn. J. Biol. Chem. 276, 2139-2152.

Chang, C.L., Hong, E., Lao-Sirieix, P., Fitzgerald, R.C., 2008. A novel role for the retinoic acid-catabolizing enzyme CYP26A1 in Barrett's associated adenocarcinoma. Oncogene 27, 2951-2960.

Chang, E., Perlman, A.J., 1988. Angiotensinogen mRNA. Regulation by cell cycle and growth factors. J. Biol. Chem. 263, 5480-5484.

Chang, S.H., Dong, C., 2007. A novel heterodimeric cytokine consisting of IL-17 and IL-17F regulates inflammatory responses. Cell Res. 17, 435-440.

Charan, N.B., Baile, E.M., Pare, P.D., 1997. Bronchial vascular congestion and angiogenesis. Eur. Respir. J. 10, 1173-1180.

Chen, M., Wang, Y.H., Wang, Y., Huang, L., Sandoval, H., Liu, Y.J., Wang, J., 2006. Dendritic cell apoptosis in the maintenance of immune tolerance. Science 311, 1160-1164.

Chen, Q., Ghilardi, N., Wang, H., Baker, T., Xie, M.H., Gurney, A., Grewal, I.S., de Sauvage, F.J., 2000. Development of Th1-type immune responses requires the type I cytokine receptor TCCR. Nature 407, 916-920.

Chen, Y., Sun, R., Han, W., Zhang, Y., Song, Q., Di, C., Ma, D., 2001. Nuclear translocation of PDCD5 (TFAR19): an early signal for apoptosis? FEBS Lett. 509, 191-196.

Cho, S.H., Kim, Y.K., Oh, H.B., Jung, J.W., Son, J.W., Lee, M.H., Jee, H.S., Kim, Y.Y., Min, K.U., 2000. Association of HLA-DRB1(*)07 and DRB1(*)04 to citrus red mite (Panonychus citri) and house dust mite sensitive asthma. Clin. Exp. Allergy 30, 1568-1575.

Chowdhary, B.P., Bailey, E., 2003. Equine genomics: galloping to new frontiers. Cytogenet Genome Res 102, 184-188.

Chu, H.W., Kraft, M., Rex, M.D., Martin, R.J., 2001. Evaluation of blood vessels and edema in the airways of asthma patients: regulation with clarithromycin treatment. Chest 120, 416-422.

Clapp, C., Thebault, S., Jeziorski, M.C., Martinez De La Escalera, G., 2009. Peptide hormone regulation of angiogenesis. Physiol. Rev. 89, 1177-1215.

Clarke, A.F., 1987. A review of environmental and host factors in relation to equine respiratory disease. Equine Vet. J. 19, 435-441.

Coffman, F.D., 2008. Chitinase 3-Like-1 (CHI3L1): a putative disease marker at the interface of proteomics and glycomics. Crit. Rev. Clin. Lab. Sci. 45, 531-562.

Cohen, D.N., Chaffin, M.K., Martens, J.G. 2002. How to Prevent and Control Pneumonia Caused by Rhodococcus equi at Affected Farms. In: Proceedings of the Annual Convention of the AAEP 2002.

Cohen, J., Burggraaf, J., Schoemaker, R.C., Sterk, P.J., Cohen, A.F., Diamant, Z., 2005a. Relationship between airway responsiveness to neurokinin A and methacholine in asthma. Pulm. Pharmacol. Ther. 18, 171-176.

Cohen, N.D., Carter, C.N., Scott, H.M., Chaffin, M.K., Smith, J.L., Grimm, M.B., Kuskie, K.R., Takai, S., Martens, R.J., 2008. Association of soil concentrations of Rhodococcus equi and incidence of pneumonia attributable to Rhodococcus equi in foals on farms in central Kentucky. Am. J. Vet. Res. 69, 385-395.

Cohen, N.D., Chaffin, M.K., Vandenplas, M.L., Edwards, R.F., Nevill, M., Moore, J.N., Martens, R.J., 2005b. Study of serum amyloid A concentrations as a means of achieving early diagnosis of Rhodococcus equi pneumonia. Equine Vet. J. 37, 212-216.

Cohen, N.D., Harrington, J., Gros, P., Del Castro, L., Meyer, D., Martens, R.J., 2004. Nramp1 deletion does not confer susceptibility to Rhodococcus equi infection in mice. Immunogenetics 56, 65-67.

Cohen, N.D., O'Conor, M.S., Chaffin, M.K., Martens, R.J., 2005c. Farm characteristics and management practices associated with development of Rhodococcus equi pneumonia in foals. J Am Vet Med Assoc 226, 404-413.

Condeelis, J., 1995. Elongation factor 1 alpha, translation and the cytoskeleton. Trends Biochem. Sci. 20, 169-170.

Corvol, P., Lamande, N., Cruz, A., Celerier, J., Gasc, J.M., 2003. Inhibition of angiogenesis: a new function for angiotensinogen and des(angiotensin I)angiotensinogen. Curr Hypertens Rep 5, 149-154.

Couetil, L.L., Art, T., de Moffarts, B., Becker, M., Melotte, D., Jaspar, F., Bureau, F., Lekeux, P., 2006. Effect of beclomethasone dipropionate and dexamethasone isonicotinate on lung function, bronchoalveolar lavage fluid cytology, and transcription factor expression in airways of horses with recurrent airway obstruction. J. Vet. Intern. Med. 20, 399-406.

Couetil, L.L., Chilcoat, C.D., DeNicola, D.B., Clark, S.P., Glickman, N.W., Glickman, L.T., 2005. Randomized, controlled study of inhaled fluticasone propionate, oral administration of prednisone, and environmental management of horses with recurrent airway obstruction. Am. J. Vet. Res. 66, 1665-1674.

Couetil, L.L., Ward, M.P., 2003. Analysis of risk factors for recurrent airway obstruction in North American horses: 1,444 cases (1990-1999). J Am Vet Med Assoc 223, 1645-1650.

Crosby, L.M., Waters, C.M., 2010. Epithelial repair mechanisms in the lung. Am J Physiol Lung Cell Mol Physiol 298, L715-731.

Custovic, A., Simpson, A., Chapman, M.D., Woodcock, A., 1998. Allergen avoidance in the treatment of asthma and atopic disorders. Thorax 53, 63-72.

Dallas, P.B., Gottardo, N.G., Firth, M.J., Beesley, A.H., Hoffmann, K., Terry, P.A., Freitas, J.R., Boag, J.M., Cummings, A.J., Kees, U.R., 2005. Gene expression levels assessed by oligonucleotide microarray analysis and quantitative real-time RT-PCR -- how well do they correlate? BMC Genomics 6, 59.

Darrah, P.A., Hondalus, M.K., Chen, Q., Ischiropoulos, H., Mosser, D.M., 2000. Cooperation between reactive oxygen and nitrogen intermediates in killing of Rhodococcus equi by activated macrophages. Infect. Immun. 68, 3587-3593.

Darrah, P.A., Monaco, M.C., Jain, S., Hondalus, M.K., Golenbock, D.T., Mosser, D.M., 2004. Innate immune responses to Rhodococcus equi. J. Immunol. 173, 1914-1924.

Dawson, T.R., Horohov, D.W., Meijer, W.G., Muscatello, G., 2010. Current understanding of the equine immune response to Rhodococcus equi. An immunological review of R. equi pneumonia. Vet. Immunol. Immunopathol. 135, 1-11.

de Almeida, S.F., Carvalho, I.F., Cardoso, C.S., Cordeiro, J.V., Azevedo, J.E., Neefjes, J., de Sousa, M., 2005. HFE cross-talks with the MHC class I antigen presentation pathway. Blood 106, 971-977.

Deaton, C.M., Deaton, L., Jose-Cunilleras, E., Vincent, T.L., Baird, A.W., Dacre, K., Marlin, D.J., 2007. Early onset airway obstruction in response to organic dust in the horse. J. Appl. Physiol. 102, 1071-1077.

Debey, M.C., Bailie, W.E., 1987. Rhodococcus equi in fecal and environmental samples from Kansas horse farms. Vet. Microbiol. 14, 251-257.

Debrue, M., Hamilton, E., Joubert, P., Lajoie-Kadoch, S., Lavoie, J.P., 2005. Chronic exacerbation of equine heaves is associated with an increased expression of interleukin-17 mRNA in bronchoalveolar lavage cells. Vet. Immunol. Immunopathol. 105, 25-31.

Dekkers, B.G., Maarsingh, H., Meurs, H., Gosens, R., 2009. Airway structural components drive airway smooth muscle remodeling in asthma. Proc Am Thorac Soc 6, 683-692.

Demmers, S., Johannisson, A., Grondahl, G., Jensen-Waern, M., 2001. Neutrophil functions and serum IgG in growing foals. Equine Vet. J. 33, 676-680.

Diehl, S., Rincon, M., 2002. The two faces of IL-6 on Th1/Th2 differentiation. Mol. Immunol. 39, 531-536.

Dirscherl, P., Grabner, A., Buschmann, H., 1993. Responsiveness of basophil granulocytes of horses suffering from chronic obstructive pulmonary disease to various allergens. Vet. Immunol. Immunopathol. 38, 217-227.

Dobbin, K., Shih, J.H., Simon, R., 2003. Statistical design of reverse dye microarrays. Bioinformatics 19, 803-810.

Dobbin, K., Simon, R., 2002. Comparison of microarray designs for class comparison and class discovery. Bioinformatics 18, 1438-1445.

Doherty, T., Broide, D., 2007. Cytokines and growth factors in airway remodeling in asthma. Curr. Opin. Immunol. 19, 676-680.

Duncan, D., Prodduturi, N., Zhang, B., 2010. WebGestalt2: an updated and expanded version of the Web-based Gene Set Analysis Toolkit. BMC Bioinformatics 11, 1-1.

Duttaroy, A., Bourbeau, D., Wang, X.-L., Wang, E., 1998. Apoptosis Rate Can Be Accelerated or Decelerated by Overexpression or Reduction of the Level of Elongation Factor-1[alpha]. Exp. Cell Res. 238, 168-176.

Eder, C., Crameri, R., Mayer, C., Eicher, R., Straub, R., Gerber, H., Lazary, S., Marti, E., 2000. Allergen-specific IgE levels against crude mould and storage mite extracts and recombinant mould allergens in sera from horses affected with chronic bronchitis. Vet. Immunol. Immunopathol. 73, 241-253.

Eleme, K., Taner, S.B., Onfelt, B., Collinson, L.M., McCann, F.E., Chalupny, N.J., Cosman, D., Hopkins, C., Magee, A.I., Davis, D.M., 2004. Cell surface organization of stress-inducible proteins ULBP and MICA that stimulate human NK cells and T cells via NKG2D. J. Exp. Med. 199, 1005-1010.

Elias, J.A., 2000. Airway remodeling in asthma. Unanswered questions. Am. J. Respir. Crit. Care Med. 161, S168-171.

Elias, J.A., Zhu, Z., Chupp, G., Homer, R.J., 1999. Airway remodeling in asthma. J. Clin. Invest. 104, 1001-1006.

Elliott, G., Lawson, G.H., Mackenzie, C.P., 1986. Rhodococcus equi infection in cats. Vet. Rec. 118, 693-694.

Fairbairn, S.M., Page, C.P., Lees, P., Cunningham, F.M., 1993. Early neutrophil but not eosinophil or platelet recruitment to the lungs of allergic horses following antigen exposure. Clin. Exp. Allergy 23, 821-828.

Fernandez-Mora, E., Polidori, M., Luhrmann, A., Schaible, U.E., Haas, A., 2005. Maturation of Rhodococcus equi-containing vacuoles is arrested after completion of the early endosome stage. Traffic 6, 635-653.

Ferraz, L.C., Bernardes, E.S., Oliveira, A.F., Ruas, L.P., Fermino, M.L., Soares, S.G., Loyola, A.M., Oliver, C., Jamur, M.C., Hsu, D.K., Liu, F.T., Chammas, R., Roque-Barreira, M.C., 2008. Lack of galectin-3 alters the balance of innate immune cytokines and confers resistance to Rhodococcus equi infection. Eur. J. Immunol. 38, 2762-2775.

Flaminio, M.J., Nydam, D.V., Marquis, H., Matychak, M.B., Giguere, S., 2009. Foal monocyte-derived dendritic cells become activated upon Rhodococcus equi infection. Clin Vaccine Immunol 16, 176-183.

Flannagan, R.S., Cosio, G., Grinstein, S., 2009. Antimicrobial mechanisms of phagocytes and bacterial evasion strategies. Nat Rev Microbiol 7, 355-366.

Flies, D.B., Chen, L., 2007. The new B7s: playing a pivotal role in tumor immunity. J. Immunother. 30, 251-260.

Follettie, M.T., Ellis, D.K., Donaldson, D.D., Hill, A.A., Diesl, V., DeClercq, C., Sypek, J.P., Dorner, A.J., Wills-Karp, M., 2006. Gene expression analysis in a murine model of allergic asthma reveals overlapping disease and therapy dependent pathways in the lung. Pharmacogenomics J 6, 141-152.

Franchini, M., Gill, U., von Fellenberg, R., Bracher, V.D., 2000. Interleukin-8 concentration and neutrophil chemotactic activity in bronchoalveolar lavage fluid of horses with chronic obstructive pulmonary disease following exposure to hay. Am. J. Vet. Res. 61, 1369-1374.

Gao, Z., Peet, N.P., 1999. Recent advances in neurokinin receptor antagonists. Curr. Med. Chem. 6, 375-388.

Gebhardt, C., Nemeth, J., Angel, P., Hess, J., 2006. S100A8 and S100A9 in inflammation and cancer. Biochem Pharmacol 72, 1622-1631.

Gerber, H., 1973. Chronic Pulmonary Disease in the Horse. Equine Vet. J. 5, 26-33.

Gerber, H., 1989. Sir Frederick Hobday Memorial Lecture. The genetic basis of some equine diseases. Equine Vet. J. 21, 244-248.

Gerber, H., Hockenjos, P., Lazary, S., Kings, M., de Weck, A., 1982. [Histamine release from equine leucocytes provoked by fungal allergens]. Dtsch. Tierarztl. Wochenschr. 89, 267-270.

Gerber, V., Baleri, D., Klukowska-Rotzler, J., Swinburne, J.E., Dolf, G., 2009a. Mixed inheritance of equine recurrent airway obstruction. J. Vet. Intern. Med. 23, 626-630.

Gerber, V., De Feijter-Rupp, H., Wagner, J., Venta, P., Harkema, J.R., Robinson, N.E., 2009b. Differential association of MUC5AC and CLCA1 expression in small cartilaginous airways of RAO-affected and control horses. Equine Vet. J. 41, 817-823.

Gerber, V., Lindberg, A., Berney, C., Robinson, N.E., 2004a. Airway mucus in recurrent airway obstruction--short-term response to environmental challenge. J. Vet. Intern. Med. 18, 92-97.

Gerber, V., Robinson, N.E., Venta, R.J., Rawson, J., Jefcoat, A.M., Hotchkiss, J.A., 2003. Mucin genes in horse airways: MUC5AC, but not MUC2, may play a role in recurrent airway obstruction. Equine Vet. J. 35, 252-257.

Gerber, V., Straub, R., Marti, E., Hauptman, J., Herholz, C., King, M., Imhof, A., Tahon, L., Robinson, N.E., 2004b. Endoscopic scoring of mucus quantity and quality: observer and horse variance and relationship to inflammation, mucus viscoelasticity and volume. Equine Vet. J. 36, 576-582.

Gerber, V., Swinburne, J.E., Blott, S.C., Nussbaumer, P., Ramseyer, A., Klukowska-Rotzler, J., Dolf, G., Marti, E., Burger, D., Leeb, T., 2008. [Genetics of recurrent airway obstruction (RAO)]. Dtsch. Tierarztl. Wochenschr. 115, 271-275.

Giguere, S., Hernandez, J., Gaskin, J., Miller, C., Bowman, J.L., 2003. Evaluation of white blood cell concentration, plasma fibrinogen concentration, and an agar gel immunodiffusion test for early identification of foals with Rhodococcus equi pneumonia. J Am Vet Med Assoc 222, 775-781.

Giguere, S., Prescott, J.F., 1997. Clinical manifestations, diagnosis, treatment, and prevention of Rhodococcus equi infections in foals. Vet. Microbiol. 56, 313-334.

Giguere, S., Prescott, J.F., 2000. Equine immunity to bacteria. Vet. Clin. North Am. Equine Pract. 16, 29-47, v-iv.

Giguere, S., Viel, L., Lee, E., MacKay, R.J., Hernandez, J., Franchini, M., 2002. Cytokine induction in pulmonary airways of horses with heaves and effect of therapy with inhaled fluticasone propionate. Vet. Immunol. Immunopathol. 85, 147-158.

Giguere, S., Wilkie, B.N., Prescott, J.F., 1999. Modulation of cytokine response of pneumonic foals by virulent Rhodococcus equi. Infect. Immun. 67, 5041-5047.

Gonzalez, S., Lopez-Soto, A., Suarez-Alvarez, B., Lopez-Vazquez, A., Lopez-Larrea, C., 2008. NKG2D ligands: key targets of the immune response. Trends Immunol 29, 397-403.

Gotoh, K., Mitsuyama, M., Imaizumi, S., Kawamura, I., Yano, I., 1991. Mycolic acid-containing glycolipid as a possible virulence factor of Rhodococcus equi for mice. Microbiol. Immunol. 35, 175-185.

Granstrom, B.W., Xu, C.B., Nilsson, E., Bengtsson, U.H., Edvinsson, L., 2004. Up-regulation of endothelin receptor function and mRNA expression in airway smooth muscle cells following Sephadex-induced airway inflammation. Basic Clin Pharmacol Toxicol 95, 43-48.

Grimm, M.B., Cohen, N.D., Slovis, N.M., Mundy, G.D., Harrington, J.R., Libal, M.C., Takai, S., Martens, R.J., 2007. Evaluation of fecal samples from mares as a source of Rhodococcus equi for their foals by use of quantitative bacteriologic culture and colony immunoblot analyses. Am. J. Vet. Res. 68, 63-71.

Ha, J., Choi, H.S., Lee, Y., Kwon, H.J., Song, Y.W., Kim, H.H., 2010. CXC chemokine ligand 2 induced by receptor activator of NF-kappa B ligand enhances osteoclastogenesis. J. Immunol. 184, 4717-4724.

Halayko, A.J., Ghavami, S., 2009. S100A8/A9: a mediator of severe asthma pathogenesis and morbidity? Can. J. Physiol. Pharmacol. 87, 743-755.

Halbert, N.D., Cohen, N.D., Slovis, N.M., Faircloth, J., Martens, R.J., 2006. Variations in equid SLC11A1 (NRAMP1) genes and associations with Rhodococcus equi pneumonia in horses. J. Vet. Intern. Med. 20, 974-979.

Halbert, N.D., Reitzel, R.A., Martens, R.J., Cohen, N.D., 2005. Evaluation of a multiplex polymerase chain reaction assay for simultaneous detection of Rhodococcus equi and the vapA gene. Am. J. Vet. Res. 66, 1380-1385.

Halliwell, R.E., Fleischman, J.B., Mackay-Smith, M., Beech, J., Gunson, D.E., 1979. The role of allergy in chronic pulmonary disease of horses. J Am Vet Med Assoc 174, 277-281.

Halliwell, R.E., McGorum, B.C., Irving, P., Dixon, P.M., 1993. Local and systemic antibody production in horses affected with chronic obstructive pulmonary disease. Vet. Immunol. Immunopathol. 38, 201-215.

Halwani, R., Al-Muhsen, S., Hamid, Q., 2010. Airway remodeling in asthma. Curr Opin Pharmacol 10, 236-245.

Hansel, N.N., Diette, G.B., 2007. Gene Expression Profiling in Human Asthma. Proc Am Thorac Soc 4, 32-36.

Hare, J.E., Viel, L., Conlon, P.D., Marshall, J.S., 1998. Evaluation of an in vitro degranulation challenge procedure for equine pulmonary mast cells. Can. J. Vet. Res. 62, 133-139.

Hare, J.E., Viel, L., Conlon, P.D., Marshall, J.S., 1999. In vitro allergen-induced degranulation of pulmonary mast cells from horses with recurrent airway obstruction (heaves). Am. J. Vet. Res. 60, 841-847.

Harrington, J.R., Golding, M.C., Martens, R.J., Halbert, N.D., Cohen, N.D., 2005. Evaluation of a real-time quantitative polymerase chain reaction assay for detection and quantitation of virulent Rhodococcus equi. Am. J. Vet. Res. 66, 755-761.

Harris, S.P., Fujiwara, N., Mealey, R.H., Alperin, D.C., Naka, T., Goda, R., Hines, S.A., 2010. Identification of Rhodococcus equi lipids recognized by host cytotoxic T lymphocytes. Microbiology 156, 1836-1847.

Harrison, T.W., Oborne, J., Newton, S., Tattersfield, A.E., 2004. Doubling the dose of inhaled corticosteroid to prevent asthma exacerbations: randomised controlled trial. Lancet 363, 271-275.

Hartung, T., Fennrich, S., Fischer, M., Montag-Lessing, T., Wendel, A., 1998. [Development and evaluation of a pyrogen test based on human whole blood]. ALTEX 15, 9-10.

Heidenfelder, B.L., Reif, D.M., Harkema, J.R., Cohen Hubal, E.A., Hudgens, E.E., Bramble, L.A., Wagner, J.G., Morishita, M., Keeler, G.J., Edwards, S.W., Gallagher, J.E., 2009. Comparative microarray analysis and pulmonary changes in Brown Norway rats exposed to ovalbumin and concentrated air particulates. Toxicol. Sci. 108, 207-221.

Heidmann, P., Madigan, J.E., Watson, J.L., 2006. Rhodococcus equi Pneumonia: Clinical Findings, Diagnosis, Treatment and Prevention. Clinical Techniques in Equine Practice 5, 203-210.

Heller, M.C., Jackson, K.A., Watson, J.L., 2010. Identification of immunologically relevant genes in mare and foal dendritic cells responding to infection by Rhodococcus equi. Vet. Immunol. Immunopathol. 136, 144-150.

Herholz, C.P., Gerber, V., Tschudi, P., Straub, R., Imhof, A., Busato, A., 2003. Use of volumetric capnography to identify pulmonary dysfunction in horses with and without clinically apparent recurrent airway obstruction. Am. J. Vet. Res. 64, 338-345.

Herszberg, B., Ramos-Barbon, D., Tamaoka, M., Martin, J.G., Lavoie, J.P., 2006. Heaves, an asthma-like equine disease, involves airway smooth muscle remodeling. J. Allergy Clin. Immunol. 118, 382-388.

Hietala, S.K., Ardans, A.A., 1987. Interaction of Rhodococcus equi with phagocytic cells from R. equi-exposed and non-exposed foals. Vet. Microbiol. 14, 307-320.

Hines, M.T. 2006. Rhodococcus equi, In: Sellon, D.C., Long, M. (Eds.) Equine Infectious Diseases. Saunders, 281-295.

Hines, M.T., Paasch, K.M., Alperin, D.C., Palmer, G.H., Westhoff, N.C., Hines, S.A., 2001. Immunity to Rhodococcus equi: antigen-specific recall responses in the lungs of adult horses. Vet. Immunol. Immunopathol. 79, 101-114.

Hines, S.A., Kanaly, S.T., Byrne, B.A., Palmer, G.H., 1997. Immunity to Rhodococcus equi. Vet. Microbiol. 56, 177-185.

Hines, S.A., Stone, D.M., Hines, M.T., Alperin, D.C., Knowles, D.P., Norton, L.K., Hamilton, M.J., Davis, W.C., McGuire, T.C., 2003. Clearance of virulent but not avirulent Rhodococcus equi from the lungs of adult horses is associated with intracytoplasmic gamma interferon production by CD4+ and CD8+ T lymphocytes. Clin. Diagn. Lab. Immunol. 10, 208-215.

Hirst, S.J., Twort, C.H., Lee, T.H., 2000. Differential effects of extracellular matrix proteins on human airway smooth muscle cell proliferation and phenotype. Am. J. Respir. Cell Mol. Biol. 23, 335-344.

Hoffman, A., Kuehn, H., Riedelberger, K., Kupcinskas, R., Miskovic, M.B., 2001. Flowmetric comparison of respiratory inductance plethysmography and pneumotachography in horses. J. Appl. Physiol. 91, 2767-2775.

Hoffman, A.M., 1999. Bronchoalveolar lavage technique and cytological diagnosis of small airway inflammatory disease. Equine Veterinary Education 11, 330-336.

Holm, A.M., Aukrust, P., Damas, J.K., Muller, F., Halvorsen, B., Froland, S.S., 2005. Abnormal interleukin-7 function in common variable immunodeficiency. Blood 105, 2887-2890.

Holznagel, D.L., Hussey, S., Mihalyi, J.E., Wilson, W.D., Lunn, D.P., 2003. Onset of immunoglobulin production in foals. Equine Vet. J. 35, 620-622.

Homer, R.J., Elias, J.A., 2005. Airway remodeling in asthma: therapeutic implications of mechanisms. Physiology (Bethesda) 20, 28-35.

Hondalus, M.K., 1997. Pathogenesis and virulence of Rhodococcus equi. Vet. Microbiol. 56, 257-268.

Horin, P., Osickova, J., Necesankova, M., Matiasovic, J., Musilova, P., Kubickova, S., Hubertova, D., Vyskocil, M., Rubes, J., 2008. Single nucleotide polymorphisms of interleukin-1 beta related genes and their associations with infection in the horse. Dev Biol (Basel) 132, 347-351.

Horin, P., Sabakova, K., Futas, J., Vychodilova, L., Necesankova, M., 2010. Immunity-related gene single nucleotide polymorphisms associated with Rhodococcus equi infection in foals. Int J Immunogenet 37, 67-71.

Horowitz, M.L., Cohen, N.D., Takai, S., Becu, T., Chaffin, M.K., Chu, K.K., Magdesian, K.G., Martens, R.J., 2001. Application of Sartwell's model (lognormal distribution of incubation periods) to age at onset and age at death of foals with Rhodococcus equi pneumonia as evidence of perinatal infection. J. Vet. Intern. Med. 15, 171-175.

Hoshino, A., Tanaka, Y., Akiba, H., Asakura, Y., Mita, Y., Sakurai, T., Takaoka, A., Nakaike, S., Ishii, N., Sugamura, K., Yagita, H., Okumura, K., 2003. Critical role for OX40 ligand in the development of pathogenic Th2 cells in a murine model of asthma. Eur. J. Immunol. 33, 861-869.

Hoshino, M., Morita, S., Iwashita, H., Sagiya, Y., Nagi, T., Nakanishi, A., Ashida, Y., Nishimura, O., Fujisawa, Y., Fujino, M., 2002. Increased expression of the human Ca2+-activated Cl- channel 1 (CaCC1) gene in the asthmatic airway. Am. J. Respir. Crit. Care Med. 165, 1132-1136.

Hotchkiss, J.W., Reid, S.W., Christley, R.M., 2007. A survey of horse owners in Great Britain regarding horses in their care. Part 2: Risk factors for recurrent airway obstruction. Equine Vet. J. 39, 301-308.

Huang, D.W., Sherman, B.T., Lempicki, R.A., 2009a. Bioinformatics enrichment tools: paths toward the comprehensive functional analysis of large gene lists. Nucleic Acids Res 37, 1-13.

Huang, D.W., Sherman, B.T., Lempicki, R.A., 2009b. Systematic and integrative analysis of large gene lists using DAVID bioinformatics resources. Nat Protoc 4, 44-57.

Huang, T., Razmovski-Naumovski, V., Kota, B., Lin, D., Roufogalis, B., 2005. The pathophysiological function of peroxisome proliferator-activated receptor-gamma in lung-related diseases. Respiratory Research 6, 102.

Hulten, C., Demmers, S., 2002. Serum amyloid A (SAA) as an aid in the management of infectious disease in the foal: comparison with total leucocyte count, neutrophil count and fibrinogen. Equine Vet. J. 34, 693-698.

Hurd, P.J., Nelson, C.J., 2009. Advantages of next-generation sequencing versus the microarray in epigenetic research. Brief Funct Genomic Proteomic 8, 174-183.

Iwata, M., Hirakiyama, A., Eshima, Y., Kagechika, H., Kato, C., Song, S.Y., 2004. Retinoic acid imprints gut-homing specificity on T cells. Immunity 21, 527-538.

Jacks, S., Giguere, S., Crawford, P.C., Castleman, W.L., 2007. Experimental infection of neonatal foals with Rhodococcus equi triggers adult-like gamma interferon induction. Clin Vaccine Immunol 14, 669-677.

Jackson, C.A., Berney, C., Jefcoat, A.M., Robinson, N.E., 2000. Environment and prednisone interactions in the treatment of recurrent airway obstruction (heaves). Equine Vet. J. 32, 432-438.

Jain, M., Petzold, C.J., Schelle, M.W., Leavell, M.D., Mougous, J.D., Bertozzi, C.R., Leary, J.A., Cox, J.S., 2007. Lipidomics reveals control of Mycobacterium tuberculosis virulence lipids via metabolic coupling. Proc. Natl. Acad. Sci. U. S. A. 104, 5133-5138.

Jefcoat, A.M., Hotchkiss, J.A., Gerber, V., Harkema, J.R., Basbaum, C.B., Robinson, N.E., 2001. Persistent mucin glycoprotein alterations in equine recurrent airway obstruction. Am J Physiol Lung Cell Mol Physiol 281, L704-712.

Jeffery, P.K., 2001. Remodeling in asthma and chronic obstructive lung disease. Am. J. Respir. Crit. Care Med. 164, S28-38.

Jia, H., Halilou, A.I., Hu, L., Cai, W., Liu, J., Huang, B., 2011. Heat shock protein 10 (Hsp10) in immune-related diseases: one coin, two sides. Int J Biochem Mol Biol 2, 47-57.

Johnson, B.J., Le, T.T., Dobbin, C.A., Banovic, T., Howard, C.B., Flores Fde, M., Vanags, D., Naylor, D.J., Hill, G.R., Suhrbier, A., 2005. Heat shock protein 10 inhibits lipopolysaccharide-induced inflammatory mediator production. J. Biol. Chem. 280, 4037-4047.

Johnson, P.R., Roth, M., Tamm, M., Hughes, M., Ge, Q., King, G., Burgess, J.K., Black, J.L., 2001. Airway smooth muscle cell proliferation is increased in asthma. Am. J. Respir. Crit. Care Med. 164, 474-477.

Joos, G.F., Vincken, W., Louis, R., Schelfhout, V.J., Wang, J.H., Shaw, M.J., Cioppa, G.D., Pauwels, R.A., 2004. Dual tachykinin NK1/NK2 antagonist DNK333 inhibits neurokinin A-induced bronchoconstriction in asthma patients. Eur. Respir. J. 23, 76-81.

Jordan, M.C., Harrington, J.R., Cohen, N.D., Tsolis, R.M., Dangott, L.J., Weinberg, E.D., Martens, R.J., 2003. Effects of iron modulation on growth and viability of Rhodococcus equi and expression of virulence-associated protein A. Am. J. Vet. Res. 64, 1337-1346.

Jose-Cunilleras, E., Kohn, C.W., Hillier, A., Saville, W.J., Lorch, G., 2001. Intradermal testing in healthy horses and horses with chronic obstructive pulmonary disease, recurrent urticaria, or allergic dermatitis. J Am Vet Med Assoc 219, 1115-1121.

Jost, U., Klukowska-Rotzler, J., Dolf, G., Swinburne, J.E., Ramseyer, A., Bugno, M., Burger, D., Blott, S., Gerber, V., 2007. A region on equine chromosome 13 is linked to recurrent airway obstruction in horses. Equine Vet. J. 39, 236-241.

Kanaly, S.T., Hines, S.A., Palmer, G.H., 1993. Failure of pulmonary clearance of Rhodococcus equi infection in CD4+ T-lymphocyte-deficient transgenic mice. Infect. Immun. 61, 4929-4932.

Karlson, A.G., Moses, H.E., Feldman, W.H., 1940. Corynebacterium equi (Magnusson, 1923) in the Submaxillary Lymph Nodes of Swine. J. Infect. Dis. 67, 243-251.

Kassuya, C.A., Rogerio, A.P., Calixto, J.B., 2008. The role of ET(A) and ET(B) receptor antagonists in acute and allergic inflammation in mice. Peptides 29, 1329-1337.

Kasuga-Aoki, H., Takai, S., Sasaki, Y., Tsubaki, S., Madarame, H., Nakane, A., 1999. Tumour necrosis factor and interferon-gamma are required in host resistance against virulent Rhodococcus equi infection in mice: cytokine production depends on the virulence levels of R. equi. Immunology 96, 122-127.

Katavolos, P., Ackerley, C.A., Clark, M.E., Bienzle, D., 2011. Clara cell secretory protein increases phagocytic and decreases oxidative activity of neutrophils. Vet. Immunol. Immunopathol. 139, 1-9.

Katavolos, P., Ackerley, C.A., Viel, L., Clark, M.E., Wen, X., Bienzle, D., 2009. Clara cell secretory protein is reduced in equine recurrent airway obstruction. Vet. Pathol. 46, 604-613.

Kedlaya, I., Ing, M.B., Wong, S.S., 2001. Rhodococcus equi infections in immunocompetent hosts: case report and review. Clin. Infect. Dis. 32, E39-46.

Kim, M.J., Wainwright, H.C., Locketz, M., Bekker, L.G., Walther, G.B., Dittrich, C., Visser, A., Wang, W., Hsu, F.F., Wiehart, U., Tsenova, L., Kaplan, G., Russell, D.G., 2010. Caseation of human tuberculosis granulomas correlates with elevated host lipid metabolism. EMBO Mol Med 2, 258-274.

Kim, S., Dougherty, E.R., Shmulevich, I., Hess, K.R., Hamilton, S.R., Trent, J.M., Fuller, G.N., Zhang, W., 2002. Identification of combination gene sets for glioma classification. Mol Cancer Ther 1, 1229-1236.

Kobayashi, T., Walsh, P.T., Walsh, M.C., Speirs, K.M., Chiffoleau, E., King, C.G., Hancock, W.W., Caamano, J.H., Hunter, C.A., Scott, P., Turka, L.A., Choi, Y., 2003a. TRAF6 is a critical factor for dendritic cell maturation and development. Immunity 19, 353-363.

Kobayashi, T., Yamaguchi, M., Kim, S., Morikawa, J., Ogawa, S., Ueno, S., Suh, E., Dougherty, E., Shmulevich, I., Shiku, H., Zhang, W., 2003b. Microarray reveals differences in both tumors and vascular specific gene expression in de novo CD5+ and CD5- diffuse large B-cell lymphomas. Cancer Res. 63, 60-66.

Kobayashi, Y., 2008. The role of chemokines in neutrophil biology. Front. Biosci. 13, 2400-2407.

Koch, P., 1957. Heredity of chronic alveolar emphysema of the lungs in horses. Dtsch. Tierarztl. Wochenschr. 64, 485-486.

Korsgren, M., 2002. NK cells and asthma. Curr. Pharm. Des. 8, 1871-1876.

Krimmer, D.I., Loseli, M., Hughes, J.M., Oliver, B.G., Moir, L.M., Hunt, N.H., Black, J.L., Burgess, J.K., 2009. CD40 and OX40 ligand are differentially regulated on asthmatic airway smooth muscle. Allergy 64, 1074-1082.

Kunzle, F., Gerber, V., Van Der Haegen, A., Wampfler, B., Straub, R., Marti, E., 2007. IgE-bearing cells in bronchoalveolar lavage fluid and allergen-specific IgE levels in sera from RAO-affected horses. J Vet Med A Physiol Pathol Clin Med 54, 40-47.

Kurosawa, N., Kanemitsu, Y., Matsui, T., Shimada, K., Ishihama, H., Muramatsu, T., 1999. Genomic analysis of a murine cell-surface sialomucin, MGC-24/CD164. Eur. J. Biochem. 265, 466-472.

Kuskie, K.R., Smith, J.L., Sinha, S., Carter, C.N., Chaffin, M.K., Slovis, N.M., Brown Ii, S.E., Stepusin, R.S., Takai, S., Cohen, N.D., 2011. Associations between the Exposure to Airborne Virulent Rhodococcus equi and the Incidence of R equi Pneumonia among Individual Foals. Journal of Equine Veterinary Science 31, 463-469.

Laan, T.T., Bull, S., Pirie, R., Fink-Gremmels, J., 2006. The role of alveolar macrophages in the pathogenesis of recurrent airway obstruction in horses. J. Vet. Intern. Med. 20, 167-174.

Laan, T.T., Bull, S., Pirie, R.S., Fink-Gremmels, J., 2005. Evaluation of cytokine production by equine alveolar macrophages exposed to lipopolysaccharide, Aspergillus fumigatus, and a suspension of hay dust. Am. J. Vet. Res. 66, 1584-1589.

Lacy, P., 2006. Mechanisms of degranulation in neutrophils. Allergy Asthma Clin Immunol 2, 98-108.

Ladron, N., Fernandez, M., Aguero, J., Gonzalez Zorn, B., Vazquez-Boland, J.A., Navas, J., 2003. Rapid identification of Rhodococcus equi by a PCR assay targeting the choE gene. J. Clin. Microbiol. 41, 3241-3245.

Lai, M.D., Xu, J., 2007. Ribosomal proteins and colorectal cancer. Curr Genomics 8, 43-49.

Lambrecht, B.N., 2005. Dendritic cells and the regulation of the allergic immune response. Allergy 60, 271-282.

Lambrecht, B.N., Hammad, H., 2010. The role of dendritic and epithelial cells as master regulators of allergic airway inflammation. Lancet 376, 835-843.

Lancas, T., Kasahara, D.I., Prado, C.M., Tiberio, I.F., Martins, M.A., Dolhnikoff, M., 2006. Comparison of early and late responses to antigen of sensitized guinea pig parenchymal lung strips. J. Appl. Physiol. 100, 1610-1616.

Lande, R., Giacomini, E., Grassi, T., Remoli, M.E., Iona, E., Miettinen, M., Julkunen, I., Coccia, E.M., 2003. IFN-alpha beta released by Mycobacterium tuberculosis-infected human dendritic cells induces the expression of CXCL10: selective recruitment of NK and activated T cells. J. Immunol. 170, 1174-1182.

Lane, P., 2000. Role of OX40 signals in coordinating CD4 T cell selection, migration, and cytokine differentiation in T helper (Th)1 and Th2 cells. J. Exp. Med. 191, 201-206.

Laprise, C., Sladek, R., Ponton, A., Bernier, M.-C., Hudson, T.J., Laviolette, M., 2004. Functional classes of bronchial mucosa genes that are differentially expressed in asthma. BMC Genomics 5, 21-21.

Lara-Marquez, M.L., Yunis, J.J., Layrisse, Z., Ortega, F., Carvallo-Gil, E., Montagnani, S., Makhatadze, N.J., Pocino, M., Granja, C., Yunis, E., 1999. Immunogenetics of atopic asthma: association of DRB1*1101 DQA1*0501 DQB1*0301

haplotype with Dermatophagoides spp.-sensitive asthma in a sample of the Venezuelan population. Clin. Exp. Allergy 29, 60-71.

Larson, K.C., Lipko, M., Dabrowski, M., Draper, M.P., 2010. Gng12 is a novel negative regulator of LPS-induced inflammation in the microglial cell line BV-2. Inflamm. Res. 59, 15-22.

Lavoie, J.-P. 2007. Recurrent Airway Obstruction (Heaves) and Summer-pasture-associated Obstructive Pulmonary Disease In: Bruce C. McGorum, P.M.D., N. Edward Robinson (Ed.) Equine respiratory medicine and surgery. Saunders Elsevier, 565-589.

Lavoie, J.P., Maghni, K., Desnoyers, M., Taha, R., Martin, J.G., Hamid, Q.A., 2001. Neutrophilic airway inflammation in horses with heaves is characterized by a Th2-type cytokine profile. Am. J. Respir. Crit. Care Med. 164, 1410-1413.

Lazaar, A.L., Panettieri, R.A., Jr., 2005. Airway smooth muscle: a modulator of airway remodeling in asthma. J. Allergy Clin. Immunol. 116, 488-495; quiz 496.

Leclere, M., Lavoie-Lamoureux, A., Gelinas-Lymburner, E., David, F., Martin, J.G., Lavoie, J.-P., 2010. Effect of Antigen Exposure on Airway Smooth Muscle Remodeling in an Equine Model of Chronic Asthma. Am. J. Respir. Cell Mol. Biol.

Leclere, M., Lavoie-Lamoureux, A., Gelinas-Lymburner, E., David, F., Martin, J.G., Lavoie, J.P., 2011a. Effect of antigenic exposure on airway smooth muscle remodeling in an equine model of chronic asthma. Am. J. Respir. Cell Mol. Biol. 45, 181-187.

Leclere, M., Lavoie-Lamoureux, A., Lavoie, J.P., 2011b. Heaves, an asthma-like disease of horses. Respirology 16, 1027-1046.

Lee, B.Y., Jethwaney, D., Schilling, B., Clemens, D.L., Gibson, B.W., Horwitz, M.A., 2010. The Mycobacterium bovis bacille Calmette-Guerin phagosome proteome. Mol Cell Proteomics 9, 32-53.

Lee, J.S., Lee, J.Y., Son, J.W., Oh, J.H., Shin, D.M., Yuk, J.M., Song, C.H., Paik, T.H., Jo, E.K., 2008. Expression and regulation of the CC-chemokine ligand 20 during human tuberculosis. Scand. J. Immunol. 67, 77-85.

Leguillette, R., 2003. Recurrent airway obstruction--heaves. Vet. Clin. North Am. Equine Pract. 19, 63-86, vi.

Li, L., Chen, Y., Zheng, R., Ma, D., Wang, D., 2000. [Expression of TFAR19 in Apoptotic Processes of Jurkat Cells Induced with Various Methods]. Zhongguo Shi Yan Xue Ye Xue Za Zhi 8, 81-84.

Linder, R., 1997. Rhodococcus equi and Arcanobacterium haemolyticum: two "coryneform" bacteria increasingly recognized as agents of human infection. Emerg. Infect. Dis. 3, 145-153.

Liu, C.-Y., Takemasa, A., Liles, W.C., Goodman, R.B., Jonas, M., Rosen, H., Chi, E., Winn, R.K., Harlan, J.M., Chuang, P.I., 2003. Broad-spectrum caspase inhibition paradoxically augments cell death in TNF-alpha -stimulated neutrophils. Blood 101, 295-304.

Liu, T., Nerren, J., Liu, M., Martens, R., Cohen, N., 2009. Basal and stimulus-induced cytokine expression is selectively impaired in peripheral blood mononuclear cells of newborn foals. Vaccine 27, 674-683.

Lloyd, C.M., Hessel, E.M., 2010. Functions of T cells in asthma: more than just T(H)2 cells. Nat Rev Immunol 10, 838-848.

Lorch, G., Hillier, A., Kwochka, K.W., Saville, W.J., Kohn, C.W., Jose-Cunilleras, E., 2001. Results of intradermal tests in horses without atopy and horses with chronic obstructive pulmonary disease. Am. J. Vet. Res. 62, 389-397.

Lou, O., Alcaide, P., Luscinskas, F.W., Muller, W.A., 2007. CD99 is a key mediator of the transendothelial migration of neutrophils. J. Immunol. 178, 1136-1143.

Lowell, F.C., 1964. Observations on Heaves. An Asthma-Like Syndrome in the Horse. J. Allergy, 322-330.

Lu, Y.C., Kim, I., Lye, E., Shen, F., Suzuki, N., Suzuki, S., Gerondakis, S., Akira, S., Gaffen, S.L., Yeh, W.C., Ohashi, P.S., 2009. Differential role for c-Rel and C/EBPbeta/delta in TLR-mediated induction of proinflammatory cytokines. J. Immunol. 182, 7212-7221.

Lugo, J., Harkema, J.R., deFeijter-Rupp, H., Bartner, L., Boruta, D., Robinson, N.E., 2006. Airway inflammation is associated with mucous cell metaplasia and increased intraepithelial stored mucosubstances in horses. Vet. J. 172, 293-301.

Luo, F.M., Wang, Z.L., Liu, X.J., Liu, C.T., Zhang, X.H., Wang, W.Z., 2003. [Expression of Clara cell secretory protein in airways of rat asthma remodel]. Zhonghua Nei Ke Za Zhi 42, 466-469.

Mann, J.S., Cushley, M.J., Holgate, S.T., 1985. Adenosine-induced bronchoconstriction in asthma. Role of parasympathetic stimulation and adrenergic inhibition. Am. Rev. Respir. Dis. 132, 1-6.

Martens, J.G., Martens, R.J., Renshaw, H.W., 1988. Rhodococcus (Corynebacterium) equi: bactericidal capacity of neutrophils from neonatal and adult horses. Am. J. Vet. Res. 49, 295-299.

Martens, R.J., Cohen, N.D., Chaffin, M.K., Takai, S., Doherty, C.L., Angulo, A.B., Edwards, R.E., 2002. Evaluation of 5 serologic assays to detect Rhodococcus equi pneumonia in foals. J Am Vet Med Assoc 221, 825-833.

Martens, R.J., Cohen, N.D., Jones, S.L., Moore, T.A., Edwards, J.F., 2005. Protective role of neutrophils in mice experimentally infected with Rhodococcus equi. Infect. Immun. 73, 7040-7042.

Marti, E., Gerber, H., Essich, G., Oulehla, J., Lazary, S., 1991. The genetic basis of equine allergic diseases. 1. Chronic hypersensitivity bronchitis. Equine Vet. J. 23, 457-460.

Marti, E., Gerber, V., Wilson, A.D., Lavoie, J.P., Horohov, D., Crameri, R., Lunn, D.P., Antczak, D., Bjornsdottir, S., Bjornsdottir, T.S., Cunningham, F., Derer, M., Frey, R., Hamza, E., Horin, P., Heimann, M., Kolm-Stark, G., Olafsdottir, G., Ramery, E., Russell, C., Schaffartzik, A., Svansson, V., Torsteinsdottir, S., Wagner, B., 2008. Report of the 3rd Havemeyer workshop on allergic diseases of

the Horse, Holar, Iceland, June 2007. Vet. Immunol. Immunopathol. 126, 351-361.

McGorum, B.C., Dixon, P.M., Halliwell, R.E., 1993. Quantification of histamine in plasma and pulmonary fluids from horses with chronic obstructive pulmonary disease, before and after 'natural (hay and straw) challenges'. Vet. Immunol. Immunopathol. 36, 223-237.

McTaggart, C., Yovich, J.V., Penhale, J., Raidal, S.L., 2001. A comparison of foal and adult horse neutrophil function using flow cytometric techniques. Res. Vet. Sci. 71, 73-79.

Meijer, W.G., Prescott, J.F., 2004. Rhodococcus equi. Vet. Res. 35, 383-396.

Moalem, S., Weinberg, E.D., Percy, M.E., 2004. Hemochromatosis and the enigma of misplaced iron: implications for infectious disease and survival. Biometals 17, 135-139.

Mobini, R., Andersson, B.A., Erjefalt, J., Hahn-Zoric, M., Langston, M.A., Perkins, A.D., Cardell, L.O., Benson, M., 2009. A module-based analytical strategy to identify novel disease-associated genes shows an inhibitory role for interleukin 7 Receptor in allergic inflammation. BMC Syst Biol 3, 19.

Mocsai, A., Ligeti, E., Lowell, C.A., Berton, G., 1999. Adhesion-dependent degranulation of neutrophils requires the Src family kinases Fgr and Hck. J. Immunol. 162, 1120-1126.

Moffatt, M.F., Schou, C., Faux, J.A., Abecasis, G.R., James, A., Musk, A.W., Cookson, W.O., 2001. Association between quantitative traits underlying asthma and the HLA-DRB1 locus in a family-based population sample. Eur. J. Hum. Genet. 9, 341-346.

Moran, G., Burgos, R., Araya, O., Folch, H., 2010. In vitro bioassay to detect reaginic antibodies from the serum of horses affected with recurrent airway obstruction. Vet. Res. Commun. 34, 91-99.

Moran, G., Folch, H., 2011. Recurrent airway obstruction in horses – an allergic inflammation: a review. Vet. Med. (Praha).

Morey, J.S., Ryan, J.C., Van Dolah, F.M., 2006. Microarray validation: factors influencing correlation between oligonucleotide microarrays and real-time PCR. Biol Proced Online 8, 175-193.

Morikawa, J., Li, H., Kim, S., Nishi, K., Ueno, S., Suh, E., Dougherty, E., Shmulevich, I., Shiku, H., Zhang, W., Kobayashi, T., 2003. Identification of signature genes by microarray for acute myeloid leukemia without maturation and acute promyelocytic leukemia with t(15;17)(q22;q12)(PML/RARalpha). Int. J. Oncol. 23, 617-625.

Mousel, M.R., Harrison, L., Donahue, J.M., Bailey, E., 2003. Rhodococcus equi and genetic susceptibility: assessing transferrin genotypes from paraffin-embedded tissues. J. Vet. Diagn. Invest. 15, 470-472.

Muller, S., Filippakopoulos, P., Knapp, S., 2011. Bromodomains as therapeutic targets. Expert Rev Mol Med 13, e29.

Muscatello, G., Anderson, G.A., Gilkerson, J.R., Browning, G.F., 2006. Associations between the ecology of virulent Rhodococcus equi and the epidemiology of R. equi pneumonia on Australian thoroughbred farms. Appl. Environ. Microbiol. 72, 6152-6160.

Muscatello, G., Leadon, D.P., Klayt, M., Ocampo-Sosa, A., Lewis, D.A., Fogarty, U., Buckley, T., Gilkerson, J.R., Meijer, W.G., Vazquez-Boland, J.A., 2007. Rhodococcus equi infection in foals: the science of 'rattles'. Equine Vet. J. 39, 470-478.

Nakanishi, A., Morita, S., Iwashita, H., Sagiya, Y., Ashida, Y., Shirafuji, H., Fujisawa, Y., Nishimura, O., Fujino, M., 2001. Role of gob-5 in mucus overproduction and airway hyperresponsiveness in asthma. Proc. Natl. Acad. Sci. U. S. A. 98, 5175-5180.

Naora, H., 1999. Involvement of ribosomal proteins in regulating cell growth and apoptosis: translational modulation or recruitment for extraribosomal activity? Immunol. Cell Biol. 77, 197-205.

Naora, H., Takai, I., Adachi, M., Naora, H., 1998. Altered Cellular Responses by Varying Expression of a Ribosomal Protein Gene: Sequential Coordination of Enhancement and Suppression of Ribosomal Protein S3a Gene Expression Induces Apoptosis. The Journal of Cell Biology 141, 741-753.

Narren, J.R., 2007. Innate immunity to rhodococcus equi: The response of adult and juvenile equine neutrophils. Texas A&M University, ProQuest Dissertations and Theses.

Nelson, H.S., Busse, W.W., Kerwin, E., Church, N., Emmett, A., Rickard, K., Knobil, K., 2000. Fluticasone propionate/salmeterol combination provides more effective asthma control than low-dose inhaled corticosteroid plus montelukast. J. Allergy Clin. Immunol. 106, 1088-1095.

Nerren, J.R., Martens, R.J., Payne, S., Murrell, J., Butler, J.L., Cohen, N.D., 2009. Age-related changes in cytokine expression by neutrophils of foals stimulated with virulent Rhodococcus equi in vitro. Vet. Immunol. Immunopathol. 127, 212-219.

Nissim Ben Efraim, A.H., Levi-Schaffer, F., 2008. Tissue remodeling and angiogenesis in asthma: the role of the eosinophil. Ther Adv Respir Dis 2, 163-171.

Nordmann, P., Ronco, E., Nauciel, C., 1992. Role of T-lymphocyte subsets in Rhodococcus equi infection. Infect. Immun. 60, 2748-2752.

O'Connor, A.M., Crawley, A.M., Angel, J.B., 2010. Interleukin-7 enhances memory CD8(+) T-cell recall responses in health but its activity is impaired in human immunodeficiency virus infection. Immunology 131, 525-536.

Ober, C., Tan, Z., Sun, Y., Possick, J.D., Pan, L., Nicolae, R., Radford, S., Parry, R.R., Heinzmann, A., Deichmann, K.A., Lester, L.A., Gern, J.E., Lemanske, R.F., Jr., Nicolae, D.L., Elias, J.A., Chupp, G.L., 2008. Effect of variation in CHI3L1 on serum YKL-40 level, risk of asthma, and lung function. N. Engl. J. Med. 358, 1682-1691.

Onsongo, G., Hongwei, X., Griffin, T.J., Carlis, J. 2008. Generating GO Slim Using Relational Database Management Systems to Support Proteomics Analysis. In: Computer-Based Medical Systems, 2008. CBMS '08. 21st IEEE International Symposium on, 17-19 June 2008, 215-217.

Pargass, I.S., Wills, T.B., Davis, W.C., Wardrop, K.J., Alperin, D.C., Hines, S.A., 2009. The influence of age and Rhodococcus equi infection on CD1 expression by equine antigen presenting cells. Vet. Immunol. Immunopathol. 130, 197-209.

Pasare, C., Medzhitov, R., 2004. Toll-like receptors: linking innate and adaptive immunity. Microbes Infect 6, 1382-1387.

Pascual, R.M., Peters, S.P., 2005. Airway remodeling contributes to the progressive loss of lung function in asthma: an overview. J. Allergy Clin. Immunol. 116, 477-486; quiz 487.

Patton, K.M., McGuire, T.C., Hines, M.T., Mealey, R.H., Hines, S.A., 2005. Rhodococcus equi-specific cytotoxic T lymphocytes in immune horses and development in asymptomatic foals. Infect. Immun. 73, 2083-2093.

Pfaffl, M.W., 2001. A new mathematical model for relative quantification in real-time RT-PCR. Nucleic Acids Res 29.

Picandet, V., Leguillette, R., Lavoie, J.P., 2003. Comparison of efficacy and tolerability of isoflupredone and dexamethasone in the treatment of horses affected with recurrent airway obstruction ('heaves'). Equine Vet. J. 35, 419-424.

Pietra, M., Peli, A., Bonato, A., Ducci, A., Cinotti, S., 2007. Equine bronchoalveolar lavage cytokines in the development of recurrent airway obstruction. Vet. Res. Commun. 31 Suppl 1, 313-316.

Platts-Mills, T.A., 2003. Allergen avoidance in the treatment of asthma and rhinitis. N. Engl. J. Med. 349, 207-208.

Polikepahad, S., Haque, M., Francis, J., Moore, R.M., Venugopal, C.S., 2008. Characterization of endothelin receptors in the peripheral lung tissues of horses unaffected and affected with recurrent airway obstruction. Can. J. Vet. Res. 72, 340-349.

Polikepahad, S., Paulsen, D.B., Moore, R.M., Costa, L.R., Venugopal, C.S., 2006. Immunohistochemical determination of the expression of endothelin receptors in bronchial smooth muscle and epithelium of healthy horses and horses affected by

summer pasture-associated obstructive pulmonary disease. Am. J. Vet. Res. 67, 348-357.

Postma, D.S., Timens, W., 2006. Remodeling in asthma and chronic obstructive pulmonary disease. Proc Am Thorac Soc 3, 434-439.

Prescott, J.F., 1991. Rhodococcus equi: an animal and human pathogen. Clin. Microbiol. Rev. 4, 20-34.

Prescott, J.F., Meijer, W.G., Boland-Vazquez, J.A. 2010. Pathogenesis of Bacterial Infections in Animals, In: Gyles, L.C., Prescott, J.F., Songer, G., Thoen, O.C. (Eds.) Pathogenesis of Bacterial Infections in Animals. 149-166.

Pusterla, N., Wilson, W.D., Mapes, S., Leutenegger, C.M., 2007. Diagnostic evaluation of real-time PCR in the detection of Rhodococcus equi in faeces and nasopharyngeal swabs from foals with pneumonia. Vet. Rec. 161, 272-275.

Raby, B.A., Van Steen, K., Lasky-Su, J., Tantisira, K., Kaplan, F., Weiss, S.T., 2009. Importin-13 genetic variation is associated with improved airway responsiveness in childhood asthma. Respir Res 10, 67.

Rachman, H., Strong, M., Ulrichs, T., Grode, L., Schuchhardt, J., Mollenkopf, H., Kosmiadi, G.A., Eisenberg, D., Kaufmann, S.H., 2006. Unique transcriptome signature of Mycobacterium tuberculosis in pulmonary tuberculosis. Infect. Immun. 74, 1233-1242.

Rahman, M.T., Parreira, V., Prescott, J.F., 2005. In vitro and intra-macrophage gene expression by Rhodococcus equi strain 103. Vet. Microbiol. 110, 131-140.

Ramalho, A.S., Beck, S., Farinha, C.M., Clarke, L.A., Heda, G.D., Steiner, B., Sanz, J., Gallati, S., Amaral, M.D., Harris, A., Tzetis, M., 2004. Methods for RNA extraction, cDNA preparation and analysis of CFTR transcripts. J Cyst Fibros 3 Suppl 2, 11-15.

Ramalho, R., Soares, R., Couto, N., Moreira, A., 2011. Tachykinin receptors antagonism for asthma: a systematic review. BMC Pulm Med 11, 41.

Ramery, E., Closset, R., Art, T., Bureau, F., Lekeux, P., 2009. Expression microarrays in equine sciences. Vet. Immunol. Immunopathol. 127, 197-202.

Ramery, E., Closset, R., Bureau, F., Art, T., Lekeux, P., 2008a. Relevance of using a human microarray to study gene expression in heaves-affected horses. Vet. J. 177, 216-221.

Ramery, E., Closset, R., Bureau, F., Art, T., Lekeux, P., 2008b. Relevance of using a human microarray to study gene expression in heaves-affected horses. Vet J 177, 216-221.

Ramery, E., Fievez, L., Fraipont, A., Bureau, F., Lekeux, P., 2010. Characterization of pentraxin 3 in the horse and its expression in airways. Vet. Res. 41, 18.

Ramseyer, A., Gaillard, C., Burger, D., Straub, R., Jost, U., Boog, C., Marti, E., Gerber, V., 2007. Effects of genetic and environmental factors on chronic lower airway disease in horses. J. Vet. Intern. Med. 21, 149-156.

Relave, F., David, F., Leclere, M., Alexander, K., Bussieres, G., Lavoie, J.P., Marcoux, M., 2008. Evaluation of a thoracoscopic technique using ligating loops to obtain large lung biopsies in standing healthy and heaves-affected horses. Vet. Surg. 37, 232-240.

Ren, J., Prescott, J.F., 2003. Analysis of virulence plasmid gene expression of intra-macrophage and in vitro grown Rhodococcus equi ATCC 33701. Vet. Microbiol. 94, 167-182.

Reyner, C.L., Wagner, B., Young, J.C., Ainsworth, D.M., 2009. Effects of in vitro exposure to hay dust on expression of interleukin-23, -17, -8, and -1beta and chemokine (C-X-C motif) ligand 2 by pulmonary mononuclear cells from horses susceptible to recurrent airway obstruction. Am. J. Vet. Res. 70, 1277-1283.

Ribatti, D., Puxeddu, I., Crivellato, E., Nico, B., Vacca, A., Levi-Schaffer, F., 2009. Angiogenesis in asthma. Clin. Exp. Allergy 39, 1815-1821.

Richter, D.C., Joubert, J.R., Nell, H., Schuurmans, M.M., Irusen, E.M., 2008. Diagnostic value of post-bronchodilator pulmonary function testing to distinguish between

stable, moderate to severe COPD and asthma. Int J Chron Obstruct Pulmon Dis 3, 693-699.

Ritchie, M.E., Silver, J., Oshlack, A., Holmes, M., Diyagama, D., Holloway, A., Smyth, G.K., 2007. A comparison of background correction methods for two-colour microarrays. Bioinformatics 23, 2700-2707.

Roberts, B., Hirst, R., 1996. Identification and characterisation of a superoxide dismutase and catalase from Mycobacterium ulcerans. J. Med. Microbiol. 45, 383-387.

Robinson, N.E. 2001. Recurrent airway obstruction (Heaves), In: Lekeux, P. (Ed.) Equine Respiratory Diseases, Document No. B0317.1101. International Veterinary Information Service (http://www.ivis.org), Ithaca, New York.

Robinson, N.E., Derksen, F.J., Berney, C., Goossens, L., 1993a. The airway response of horses with recurrent airway obstruction (heaves) to aerosol administration of ipratropium bromide. Equine veterinary journal 25, 299-303.

Robinson, N.E., Derksen, F.J., Berney, C., Goossens, L., 1993b. The airway response of horses with recurrent airway obstruction (heaves) to aerosol administration of ipratropium bromide. Equine Vet J 25, 299-303.

Robinson, N.E., Derksen, F.J., Olszewski, M.A., Buechner-Maxwell, V.A., 1996. The pathogenesis of chronic obstructive pulmonary disease of horses. Br. Vet. J. 152, 283-306.

Robinson, N.E., Jackson, C., Jefcoat, A., Berney, C., Peroni, D., Derksen, F.J., 2002. Efficacy of three corticosteroids for the treatment of heaves. Equine Vet. J. 34, 17-22.

Rodriguez-Lazaro, D., Lewis, D.A., Ocampo-Sosa, A.A., Fogarty, U., Makrai, L., Navas, J., Scortti, M., Hernandez, M., Vazquez-Boland, J.A., 2006. Internally controlled real-time PCR method for quantitative species-specific detection and vapA genotyping of Rhodococcus equi. Appl. Environ. Microbiol. 72, 4256-4263.

Romagnani, S., 2002. Cytokines and chemoattractants in allergic inflammation. Mol. Immunol. 38, 881-885.

Ross, T.L., Balson, G.A., Miners, J.S., Smith, G.D., Shewen, P.E., Prescott, J.F., Yager, J.A., 1996. Role of CD4+, CD8+ and double negative T-cells in the protection of SCID/beige mice against respiratory challenge with Rhodococcus equi. Can. J. Vet. Res. 60, 186-192.

Rousseau, K., Kirkham, S., McKane, S., Newton, R., Clegg, P., Thornton, D.J., 2007. Muc5b and Muc5ac are the major oligomeric mucins in equine airway mucus. Am J Physiol Lung Cell Mol Physiol 292, L1396-1404.

Ruland, J., 2008. CARD9 signaling in the innate immune response. Ann. N. Y. Acad. Sci. 1143, 35-44.

Ryan, C., Giguere, S., Hagen, J., Hartnett, C., Kalyuzhny, A.E., 2010. Effect of age and mitogen on the frequency of interleukin-4 and interferon gamma secreting cells in foals and adult horses as assessed by an equine-specific ELISPOT assay. Vet. Immunol. Immunopathol. 133, 66-71.

Ryckman, C., Vandal, K., Rouleau, P., Talbot, M., Tessier, P.A., 2003. Proinflammatory activities of S100: proteins S100A8, S100A9, and S100A8/A9 induce neutrophil chemotaxis and adhesion. J. Immunol. 170, 3233-3242.

Ryhner, T., Muller, N., Balmer, V., Gerber, V., 2008. Increased mucus accumulation in horses chronically affected with recurrent airway obstruction is not associated with up-regulation of CLCA1, EGFR, MUC5AC, Bcl-2, IL-13 and INF-gamma expression. Vet. Immunol. Immunopathol. 125, 8-17.

S. Varma, G.M., J. Wang, A. Hinds, BS, D. Kotton, M. I. Ramirez 2009. Role of Grainyhead−Like Transcription Factors Grhl2 and Grhl3 in Morphogenesis of Alveolar Epithelial Cells.

Saatian, B., Yu, X.Y., Lane, A.P., Doyle, T., Casolaro, V., Spannhake, E.W., 2004. Expression of genes for B7-H3 and other T cell ligands by nasal epithelial cells during differentiation and activation. Am J Physiol Lung Cell Mol Physiol 287, L217-225.

Sano, H., Hsu, D.K., Apgar, J.R., Yu, L., Sharma, B.B., Kuwabara, I., Izui, S., Liu, F.T., 2003. Critical role of galectin-3 in phagocytosis by macrophages. J. Clin. Invest. 112, 389-397.

Schaeper, W., 1939. Untersuchungen über die Erblichkeit und das Wesen des Lungendampfes beim Pferd Investigation into the nature and heritability of heaves in the horse. Tierärztliche Rundschau 31, 595-599.

Schelfhout, V., Van De Velde, V., Maggi, C., Pauwels, R., Joos, G., 2009. The effect of the tachykinin NK(2) receptor antagonist MEN11420 (nepadutant) on neurokinin A-induced bronchoconstriction in asthmatics. Ther Adv Respir Dis 3, 219-226.

Schnare, M., Barton, G.M., Holt, A.C., Takeda, K., Akira, S., Medzhitov, R., 2001. Toll-like receptors control activation of adaptive immune responses. Nat Immunol 2, 947-950.

Schuh, J.M., Blease, K., Hogaboam, C.M., 2001. The role of CC chemokine receptor 5 (CCR5) and RANTES/CCL5 during chronic fungal asthma in mice1. The FASEB Journal.

Schutyser, E., Struyf, S., Van Damme, J., 2003. The CC chemokine CCL20 and its receptor CCR6. Cytokine Growth Factor Rev. 14, 409-426.

Schwartz, M.A., Assoian, R.K., 2001. Integrins and cell proliferation: regulation of cyclin-dependent kinases via cytoplasmic signaling pathways. J. Cell Sci. 114, 2553-2560.

Sellon, D.C., Besser, T.E., Vivrette, S.L., McConnico, R.S., 2001. Comparison of nucleic acid amplification, serology, and microbiologic culture for diagnosis of Rhodococcus equi pneumonia in foals. J. Clin. Microbiol. 39, 1289-1293.

Sheoran, A.S., Timoney, J.F., Holmes, M.A., Karzenski, S.S., Crisman, M.V., 2000. Immunoglobulin isotypes in sera and nasal mucosal secretions and their neonatal transfer and distribution in horses. Am. J. Vet. Res. 61, 1099-1105.

Shizuo, A., 2003. Mammalian Toll-like receptors. Curr. Opin. Immunol. 15, 5-11.

Simcock, D.E., Kanabar, V., Clarke, G.W., Mahn, K., Karner, C., O'Connor, B.J., Lee, T.H., Hirst, S.J., 2008. Induction of angiogenesis by airway smooth muscle from patients with asthma. Am. J. Respir. Crit. Care Med. 178, 460-468.

Simon, R.M., Dobbin, K., 2003. Experimental design of DNA microarray experiments. Biotechniques Suppl, 16-21.

Simpson, A., Custovic, A., 2004. Allergen avoidance in the primary prevention of asthma. Curr Opin Allergy Clin Immunol 4, 45-51.

Smyth, G.K., 2004. Linear models and empirical bayes methods for assessing differential expression in microarray experiments. Stat Appl Genet Mol Biol 3.

Smyth, G.K. 2005. Individual Channel Analysis of Two-Colour Microarrays. In: Proceedings of the 55th Session of the International Statistics Institute, Sydney, Australia.

Smyth, G.K., Speed, T., 2003a. Normalization of cDNA microarray data. Methods 31, 265-273.

Smyth, G.K., Speed, T., 2003b. Normalization of cDNA microarray data. Methods 31, 265-273.

Spinetti, G., Bernardini, G., Camarda, G., Mangoni, A., Santoni, A., Capogrossi, M.C., Napolitano, M., 2003. The chemokine receptor CCR8 mediates rescue from dexamethasone-induced apoptosis via an ERK-dependent pathway. J. Leukoc. Biol. 73, 201-207.

Starner, T.D., Barker, C.K., Jia, H.P., Kang, Y., McCray, P.B., Jr., 2003. CCL20 is an inducible product of human airway epithelia with innate immune properties. Am. J. Respir. Cell Mol. Biol. 29, 627-633.

Stears, R.L., Getts, R.C., Gullans, S.R., 2000. A novel, sensitive detection system for high-density microarrays using dendrimer technology. Physiol Genomics 3, 93-99.

Steinberger, P., Majdic, O., Derdak, S.V., Pfistershammer, K., Kirchberger, S., Klauser, C., Zlabinger, G., Pickl, W.F., Stockl, J., Knapp, W., 2004. Molecular characterization of human 4Ig-B7-H3, a member of the B7 family with four Ig-like domains. J. Immunol. 172, 2352-2359.

Suh, W.K., Gajewska, B.U., Okada, H., Gronski, M.A., Bertram, E.M., Dawicki, W., Duncan, G.S., Bukczynski, J., Plyte, S., Elia, A., Wakeham, A., Itie, A., Chung, S., Da Costa, J., Arya, S., Horan, T., Campbell, P., Gaida, K., Ohashi, P.S., Watts, T.H., Yoshinaga, S.K., Bray, M.R., Jordana, M., Mak, T.W., 2003. The B7 family member B7-H3 preferentially down-regulates T helper type 1-mediated immune responses. Nat Immunol 4, 899-906.

Sumi, Y., Hamid, Q., 2007. Airway remodeling in asthma. Allergol Int 56, 341-348.

Sun, J.C., Liang, X.T., Pan, K., Wang, H., Zhao, J.J., Li, J.J., Ma, H.Q., Chen, Y.B., Xia, J.C., 2010. High expression level of EDIL3 in HCC predicts poor prognosis of HCC patients. World J Gastroenterol 16, 4611-4615.

Swinburne, J.E., Bogle, H., Klukowska-Rotzler, J., Drogemuller, M., Leeb, T., Temperton, E., Dolf, G., Gerber, V., 2009. A whole-genome scan for recurrent airway obstruction in Warmblood sport horses indicates two positional candidate regions. Mamm. Genome 20, 504-515.

Syed, F., Panettieri, R.A., Tliba, O., Huang, C., Li, K., Bracht, M., Amegadzie, B., Griswold, D., Li, L., Amrani, Y., 2005. The effect of IL-13 and IL-13R130Q, a naturally occurring IL-13 polymorphism, on the gene expression of human airway smooth muscle cells. Respir Res 6, 9-9.

Tahon, L., Baselgia, S., Gerber, V., Doherr, M.G., Straub, R., Robinson, N.E., Marti, E., 2009. In vitro allergy tests compared to intradermal testing in horses with recurrent airway obstruction. Vet. Immunol. Immunopathol. 127, 85-93.

Takai, S., 1997. Epidemiology of Rhodococcus equi infections: a review. Vet. Microbiol. 56, 167-176.

Takai, S., Chaffin, M.K., Cohen, N.D., Hara, M., Nakamura, M., Kakuda, T., Sasaki, Y., Tsubaki, S., Martens, R.J., 2001. Prevalence of virulent Rhodococcus equi in soil from five R. equi-endemic horse-breeding farms and restriction fragment length

polymorphisms of virulence plasmids in isolates from soil and infected foals in Texas. J. Vet. Diagn. Invest. 13, 489-494.

Takai, S., Fujimori, T., Katsuzaki, K., Tsubaki, S., 1987. Ecology of Rhodococcus equi in horses and their environment on horse-breeding farms. Vet. Microbiol. 14, 233-239.

Takai, S., Fukunaga, N., Kamisawa, K., Imai, Y., Sasaki, Y., Tsubaki, S., 1996. Expression of virulence-associated antigens of Rhodococcus equi is regulated by temperature and pH. Microbiol. Immunol. 40, 591-594.

Takai, S., Hines, S.A., Sekizaki, T., Nicholson, V.M., Alperin, D.A., Osaki, M., Takamatsu, D., Nakamura, M., Suzuki, K., Ogino, N., Kakuda, T., Dan, H., Prescott, J.F., 2000. DNA sequence and comparison of virulence plasmids from Rhodococcus equi ATCC 33701 and 103. Infect. Immun. 68, 6840-6847.

Takai, S., Ikeda, T., Sasaki, Y., Watanabe, Y., Ozawa, T., Tsubaki, S., Sekizaki, T., 1995a. Identification of virulent Rhodococcus equi by amplification of gene coding for 15- to 17-kilodalton antigens. J. Clin. Microbiol. 33, 1624-1627.

Takai, S., Imai, Y., Fukunaga, N., Uchida, Y., Kamisawa, K., Sasaki, Y., Tsubaki, S., Sekizaki, T., 1995b. Identification of virulence-associated antigens and plasmids in Rhodococcus equi from patients with AIDS. J. Infect. Dis. 172, 1306-1311.

Takai, S., Kawazu, S., Tsubaki, S., 1985. Enzyme-linked immunosorbent assay for diagnosis of Corynebacterium (Rhodococcus) equi infection in foals. Am. J. Vet. Res. 46, 2166-2170.

Takai, S., Martens, R.J., Julian, A., Garcia Ribeiro, M., Rodrigues de Farias, M., Sasaki, Y., Inuzuka, K., Kakuda, T., Tsubaki, S., Prescott, J.F., 2003. Virulence of Rhodococcus equi isolated from cats and dogs. J. Clin. Microbiol. 41, 4468-4470.

Takai, S., Narita, K., Ando, K., Tsubaki, S., 1986. Ecology of Rhodococcus (Corynebacterium) equi in soil on a horse-breeding farm. Vet. Microbiol. 12, 169-177.

Takai, S., Ohbushi, S., Koike, K., Tsubaki, S., Oishi, H., Kamada, M., 1991. Prevalence of virulent Rhodococcus equi in isolates from soil and feces of horses from horse-breeding farms with and without endemic infections. J. Clin. Microbiol. 29, 2887-2889.

Takai, S., Watanabe, Y., Ikeda, T., Ozawa, T., Matsukura, S., Tamada, Y., Tsubaki, S., Sekizaki, T., 1993. Virulence-associated plasmids in Rhodococcus equi. J. Clin. Microbiol. 31, 1726-1729.

Takeda, A., Hamano, S., Yamanaka, A., Hanada, T., Ishibashi, T., Mak, T.W., Yoshimura, A., Yoshida, H., 2003. Cutting edge: role of IL-27/WSX-1 signaling for induction of T-bet through activation of STAT1 during initial Th1 commitment. J. Immunol. 170, 4886-4890.

Takizawa, H., 2007. Novel strategies for the treatment of asthma. Recent Pat Inflamm Allergy Drug Discov 1, 13-19.

Tanaka, T., Akira, S., Yoshida, K., Umemoto, M., Yoneda, Y., Shirafuji, N., Fujiwara, H., Suematsu, S., Yoshida, N., Kishimoto, T., 1995. Targeted disruption of the NF-IL6 gene discloses its essential role in bacteria killing and tumor cytotoxicity by macrophages. Cell 80, 353-361.

Tao, T., Lan, J., Lukacs, G.L., Hache, R.J., Kaplan, F., 2006. Importin 13 regulates nuclear import of the glucocorticoid receptor in airway epithelial cells. Am. J. Respir. Cell Mol. Biol. 35, 668-680.

Tobian, A.A., Harding, C.V., Canaday, D.H., 2005. Mycobacterium tuberculosis heat shock fusion protein enhances class I MHC cross-processing and -presentation by B lymphocytes. J. Immunol. 174, 5209-5214.

van Erck, E., Votion, D.M., Kirschvink, N., Art, T., Lekeux, P., 2003. Use of the impulse oscillometry system for testing pulmonary function during methacholine bronchoprovocation in horses. Am. J. Vet. Res. 64, 1414-1420.

Van Vyve, T., Chanez, P., Bernard, A., Bousquet, J., Godard, P., Lauwerijs, R., Sibille, Y., 1995. Protein content in bronchoalveolar lavage fluid of patients with asthma and control subjects. J. Allergy Clin. Immunol. 95, 60-68.

Vandal, K., Rouleau, P., Boivin, A., Ryckman, C., Talbot, M., Tessier, P.A., 2003. Blockade of S100A8 and S100A9 suppresses neutrophil migration in response to lipopolysaccharide. J Immunol 171, 2602-2609.

Vandenput, S., Duvivier, D.H., Votion, D., Art, T., Lekeux, P., 1998. Environmental control to maintain stabled COPD horses in clinical remission: effects on pulmonary function. Equine Vet. J. 30, 93-96.

Vandenput, S., Istasse, L., Nicks, B., Lekeux, P., 1997. Airborne dust and aeroallergen concentrations in different sources of feed and bedding for horses. Vet. Q. 19, 154-158.

Veenman, L., Papadopoulos, V., Gavish, M., 2007. Channel-like functions of the 18-kDa translocator protein (TSPO): regulation of apoptosis and steroidogenesis as part of the host-defense response. Curr. Pharm. Des. 13, 2385-2405.

Venugopal, C.S., Holmes, E.P., Polikepahad, S., Laborde, S., Kearney, M., Moore, R.M., 2009. Neurokinin receptors in recurrent airway obstruction: a comparative study of affected and unaffected horses. Can. J. Vet. Res. 73, 25-33.

Venugopal, C.S., Mendes, L.C., Peiro, J.R., Laborde, S.S., Stokes, A.M., Moore, R.M., 2010a. Transcriptional changes associated with recurrent airway obstruction in affected and unaffected horses. Am. J. Vet. Res. 71, 476-482.

Venugopal, C.S., Mendes, L.C.N., Peiro, J.R., Laborde, S.S., Stokes, A.M., Moore, R.M., 2010b. Transcriptional changes associated with recurrent airway obstruction in affected and unaffected horses. Am. J. Vet. Res. 71, 476-482.

Venugopal, C.S., Polikepahad, S., Holmes, E.P., Heuvel, J.V., Leas, T.L., Moore, R.M., 2006. Endothelin receptor alterations in equine airway hyperreactivity. Can. J. Vet. Res. 70, 50-57.

Viemari, J.C., Bevengut, M., Burnet, H., Coulon, P., Pequignot, J.M., Tiveron, M.C., Hilaire, G., 2004. Phox2a gene, A6 neurons, and noradrenaline are essential for development of normal respiratory rhythm in mice. J. Neurosci. 24, 928-937.

Vignola, A.M., Gagliardo, R., Siena, A., Chiappara, G., Bonsignore, M.R., Bousquet, J., Bonsignore, G., 2001. Airway remodeling in the pathogenesis of asthma. Curr Allergy Asthma Rep 1, 108-115.

Vignola, A.M., Kips, J., Bousquet, J., 2000. Tissue remodeling as a feature of persistent asthma. J. Allergy Clin. Immunol. 105, 1041-1053.

Vignola, A.M., Mirabella, F., Costanzo, G., Di Giorgi, R., Gjomarkaj, M., Bellia, V., Bonsignore, G., 2003. Airway remodeling in asthma. Chest 123, 417S-422S.

Vigorito, E., Bell, S., Hebeis, B.J., Reynolds, H., McAdam, S., Emson, P.C., McKenzie, A., Turner, M., 2004. Immunological function in mice lacking the Rac-related GTPase RhoG. Mol. Cell. Biol. 24, 719-729.

Vigorito, E., Billadeu, D.D., Savoy, D., McAdam, S., Doody, G., Fort, P., Turner, M., 2003. RhoG regulates gene expression and the actin cytoskeleton in lymphocytes. Oncogene 22, 330-342.

Vincent, S., Jeanteur, P., Fort, P., 1992. Growth-regulated expression of rhoG, a new member of the ras homolog gene family. Mol. Cell. Biol. 12, 3138-3148.

von Bargen, K., Haas, A., 2009. Molecular and infection biology of the horse pathogen Rhodococcus equi. FEMS Microbiol. Rev. 33, 870-891.

von Bargen, K., Polidori, M., Becken, U., Huth, G., Prescott, J.F., Haas, A., 2009. Rhodococcus equi virulence-associated protein A is required for diversion of phagosome biogenesis but not for cytotoxicity. Infect. Immun. 77, 5676-5681.

Vranjkovic, A., Crawley, A.M., Gee, K., Kumar, A., Angel, J.B., 2007. IL-7 decreases IL-7 receptor alpha (CD127) expression and induces the shedding of CD127 by human CD8+ T cells. Int. Immunol. 19, 1329-1339.

Wada, H., Noguchi, Y., Marino, M.W., Dunn, A.R., Old, L.J., 1997. T cell functions in granulocyte/macrophage colony-stimulating factor deficient mice. Proc. Natl. Acad. Sci. U. S. A. 94, 12557-12561.

Wagner, B., 2009. IgE in horses: occurrence in health and disease. Vet. Immunol. Immunopathol. 132, 21-30.

Wagner, B., Miller, D.C., Lear, T.L., Antczak, D.F., 2004. The complete map of the Ig heavy chain constant gene region reveals evidence for seven IgG isotypes and for IgD in the horse. J. Immunol. 173, 3230-3242.

Wang, J.P., Rought, S.E., Corbeil, J., Guiney, D.G., 2003. Gene expression profiling detects patterns of human macrophage responses following Mycobacterium tuberculosis infection. FEMS Immunol. Med. Microbiol. 39, 163-172.

Wang, Y.H., Liu, Y.J., 2007. OX40-OX40L interactions: a promising therapeutic target for allergic diseases? J. Clin. Invest. 117, 3655-3657.

Wang, Z., Gerstein, M., Snyder, M., 2009. RNA-Seq: a revolutionary tool for transcriptomics. Nat Rev Genet 10, 57-63.

Watson, J.L., Stott, J.L., Blanchard, M.T., Lavoie, J.P., Wilson, W.D., Gershwin, L.J., Wilson, D.W., 1997. Phenotypic characterization of lymphocyte subpopulations in horses affected with chronic obstructive pulmonary disease and in normal controls. Vet. Pathol. 34, 108-116.

Weinstock, D.M., Brown, A.E., 2002. Rhodococcus equi: an emerging pathogen. Clin. Infect. Dis. 34, 1379-1385.

Werth, M., Walentin, K., Aue, A., Schonheit, J., Wuebken, A., Pode-Shakked, N., Vilianovitch, L., Erdmann, B., Dekel, B., Bader, M., Barasch, J., Rosenbauer, F., Luft, F.C., Schmidt-Ott, K.M., 2010. The transcription factor grainyhead-like 2 regulates the molecular composition of the epithelial apical junctional complex. Development 137, 3835-3845.

Wichtel, M.G., Anderson, K.L., Johnson, T.V., Nathan, U., Smith, L., 1991. Influence of age on neutrophil function in foals. Equine Vet. J. 23, 466-469.

Williams, I.R., 2006. CCR6 and CCL20: partners in intestinal immunity and lymphorganogenesis. Ann. N. Y. Acad. Sci. 1072, 52-61.

Wolanczyk-Medrala, A., Barg, W., Liebhart, J., Panaszek, B., Nadobna, G., Litwa, M., Gogolewski, G., Medrala, W., 2010. Validation of Basophil CD164 Upregulation for Pollen Allergy Diagnosis. Arch. Immunol. Ther. Exp. (Warsz). 58, 459-465.

Wolf, A.M., Wolf, D., Rumpold, H., Enrich, B., Tilg, H., 2004. Adiponectin induces the anti-inflammatory cytokines IL-10 and IL-1RA in human leukocytes. Biochem. Biophys. Res. Commun. 323, 630-635.

Wong, D.M., Buechner-Maxwell, V.A., Manning, T.O., Ward, D.L., 2005. Comparison of results for intradermal testing between clinically normal horses and horses affected with recurrent airway obstruction. Am. J. Vet. Res. 66, 1348-1355.

Woodcock, A., Bateman, E.D., Busse, W.W., Lotvall, J., Snowise, N.G., Forth, R., Jacques, L., Haumann, B., Bleecker, E.R., 2011. Efficacy in asthma of once-daily treatment with fluticasone furoate: a randomized, placebo-controlled trial. Respir Res 12, 132.

Woods, P.S., Robinson, N.E., Swanson, M.C., Reed, C.E., Broadstone, R.V., Derksen, F.J., 1993. Airborne dust and aeroallergen concentration in a horse stable under two different management systems. Equine Vet. J. 25, 208-213.

Woolcock, J.B., Rudduck, H.B., 1973. Corynebacterium equi in cattle. Aust Vet J 49, 319.

Wrobel, L.J., Ogier, M., Chatonnet, F., Autran, S., Mezieres, V., Thoby-Brisson, M., McLean, H., Taeron, C., Champagnat, J., 2007. Abnormal inspiratory depth in Phox2a haploinsufficient mice. Neuroscience 145, 384-392.

Xisto, D.G., Farias, L.L., Ferreira, H.C., Picanco, M.R., Amitrano, D., Lapa, E.S.J.R., Negri, E.M., Mauad, T., Carnielli, D., Silva, L.F., Capelozzi, V.L., Faffe, D.S., Zin, W.A., Rocco, P.R., 2005. Lung parenchyma remodeling in a murine model of chronic allergic inflammation. Am. J. Respir. Crit. Care Med. 171, 829-837.

Ye, J., Ji, S., 2009. Discriminant Analysis for Dimensionality Reduction: An Overview of Recent Developments. John Wiley & Sons, Inc., 1-19 pp.

Yi, K.H., Chen, L., 2009. Fine tuning the immune response through B7-H3 and B7-H4. Immunol. Rev. 229, 145-151.

Young-Pearse, T.L., Ivic, L., Kriegstein, A.R., Cepko, C.L., 2006. Characterization of mice with targeted deletion of glycine receptor alpha 2. Mol. Cell. Biol. 26, 5728-5734.

Zhang, B., Kirov, S., Snoddy, J., 2005. WebGestalt: an integrated system for exploring gene sets in various biological contexts. Nucleic Acids Res 33, W741-748.

Zhang, X., Mahmudi-Azer, S., Connett, J., Anthonisen, N., He, J.-Q., Paré, P., Sandford, A., 2007. Association of Hck genetic polymorphisms with gene expression and COPD. Hum. Genet. 120, 681-690.

Zhao, C., Ivanov, I., Dougherty, E.R., Hartman, T.J., Lanza, E., Bobe, G., Colburn, N.H., Lupton, J.R., Davidson, L.A., Chapkin, R.S., 2009. Noninvasive detection of candidate molecular biomarkers in subjects with a history of insulin resistance and colorectal adenomas. Cancer Prev Res (Phila) 2, 590-597.

Zhong, J., Yang, P., Muta, K., Dong, R., Marrero, M., Gong, F., Wang, C.Y., 2010. Loss of Jak2 selectively suppresses DC-mediated innate immune response and protects mice from lethal dose of LPS-induced septic shock. PLoS One 5, e9593.

Zimmermann, N., King, N.E., Laporte, J., Yang, M., Mishra, A., Pope, S.M., Muntel, E.E., Witte, D.P., Pegg, A.A., Foster, P.S., Hamid, Q., Rothenberg, M.E., 2003. Dissection of experimental asthma with DNA microarray analysis identifies arginase in asthma pathogenesis. J. Clin. Invest. 111, 1863-1874.

Zink, M.C., Yager, J.A., Smart, N.L., 1986. Corynebacterium equi Infections in Horses, 1958-1984: A Review of 131 Cases. Can. Vet. J. 27, 213-217.

Zou, J., Young, S., Zhu, F., Gheyas, F., Skeans, S., Wan, Y., Wang, L., Ding, W., Billah, M., McClanahan, T., Coffman, R.L., Egan, R., Umland, S., 2002. Microarray profile of differentially expressed genes in a monkey model of allergic asthma. Genome Biol 3.

Zuyderduyn, S., Sukkar, M.B., Fust, A., Dhaliwal, S., Burgess, J.K., 2008. Treating asthma means treating airway smooth muscle cells. Eur. Respir. J. 32, 265-274.

APPENDIX A

Table A-1: Gene Ontology analysis of differentially expressed (DE) genes from RAO-affected exposed to allergen compared to baseline.

Category	Term	Pvalue	Genes
Biological process	GO:0006414~translational elongation	0.035272	RPS3A, RPS15A
Cellular component	GO:0022627~cytosolic small ribosomal subunit	0.012511	RPS3A, RPS15A
	GO:0015935~small ribosomal subunit	0.019648	RPS3A, RPS15A
	GO:0005737~cytoplasm	0.0206	ELAVL1, FDFT1, KIF2A,PFCP,RPS15A,RPS3A
	GO:0022626~cytosolic ribosome	0.025204	RPS3A, RPS15A
	GO:0033279~ribosomal subunit	0.039594	RPS3A, RPS15A
	GO:0044445~cytosolic part	0.046876	RPS3A, RPS15A
	GO:0005840~ribosome	0.065782	RPS3A, RPS15A
Molecular function	GO:0003723~RNA binding	0.020402	ELAVL1,RPS3A,RPS15A
	GO:0003735~structural constituent of ribosome	0.054261	RPS3A, RPS15A

Table A-2: Gene Ontology analysis for DE genes from control horses exposed to allergen compared to baseline.

Category	Term	Pvalue	Genes
Biological Process	GO:0030155~regulation of cell adhesion	0.007883	PPP2CA, ADA, PIK3R1
	GO:0006144~purine base metabolic process	0.013802	ADA, AMPD1
	GO:0009168~purine ribonucleoside monophosphate biosynthetic process	0.017713	ADA, AMPD1
	GO:0009127~purine nucleoside monophosphate biosynthetic process	0.017713	ADA, AMPD1
	GO:0009126~purine nucleoside monophosphate metabolic process	0.019663	ADA, AMPD1
	GO:0009167~purine ribonucleoside monophosphate metabolic process	0.019663	ADA, AMPD1
	GO:0009156~ribonucleoside monophosphate biosynthetic process	0.022581	ADA, AMPD1
	GO:0009112~nucleobase metabolic process	0.022581	ADA, AMPD1
	GO:0009161~ribonucleoside monophosphate metabolic process	0.024522	ADA, AMPD1
	GO:0046483~heterocycle metabolic process	0.042108	P4HA2, ADA, AMPD1
	GO:0030183~B cell differentiation	0.046589	ADA, PIK3R1
	GO:0009124~nucleoside monophosphate biosynthetic process	0.048485	ADA, AMPD1

Table A-2 Continued

Category	Term	Pvalue	Genes
	GO:0005737~cytoplasm	0.013886	OPA3, P4HA2, RPL7, EXOC8, PPP2CA, UBE2G2, GLCCI1, DPP7, GRHL2, NLRP1, ADA, PIK3R1
	GO:0044444~cytoplasmic part	0.036444	OPA3, P4HA2, RPL7, EXOC8, PPP2CA, UBE2G2, DPP7, ADA, PIK3R1
Molecular Function	GO:0019239~deaminase activity	0.022876	ADA, AMPD1
	GO:0016814~hydrolase activity, acting on carbon-nitrogen (but not peptide) bonds, in cyclic amidines	0.028294	ADA, AMPD1

Table A-3: Gene Ontology analysis for DE genes from RAO-affected horses versus control at baseline.

Category	Term	Pvalue	Genes
Biological Process	GO:0008217~regulation of blood pressure	0.012397	PTGS2, ACTA2, AGT, HBB
	GO:0031399~regulation of protein modification process	0.013757	UBE2N, PSMA1, CLCF1, AGT, PAX5, CBS
	GO:0032268~regulation of cellular protein metabolic process	0.026343	UBE2N, PSMA1, CLCF1, AGT, PAIP1, PAX5, CBS
	GO:0035150~regulation of tube size	0.026908	ACTA2, AGT, HBB
	GO:0050880~regulation of blood vessel size	0.026908	ACTA2, AGT, HBB
	GO:0003018~vascular process in circulatory system	0.031787	ACTA2, AGT, HBB
	GO:0010627~regulation of protein kinase cascade	0.031969	UBE2N, CLCF1, ERBB2, AGT, CBS
	GO:0014065~phosphoinositide 3-kinase cascade	0.033244	ERBB2, PIK3R1
	GO:0002520~immune system development	0.043978	POLL, TNFRSF11A, CLCF1, CD164, PIK3R1
	GO:0010740~positive regulation of protein kinase cascade	0.046619	UBE2N, CLCF1, ERBB2, AGT
	GO:0051246~regulation of protein metabolic process	0.047347	UBE2N, PSMA1, CLCF1, AGT, PAIP1, PAX5, CBS
	GO:0030384~phosphoinositide metabolic process	0.048273	SEMA6D, PIGW, PIK3R1
	GO:0002376~immune system process	0.049142	POLL, UBE2N, LAT, TNFRSF11A, VTCN1, CLCF1, HFE, PAX5, CD164, PIK3R1
Cellular Component	GO:0044444~cytoplasmic part	1.08E-03	TYRP1, CYP2F1, PTGS2, CYP2B6, AP1G1, EXOC8, ERBB2, TIMM17B, MRFAP1, RPS15A, HFE, TPM3, EIF3CL, PGRMC1, AGT, DAO, HSPE1, HBB, PIK3R1, KIF2A, ACTA2, TP53BP2, PIGW, BTBD6, CD164, ATG3, MARK2, AGTRAP, CCT7, PSMA1, LAMP1, MRPL21, RPL13A, USO1, VAMP4, CALR3, CBS, RCN2

Table A-3 Continued

Category	Term	Pvalue	Genes
	GO:0005737~cytoplasm	0.002828	PTGS2, AP1G1, COPS3, TIMM17B, MRFAP1, MYLIP, EIF3CL, ACTR2, PGRMC1, DAO, KIF2A, ACTA2, PIGW, BTBD6, CD164, MARK2, UBE2N, PSMA1, SERPINB7, USO1, VAMP4, CALR3, TYRP1, CYP2F1, PLEK2, CYP2B6, EXOC8, ERBB2, HFE, CDC42SE1, RPS15A, TPM3, AGT, WIPF2, HSPE1, HBB, PIK3R1, TP53BP2, PAIP1, ELAVL1, ATG3, AGTRAP, CCT7, LAMP1, MRPL21, SEMA6D, RPL13A, CBS, RCN2
	GO:0045178~basal part of cell	0.009215	ERBB2, HFE, MARK2
	GO:0048471~perinuclear region of cytoplasm	0.012865	TP53BP2, AP1G1, ERBB2, USO1, HFE, MRFAP1
	GO:0044425~membrane part	0.013064	TYRP1, CYP2F1, PTGS2, PLEK2, CYP2B6, AP1G1, VTCN1, TSPAN4, ERBB2, OR2T4, TIMM17B, EFNA3, HFE, CDC42SE1, MYLIP, LRRC15, TMEM61, SLC7A7, OR4D1, VN1R4, TNFRSF11A, OR6C2, PGRMC1, OR13C8, ABCA13, PIGW, SIGLEC10, CD164, MARK2, AGTRAP, OR5B3, LRRC25, LAT, LAMP1, TMEM66, RPAP2, SEMA6D, USO1, VAMP4, OR2D3, TMPO, OMG, ACCN5
	GO:0044432~endoplasmic reticulum part	0.026426	CYP2F1, PTGS2, CYP2B6, PIGW, CALR3, RCN2
	GO:0005792~microsome	0.027906	CYP2F1, PTGS2, CYP2B6, PGRMC1, USO1
	GO:0044464~cell part	0.028928	PTGS2, VTCN1, AP1G1, TSPAN4, COPS3, TIMM17B, EFNA3, MRFAP1, PAX5, MYLIP, LRRC15, TMEM61, SLC7A7, OR4D1, ACTR2, VN1R4, EIF3CL, TNFRSF11A, WDR36, OR6C2, PGRMC1, DAO, KIF2A, POLL, ACTA2, PIGW, SIGLEC10, BTBD6, CD164, LRRC25, MARK2, UBE2N, PSMA1, TMEM66, SERPINB7, USO1, VAMP4, CALR3, OR2D3, TYRP1, CYP2F1, PLEK2, EXOC8, CYP2B6, OR2T4, ERBB2, RPS15A, HFE, CDC42SE1, TPM3, AGT, WIPF2, HSPE1, OR13C8, HBB, PIK3R1, ABCA13, C17ORF49, MYO1B, TP53BP2, PAIP1, ELAVL1, ATG3, OR5B3, AGTRAP, CCT7, LAMP1, LAT, MRPL21, RPAP2, SEMA6D, RPL13A, TMPO, OMG, ACCN5, RCN2, CBS

Table A-3 Continued

Category	Term	Pvalue	Genes
	GO:0005623~cell	0.029054	PTGS2, VTCN1, AP1G1, TSPAN4, COPS3, TIMM17B, EFNA3, MRFAP1, PAX5, MYLIP, LRRC15, TMEM61, SLC7A7, OR4D1, ACTR2, VN1R4, EIF3CL, TNFRSF11A, WDR36, OR6C2, PGRMC1, DAO, KIF2A, POLL, ACTA2, PIGW, SIGLEC10, BTBD6, CD164, LRRC25, MARK2, UBE2N, PSMA1, TMEM66, SERPINB7, USO1, VAMP4, CALR3, OR2D3, TYRP1, CYP2F1, PLEK2, EXOC8, CYP2B6, OR2T4, ERBB2, RPS15A, HFE, CDC42SE1, TPM3, AGT, WIPF2, HSPE1, OR13C8, HBB, PIK3R1, ABCA13, C17ORF49, MYO1B, TP53BP2, PAIP1, ELAVL1, ATG3, OR5B3, AGTRAP, CCT7, LAMP1, LAT, MRPL21, RPAP2, SEMA6D, RPL13A, TMPO, OMG, ACCN5, RCN2, CBS
	GO:0042598~vesicular fraction	0.0306	CYP2F1, PTGS2, CYP2B6, PGRMC1, USO1
	GO:0019898~extrinsic to membrane	0.032343	CYP2F1, PTGS2, PLEK2, CYP2B6, USO1, MYLIP, MARK2
	GO:0044445~cytosolic part	0.037448	CCT7, RPS15A, HBB, PIK3R1
	GO:0016020~membrane	0.046637	TYRP1, CYP2F1, PTGS2, PLEK2, CYP2B6, AP1G1, VTCN1, TSPAN4, OR2T4, ERBB2, TIMM17B, EFNA3, HFE, CDC42SE1, MYLIP, LRRC15, TMEM61, SLC7A7, OR4D1, VN1R4, TNFRSF11A, OR6C2, PGRMC1, OR13C8, ABCA13, PIK3R1, PIGW, SIGLEC10, CD164, MARK2, AGTRAP, OR5B3, LRRC25, LAT, LAMP1, TMEM66, RPAP2, SEMA6D, USO1, VAMP4, OR2D3, TMPO, OMG, ACCN5
	GO:0031224~intrinsic to membrane	0.049187	TYRP1, VTCN1, TSPAN4, ERBB2, OR2T4, EFNA3, TIMM17B, HFE, CDC42SE1, LRRC15, TMEM61, SLC7A7, OR4D1, VN1R4, TNFRSF11A, OR6C2, PGRMC1, OR13C8, ABCA13, PIGW, SIGLEC10, CD164, AGTRAP, LRRC25,
Molecular function	GO:0020037~heme binding	3.11E-04	CYP2F1, PTGS2, CYP2B6, PGRMC1, HBB, CBS
	GO:0046906~tetrapyrrole binding	4.18E-04	CYP2F1, PTGS2, CYP2B6, PGRMC1, HBB, CBS
	GO:0005506~iron ion binding	0.00392	CYP2F1, PTGS2, CYP2B6, PGRMC1, HFE, HBB, CBS
	GO:0019825~oxygen binding	0.018694	CYP2F1, CYP2B6, HBB
	GO:0043125~ErbB-3 class receptor binding	0.019406	ERBB2, PIK3R1

Table A-3 Continued

Category	Term	Pvalue	Genes
	GO:0005515~protein binding	0.020697	PTGS2, AP1G1, COPS3, TSPAN4, TIMM17B, MRFAP1, PAX5, MYLIP, LRRC15, EIF3CL, SH2D4B, ACTR2, TNFRSF11A, CLCF1, PGRMC1, ACTA2, SIGLEC10, BTBD6, CD164, MARK2, UBE2N, PSMA1, USO1, CALR3, TYRP1, EXOC8, ERBB2, HFE, CDC42SE1, LRRC36, RPS15A, TPM3, AGT, WIPF2, HSPE1, UNK, HBB, PIK3R1, MYO1B, TP53BP2, PAIP1, ELAVL1, ATG3, AGTRAP, CCT7, LAT, TMPO, OMG, CBS, RCN2
	GO:0016705~oxidoreductase activity, acting on paired donors, with incorporation or reduction of molecular oxygen	0.028383	TYRP1, CYP2F1, PTGS2, CYP2B6

Table A-4: Gene ontology analysis for DE genes from RAO-affected versus control horses after 30-day allergen exposure.

Gene Ontology Category	Term	Pvalue	Genes
Biological Process	GO:0006414~translational elongation	0.003806	EEF1A1, RPS3A, RPL13A, RPLP1
	GO:0006412~translation	0.019292	EEF1A1, MRPL21, RPS3A, RPL13A, RPLP1
Cellular Component	GO:0005737~cytoplasm	0.017422	TYRP1, COPS3, IGFBP6, ALDOB, COX7C, COPS7B, CCL5, ZNRF2, SLC25A21, ACTR2, SH2D1A, RPS3A, C4ORF35, EMID2, RPLP1, HSPE1, SLC25A1, HBB, EEF1A1, HCK, SPHK1, DDN, GRHL2, GCC1, UBE2N, EYA4, SGSM1, GAPVD1, MRPL21, RPL13A, ATF7, PLA2G5, CBS
	GO:0008180~signalosome	0.03222	COPS3, COPS7B
	GO:0005840~ribosome	0.033144	MRPL21, RPS3A, RPL13A, RPLP1
Molecular Function	GO:0003735~structural constituent of ribosome	0.014363	MRPL21, RPS3A, RPL13A, RPLP1

Table A-5: GO Term Mapper results for DE genes from RAO-affected versus control horses at baseline.

GO Term (GO ID)	GO Term Usage in Gene List	Genome Frequency of Use
cellular component organization (GO:0016043)	22 of 90 genes, 24.44%	3370 of 18410 annotated genes, 18.31%
protein metabolic process (GO:0019538)	20 of 90 genes, 22.22%	3090 of 18410 annotated genes, 16.78%
transport (GO:0006810)	20 of 90 genes, 22.22%	3061 of 18410 annotated genes, 16.63%
multicellular organismal development (GO:0007275)	18 of 90 genes, 20.00%	3292 of 18410 annotated genes, 17.88%
response to stress (GO:0006950)	15 of 90 genes, 16.67%	2248 of 18410 annotated genes, 12.21%
signal transduction (GO:0007165)	13 of 90 genes, 14.44%	2432 of 18410 annotated genes, 13.21%
protein modification process (GO:0006464)	12 of 90 genes, 13.33%	1851 of 18410 annotated genes, 10.05%
death (GO:0016265)	10 of 90 genes, 11.11%	1397 of 18410 annotated genes, 7.59%
cell differentiation (GO:0030154)	10 of 90 genes, 11.11%	2039 of 18410 annotated genes, 11.08%
cell death (GO:0008219)	10 of 90 genes, 11.11%	1394 of 18410 annotated genes, 7.57%
cell communication (GO:0007154)	9 of 90 genes, 10.00%	1624 of 18410 annotated genes, 8.82%
organelle organization (GO:0006996)	9 of 90 genes, 10.00%	1599 of 18410 annotated genes, 8.69%
catabolic process (GO:0009056)	9 of 90 genes, 10.00%	1364 of 18410 annotated genes, 7.41%
reproduction (GO:0000003)	7 of 90 genes, 7.78%	989 of 18410 annotated genes, 5.37%
response to external stimulus (GO:0009605)	7 of 90 genes, 7.78%	983 of 18410 annotated genes, 5.34%
protein transport (GO:0015031)	6 of 90 genes, 6.67%	904 of 18410 annotated genes, 4.91%
response to biotic stimulus (GO:0009607)	6 of 90 genes, 6.67%	501 of 18410 annotated genes, 2.72%
lipid metabolic process (GO:0006629)	6 of 90 genes, 6.67%	999 of 18410 annotated genes, 5.43%
cell proliferation (GO:0008283)	6 of 90 genes, 6.67%	1191 of 18410 annotated genes, 6.47%
translation (GO:0006412)	5 of 90 genes, 5.56%	425 of 18410 annotated genes, 2.31%
viral reproduction (GO:0016032)	4 of 90 genes, 4.44%	420 of 18410 annotated genes, 2.28%
mitochondrion organization (GO:0007005)	3 of 90 genes, 3.33%	143 of 18410 annotated genes, 0.78%
response to endogenous stimulus (GO:0009719)	3 of 90 genes, 3.33%	608 of 18410 annotated genes, 3.30%
cellular homeostasis (GO:0019725)	3 of 90 genes, 3.33%	513 of 18410 annotated genes, 2.79%
behavior (GO:0007610)	2 of 90 genes, 2.22%	360 of 18410 annotated genes, 1.96%
secondary metabolic process (GO:0019748)	1 of 90 genes, 1.11%	63 of 18410 annotated genes, 0.34%

Table A-6: GO Term Mapper results for DE genes from RAO-affected versus control horses after 30-day allergen exposure.

GO Term (GO ID)	GO Term Usage in Gene List	Genome Frequency of Use
biosynthetic process (GO:0009058)	16 of 56 genes, 28.57%	4533 of 18302 annotated genes, 24.77%
transport (GO:0006810)	12 of 56 genes, 21.43%	2917 of 18302 annotated genes, 15.94%
cellular component organization (GO:0016043)	11 of 56 genes, 19.64%	2996 of 18302 annotated genes, 16.37%
response to stress (GO:0006950)	9 of 56 genes, 16.07%	1936 of 18302 annotated genes, 10.58%
signal transduction (GO:0007165)	8 of 56 genes, 14.29%	2350 of 18302 annotated genes, 12.84%
catabolic process (GO:0009056)	7 of 56 genes, 12.50%	1255 of 18302 annotated genes, 6.86%
cell communication (GO:0007154)	6 of 56 genes, 10.71%	1502 of 18302 annotated genes, 8.21%
death (GO:0016265)	5 of 56 genes, 8.93%	1318 of 18302 annotated genes, 7.20%
translation (GO:0006412)	5 of 56 genes, 8.93%	420 of 18302 annotated genes, 2.29%
cell death (GO:0008219)	5 of 56 genes, 8.93%	1315 of 18302 annotated genes, 7.19%
ion transport (GO:0006811)	5 of 56 genes, 8.93%	843 of 18302 annotated genes, 4.61%
response to endogenous stimulus (GO:0009719)	4 of 56 genes, 7.14%	526 of 18302 annotated genes, 2.87%
lipid metabolic process (GO:0006629)	4 of 56 genes, 7.14%	926 of 18302 annotated genes, 5.06%
reproduction (GO:0000003)	3 of 56 genes, 5.36%	855 of 18302 annotated genes, 4.67%
DNA metabolic process (GO:0006259)	3 of 56 genes, 5.36%	619 of 18302 annotated genes, 3.38%
response to biotic stimulus (GO:0009607)	3 of 56 genes, 5.36%	482 of 18302 annotated genes, 2.63%
response to external stimulus (GO:0009605)	3 of 56 genes, 5.36%	773 of 18302 annotated genes, 4.22%
cell-cell signaling (GO:0007267)	3 of 56 genes, 5.36%	728 of 18302 annotated genes, 3.98%
generation of precursor metabolites and energy (GO:0006091)	2 of 56 genes, 3.57%	305 of 18302 annotated genes, 1.67%
cell growth (GO:0016049)	2 of 56 genes, 3.57%	288 of 18302 annotated genes, 1.57%
growth (GO:0040007)	2 of 56 genes, 3.57%	570 of 18302 annotated genes, 3.11%
viral reproduction (GO:0016032)	1 of 56 genes, 1.79%	166 of 18302 annotated genes, 0.91%
secondary metabolic process (GO:0019748)	1 of 56 genes, 1.79%	63 of 18302 annotated genes, 0.34%

Table A-7: Linear discriminant analysis of control animals after allergen exposure compared to baseline. The top ten one-, two-, and three-gene LDA classifiers are shown in the table below. $\varepsilon_{bolstered}$ represents the bolstered resubstitution error for the respective gene classifier and $\Delta\varepsilon_{bolstered}$ represents the decrease in error for each feature set relative to its highest ranked subset of genes.

1 feature	2 feature	3 feature	$\varepsilon_{bolstered}$	$\Delta\varepsilon_{bolstered}$
PPP2CA			0.1445	
DPP7			0.1576	
ADA			0.1661	
P4HA2			0.1935	
OPA3			0.2049	
NLRP1			0.2134	
EXOC8			0.221	
CT020013A20H09.ab1			0.2234	
RPL7			0.2359	
HL020010000_PLT_A12_89_087.ab1			0.2552	
CT020019B20A11.ab1	OPA3		0.1083	0.0966
DPP7	PPP2CA		0.1216	0.0229
PPP2CA	ADA		0.1346	0.0099
OPA3	CT020013A20H09.ab1		0.1378	0.0671
DPP7	CT020012B20E04.ab1		0.1387	0.0189
PPP2CA	EXOC8		0.14	0.0045
P4HA2	ADA		0.1413	0.0248
GLCCI1	CT020013A20H09.ab1		0.1456	0.0778
CT020012B20E04.ab1	CT02035B1A10.f1.ab1		0.1479	0.1097
GLCCI1	ADA		0.1518	0.0143
CT020019B20A11.ab1	OPA3	CT020013A20H09.ab1	0.0595	0.0488
GLCCI1	DPP7	CT020012B20E04.ab1	0.071	0.0677
GLCCI1	CT020013A20H09.ab1	ADA	0.0731	0.0725
CT020019B20A11.ab1	OPA3	ADA	0.0749	0.0334
CT020019B20A11.ab1	GLCCI1	OPA3	0.0846	0.0237
CT020019B20A11.ab1	OPA3	EXOC8	0.0893	0.019
GLCCI1	CT020013A20H09.ab1	EXOC8	0.0931	0.0525
CT020019B20A11.ab1	PPP2CA	OPA3	0.0958	0.0125
CT020019B20A11.ab1	OPA3	P4HA2	0.0993	0.009
CT020019B20A11.ab1	OPA3	CT020012B20E04.ab1	0.1033	0.005

Table A-8: Linear discriminant analysis for allergen exposed RAO-affected horses compared to baseline. The top ten one-, two-, and three-gene LDA classifiers are shown in the table below. $\varepsilon_{bolstered}$ represents the bolstered resubstitution error for the respective gene classifier and $\Delta\varepsilon_{bolstered}$ represents the decrease in error for each feature set relative to its highest ranked subset of genes.

1 feature	2 feature	3 feature	$\varepsilon_{bolstered}$	$\Delta\varepsilon_{bolstered}$
KIF2A			0.1377	
FDFT1			0.1853	
ELAVL1			0.2497	
CT020014A10G07.ab1			0.2816	
CT020014A10G07.ab1			0.3085	
RPS3A			0.3601	
RPS15A			0.3785	
KIF2A	FDFT1		0.1438	-0.0061
RPS15A	KIF2A		0.1625	-0.0248
RPS15A	FDFT1		0.2089	-0.0236
RPS3A	FDFT1		0.2385	-0.0532
KIF2A	RPS3A		0.2439	-0.1062
CT020014A10G07.ab1	ELAVL1		0.25	-0.0003
CT020014A10G07.ab1	CT020014A10G07.ab1		0.2531	0.0285
RPS15A	KIF2A	FDFT1	0.1859	-0.0421
KIF2A	RPS3A	FDFT1	0.19	-0.0462
CT020014A10G07.ab1	CT020014A10G07.ab1	ELAVL1	0.2397	0.0103
RPS15A	RPS3A	FDFT1	0.2454	-0.0365
RPS15A	KIF2A	RPS3A	0.2794	-0.1169
CT020014A10G07.ab1	CT020014A10G07.ab1	RPS15A	0.3473	-0.0942
CT020014A10G07.ab1	RPS15A	KIF2A	0.3564	-0.1939

Table A-9: List of differentially expressed genes (pvalue<0.05) for allergen exposed RAO-affected horses compared to baseline. ** Represents genes with pvalue<0.05 and fold change ≥ 0.58 or ≤ -0.58 selected for qPCR.

Gene symbol	NCBI accession	RefSeq accession	Log fold change	Pvalue
ABCA13	XM_001496546	XP_001496596	-0.56289	0.014525
ABO	XM_001491153	XP_001491203	-0.28231	0.022564
ANKRA2	XM_001504688	XP_001504738	0.276074	0.035059
ANKRD38	XM_001500075	XP_001500125	0.245804	0.048664
ANXA11	XM_001504023	XP_001504073	0.316336	0.036306
ARF1	XM_001494630	XP_001494680	0.174403	0.039539

Table A-9 Continued

Gene symbol	NCBI accession	RefSeq accession	Log fold change	Pvalue
ARHGEF10	XR_036140	NULL	0.191463	0.033482
ARL5A	XM_001488594	XP_001488644	-0.12865	0.042757
C12orf60	XM_001497318	XP_001497368	0.24732	0.036306
C17orf56	XM_001489994	XP_001490044	0.213744	0.0336
C20orf177	XM_001490535	XP_001490585	-0.11794	0.04638
CCBP2	XM_001497290	XP_001497340	-0.1504	0.04585
CD1A	XM_001490547	XP_001490597	0.269643	0.027989
CD82	XM_001489923	XP_001489973	0.419028	0.020188
CDK9	CX605189	NULL	0.270423	0.038016
CERK	XM_001488742	XP_001488792	-0.18976	0.010087
CMTM5	CX594400	XP_001489647	0.443946	0.020844
COX7C	XM_001504630	NULL	0.184777	0.026098
DAO	XM_001500936	XP_001500986	-0.14051	0.041508
DCXR	XM_001489215	NULL	0.247633	0.014717
DR1	XM_001491648	XP_001491698	0.394033	0.016238
EIF4B	CX604925	NULL	-0.19675	0.027704
ELAVL1	XM_001497883	XP_001497933	-0.63751	0.009965
ENTPD8	XM_001490804	XP_001490854	-0.16128	0.040257
EPB41L4A	XM_001504580	XP_001504630	-0.15229	0.043272
EWSR1	XM_001495303	XP_001495353	0.211883	0.045809
FDFT1	XR_036232	NULL	-0.651	0.047877
FLJ22222	XM_001490418	XP_001490468	-0.29984	0.008046
FXR1	XM_001495885	XP_001495935	0.147859	0.032671
GALNTL2	XM_001496032	XP_001496082	-0.154	0.037805
GBL	NULL	NULL	0.49018	0.042397
GEMIN7	XM_001502450	XP_001502500	-0.13277	0.047512
GJD3	XM_001497718	XP_001497768	0.332869	0.023295
GLYAT	XM_001504695	XP_001504745	-0.27249	0.042987
HIST1H2AG	XM_001494400	XP_001494450	0.235065	0.024662
HLA-DRB1	XM_001495531	XP_001495581	0.172331	0.038692
HRH4	XM_001494911	XP_001494961	0.216031	0.035668
HSPA9	XM_001502530	XP_001502580	0.355392	0.02675
KIF27	XM_001488810	XP_001488860	-0.22622	0.03835
KIF2A**	**XM_001493976**	**XP_001494026**	**-0.58275**	**0.018499**
LAIR1	XM_001488882	XP_001488932	-0.15478	0.035582
LOC645638	XM_001503882	NULL	0.292343	0.03972
LOC651536	XM_001493214	XP_001493264	0.23644	0.047877
LUZP1	XM_001504239	XP_001504289	-0.11806	0.035944
MAL	XM_001494113	XP_001494163	0.367886	0.047754
MTHFD1L	XM_001503676	XP_001503726	0.424522	0.029772
NUCKS1	XM_001489449	XP_001489499	-0.25888	0.03597

Table A-9 Continued

Gene symbol	NCBI accession	RefSeq accession	Log fold change	Pvalue
NULL	DN511058	NULL	-0.15791	0.022052
NULL	XM_001504718	XP_001504768	0.206873	0.03212
NULL	CX594544	NULL	0.55437	0.034214
NULL	DN509646	NULL	0.214341	0.036032
NULL	CX602146	NULL	-0.17521	0.036646
NULL	XR_035802	NULL	0.15049	0.037322
NULL	DN509801	NULL	0.154664	0.038794
OR12D3	XM_001491536	XP_001491586	-0.22555	0.042161
OR2A14	XM_001504219	XP_001504269	-0.19007	0.044514
OR2S2	XM_001504440	XP_001504490	-0.19947	0.037691
OR4A15	XM_001495924	NULL	0.199356	0.027319
OR6C4	XM_001504715	XP_001504765	-0.21596	0.014641
P4HA3	XM_001495901	XP_001495951	0.201425	0.029781
PDPR	XM_001501064	XP_001501114	0.315757	0.028449
PGCP**	**XM_001490623**	**XP_001490673**	**1.317639**	**0.004671**
PHF12	XM_001504186	XP_001504236	-0.25994	0.038917
PHF16	XM_001491297	XP_001491347	-0.17259	0.046324
PHOX2A	XM_001499157	XP_001499207	0.240919	0.043696
PLA2G10	XM_001489049	XP_001489099	-0.43093	0.034256
PLUNC	XM_001498706	XP_001498756	-0.19161	0.029585
RAB3D	XM_001489914	XP_001489964	0.21887	0.028999
RELL2	XM_001503977	XP_001504027	-0.15318	0.03434
RHBG	XM_001500143	XP_001500193	0.542523	0.030661
RPS15A	CD468996	NULL	0.457876	0.025843
RPS15A	CD467047	NULL	0.776104	0.026463
RPS27A	NULL	NULL	0.243014	0.037853
RPS3A	XM_001490864	NULL	-1.03708	0.027548
S100A9	XM_001493485	XP_001493535	0.219545	0.023185
SCARB2	XM_001491232	XP_001491282	0.182691	0.041357
SLC16A10	XM_001502292	XP_001502342	-0.20701	0.049061
SLC25A1	XM_001488569	XP_001488619	0.397017	0.031063
SLC2A2	AJ715983	NP_001075348	0.506324	0.016794
SLC38A5	XM_001493333	XP_001493383	0.228724	0.037214
SLC9A8	XM_001501184	XP_001501234	0.237754	0.016015
SPTA1	XM_001490255	XP_001490305	0.128038	0.038389
SSFA2	XM_001501268	NULL	-0.23099	0.031803
ST6GALNAC1	XM_001491565	XP_001491615	-0.15578	0.042985
TBX6	XR_036396	NULL	-0.19838	0.037551
TCTN3	XM_001500642	XP_001500692	-0.21303	0.025011
TOR2A	XM_001501467	XP_001501517	0.379833	0.014873
TP53	EF627477	NULL	0.33727	0.038955

Table A-9 Continued

Gene symbol	NCBI accession	RefSeq accession	Log fold change	Pvalue
TRAF6	NULL	NULL	-0.46026	0.038984
TRIM50	XM_001504491	XP_001504541	0.346829	0.048596
TSPAN18	XM_001490050	XP_001490100	-0.16211	0.03481
TTBK2	AB292108	NP_001075250	0.462038	0.033517
TXNDC9	XM_001490270	XP_001490320	0.152967	0.040947
UBC	XM_001499082	XP_001499132	0.336627	0.040326
UNC13B	XM_001504528	NULL	-0.1499	0.043334
UPK2	XM_001503043	XP_001503093	-0.17234	0.025518
WDR36	XM_001503571	XP_001503621	-0.41988	0.038431
YIPF2	NULL	NULL	-0.13495	0.026752

Table A-10: List of differentially expressed genes (pvalue<0.05) for control horses after allergen exposure compared to baseline. ** Represents genes with pvalue<0.05 and fold change ≥ 0.58 or ≤ -0.58 selected for qPCR.

Gene Symbol	NCBI accession	RefSeq accession	Log fold change	Pvalue
ABCC8	XM_001501642	XP_001501692	-0.28736	0.02648
ACTG1	BM735136	NULL	0.382464	0.036253
ADA	XM_001500443	XP_001500493	-0.65874	0.042177
AGT	DN510402	NULL	-0.55413	0.031435
ALDOB	XM_001504011	XP_001504061	0.478568	0.047262
ALG3	XM_001497526	XP_001497576	0.515755	0.037369
AMPD1	NULL	NULL	0.954384	0.005189
ANKRD46	XM_001492490	XP_001492540	-0.25017	0.008314
ANKS3	NULL	NULL	-0.41365	0.008631
APIP	XM_001493072	XP_001493122	-0.17689	0.042824
ARSA	XM_001490463	XP_001490513	-0.37952	0.020896
ARX	XM_001493047	NULL	-0.44152	0.024878
ASB1	XM_001496907	XP_001496957	0.260529	0.049957
ASCC3L1	XM_001492679	XP_001492729	0.251776	0.024469
ATAD2	XM_001497188	XP_001497238	0.723817	0.023879
ATF7	XM_001504543	XP_001504593	0.566171	0.04658
ATG7	XM_001493002	XP_001493052	0.184386	0.039075
ATP5C1	NULL	NULL	0.54808	0.01767
ATPIF1	DN507063	XP_001504043	0.215821	0.021334
BCOR	XM_001488901	NULL	-0.18082	0.02417
BHMT	XM_001504652	XP_001504702	0.297368	0.009834
BLCAP	XM_001502351	XP_001502401	0.529198	0.024666
BTBD1	CX601378	NULL	0.359597	0.045596

Table A-10 Continued

Gene Symbol	NCBI accession	RefSeq accession	Log fold change	Pvalue
C12orf48	XM_001497513	XP_001497563	-0.22759	0.025501
C12orf53	XM_001496868	XP_001496918	0.318913	0.008198
C12orf60	XM_001497318	XP_001497368	-0.10904	0.047529
C14orf50	XM_001493918	XP_001493968	0.112401	0.035554
C17orf68	XM_001503195	XP_001503245	0.194422	0.04506
C1QA	XM_001504261	XP_001504311	-0.24793	0.035635
C1QTNF8	CX602825	NULL	-0.14524	0.042302
C21orf56	XM_001488132	XP_001488182	0.129936	0.021444
C2orf47	NULL	NULL	0.234285	0.022549
C2orf50	XM_001503531	XP_001503581	0.230749	0.042411
C3orf37	XM_001495046	XP_001495096	0.157194	0.046541
C3orf52	XM_001501326	XP_001501376	-0.43246	0.025775
C5orf21	XM_001503716	XP_001503766	-0.47471	0.000374
C6orf192	XM_001503393	XP_001503443	0.225104	0.019186
C7orf23	DN508473	NULL	-0.36892	0.006763
CASP4	XM_001499070	XP_001499120	-0.23161	0.049906
CATSPER1	XM_001491133	XP_001491183	0.554645	0.017303
CBFB	XM_001496237	XP_001496287	-0.12229	0.028415
CBLN3	XM_001488806	XP_001488856	-0.12933	0.019709
CCBP2	XM_001497290	XP_001497340	0.145647	0.042516
CCDC106	XM_001496086	XP_001496136	0.236705	0.027563
CCNYL1	XM_001498888	XP_001498938	0.159102	0.046413
CD40LG	XM_001490011	XP_001490061	0.13724	0.036134
CDC42	XM_001493198	XP_001493248	-0.48628	0.025385
CDIPT	XM_001501701	XP_001501751	0.32878	0.01138
CHAT	XM_001494138	XP_001494188	-0.19806	0.038428
CHCHD6	XM_001492700	XP_001492750	0.153303	0.046125
CHEK1	XM_001505083	XP_001505133	0.22364	0.03904
CHST8	XM_001489047	XP_001489097	-0.21969	0.022875
CLPX	XM_001498202	XP_001498252	-0.2739	0.024605
CNOT10	XM_001491886	XP_001491936	0.454001	0.006565
CNPY4	XM_001505053	XP_001505103	0.116868	0.048801
CNTNAP5	XM_001489205	XP_001489255	-0.24302	0.0394
COX5B	XM_001493723	XP_001493773	0.118438	0.049893
CPEB1	XM_001498253	XP_001498303	0.343802	0.027005
CPN2	XM_001498855	NULL	0.364045	0.035331
CREB3L2	XM_001499610	XP_001499660	0.158716	0.044214
CREBBP	XM_001499349	XP_001499399	0.48091	0.022536
CYP11B2	XM_001505011	NULL	-0.23419	0.025429
CYP2C19	XM_001502162	XP_001502212	0.256779	0.040061
CYP2F1	XM_001498170	XP_001498220	-0.33643	0.026136
DCBLD1	XM_001502824	XP_001502874	0.200435	0.032127
DDB2	XM_001490725	XP_001490775	-0.22609	0.024481
DDN	XM_001491707	XP_001491757	0.347831	0.017498

Table A-10 Continued

Gene Symbol	NCBI accession	RefSeq accession	Log fold change	Pvalue
C12orf48	XM_001497513	XP_001497563	-0.22759	0.025501
C12orf53	XM_001496868	XP_001496918	0.318913	0.008198
C12orf60	XM_001497318	XP_001497368	-0.10904	0.047529
C14orf50	XM_001493918	XP_001493968	0.112401	0.035554
C17orf68	XM_001503195	XP_001503245	0.194422	0.04506
C1QA	XM_001504261	XP_001504311	-0.24793	0.035635
C1QTNF8	CX602825	NULL	-0.14524	0.042302
C21orf56	XM_001488132	XP_001488182	0.129936	0.021444
C2orf47	NULL	NULL	0.234285	0.022549
C2orf50	XM_001503531	XP_001503581	0.230749	0.042411
C3orf37	XM_001495046	XP_001495096	0.157194	0.046541
C3orf52	XM_001501326	XP_001501376	-0.43246	0.025775
C5orf21	XM_001503716	XP_001503766	-0.47471	0.000374
C6orf192	XM_001503393	XP_001503443	0.225104	0.019186
C7orf23	DN508473	NULL	-0.36892	0.006763
CASP4	XM_001499070	XP_001499120	-0.23161	0.049906
CATSPER1	XM_001491133	XP_001491183	0.554645	0.017303
CBFB	XM_001496237	XP_001496287	-0.12229	0.028415
CBLN3	XM_001488806	XP_001488856	-0.12933	0.019709
CCBP2	XM_001497290	XP_001497340	0.145647	0.042516
CCDC106	XM_001496086	XP_001496136	0.236705	0.027563
CCNYL1	XM_001498888	XP_001498938	0.159102	0.046413
CD40LG	XM_001490011	XP_001490061	0.13724	0.036134
CDC42	XM_001493198	XP_001493248	-0.48628	0.025385
CDIPT	XM_001501701	XP_001501751	0.32878	0.01138
CHAT	XM_001494138	XP_001494188	-0.19806	0.038428
CHCHD6	XM_001492700	XP_001492750	0.153303	0.046125
CHEK1	XM_001505083	XP_001505133	0.22364	0.03904
CHST8	XM_001489047	XP_001489097	-0.21969	0.022875
CLPX	XM_001498202	XP_001498252	-0.2739	0.024605
CNOT10	XM_001491886	XP_001491936	0.454001	0.006565
CNPY4	XM_001505053	XP_001505103	0.116868	0.048801
CNTNAP5	XM_001489205	XP_001489255	-0.24302	0.0394
COX5B	XM_001493723	XP_001493773	0.118438	0.049893
CPEB1	XM_001498253	XP_001498303	0.343802	0.027005
CPN2	XM_001498855	NULL	0.364045	0.035331
CREB3L2	XM_001499610	XP_001499660	0.158716	0.044214
CREBBP	XM_001499349	XP_001499399	0.48091	0.022536
CYP11B2	XM_001505011	NULL	-0.23419	0.025429
CYP2C19	XM_001502162	XP_001502212	0.256779	0.040061
CYP2F1	XM_001498170	XP_001498220	-0.33643	0.026136
DCBLD1	XM_001502824	XP_001502874	0.200435	0.032127
DDB2	XM_001490725	XP_001490775	-0.22609	0.024481
DDN	XM_001491707	XP_001491757	0.347831	0.017498

Table A-10 Continued

Gene Symbol	NCBI accession	RefSeq accession	Log fold change	Pvalue
DDR2	XM_001492493	XP_001492543	0.525399	0.014439
DDX11	XM_001490596	XP_001490646	-0.21617	0.025034
DKFZp686D0972	XM_001495321	XP_001495371	0.334511	0.020193
DMRTC2	XM_001499585	XP_001499635	0.272045	0.003553
DOCK1	XM_001489764	XP_001489814	0.285689	0.049323
DPP7	XM_001492340	XP_001492390	0.621615	0.021717
DRD2	XM_001501996	XP_001502046	0.158282	0.027737
E4F1	XM_001498135	XP_001498185	-0.34871	0.006322
ECHDC3	XM_001499215	XP_001499265	-0.17476	0.045254
EFCAB6	XM_001487867	XP_001487917	0.200027	0.023574
EIF2B4	XM_001502278	XP_001502328	-0.47666	0.033778
EIF2S3	XM_001494201	XP_001494251	-0.17337	0.027287
ELAVL1	XM_001497883	XP_001497933	0.558273	0.025783
ELOF1	XM_001490341	XP_001490391	-0.18687	0.040113
EMR3	XM_001495605	XP_001495655	0.458319	0.046023
EPO	AB100030	NP_001075294	0.178845	0.031493
EXOC8	XM_001494038	XP_001494088	-0.66813	0.021026
FAM107A	XM_001488861	XP_001488911	-0.25554	0.017673
FAM91A1	XM_001497901	XP_001497951	0.220126	0.041142
FANCD2	XM_001494041	XP_001494091	-0.18318	0.033523
FASTKD2	XM_001498513	XP_001498563	0.314497	0.03658
FBXL11	XM_001497095	XP_001497145	-0.23001	0.019622
FBXO11	XM_001498271	XP_001498321	0.137258	0.049045
FERMT1	XM_001493949	XP_001493999	-0.19588	0.025881
FGA	BM780427	NULL	-0.21398	0.005842
FGF2	NULL	NULL	0.133195	0.042356
FLJ21865	XM_001490670	XP_001490720	-0.19076	0.041819
FLJ46321	N/A	N/A	0.202494	0.024876
FLJ46321	XM_001488510	NULL	-0.2933	0.030105
FLJ46321	N/A	N/A	0.168935	0.039239
FLVCR1	XM_001488684	XP_001488734	-0.31062	0.005169
FMO3	XM_001495951	XP_001496001	0.206273	0.014022
FOLH1	XM_001489017	XP_001489067	0.185224	0.030348
FOXN4	XM_001496911	XP_001496961	-0.36655	0.005968
GATA2	XM_001488164	XP_001488214	0.446997	0.048959
GEMIN8	XM_001489578	NULL	0.291336	0.024218
GLCCI1	XM_001495201	XP_001495251	0.785274	0.017472
GOLPH3	XM_001500613	XP_001500663	0.31076	0.046624
GPR151	XM_001503885	XP_001503935	0.280873	0.021988
GPX3	NM_001115158	NP_001108630	-0.28061	0.04535
GRHL2	XM_001493287	XP_001493337	0.910797	0.01957
HBE1	XM_001504191	XP_001504241	-0.17099	0.013871
HCK	CD465568	NULL	-0.26801	0.007001
HECA	XM_001495962	XP_001496012	0.158119	0.040098

Table A-10 Continued

Gene Symbol	NCBI accession	RefSeq accession	Log fold change	Pvalue
HIBADH	XM_001499874	XP_001499924	-0.54107	0.017333
HIST1H4J	XM_001498048	XP_001498098	0.195906	0.020184
HLA-DRB1	XM_001495531	XP_001495581	-0.22221	0.017836
HMGB2	NULL	NULL	0.246214	0.008762
HMGN1	NULL	NULL	0.22359	0.04144
HTR7	XM_001501255	XP_001501305	0.17498	0.048014
HTRA4	XM_001491574	XP_001491624	-0.18611	0.0271
IFI44	XM_001497882	XP_001497932	-0.33711	0.025669
IGFBP6	NULL	NULL	-0.33601	0.022968
IIP45	XM_001489888	XP_001489938	-0.23947	0.016327
IL1RL1	XM_001491350	XP_001491400	-0.32791	0.038072
KCNC4	XM_001496175	NULL	0.418141	0.025487
KCNE4	XM_001495661	XP_001495711	-0.1476	0.027269
KCNIP1	XM_001503162	XP_001503212	0.29794	0.018114
KIAA0652	XM_001489922	NULL	0.20253	0.017528
KIF2A	XM_001493976	XP_001494026	0.30307	0.017625
KITLG	XM_001491749	XP_001491799	0.150915	0.047963
KLF4	XM_001492981	NULL	-0.20009	0.04385
KLRD1	XM_001494069	XP_001494119	0.169488	0.043248
LCA5	XM_001503637	XP_001503687	0.503378	0.020068
LHFPL1	XM_001488695	XP_001488745	0.348849	0.044286
LILRB4	XM_001489413	XP_001489463	0.162521	0.031188
LINGO2	XM_001498518	XP_001498568	-0.29399	0.012915
LIPG	XM_001499159	XP_001499209	0.280005	0.014571
LIPJ	XM_001501539	XP_001501589	0.187562	0.029423
LOC340156	XM_001488066	XP_001488116	0.844356	0.0325
LOC4951	XM_001494035	XP_001494085	-0.1814	0.041105
LOC651536	XM_001502913	XP_001502963	0.191004	0.036871
LOC728447	XM_001494321	XP_001494371	0.37434	0.049943
LOC728464	XM_001502209	XP_001502259	-0.19277	0.023366
LRRC39	XM_001488705	XP_001488755	0.262233	0.020636
LRRN2	XM_001489200	XP_001489250	0.189625	0.007082
LYK5	XM_001495479	XP_001495529	-0.22873	0.042064
MAOB	AB178283	NP_001075302	0.159384	0.049059
MAP1LC3B	XM_001500241	NULL	-0.25273	0.048179
MAP2K6	XM_001498752	XP_001498802	0.123403	0.044617
MC3R	XM_001489123	XP_001489173	-0.42292	0.035993
MFSD11	XM_001492704	XP_001492754	-0.13936	0.043888
MGC23985	XM_001503845	XP_001503895	0.160148	0.040733
MGC50722	XM_001498447	XP_001498497	0.260469	0.011222
MOCOS	XM_001497515	XP_001497565	0.169281	0.011422
MPST	CX605060	NULL	0.171037	0.027473
MRPL11	XM_001496069	XP_001496119	-0.1725	0.012575
MRPL15	CX598344	NULL	-0.4632	0.049464

Table A-10 Continued

Gene Symbol	NCBI accession	RefSeq accession	Log fold change	Pvalue
MRPL55	DN509267	XP_001494804	-0.43127	0.004726
MTERFD2	XM_001497592	XP_001497642	0.161427	0.01816
MYOZ2	XM_001503234	XP_001503284	0.210234	0.015215
MYST2	XM_001502506	XP_001502556	0.2297	0.024376
NADK	XM_001503443	XP_001503493	-0.26861	0.036858
NDUFB5	DN508847	XP_001495558	0.197419	0.03774
NFYC	XM_001503250	XP_001503300	0.206316	0.016469
NKIRAS2	XM_001495362	XP_001495412	-0.27577	0.022311
NLRP1**	**XM_001502829**	**XP_001502879**	**0.879117**	**0.038263**
NME1-NME2	DN510443	NULL	-0.19402	0.009184
NOC3L	CX603641	NULL	0.288471	0.017359
NPAL1	DN510209	NULL	-0.5065	0.010381
NPM1	NULL	NULL	-0.18544	0.022126
NPR3	XM_001500398	XP_001500448	-0.16671	0.017961
NPTXR	CX594481	NULL	-0.25043	0.047288
NR1H4	XM_001496056	XP_001496106	-0.20849	0.049551
NR2E3	XM_001494954	XP_001495004	0.275625	0.022754
NTAN1	NULL	NULL	0.160111	0.034946
NUDT4	XM_001495348	XP_001495398	0.356541	0.045166
NUDT8	XM_001492186	NULL	0.410626	0.032351
NULL	CX603838	NULL	-0.26316	0.003618
NULL	DN510982	NULL	-0.34284	0.003826
NULL	CX597518	NULL	0.32561	0.004362
NULL	XM_001491511	NULL	-0.38713	0.00611
NULL	DN508304	NULL	-0.17229	0.007647
NULL	DN509075	NULL	-0.18996	0.007979
NULL	XR_036258	NULL	-0.35068	0.011203
NULL	CX598059	NULL	-0.34524	0.011675
NULL	CX602673	NULL	-0.20763	0.011809
NULL	XM_001495673	NULL	0.26954	0.01203
NULL	DN509646	NULL	-0.27243	0.012771
NULL	XM_001499091	XP_001499141	-0.30197	0.012947
NULL	CX605794	NULL	-0.25747	0.013891
NULL	DN510407	NULL	-0.22756	0.015263
NULL	CX603890	NULL	-0.3292	0.015421
NULL	CX602249	NULL	-0.40041	0.015669
NULL	XR_036349	NULL	-0.17858	0.016135
NULL	CX604190	NULL	-0.355	0.016504
NULL	CX604012	NULL	0.287679	0.016893
NULL	DN510417	NULL	0.403233	0.017168
NULL	DN509230	NULL	-0.34225	0.017823
NULL	CX602423	NULL	0.356203	0.020874
NULL	CX602962	NULL	-0.32357	0.021541
NULL	CX605229	NULL	-0.16713	0.021921

Table A-10 Continued

Gene Symbol	NCBI accession	RefSeq accession	Log fold change	Pvalue
NULL	DN511060	NULL	-0.20142	0.022355
NULL	CX602999	NULL	0.372858	0.023793
NULL	XM_001491766	NULL	-0.20418	0.024842
NULL	CX605497	NULL	0.166509	0.027773
NULL	DN510227	NULL	-0.30624	0.028065
NULL	CX597125	NULL	-0.15902	0.028866
NULL	XM_001503568	NULL	0.253451	0.031333
NULL	CX603914	NULL	-0.18911	0.032286
NULL	CD536420	NULL	-0.13801	0.032654
NULL	CX604033	NULL	-0.26169	0.03318
NULL	DN509048	NULL	-0.34883	0.033232
NULL	CX602671	NULL	-0.51486	0.034018
NULL	DN509184	NULL	-0.38082	0.03435
NULL	DN507905	NULL	0.354473	0.034748
NULL	CD470590	NULL	-0.55033	0.040211
NULL	CX604149	NULL	0.220966	0.041461
NULL	CD528773	NULL	-0.27521	0.043312
NULL	CD470227	NULL	-0.46914	0.043705
NULL	CX600034	NULL	-0.96456	0.045322
NULL	CX599655	NULL	0.222764	0.045956
NULL	DN506142	NULL	0.199536	0.046189
NULL	CX594703	NULL	0.208985	0.046428
NULL	DN509452	NULL	0.230574	0.046692
NULL	CX601539	NULL	0.148762	0.047775
NULL	CD467057	NULL	-0.25517	0.047784
NULL	DN504828	NULL	-0.40229	0.047866
NULL	BI960932	NULL	0.357004	0.047919
NULL	CX603562	NULL	0.351948	0.049321
NULL	CX603403	NULL	-0.21629	0.049484
OPA3	DN509316	NULL	-0.8072	0.000239
OR10A4	XM_001500066	XP_001500116	0.190027	0.047697
OR10C1	XM_001489021	XP_001489071	0.12307	0.04753
OR11H6	XM_001502302	XP_001502352	0.268459	0.045998
OR13H1	XM_001491485	NULL	0.240546	0.039581
OR1F1	XM_001499014	XP_001499064	0.173465	0.039443
OR1L1	XM_001501254	XP_001501304	0.216243	0.048029
OR1N2	XM_001497814	XP_001497864	0.45279	0.018868
OR2B11	XM_001504074	XP_001504124	0.447462	0.027603
OR2D3**	**XM_001500110**	**XP_001500160**	**0.854773**	**0.003415**
OR2L8	XM_001499162	NULL	-0.50719	0.023318
OR2T33	XM_001497754	NULL	0.175891	0.022634
OR2T33	XM_001491345	NULL	-0.2515	0.033996
OR2W1	XM_001494282	XP_001494332	0.174815	0.02704
OR4C11	XM_001495311	XP_001495361	0.242508	0.027577

Table A-10 Continued

Gene Symbol	NCBI accession	RefSeq accession	Log fold change	Pvalue
OR4C16	XM_001494914	XP_001494964	-0.32212	0.042627
OR4F15	XM_001501753	XP_001501803	0.230348	0.014142
OR4K13	XM_001501955	XP_001502005	0.260309	0.030299
OR4P4	XM_001495187	XP_001495237	0.542067	0.014848
OR51A7	XM_001497708	XP_001497758	0.423374	0.038104
OR51G2	XM_001498435	NULL	0.348326	0.002337
OR51I1	XM_001503971	XP_001504021	0.288524	0.025677
OR52E8	XM_001498450	XP_001498500	0.291408	0.011323
OR52J3	XM_001498495	NULL	0.20133	0.040383
OR5A2	XM_001495642	XP_001495692	0.216045	0.024005
OR5BU1	XM_001495626	XP_001495676	0.510988	0.007688
OR5P2	XM_001500307	XP_001500357	0.335611	0.012578
OR6C1	XM_001490296	XP_001490346	0.206577	0.028519
OR6C2	XM_001489553	NULL	0.265508	0.010738
OR6C2	XM_001491120	XP_001491170	0.202785	0.01975
OR6C70	XM_001490802	XP_001490852	0.28592	0.029728
OR7E24	XM_001493590	XP_001493640	0.543819	0.034561
OR8B3	XM_001501921	NULL	0.648596	0.013265
OR8B3	XM_001501664	XP_001501714	0.340618	0.024416
P2RX3	XM_001504914	XP_001504964	-0.35219	0.007107
P4HA2	XM_001502946	XP_001502996	-0.73316	0.040654
PANK3	XM_001503241	XP_001503291	0.220359	0.044781
PCDHGB3	XM_001502136	XP_001502186	0.360144	0.033932
PCK2	XM_001489336	XP_001489386	0.311448	0.015789
PCSK2	XM_001491591	XP_001491641	0.349811	0.017213
PDCD1LG2	XM_001492097	XP_001492147	0.147122	0.026782
PDE3B	XM_001501420	XP_001501470	0.177111	0.022396
PFDN1	XM_001499395	XP_001499445	-0.25215	0.034877
PGRMC1	DN509190	NULL	-0.21395	0.049152
PIK3R1	XM_001491571	XP_001491621	-0.68522	0.026548
PIK3R4	XM_001496778	XP_001496828	0.257827	0.043563
PITPNB	XM_001499699	XP_001499749	-0.249	0.039968
PITPNC1	XM_001499960	XP_001500010	-0.17096	0.024152
PLUNC	XM_001498706	XP_001498756	0.294584	0.034644
PPP2CA	XR_036429	NULL	0.652938	0.034851
PPP6C	XM_001500587	XP_001500637	0.441911	0.032121
PQLC3	XM_001502263	XP_001502313	0.115683	0.04322
PRCC	XM_001500494	XP_001500544	-0.28742	0.04078
PRKCDBP	XM_001499633	XP_001499683	-0.41415	0.040801
PRKCQ	XM_001499872	XP_001499922	-0.32081	0.048945
PSME4	XM_001497080	XP_001497130	-0.27736	0.004814
PTP4A2	NULL	NULL	0.207895	0.033241
QRSL1	XM_001503943	XP_001503993	-0.32415	0.012343
QSOX1	XM_001488615	XP_001488665	-0.28399	0.028888

Table A-10 Continued

Gene Symbol	NCBI accession	RefSeq accession	Log fold change	Pvalue
RBM35B	XM_001498872	XP_001498922	-0.18307	0.048584
RGS5	XM_001492029	XP_001492079	0.119258	0.04492
RING1	XM_001493382	XP_001493432	-0.2514	0.048376
RNF152	XM_001489933	XP_001489983	-0.14793	0.019968
RPL37	BI961238	XP_001499005	-0.39546	0.016148
RPL7	XM_001491982	XP_001492032	-0.67362	0.032564
RPRM	XM_001491352	XP_001491402	0.177594	0.048717
RQCD1	XM_001491531	XP_001491581	0.523039	0.045376
SELO	XM_001496075	XP_001496125	0.174708	0.038087
SERF2	XM_001500420	XP_001500470	0.215438	0.012303
SERINC5	XM_001503874	XP_001503924	-0.38581	0.02252
SERTAD1	XR_036272	NULL	-0.19328	0.028736
SH3BGRL	XM_001501152	XP_001501202	0.14636	0.023908
SH3GL1	XM_001494308	NULL	0.420738	0.025007
SHROOM2	XM_001488393	XP_001488443	0.131121	0.046404
SIGLEC14	XM_001496296	XP_001496346	-0.32211	0.036327
SLC16A1	XM_001495158	XP_001495208	0.188788	0.036625
SLC16A14	XM_001497261	XP_001497311	-0.20989	0.029197
SLC18A1	XM_001490140	XP_001490190	0.261434	0.02371
SLC35A4	XM_001504164	XP_001504214	0.232301	0.018334
SLC39A13	XM_001491132	XP_001491182	-0.294	0.036139
SLC39A9	XM_001500384	XP_001500434	0.224154	0.020065
SLC6A8	XM_001491633	XP_001491683	0.465186	0.030494
SLC7A4	BI961888	XP_001492952	0.398226	0.02824
SLC7A7	CD535752	NULL	-0.38915	0.013448
SLMO1	XM_001489476	XP_001489526	0.162967	0.048988
SOX4	NULL	NULL	0.219273	0.027637
SPHK1	XM_001491689	XP_001491739	0.222634	0.04825
SURF4	XM_001499090	XP_001499140	0.156427	0.029156
SYF2	XM_001501117	XP_001501167	0.185125	0.010552
TAAR8	XM_001503349	XP_001503399	-0.3475	0.006339
TEX11	XM_001490344	XP_001490394	0.22371	0.026907
TFAM	XM_001503382	XP_001503432	0.286302	0.019479
TFE3	XM_001494896	XP_001494946	0.297885	0.045961
TGM3	CD469900	NULL	-0.25928	0.027262
THAP3	XM_001491823	XP_001491873	-0.30618	0.007553
THSD1	XR_035821	NULL	-0.13005	0.049763
TICAM1	XM_001493990	XP_001494040	-0.11966	0.032748
TM2D2	XM_001491499	XP_001491549	-0.26594	0.032277
TMCO6	XM_001504162	XP_001504212	0.183063	0.032356
TMEM167	XM_001504639	NULL	0.290951	0.039732
TMEM171	XM_001504691	XP_001504741	0.305715	0.015251
TMEM5	NULL	NULL	-0.55048	0.007448
TMEM58	XM_001494838	XP_001494888	-0.56743	0.012298

Table A-10 Continued

Gene Symbol	NCBI accession	RefSeq accession	Log fold change	Pvalue
TMEM71	XM_001499201	XP_001499251	0.348118	0.035967
TMEM95	XM_001503064	XP_001503114	0.166907	0.045127
TMOD3	XM_001499393	XP_001499443	0.139338	0.030561
TMPRSS11E2	XM_001501361	XP_001501411	-0.47637	0.04511
TNFRSF10A	XM_001503050	XP_001503100	-0.2383	0.011352
TPR	NULL	NULL	-0.20522	0.01265
TRH	XM_001491273	XP_001491323	0.153682	0.043842
TRIM39	XM_001492176	XP_001492226	0.379216	0.04574
TSPO	XM_001503143	XP_001503193	0.251579	0.043451
TTR	XM_001495182	XP_001495232	0.214415	0.012757
TUBA3C	XM_001488340	XP_001488390	-0.29746	0.017159
UACA	XM_001495340	NULL	-0.19096	0.041346
UBC	XM_001499082	XP_001499132	-0.3403	0.044822
UBE2G2	XM_001490079	NULL	0.715065	0.037124
UBXD8	XM_001502650	XP_001502700	0.468242	0.000969
UGCGL1	XM_001504931	XP_001504981	0.103581	0.044813
UPK2	XM_001503043	XP_001503093	0.242261	0.009669
USP32	XM_001503781	XP_001503831	0.183872	0.038464
USP6NL	XM_001489534	XP_001489584	-0.27901	0.045073
USP8	XM_001501926	XP_001501976	-0.23152	0.038994
VN1R1	XM_001490632	NULL	0.34542	0.030136
VPS29	XM_001495099	XP_001495149	0.20264	0.04716
VPS35	XM_001490225	XP_001490275	0.251023	0.035081
VTN	XM_001504123	XP_001504173	0.231365	0.029878
XKRX	XM_001492403	XP_001492453	0.429293	0.035877
ZC3H12D	XM_001495556	XP_001495606	-0.1269	0.024606
ZCCHC9	XM_001504642	XP_001504692	0.171532	0.047382
ZDHHC17	DN510703	NULL	-0.39825	0.036697
ZKSCAN4	DN509499	NULL	-0.32777	0.014806
ZNF234	XM_001500100	XP_001500150	-0.1708	0.048093
ZNF407	NULL	NULL	-0.44057	0.004587
ZNF512	XM_001502165	XP_001502215	0.275094	0.047046
ZNF575	XM_001499856	XP_001499906	0.331743	0.039215
TFE3	XM_001494896	XP_001494946	0.297885	0.045961
TGM3	CD469900	NULL	-0.25928	0.027262
THAP3	XM_001491823	XP_001491873	-0.30618	0.007553
THSD1	XR_035821	NULL	-0.13005	0.049763
TICAM1	XM_001493990	XP_001494040	-0.11966	0.032748
TM2D2	XM_001491499	XP_001491549	-0.26594	0.032277
TMCO6	XM_001504162	XP_001504212	0.183063	0.032356
TMEM167	XM_001504639	NULL	0.290951	0.039732
TMEM171	XM_001504691	XP_001504741	0.305715	0.015251
TMEM5	NULL	NULL	-0.55048	0.007448
TMEM58	XM_001494838	XP_001494888	-0.56743	0.012298

Table A-11: List of differentially expressed genes (pvalue<0.05) for RAO-affected horses compared to control at baseline. ** Represents genes with pvalue<0.05 and fold change ≥ 0.58 or ≤ -0.58 selected for qPCR.

Gene Symbol	NCBI accession	RefSeq accession	Log fold change	Pvalue
ABCA13	XM_001496546	XP_001496596	1.037721	0.012461
ABCA4	XM_001491597	XP_001491647	-0.20234	0.046607
ABI2	XM_001497656	XP_001497706	0.579302	0.005247
ABO	XM_001491153	XP_001491203	0.486945	0.006452
ACCN5	XM_001500739	XP_001500789	0.771025	0.028665
ACSS2	XM_001501341	XP_001501391	-0.46807	0.039853
ACTA2	XM_001503035	XP_001503085	0.703496	0.02659
ACTR2	XM_001494389	XP_001494439	-2.07064	0.001165
ADAM28	XM_001491580	XP_001491630	-0.56749	0.046506
AGT	DN510402	NULL	-0.60305	0.02028
AGTRAP	XM_001492019	XP_001492069	-0.79757	0.043198
AKAP14	XM_001491634	NULL	0.267078	0.049638
ALDOA	NULL	NULL	-0.36301	0.044038
ALKBH3	XM_001489694	XP_001489744	-0.1968	0.029472
ALKBH6	XM_001492599	XP_001492649	-0.33154	0.021518
ALPL	XM_001504312	XP_001504362	0.560444	0.017596
ALS2CR8	XM_001497530	XP_001497580	-0.27154	0.046495
AP1G1	XM_001500479	NULL	1.055121	0.012305
APPL1	XM_001491548	XP_001491598	0.334809	0.01894
ARL6	XM_001504416	XP_001504466	0.243138	0.046286
ARPM1	XM_001491136	XP_001491186	0.473668	0.027702
ART3	XM_001490592	XP_001490642	-0.33842	0.008631
ASB11	XM_001489836	XP_001489886	-0.67643	0.048175
ATF4	XM_001499993	XP_001500043	-0.21397	0.039679
ATG3	CD528901	NULL	-0.72757	0.038941
ATG7	XM_001493002	XP_001493052	0.348071	0.040517
ATM	XM_001501161	XP_001501211	-0.45027	0.001899
ATOH1	XM_001495691	XP_001495741	-0.23704	0.025404
ATP11B	XM_001496792	XP_001496842	-0.27704	0.039211
ATP6AP1	XM_001494850	NULL	-0.37601	0.017738
AVPR1B	XM_001489521	XP_001489571	-0.15627	0.018305
B4GALT3	XM_001503814	XP_001503864	-0.41842	0.024535
bA16L21.2.1	XM_001491058	XP_001491108	0.468213	0.039446
BAG4	XM_001493179	XP_001493229	0.212958	0.014436
BAZ1A	XM_001490894	XP_001490944	-0.5496	0.017181
BCKDK	XM_001500782	XP_001500832	-0.31719	0.037365
BDKRB1	XM_001489223	XP_001489273	-0.52687	0.028964
BHLHB9	XM_001504604	XP_001504654	0.522902	0.000104
BMPR1A	XM_001500907	XP_001500957	0.540654	0.012881
BMS1	XM_001489945	XP_001489995	-0.38849	0.033776
BMX	XM_001490091	XP_001490141	-0.32058	0.040133
BSDC1	XM_001503784	XP_001503834	-0.23987	0.009126
BTBD16	XM_001495476	XP_001495526	0.252625	0.017797
BTBD6	NULL	NULL	-0.7423	0.009073
C11orf41	XM_001492058	XP_001492108	-0.43351	0.012116
C11orf60	XM_001502961	XP_001503011	0.367626	0.01651
C12orf34	XM_001496801	NULL	-0.58296	0.020218

Table A-11 Continued

Gene Symbol	NCBI accession	RefSeq accession	Log fold change	Pvalue
C12orf57	CX604375	XP_001497722	-0.1585	0.041625
C14orf68	XM_001488578	NULL	-0.31614	0.006199
C17orf49	NULL	NULL	0.722099	0.015115
C17orf63	XM_001504183	XP_001504233	-0.69946	0.030039
C17orf68	XM_001503195	XP_001503245	0.359327	0.009729
C17orf75	XM_001504001	XP_001504051	-0.35747	0.02246
C18orf22	XM_001496059	XP_001496109	0.234633	0.036686
C19orf45	XM_001496690	XP_001496740	-0.3325	0.016977
C1orf182	XM_001495120	NULL	0.701534	0.043444
C1QA	XM_001504261	XP_001504311	-0.49162	0.033785
C20orf152	XM_001501888	XP_001501938	-0.22185	0.036937
C3orf37	XM_001495046	XP_001495096	0.248819	0.018123
C3orf63	XM_001490512	XP_001490562	0.238418	0.033175
C4orf20	XM_001490682	XP_001490732	-0.49584	0.04532
C4orf26	XM_001490823	XP_001490873	0.33728	0.036499
C5orf21	XM_001503716	XP_001503766	-0.67135	0.033617
C6orf166	XM_001500351	XP_001500401	0.437393	0.005069
C8orf37	XM_001490155	XP_001490205	-0.33855	0.01189
C8orf70	XM_001491870	XP_001491920	-0.29263	0.047506
C8orf80	XM_001492998	XP_001493048	0.223111	0.032251
C9orf131	XM_001498113	XP_001498163	-0.42936	0.006311
CALR3	XM_001502873	XP_001502923	-1.72919	0.045369
CAPN9	XM_001494410	XP_001494460	-0.3399	0.032075
CASC5	XM_001501097	XP_001501147	-0.29271	0.01074
CASR	XM_001502152	XP_001502202	0.427202	0.047735
CBLN3	XM_001488806	XP_001488856	-0.29656	0.03575
CBS	XM_001490849	NULL	1.186991	0.006148
CCDC25	XM_001492881	XP_001492931	0.735653	0.01888
CCDC86	XM_001501625	XP_001501675	-0.36668	0.043493
CCDC99	XM_001503223	XP_001503273	-0.26275	0.039019
CCL11	AJ251188	NP_001075340	0.242455	0.020013
CCL4	CD536661	XP_001503938	-0.30715	0.007157
CCT7	XM_001488366	XP_001488416	-1.00489	0.028476
CD164**	**BM414616**	**NULL**	**0.623907**	**0.030197**
CD200R2	XM_001501232	XP_001501282	-0.31167	0.046973
CD300E	XM_001492757	XP_001492807	0.27282	0.035827
CD82	XM_001489923	XP_001489973	-0.56017	0.032673
CDC42SE1	XM_001491452	NULL	0.715237	0.04539
CDS2	XM_001496234	XP_001496284	0.331344	0.048142
CEACAM1	DN510800	NULL	-0.19695	0.011575
CFB	XM_001492552	XP_001492602	0.250238	0.029272
CGGBP1	NULL	NULL	-0.57567	0.033939
CHAT	XM_001494138	XP_001494188	-0.42505	0.020786
CHCHD1	XM_001503907	XP_001503957	-0.27602	0.039856
CHD1	XM_001504605	XP_001504655	0.413024	0.012356
CLCF1	XM_001495767	XP_001495817	-0.60471	0.031767
CLEC4G	XM_001496849	XP_001496899	-0.49977	0.005775
CLPX	XM_001498202	XP_001498252	-0.35828	0.015643
CLRN1	XM_001489624	XP_001489674	-0.50704	0.043534
CNTN5	XM_001499420	XP_001499470	-0.48395	0.018772

Table A-11 Continued

Gene Symbol	NCBI accession	RefSeq accession	Log fold change	Pvalue
COPS3	XM_001489781	XP_001489831	1.317346	0.006002
COQ5	XM_001488871	XP_001488921	-0.362	0.040116
COX7B2	XM_001496055	NULL	0.418043	0.003373
CRTAC1	XM_001501238	XP_001501288	-0.344	0.017977
CRYGS	XM_001499197	XP_001499247	-0.32412	0.018514
CTDSPL2	XM_001502847	XP_001502897	-0.28197	0.046758
CTNNA1	XM_001504256	XP_001504306	0.347933	0.01988
CYP11A1	NM_001082521	NULL	-0.26564	0.012307
CYP2B6	XM_001498389	XP_001498439	-0.9925	0.039791
CYP2F1	XM_001498170	XP_001498220	-0.58941	0.04966
D2HGDH	XM_001503152	XP_001503202	-0.35464	0.015085
DAO	XM_001500936	XP_001500986	0.604679	0.005247
DARC	XM_001490641	XP_001490691	-0.43282	0.037625
DCP1B	XM_001489775	NULL	-0.43519	0.028676
DCP2	XM_001503544	XP_001503594	0.520618	0.00031
DDT	NULL	NULL	0.365224	0.028522
DECR2	XM_001495338	XP_001495388	0.421156	0.001778
DHCR7	XM_001497598	XP_001497648	-0.32826	0.040516
DLEU7	XM_001488517	XP_001488567	0.32917	0.042681
DLX6	XM_001494576	XP_001494626	-0.2854	0.049404
DMAP1	XM_001496404	XP_001496454	0.128217	0.006903
DNAJB5	XM_001498146	XP_001498196	-0.34425	0.015034
DUT	XM_001499877	XP_001499927	0.536045	0.018876
DZIP1	XM_001492095	XP_001492145	0.427997	0.016201
ECM2	XM_001491513	XP_001491563	-0.31136	0.025311
EEF1A1	NULL	NULL	-0.36645	0.041193
EEF1E1	XM_001490875	XP_001490925	0.390926	0.040527
EFNA3	XM_001498265	XP_001498315	-0.58867	0.003751
EIF2C1	XM_001503662	NULL	-0.28284	0.019496
EIF3CL	DN509049	NULL	-0.69744	0.009602
EIF3CL	CX603489	NULL	-0.3145	0.017678
ELAVL1**	**XM_001497883**	**XP_001497933**	**1.018199**	**0.006986**
EMP2	XM_001492271	NULL	0.391436	0.026733
EMR3	XM_001495605	XP_001495655	0.487905	0.048778
ENO3	NULL	NULL	-0.38754	0.018971
ERBB2	XM_001501105	XP_001501155	-0.81754	0.039115
EXOC8	XM_001494038	XP_001494088	-1.19338	0.008229
FAM107B	XM_001498585	XP_001498635	-0.37907	0.002294
FAM45A	CX598831	NULL	1.481584	0.024642
FBXL10	DN504171	NULL	-0.55947	0.035738
FBXL11	XM_001497095	XP_001497145	-0.34449	0.008827
FBXL15	XM_001499655	XP_001499705	-0.24886	0.043512
FBXL22	XM_001499127	NULL	-0.31008	0.017224
FCF1	XM_001490976	XP_001491026	-0.31983	0.048569
FES	XM_001498763	NULL	-0.45435	0.035789
FEZ2	XM_001499974	XP_001500024	0.173831	0.038165
FGA	BM780427	NULL	-0.43454	0.021822
FLJ12993	XM_001493769	XP_001493819	-0.46767	0.00952
FLJ20254	XM_001502643	XP_001502693	0.340071	0.010832
FLJ25006	XM_001501927	XP_001501977	-0.31047	0.013722

Table A-11 Continued

Gene Symbol	NCBI accession	RefSeq accession	Log fold change	Pvalue
FLJ31818	XM_001500571	XP_001500621	0.289857	0.008696
FLJ40243	XM_001496447	XP_001496497	0.406214	0.035389
FLJ46321	#N/A	#N/A	-0.43179	0.011405
FLJ46321	#N/A	#N/A	-0.29692	0.01998
FLRT2	XM_001495071	XP_001495121	0.302181	0.013902
FMO3	XM_001495951	XP_001496001	0.523709	0.009847
FN3KRP	XM_001490260	XP_001490310	0.318488	0.022715
FOXP4	XM_001501047	XP_001501097	0.316174	0.022606
FRYL	NULL	NULL	-0.34467	0.005715
FTL	XM_001488775	XP_001488825	-0.35257	0.038442
GABRA2	XM_001496096	XP_001496146	0.495879	0.035691
GATAD1	XM_001493322	XP_001493372	0.522085	0.037253
GBA	XM_001498650	XP_001498700	0.270754	0.026967
GBA2	XM_001497746	XP_001497796	0.163072	0.01766
GEMIN6	XM_001500469	XP_001500519	-0.13552	0.041607
GMIP	XM_001503515	XP_001503565	-0.15845	0.029161
GOLPH3	XM_001500613	XP_001500663	0.418452	0.043142
GORASP1	XM_001498286	XP_001498336	-0.17059	0.015596
GPRC6A	XM_001504147	XP_001504197	-0.45449	0.01586
GRINA	XM_001493306	XP_001493356	0.539736	0.049361
GTSE1	XM_001488648	XP_001488698	-0.48555	0.046174
HBB	XM_001504190	XP_001504240	1.436502	0.0228
HDAC3	XM_001503978	XP_001504028	0.198928	0.042852
HFE	XM_001505039	XP_001505089	0.677802	0.024956
HIST1H3B	XM_001493440	XP_001493490	0.173631	0.049382
HIST2H2AB	XM_001488506	XP_001488556	-0.13196	0.018501
HNRPDL	AY246721	NULL	-0.43276	0.016786
HRAS	XM_001488899	NULL	0.406556	0.019443
HSD11B2	AF126744	NP_001075395	-0.39177	0.043871
HSPBP1	NULL	NULL	-0.49075	0.030163
HSPE1	NULL	NULL	1.359839	0.039948
HTR4	AY263357	NULL	-0.28813	0.026755
IDH3G	XM_001493411	XP_001493461	-0.23873	0.045309
IFNW1	XM_001497115	XP_001497165	-0.12699	0.039297
IFT57	XM_001503311	XP_001503361	-0.46961	0.027765
IGSF21	XM_001498665	XP_001498715	-0.39913	0.033873
IGSF8	XM_001491262	XP_001491312	0.480286	0.046656
IL1RL1	XM_001491350	XP_001491400	-0.538	0.038873
IL3	XM_001504454	NULL	-0.50156	0.035707
ILK	XM_001504599	XP_001504649	-0.30422	0.01894
ING5	XM_001497795	XP_001497845	-0.35798	0.040122
INTS12	XM_001503610	XP_001503660	-0.31402	0.006822
ITGAL	XM_001496070	XP_001496120	-0.33171	0.022815
JAK2	XM_001500499	XP_001500549	-0.51016	0.010581
JMJD3	XR_036443	NULL	0.324232	0.048903
KCNH8	XM_001495463	XP_001495513	-0.4725	0.015057
KCTD11	NULL	NULL	-0.52284	0.03645
KDELC1	XM_001493228	XP_001493278	0.372368	0.016248
KIAA0226	XM_001499814	XP_001499864	0.827202	0.038863
KIAA0907	XM_001499401	XP_001499451	0.148796	0.049374

Table A-11 Continued

Gene Symbol	NCBI accession	RefSeq accession	Log fold change	Pvalue
KIAA1853	XM_001490434	XP_001490484	-0.32549	0.038302
KIF2A	XM_001493976	XP_001494026	1.04902	0.001648
KIF5B	XM_001493254	XP_001493304	-0.23622	0.046619
KL	XM_001495612	XP_001495662	-0.37402	0.019868
KLK8	XM_001497389	XP_001497439	0.245556	0.025008
KLRD1	XM_001494069	XP_001494119	0.260962	0.034785
KLRK1	XM_001499819	XP_001499869	-0.35753	0.044149
KRTAP10-7	XM_001490330	XP_001490380	-0.4848	0.026736
KTELC1	XM_001500712	XP_001500762	0.357019	0.031305
LAMP1	XM_001495652	XP_001495702	-0.68662	0.025885
LAT	XM_001502343	XP_001502393	1.094573	0.04829
LBP	XM_001499815	XP_001499865	0.27448	0.038729
LDHB	XM_001502203	XP_001502253	-0.3092	0.026803
LHX6	XM_001501453	NULL	-0.3683	0.038979
LHX9	XM_001492961	NULL	0.238433	0.026941
LILRB3	XM_001488558	XP_001488608	-0.10361	0.048875
LMBR1L	XM_001504157	XP_001504207	-0.49004	0.005773
LOC255809	XM_001490886	NULL	-0.30213	0.0277
LOC283677	XM_001494312	XP_001494362	-0.50036	0.008356
LOC401934	XM_001496605	NULL	0.225593	0.044584
LOC729533	XM_001489563	NULL	0.55112	0.028664
LONRF1	XM_001494722	XP_001494772	0.368876	0.005907
LRMP	XM_001498588	XP_001498638	-0.37691	0.036073
LRRC15	XM_001500569	XP_001500619	-0.7499	0.045015
LRRC25	XM_001500641	XP_001500691	1.076904	0.002838
LRRC36	XM_001496409	XP_001496459	1.085917	0.043118
LRRC41	NULL	NULL	0.311386	0.029295
LYNX1	XM_001496732	XP_001496782	-0.43004	0.019176
MAGED1	CX595349	NULL	-0.2497	0.048527
MAL	XM_001494676	NULL	-0.42252	0.003718
MAL	XM_001494113	XP_001494163	-0.48321	0.020482
MAML1	XM_001497397	XP_001497447	0.419366	0.022563
MAP4K3	XM_001499556	XP_001499606	0.279908	0.012328
MARK2	NULL	NULL	-1.27109	0.009214
MAT2A	XM_001497416	XP_001497466	-0.23636	0.022092
MC3R	XM_001489123	XP_001489173	-0.55662	0.024977
MCM8	XM_001496114	XP_001496164	0.302788	0.035381
MEIS3	XM_001503175	XP_001503225	0.230872	0.03966
MMD	XM_001500221	XP_001500271	0.260309	0.035177
MNDA	XM_001490503	XP_001490553	0.263727	0.043212
MPP5	XM_001499684	XP_001499734	-0.25067	0.033853
MPZL3	XM_001500915	XP_001500965	0.445297	0.040927
MRFAP1	CX594991	NULL	-0.67634	0.048577
MRPL1	XM_001491866	XP_001491916	-0.18196	0.020208
MRPL21	CX604559	XP_001499094	0.994656	0.012171
MRPL47	XM_001495484	XP_001495534	0.306573	0.016678
MSRB2	XM_001495858	NULL	-0.38218	0.013082
MTERFD2	XM_001497592	XP_001497642	0.242095	0.043465
MTFR1	XM_001495100	XP_001495150	-0.54029	0.011643
MTHFD2L	XM_001490173	XP_001490223	-0.32808	0.037074

Table A-11 Continued

Gene Symbol	NCBI accession	RefSeq accession	Log fold change	Pvalue
MTNR1A	XM_001490171	XP_001490221	-0.16377	0.018636
MX2	U55216	NP_001075961	-0.42476	0.012707
MXD4	XM_001488540	XP_001488590	-0.4782	0.047791
MYEOV2	XM_001497339	XP_001497389	0.801473	0.030051
MYLIP	XM_001493152	XP_001493202	0.602705	0.000216
MYO1B	XM_001502243	XP_001502293	-0.76223	0.027856
NAE1	XM_001496095	XP_001496145	0.308608	0.0113
NAGA	XM_001502709	XP_001502759	0.342072	0.028904
NARG1	XM_001502496	XP_001502546	-0.30179	0.017191
NBPF6	XM_001491713	NULL	-0.16598	0.032227
NDUFA3	XM_001488784	NULL	-0.4914	0.025004
NFYA	XM_001500879	XP_001500929	0.196692	0.034159
NHLRC1	XM_001496559	XP_001496609	0.425955	0.027616
NID1	NULL	NULL	-0.27056	0.040337
NID2	XM_001497325	XP_001497375	-0.16267	0.040769
NKIRAS2	XM_001495362	XP_001495412	-0.48614	0.049914
NMBR	XM_001502752	XP_001502802	-0.22195	0.03695
NNMT	XM_001500480	XP_001500530	0.444659	0.040034
NOTCH3	NULL	NULL	-0.2651	0.015905
NPEPPS	XM_001498919	XP_001498969	0.172038	0.024811
NPTXR	CX594481	NULL	-0.46787	0.031628
NSD1	XM_001502429	XP_001502479	0.531832	0.031273
NULL	CX601100	NULL	-0.67773	0.00164
NULL	BM735205	NULL	-0.7024	0.003485
NULL	XM_001499091	XP_001499141	-0.79201	0.003809
NULL	DN507943	NULL	-0.64088	0.003851
NULL	DN508635	NULL	-0.48034	0.004784
NULL	CX601827	NULL	-1.08591	0.005241
NULL	CD468792	NULL	-0.57139	0.005412
NULL	CX604012	NULL	0.363557	0.005468
NULL	DN504496	NULL	0.332039	0.0057
NULL	CX602321	NULL	0.500311	0.005783
NULL	CX602251	NULL	-0.60126	0.006089
NULL	DN506707	NULL	-0.34604	0.008084
NULL	CX598059	NULL	-0.41728	0.009811
NULL	DN505730	NULL	0.409894	0.010636
NULL	CX593209	NULL	0.145297	0.011794
NULL	CX605433	NULL	-0.45932	0.012188
NULL	XM_001498676	XP_001498726	-0.42284	0.012976
NULL	XM_001499079	XP_001499129	-0.28088	0.014014
NULL	CX603887	NULL	0.343868	0.014105
NULL	CX603684	NULL	-0.36693	0.015477
NULL	CX595318	NULL	0.264926	0.015884
NULL	DN508766	NULL	-0.44952	0.016605
NULL	XM_001500257	NULL	0.447962	0.017507
NULL	CX603713	NULL	-0.35958	0.018491
NULL	DN510407	NULL	-0.24818	0.018983
NULL	CD464196	NULL	0.558409	0.019886
NULL	NULL	NULL	0.35697	0.019998
NULL	DN508159	NULL	-0.56657	0.020105

Table A-11 Continued

Gene Symbol	NCBI accession	RefSeq accession	Log fold change	Pvalue
NULL	BM735424	NULL	1.520936	0.020466
NULL	XM_001503536	XP_001503586	-0.54449	0.021203
NULL	CX593935	NULL	-0.42233	0.02156
NULL	CX596903	NULL	0.464739	0.021816
NULL	XM_001490812	NULL	-0.39431	0.022622
NULL	CX604190	NULL	-0.62638	0.024814
NULL	CX602929	NULL	0.271464	0.025325
NULL	CD467522	NULL	-0.45779	0.025506
NULL	DN509048	NULL	-0.75683	0.026148
NULL	DN510495	NULL	-0.18871	0.027206
NULL	CD465619	NULL	1.250059	0.028296
NULL	CX599439	NULL	-0.38836	0.028907
NULL	XR_036039	NULL	0.413724	0.029429
NULL	XM_001498663	NULL	-0.2136	0.02979
NULL	CX600740	NULL	-0.67915	0.032207
NULL	DN509646	NULL	-0.3427	0.033119
NULL	DN504061	NULL	0.126985	0.035378
NULL	CX599268	NULL	0.241347	0.036262
NULL	CX603914	NULL	-0.32499	0.037032
NULL	CX601732	NULL	-0.42339	0.037134
NULL	CX601151	NULL	0.248239	0.03816
NULL	XR_036258	NULL	-0.56344	0.039309
NULL	XM_001496940	NULL	-0.45673	0.039553
NULL	CX602249	NULL	-0.58671	0.039715
NULL	CD528873	NULL	-0.28557	0.039772
NULL	CX604208	NULL	-0.24671	0.04007
NULL	XM_001492225	XP_001492275	-0.3243	0.040092
NULL	XM_001503568	NULL	0.345419	0.04114
NULL	CX605182	NULL	-0.20818	0.041375
NULL	XM_001493134	NULL	0.272965	0.042045
NULL	CX594596	NULL	-0.95861	0.042623
NULL	DN507767	NULL	-0.56498	0.043055
NULL	XM_001496228	XP_001496278	0.112603	0.043923
NULL	CX597119	NULL	-0.55971	0.045049
NULL	DN509404	NULL	0.328628	0.045736
NULL	NULL	NULL	0.289731	0.046468
NULL	NULL	NULL	0.322679	0.046653
NULL	NULL	NULL	0.134845	0.046877
NULL	DN509184	NULL	-0.68031	0.047685
NULL	BM780537	NULL	1.344317	0.048789
NULL	DN510522	NULL	-0.33785	0.048892
NULL	CX596762	NULL	-0.71837	0.049943
NUP85	XM_001496162	XP_001496212	0.30659	0.033569
ODZ3	NULL	NULL	0.30416	0.027222
OMG	XM_001504036	XP_001504086	0.903839	0.036137
OR12D2	XM_001499509	NULL	0.315713	0.028131
OR13C8	XM_001493303	XP_001493353	0.596551	0.038654
OR1N1	XM_001501095	XP_001501145	-0.47512	0.006692
OR2D3	XM_001500110	XP_001500160	0.725878	0.027357
OR2D3	XM_001499982	XP_001500032	0.447959	0.041069

Table A-11 Continued

Gene Symbol	NCBI accession	RefSeq accession	Log fold change	Pvalue
OR2G3	XM_001491712	XP_001491762	-0.32043	0.039956
OR2L2	XM_001497233	XP_001497283	-0.40817	0.020941
OR2T1	XM_001502542	XP_001502592	-0.44488	0.045203
OR2T4	XM_001504685	XP_001504735	1.089059	0.026307
OR2T4	XM_001490238	NULL	-0.3494	0.031239
OR4A16	XM_001495905	NULL	0.489512	0.028438
OR4A47	XM_001495702	XP_001495752	-0.465	0.040039
OR4D1	XM_001503470	NULL	-0.80203	0.01943
OR4D9	XM_001495337	NULL	0.348727	0.026342
OR51F1	XM_001497409	XP_001497459	-0.45656	0.001096
OR52A1	XM_001498165	XP_001498215	-0.31527	0.045603
OR52E8	XM_001496727	XP_001496777	-0.41831	0.005041
OR5AT1	XM_001488321	XP_001488371	-0.89421	0.014204
OR5B3	XM_001497677	XP_001497727	-0.66089	0.029936
OR6C2	XM_001491344	XP_001491394	0.728612	0.014376
OR6C2	XM_001489614	XP_001489664	-0.63834	0.021204
OR6C2	XM_001489573	XP_001489623	-0.38728	0.023382
OR6F1	XM_001497005	XP_001497055	-0.39749	0.002335
OR7G2	XM_001494401	XP_001494451	-0.47589	0.001555
OR8B3	XM_001502010	XP_001502060	0.337228	0.010235
OR8B3	XM_001501965	XP_001502015	-0.44819	0.02263
OR8B3	XM_001501664	XP_001501714	0.415064	0.024793
OR8B3	XM_001501870	XP_001501920	-0.37101	0.035763
OR8G2	XM_001501835	XP_001501885	-0.38882	0.007602
OR9I1	XM_001497370	XP_001497420	-0.29027	0.024997
OR9I1	XM_001497800	XP_001497850	0.284142	0.025185
OSBPL11	XM_001501564	XP_001501614	0.337289	0.008461
OTOA	XM_001498662	XP_001498712	-0.38073	0.032787
PAFAH1B3	XM_001501179	XP_001501229	-0.39568	0.021092
PAIP1	NULL	NULL	-0.61037	0.00168
PAMCI	XM_001491284	XP_001491334	-0.28221	0.028922
PASK	XM_001497609	XP_001497659	0.262052	0.006837
PAX2	XM_001499985	XP_001500035	0.5136	0.038219
PAX5	XM_001504306	XP_001504356	-0.67071	0.0113
PBXIP1	NULL	NULL	-0.56141	0.034118
PCDHGA1	XM_001502164	XP_001502214	0.295804	0.044348
PDCD1LG2	XM_001492097	XP_001492147	0.333714	0.042233
PDCD5**	**CX600347**	**NULL**	**0.595991**	**0.034822**
PEO1	XM_001499940	XP_001499990	0.908884	0.01853
PEX1	XM_001493365	XP_001493415	-0.33281	0.036541
PFDN1	XM_001499395	XP_001499445	-0.25002	0.031685
PGRMC1	DN509190	NULL	-0.6774	0.047156
PHLDB2	XM_001501356	XP_001501406	-0.34437	0.039855
PHOX2A	XM_001499157	XP_001499207	-0.48986	0.044225
PIBF1	XM_001496359	XP_001496409	0.579437	0.038817
PIGW	XM_001503800	XP_001503850	0.605626	0.005669
PIK3R1**	**XM_001491571**	**XP_001491621**	**-1.45857**	**0.000769**
PIWIL4	XM_001498511	XP_001498561	-0.37208	0.005277
PLA2G4B	XM_001500747	XP_001500797	0.238702	0.028487
PLAC8	DN503804	NULL	-0.25129	0.024623

Table A-11 Continued

Gene Symbol	NCBI accession	RefSeq accession	Log fold change	Pvalue
PLCL1	XM_001500272	XP_001500322	0.384306	0.021737
PLCXD2	XM_001501392	XP_001501442	-0.32069	0.036216
PLEK2	XM_001499816	XP_001499866	-0.69179	0.022386
PNKD	CX600626	NULL	-0.4653	0.023308
POLL	XM_001499802	XP_001499852	-0.96154	0.024432
POLR1C	XM_001502041	XP_001502091	0.543719	0.030209
POLR2C	XM_001494211	XP_001494261	-0.44105	0.007487
POLR2H	XM_001498245	XP_001498295	-0.24263	0.030994
PPAPDC3	XM_001498987	XP_001499037	-0.24863	0.036815
PPCDC	XM_001491716	XP_001491766	-0.44417	0.002218
PPM1M	XM_001492660	NULL	0.189241	0.04209
PQBP1	XM_001494409	XP_001494459	-0.28915	0.02038
PRIMA1	XM_001495263	XP_001495313	0.27794	0.037698
PRKAB1	XM_001490253	XP_001490303	-0.49682	0.009982
PRKAR1A	NULL	NULL	-0.29288	0.019041
PRPF4	XM_001488863	XP_001488913	-0.24401	0.011598
PRPSAP2	XM_001488362	XP_001488412	-0.13886	0.029364
PRSS27	XM_001498358	XP_001498408	-0.24355	0.049024
PSMA1	XM_001504944	XP_001504994	1.403976	0.033914
PSMA2	XM_001495200	XP_001495250	-0.17599	0.043855
PSTK	XM_001490298	XP_001490348	-0.32289	0.047575
PTCRA	XM_001497178	XP_001497228	0.511121	0.043665
PTGS2	AB041771	NULL	-0.61131	0.003264
PTPRA	XM_001497046	XP_001497096	-0.49236	0.039803
PTPRM	NULL	NULL	0.242835	0.026959
PWWP2B	XM_001488078	XP_001488128	-0.32772	0.007807
RAB10	XM_001502813	XP_001502863	0.541243	0.049004
RAB39	XM_001501007	XP_001501057	0.465332	0.031408
RAB9A	XM_001488986	XP_001489036	0.288793	0.029713
RAD51C	XM_001500643	XP_001500693	0.427758	0.037929
RAG1AP1	XM_001498337	XP_001498387	-0.29493	0.022318
RASGEF1C	XM_001501051	XP_001501101	0.309668	0.019989
RCL1	XM_001491924	XP_001491974	-0.45125	0.012265
RCN1	NULL	NULL	-0.44143	0.005236
RCN2	XM_001493149	XP_001493199	1.128578	0.011424
RECQL	NULL	NULL	-0.35707	0.048399
RHBDD1	XM_001496411	XP_001496461	-0.25906	0.020625
RIT2	XM_001497798	XP_001497848	0.384162	0.047161
RNASET2	XM_001489592	XP_001489642	-0.33638	0.035311
RNF6	NULL	NULL	0.290255	0.018977
RNH1	XM_001488475	XP_001488525	-0.52832	0.027001
ROR2	XM_001495538	XP_001495588	-0.15183	0.034363
RPAP2	XM_001492375	XP_001492425	1.616473	0.04193
RPL13A	XM_001491876	XP_001491926	1.157148	0.005014
RPL9	XM_001498163	XP_001498213	-0.11745	0.033947
RPS15A	CD467047	NULL	-0.82898	0.009938
RPS18	NULL	NULL	-0.52733	0.032222
RSU1	XM_001498053	XP_001498103	-0.23718	0.020765
RUSC2	XM_001504521	XP_001504571	-0.38864	0.006565
RXFP1	XM_001500397	XP_001500447	0.479782	0.036678

Table A-11 Continued

Gene Symbol	NCBI accession	RefSeq accession	Log fold change	Pvalue
RYBP	XM_001493974	XP_001494024	0.551866	0.037589
S100A2	CX598422	XP_001494717	-0.28614	0.000633
SAAL1	XM_001501683	XP_001501733	-0.42161	0.009864
SAMM50	XM_001487978	XP_001488028	-0.46664	0.016864
SCO2	XM_001490346	XP_001490396	-0.5202	0.020918
SCYL1BP1	CX603672	NULL	0.476634	0.016104
SDHB	XM_001488214	XP_001488264	-0.4021	0.037353
SEC14L2	XM_001498151	XP_001498201	-0.31864	0.016432
SEMA6D	XM_001502470	NULL	1.611118	0.041064
SENP5	XM_001499415	XP_001499465	-0.2666	0.021735
SERPINA10	XM_001495713	XP_001495763	-0.22057	0.016413
SERPINB5	XM_001490854	XP_001490904	0.290265	0.034924
SERPINB7	XM_001491729	XP_001491779	-0.6862	0.009143
SESN2	XM_001503991	XP_001504041	0.380826	0.032296
SFT2D2	XM_001490765	NULL	-0.36743	0.014426
SH2D4B	XM_001501404	XP_001501454	-1.04133	0.041784
SHCBP1	XM_001490125	XP_001490175	0.251866	0.018841
SIGLEC10	XM_001496570	XP_001496620	1.824777	0.033051
SLBP	XM_001488379	XP_001488429	-0.41802	0.025112
SLC12A3	XM_001502571	XP_001502621	-0.27332	0.008323
SLC19A2	XM_001491417	XP_001491467	-0.33836	0.026902
SLC22A18	XM_001492540	XP_001492590	0.376234	0.038742
SLC25A13	XM_001494425	XP_001494475	-0.44461	0.007677
SLC26A9	XM_001490825	XP_001490875	0.432121	0.033086
SLC29A3	XM_001502808	XP_001502858	-0.49362	0.027257
SLC2A3	XM_001498757	XP_001498807	-0.46009	0.049435
SLC30A9	XM_001494445	XP_001494495	-0.5714	0.017555
SLC36A2	XM_001501324	XP_001501374	-0.21357	0.03344
SLC39A9	XM_001500384	XP_001500434	0.278338	0.049063
SLC7A4	XM_001488939	XP_001488989	-0.43406	0.039078
SLC7A7	CD535752	NULL	-0.91116	0.004926
SLC9A8	XM_001501184	XP_001501234	-0.49589	0.006665
SNAI2	XM_001488056	XP_001488106	0.227857	0.034827
SP3	XM_001495258	XP_001495308	0.397893	0.034462
SPATS2	NULL	NULL	0.359554	0.045724
SPRY3	XM_001498267	XP_001498317	0.43798	0.036341
SPSB3	XM_001497802	XP_001497852	0.296659	0.020542
SRD5A2	XM_001501522	XP_001501572	0.446924	0.019614
SSRP1	XM_001497090	XP_001497140	-0.21896	0.028055
STAMBPL1	XM_001503046	XP_001503096	0.648776	0.048185
STARD8	XM_001496620	XP_001496670	-0.15655	0.023873
STMN2	XM_001490291	XP_001490341	-0.4201	0.005985
TAAR8	XM_001503349	XP_001503399	-0.37331	0.039089
TATDN1	CX598673	NULL	-0.33175	0.049004
TBC1D16	XM_001490266	XP_001490316	-0.51957	0.03238
TBP	XM_001499329	XP_001499379	-0.57815	0.035184
TBX5	NULL	NULL	-0.41324	0.007684
TCAP	XM_001501165	XP_001501215	-0.43643	0.049727
TCERG1	NULL	NULL	0.367793	0.021478
TFPI2	XM_001492769	XP_001492819	0.523447	0.020102

Table A-11 Continued

Gene Symbol	NCBI accession	RefSeq accession	Log fold change	Pvalue
THAP3	XM_001491823	XP_001491873	-0.42859	0.016419
THEM4	XR_036022	NULL	-0.20629	0.018377
THNSL1	XM_001495489	XP_001495539	0.892391	0.04134
THUMPD2	XM_001499458	XP_001499508	-0.22917	0.011271
TIMM17B	CX602842	XP_001494391	-0.72716	0.015399
TLOC1	XM_001494700	XP_001494750	0.615924	0.004561
TMEM107	CX602840	XP_001504860	-0.49671	0.019149
TMEM186	XM_001490868	XP_001490918	-0.17676	0.04649
TMEM58	XM_001494838	XP_001494888	-0.58807	0.04332
TMEM61	XM_001492579	XP_001492629	-0.84275	0.046517
TMEM66	XM_001494229	XP_001494279	-0.64837	0.03537
TMPO	XM_001496532	XP_001496582	0.592739	0.002712
TMPRSS11B	XM_001497493	XP_001497543	0.322418	0.039678
TMPRSS11E2	XM_001501361	XP_001501411	-0.49099	0.018928
TMPRSS11F	XM_001497462	XP_001497512	-0.18015	0.04736
TNFRSF11A	XM_001490290	NULL	-0.60134	0.021882
TNNI1	NULL	NULL	-0.42858	0.029371
TNNI3	AY819020	NP_001075373	-0.14174	0.048887
TOR3A	XM_001494447	XP_001494497	0.368171	0.022678
TP53BP1	XM_001503090	XP_001503140	-0.53399	0.022722
TP53BP2	XM_001489738	XP_001489788	-0.59972	0.001774
TPM2	NULL	NULL	0.410223	0.039612
TPM3	XM_001496060	XP_001496110	0.790491	0.049503
TPPP	XM_001490990	NULL	-0.13979	0.031393
TPR	NULL	NULL	-0.3308	0.039404
TRAF3IP3	XM_001490981	NULL	-0.11419	0.038281
TRAT1	XM_001501680	NULL	-0.36617	0.027302
TSC1	XM_001498348	XP_001498398	-0.25102	0.041166
TSPAN17	XM_001492295	NULL	0.293128	0.034302
TSPAN17	NULL	NULL	-0.22306	0.04522
TSPAN4	XM_001494692	XP_001494742	-0.76231	0.045128
TSSK1B	XM_001495808	XP_001495858	-0.39324	0.038658
TTC17	XM_001489510	XP_001489560	-0.26205	0.049193
TTC29	XM_001500442	XP_001500492	0.222961	0.017177
TTC32	XM_001503379	XP_001503429	-0.36951	0.011026
TTN	NULL	NULL	-0.3528	0.036569
TUBGCP2	NULL	NULL	0.316341	0.002595
TYRP1	NM_001081840	NULL	-0.64773	0.009289
UBC	XM_001499082	XP_001499132	-0.50371	0.016492
UBE2N	XM_001495374	XP_001495424	-1.40564	0.009958
UBR1	NULL	NULL	0.34222	0.04028
UGCGL2	XR_035970	NULL	1.321114	0.008578
UNC93B1	XR_035965	NULL	0.395064	0.002776
UNK	XM_001492039	XP_001492089	-0.64874	0.006525
USF2	XM_001491920	NULL	-0.48562	0.040525
USO1	XM_001490004	XP_001490054	-0.74932	0.028564
USP26	XM_001490646	XP_001490696	-0.20627	0.043552
USP37	XM_001491830	XP_001491880	0.278041	0.019774
VAMP4	XM_001496519	XP_001496569	-0.61482	0.006003
VAX2	XM_001492525	XP_001492575	-0.11692	0.034143

Table A-11 Continued

Gene Symbol	NCBI accession	RefSeq accession	Log fold change	Pvalue
VN1R4	XM_001495698	NULL	-0.76408	0.008464
VN1R4	XM_001495663	XP_001495713	-0.52895	0.008648
VPS25	DN506327	NULL	-0.4429	0.024473
VPS8	XM_001498641	XP_001498691	-0.44364	0.038505
VTCN1	XM_001496634	XP_001496684	0.826387	0.039715
VWA3A	XM_001491541	NULL	0.196857	0.038463
WASF3	XM_001491084	XP_001491134	-0.26094	0.019494
WDR1	XM_001501013	XP_001501063	0.178524	0.0446
WDR19	XM_001498365	XP_001498415	-0.31339	0.030455
WDR36	XM_001503571	XP_001503621	0.71301	0.045841
WDR52	XM_001501172	XP_001501222	-0.32261	0.013713
WIPF2	XM_001500432	XP_001500482	0.580661	0.013572
ZFYVE26	XM_001500061	XP_001500111	-0.24851	0.013307
ZNF24	XM_001496673	XP_001496723	0.493909	0.027197
ZNF384	XM_001492314	XP_001492364	-0.14402	0.048108
ZNF385B	XM_001501085	XP_001501135	-0.27851	0.03744
ZNF454	XM_001501556	XP_001501606	-0.48612	0.045934
ZNF571	XM_001493743	XP_001493793	0.382406	0.011424
ZNF704	XM_001491115	XP_001491165	-0.28161	0.040396
ZNF709	XM_001496693	XP_001496743	0.271299	0.015172
ZSWIM6	XM_001492480	XP_001492530	-0.4768	0.039998

Table A-12: List of differentially expressed genes (pvalue<0.05) for RAO-affected horses compared to control after the 30-day allergen challenge. ** Represents genes with pvalue<0.05 and fold change ≥ 0.58 or ≤ -0.58 selected for qPCR.

Gene symbol	NCBI accession	RefSeq accession	Log fold change	Pvalue
39509	XM_001487921	XP_001487971	-0.21501	0.008258
ABCA4	XM_001491597	XP_001491647	-0.24088	0.020179
ABCC1	DQ418453	NP_001075232	-0.37076	0.004618
ACAA1	XM_001488559	XP_001488609	0.439247	0.014224
ACCN5	XM_001500739	XP_001500789	0.697107	0.045548
ACTR2	XM_001494389	XP_001494439	-1.92631	0.002144
ADCY4	XM_001489040	XP_001489090	0.394923	0.025122
AGPAT1	XM_001492068	XP_001492118	-0.52109	0.046043
AGTRL1	XM_001504912	XP_001504962	-0.15371	0.048224
AHRR	XM_001490918	XP_001490968	0.404589	0.017294
AJAP1	XM_001492529	XP_001492579	0.41276	0.043132
ALDOB	XM_001504011	XP_001504061	-0.61132	0.020628
ALKBH3	XM_001489694	XP_001489744	-0.25528	0.006483
ALKBH6	XM_001492599	XP_001492649	-0.31432	0.028275
ARHGAP11A	XM_001503656	XP_001503706	-0.27127	0.049702
ARID5B	XM_001503500	XP_001503550	-0.36463	0.02885
ART3	XM_001490592	XP_001490642	-0.24265	0.049635
ATF7	XM_001504543	XP_001504593	-0.69194	0.005127
ATG9B	XM_001495054	XP_001495104	-0.43453	0.008089
ATOH1	XM_001495691	XP_001495741	-0.26671	0.01328
ATP11B	XM_001496792	XP_001496842	-0.2865	0.033604
ATP5G1	XM_001499269	XP_001499319	-0.13855	0.025869
ATP6AP1	XM_001494850	NULL	-0.36204	0.02178
AUP1	XR_036315	NULL	0.193886	0.021566
B4GALT3	XM_001503814	XP_001503864	-0.4411	0.018534
BHLHB3	CX604838	NULL	-0.26255	0.008899
BHLHB9	XM_001504604	XP_001504654	0.278385	0.018121
BMS1	XM_001489945	XP_001489995	-0.40133	0.028896
BTBD16	XM_001495476	XP_001495526	0.31356	0.004471
BTN3A3	XM_001492121	XP_001492171	-0.4129	0.022899
C10orf11	XM_001503070	XP_001503120	-0.27753	0.028051
C10orf35	XM_001503697	XP_001503747	-0.33961	0.047171
C11orf41	XM_001492058	XP_001492108	-0.37076	0.028522
C17orf49	NULL	NULL	1.108573	0.000595
C17orf63	XM_001504183	XP_001504233	-0.7154	0.02688
C17orf75	XM_001504001	XP_001504051	-0.40659	0.010759
C1orf149	XM_001498954	XP_001499004	0.113634	0.039654
C1orf182	XM_001495120	NULL	0.701324	0.0435
C2	XM_001492501	XP_001492551	0.298633	0.038245

Table A-12 Continued

Gene symbol	NCBI accession	RefSeq accession	Log fold change	Pvalue
C20orf149	NULL	NULL	1.015525	0.048434
C4orf35	XM_001502161	XP_001502211	0.605399	0.044016
C6orf128	XM_001495299	XP_001495349	0.312798	0.036258
C7orf42	XM_001499915	XP_001499965	-0.23991	0.044483
C8orf33	XM_001494951	NULL	-0.37805	0.017016
C9orf125	XM_001504009	XP_001504059	0.414458	0.037869
C9orf23	DN510873	XP_001498436	-0.6268	0.000469
CASC5	XM_001501097	XP_001501147	-0.23901	0.032447
CASR	XM_001502152	XP_001502202	0.445185	0.039913
CATSPERB	XM_001494573	XP_001494623	-0.32921	0.042172
CBS	XM_001490849	NULL	1.088121	0.01086
CCDC142	XM_001498892	XP_001498942	-0.3235	0.045393
CCDC38	XM_001496074	XP_001496124	0.492362	0.022565
CCDC68	XM_001488458	XP_001488508	-0.14245	0.021078
CCL11	AJ251188	NP_001075340	0.225497	0.029067
CCL5	AF506970	NP_001075332	0.739873	0.035852
CCL8	AF506972	NP_001075333	0.395796	0.034808
CCNG1	XM_001503358	XP_001503408	0.322989	0.045921
CDC23	XM_001504289	XP_001504339	0.357997	0.034333
CHMP2A	XM_001495629	XP_001495679	0.531585	0.036436
CLRN1	XM_001489624	XP_001489674	-0.58661	0.021593
CLRN2	XM_001498507	XP_001498557	-0.22687	0.044594
CNIH2	XM_001491221	NULL	-0.18796	0.033759
CNTNAP5	XM_001489205	XP_001489255	0.421424	0.044733
COPS3	XM_001489781	XP_001489831	1.695628	0.00079
COPS7B	XM_001498509	XP_001498559	-0.80484	0.022268
CORO1C	XM_001500961	XP_001501011	-0.19039	0.037091
COX18	XM_001488484	XP_001488534	-0.33021	0.027109
COX5A	DN504112	XP_001491906	0.225113	0.039324
COX7C	XM_001504630	NULL	0.84929	0.019084
CREB3L2	XM_001499610	XP_001499660	-0.23417	0.011386
CRTAC1	XM_001501238	XP_001501288	-0.34228	0.018482
CTDSPL2	XM_001502847	XP_001502897	-0.46335	0.002379
CYP39A1	XM_001498174	XP_001498224	-0.22456	0.047946
DAPP1	DN504745	NULL	0.375578	0.037677
DCP2	XM_001503544	XP_001503594	0.307228	0.018115
DDN	XM_001491707	XP_001491757	-0.58105	0.002249
DDR1	XM_001490798	XP_001490848	0.179244	0.023285
DDT	NULL	NULL	0.523196	0.002997
DECR2	XM_001495338	XP_001495388	0.244986	0.048646
DLX6	XM_001494576	XP_001494626	-0.35271	0.017734
DMAP1	XM_001496404	XP_001496454	0.16191	0.001128

Table A-12 Continued

Gene symbol	NCBI accession	RefSeq accession	Log fold change	Pvalue
DMRTC2	XM_001499585	XP_001499635	-0.25159	0.044309
DNAJB5	XM_001498146	XP_001498196	-0.34228	0.015538
DNAJC16	XM_001489768	XP_001489818	-0.21894	0.040372
DNAJC21	XM_001497983	XP_001498033	0.257368	0.049391
DNASE1L3	XM_001491051	XP_001491101	1.059955	0.041287
DZIP1	XM_001492095	XP_001492145	0.508085	0.005456
EEF1A1	NULL	NULL	1.077461	0.04369
EFNA3	XM_001498265	XP_001498315	-0.50762	0.010359
EIF2C1	XM_001503662	NULL	-0.2827	0.019545
EMID2**	**XM_001492651**	**XP_001492701**	**1.179418**	**0.005997**
ENDOGL1	XM_001488144	XP_001488194	-0.22543	0.033927
ETAA1	XM_001492658	XP_001492708	0.280771	0.047149
ETFDH	XM_001500342	XP_001500392	-0.12258	0.046647
EXOC5	XM_001491407	XP_001491457	-0.29879	0.011841
EYA4	XM_001504359	NULL	-0.6815	0.005129
FAM107B	XM_001498585	XP_001498635	-0.29336	0.013603
FAM108B1	XM_001488520	XP_001488570	-0.31686	0.028521
FARSA	XM_001504881	XP_001504931	0.153892	0.009352
FBXL15	XM_001499655	XP_001499705	-0.28166	0.024202
FBXL22	XM_001499127	NULL	-0.29888	0.02106
FBXO2	XM_001492274	XP_001492324	0.349863	0.047672
FBXO30	XM_001502353	XP_001502403	-0.20567	0.03598
FCF1	XM_001490976	XP_001491026	-0.42613	0.011148
FERMT2	XM_001494661	XP_001494711	-0.42347	0.048057
FGFR2	XM_001491765	XP_001491815	-0.28711	0.044411
FLJ11171	XM_001498320	XP_001498370	-0.50677	0.030762
FLJ12993	XM_001493769	XP_001493819	-0.4646	0.009925
FLJ46321	XM_001488510	NULL	0.958958	0.005997
FLJ46321	N/A	N/A	-0.21903	0.044957
FPRL1	XM_001489967	XP_001490017	-0.30868	0.009139
FRK	XM_001504096	XP_001504146	0.437822	0.040077
FTH1	XM_001488238	NULL	-0.18888	0.046372
GALNT5	XM_001491135	XP_001491185	0.130806	0.042747
GAPVD1	XR_036393	NULL	0.679605	0.008361
GBA	XM_001498650	XP_001498700	0.368033	0.004092
GBA2	XM_001497746	XP_001497796	0.177416	0.010756
GCC1	XM_001502547	XP_001502597	0.798215	0.043716
GJB1	AY286490	NP_001075360	-0.24453	0.035921
GPAM	XM_001496479	XP_001496529	-0.34893	0.031211
GPBAR1	XM_001491146	XP_001491196	-0.44605	0.02938
GPR110	XM_001498273	XP_001498323	-0.45149	0.023833
GPR152	XM_001491968	XP_001492018	-0.95856	0.013787

Table A-12 Continued

Gene symbol	NCBI accession	RefSeq accession	Log fold change	Pvalue
GPR161	XM_001493957	XP_001494007	-0.32022	0.047479
GPR31	XM_001489448	XP_001489498	-0.27566	0.013579
GRHL2**	**XM_001493287**	**XP_001493337**	**-1.44125**	**0.000166**
GRIA4	XM_001500730	NULL	0.193427	0.044726
GSG1L	XM_001502403	XP_001502453	-0.25204	0.02885
GTPBP2	XM_001497559	XP_001497609	-0.23995	0.015556
GZMK	XM_001497014	XP_001497064	0.140809	0.048632
H3F3A	CD468247	NULL	0.62422	0.032925
HBB	XM_001504190	XP_001504240	1.414061	0.024735
HCK**	**CD465568**	**NULL**	**0.59042**	**0.019787**
HIST1H2BI	XM_001498344	XP_001498394	-0.27937	0.04005
HK1	CX601616	NULL	-0.18104	0.046972
HLA-DRB1	XM_001495531	XP_001495581	0.531712	0.000256
HOXB1	XM_001499152	XP_001499202	-0.29727	0.005543
HRAS	XM_001488899	NULL	0.562831	0.002187
HS3ST2	XM_001500813	XP_001500863	0.374906	0.033424
HSPE1	NULL	NULL	1.82398	0.008014
HTATSF1	DN506841	NULL	-0.33914	0.047444
HTT	XM_001488793	XP_001488843	-0.55307	0.032434
IDE	XM_001501035	XP_001501085	-0.17776	0.011112
IGFBP6	NULL	NULL	0.687531	0.008746
IGFBP7	XM_001491171	XP_001491221	0.492022	0.048569
IL22RA2	XM_001503573	XP_001503623	-0.33945	0.023025
IMP5	XM_001496121	NULL	0.314868	0.021224
INSR	XM_001496584	XP_001496634	-0.25966	0.027761
INTS12	XM_001503610	XP_001503660	-0.2701	0.017283
IQGAP2	XM_001503963	XP_001504013	-0.17378	0.012993
IRF4	XM_001487865	XP_001487915	-0.40285	0.044287
ITGBL1	XM_001494267	XP_001494317	0.684289	0.038352
JMJD2C	XM_001492601	XP_001492651	0.215892	0.045166
KCNA1	XM_001494973	XP_001495023	-0.42141	0.047751
KCNE3	XM_001498182	XP_001498232	-0.27853	0.028716
KCNH8	XM_001495463	XP_001495513	-0.48107	0.013556
KCTD15	XM_001489117	XP_001489167	-1.35609	0.033293
KIAA0141	XM_001503967	XP_001504017	0.443343	0.024048
KIAA0515	XM_001498956	XP_001499006	-0.21349	0.022052
KIAA1166	XM_001504860	XP_001504910	0.348703	0.036559
KIF17	XM_001504329	XP_001504379	0.444891	0.017319
KITLG	XM_001491749	XP_001491799	-0.4293	0.003208
KLHDC8B	XM_001498158	XP_001498208	-0.28733	0.030014
KRTAP26-1	XM_001495932	XP_001495982	-0.63053	0.048573
LIPG	XM_001499159	XP_001499209	-0.32741	0.028016

Table A-12 Continued

Gene symbol	NCBI accession	RefSeq accession	Log fold change	Pvalue
LMAN1L	XM_001493866	XP_001493916	-0.51913	0.028414
LMBR1L	XM_001504157	XP_001504207	-0.40519	0.018797
LOC152485	XM_001500552	XP_001500602	0.724353	0.04312
LOC345222	XM_001490014	XP_001490064	-0.22755	0.028129
LOC401498	XM_001498934	XP_001498984	-0.46916	0.029612
LOC644444	XM_001502201	XP_001502251	-0.14474	0.040538
LOC648672	XM_001488728	XP_001488778	-0.23577	0.037284
LOC728772	XM_001491967	XP_001492017	0.580286	0.041238
LOC728937	NULL	NULL	0.49753	0.042804
LOC730491	XM_001488498	XP_001488548	-0.32795	0.021633
LOC731062	X75612	CAA53284	0.90197	0.012465
LONRF1	XM_001494722	XP_001494772	0.309904	0.017531
LRFN2	XM_001496300	XP_001496350	-0.2559	0.033191
LRPAP1	CX602308	NULL	0.156946	0.022387
LRPPRC	XM_001498869	XP_001498919	-0.31371	0.024851
LRRC41	NULL	NULL	0.286663	0.042943
LRRC8D	XM_001493936	XP_001493986	0.413924	0.03701
LYPLA1	XM_001489457	NULL	-0.30844	0.037274
MAL	XM_001494676	NULL	-0.4395	0.002748
MAL2	XM_001496457	XP_001496507	0.315626	0.032243
MAML1	XM_001497397	XP_001497447	0.451541	0.015019
MAN2A2	NULL	NULL	-0.38682	0.029215
MB	NULL	NULL	-0.22733	0.02535
MBOAT4	XM_001494172	XP_001494222	-0.36283	0.034479
MECR	BM735250	NULL	-0.17506	0.047716
MED7	DN510032	NULL	-0.1466	0.043135
MGC23985	XM_001503845	XP_001503895	-0.31588	0.036821
MGC24975	XM_001495805	NULL	-0.32261	0.035594
MGC4655	XM_001496288	XP_001496338	-0.47118	0.011122
MGC50722	XM_001498447	XP_001498497	-0.47108	0.019641
MICB	AB126064	NULL	-0.23536	0.011169
MLZE	XM_001498324	XP_001498374	-0.32635	0.024704
MRPL21	CX604559	XP_001499094	1.061571	0.008074
MRPL47	XM_001495484	XP_001495534	0.257987	0.039781
MVP	XM_001501685	XP_001501735	-0.39093	0.025236
MYEOV2	XM_001497339	XP_001497389	0.909018	0.01544
MYL2	NULL	NULL	0.382941	0.045384
MYLIP	XM_001493152	XP_001493202	0.374966	0.010823
NAT1	XM_001487857	XP_001487907	0.542205	0.005775
NBPF6	XM_001491713	NULL	-0.16287	0.035219
NCAPG2	XR_035925	NULL	0.378977	0.046848
NDUFA12L	XM_001494417	XP_001494467	-0.24762	0.040189

Table A-12 Continued

Gene symbol	NCBI accession	RefSeq accession	Log fold change	Pvalue
NEB	NULL	NULL	-0.1953	0.008036
NENF	NULL	NULL	0.755207	0.005771
NKAIN1	XM_001500148	XP_001500198	-0.26922	0.048009
NLE1	XM_001503942	XP_001503992	0.456578	0.004181
NMD3	XM_001493928	XP_001493978	0.144493	0.043712
NPEPPS	XM_001498919	XP_001498969	0.156847	0.038691
NQO1	XM_001497333	XP_001497383	0.163082	0.01344
NR1I3	XM_001503792	XP_001503842	-0.28748	0.04936
NUDCD3	XM_001495776	XP_001495826	1.15546	0.01093
NULL	DN510495	NULL	-0.29115	0.001519
NULL	CX601100	NULL	-0.63069	0.002934
NULL	CD528461	NULL	-0.55488	0.003523
NULL	DN505730	NULL	0.466296	0.00446
NULL	XM_001498676	XP_001498726	-0.45457	0.008256
NULL	DN504496	NULL	0.308781	0.009264
NULL	CX593935	NULL	-0.47838	0.010519
NULL	CX598740	NULL	-0.44108	0.011666
NULL	XM_001501528	NULL	-0.37123	0.012526
NULL	CD469043	NULL	-0.36502	0.012804
NULL	CX604150	NULL	-0.48215	0.013588
NULL	CD465841	NULL	1.03321	0.013937
NULL	CD465619	NULL	1.377777	0.016941
NULL	DN509075	NULL	0.334493	0.017014
NULL	CX599557	NULL	0.184822	0.018528
NULL	XM_001499079	XP_001499129	-0.26389	0.01992
NULL	XM_001502810	NULL	0.465699	0.020151
NULL	CD468792	NULL	-0.4564	0.021556
NULL	CD535786	NULL	-0.39812	0.022838
NULL	XM_001500869	NULL	0.604523	0.022854
NULL	XM_001500257	NULL	0.425431	0.023123
NULL	CX601539	NULL	-0.36929	0.025992
NULL	CX597518	NULL	-0.27243	0.028562
NULL	XR_035913	NULL	0.727238	0.030052
NULL	CD465531	NULL	0.570342	0.030387
NULL	DN505697	NULL	0.4977	0.030721
NULL	XM_001491362	XP_001491412	0.500122	0.034607
NULL	CX604208	NULL	-0.24763	0.039409
NULL	CD466767	NULL	-0.65138	0.039784
NULL	XM_001498702	NULL	-0.19587	0.039845
NULL	CX592735	NULL	1.06049	0.040585
NULL	CX595725	NULL	-0.17242	0.041027
NULL	XM_001493892	NULL	-0.4473	0.044512

Table A-12 Continued

Gene symbol	NCBI accession	RefSeq accession	Log fold change	Pvalue
NULL	CD468899	NULL	0.461399	0.044934
NULL	DN507862	NULL	-0.2436	0.045068
NULL	DN509644	NULL	-0.27954	0.045367
NULL	CD528231	NULL	-0.15912	0.0458
NULL	CD471233	NULL	-0.28895	0.046984
NULL	CX602929	NULL	0.236282	0.048182
OBSL1	CX603384	NULL	0.168987	0.016025
ODAM	XM_001502141	XP_001502191	0.810894	0.04895
OR11L1	XM_001498040	NULL	-0.28901	0.039886
OR13A1	XM_001497194	XP_001497244	-0.40502	0.02689
OR1L6	XM_001500920	XP_001500970	0.339785	0.022104
OR1N1	XM_001501095	XP_001501145	-0.38801	0.022541
OR1N2	XM_001497814	XP_001497864	-0.46837	0.039316
OR2B11	XM_001491893	XP_001491943	-0.37587	0.02802
OR2L2	XM_001497233	XP_001497283	-0.3471	0.045558
OR2L8	XM_001499037	NULL	-1.05989	0.040685
OR2T33	XM_001491345	NULL	0.455463	0.034616
OR2W1	XM_001494282	XP_001494332	-0.27689	0.010633
OR4A16	XM_001495905	NULL	0.461048	0.037763
OR4C13	XM_001494731	XP_001494781	-0.25656	0.032483
OR4D9	XM_001495337	NULL	0.411979	0.010305
OR4F15	XM_001502286	XP_001502336	-0.34222	0.048646
OR4F6	XM_001501987	XP_001502037	-0.33232	0.009043
OR51E2	XM_001497263	XP_001497313	-0.39032	0.030857
OR51F1	XM_001497409	XP_001497459	-0.32001	0.014553
OR51I1	XM_001503971	XP_001504021	-0.69163	0.00464
OR51I2	XM_001498875	XP_001498925	-0.42474	0.045744
OR52E8	XM_001496727	XP_001496777	-0.40421	0.006407
OR52H1	XM_001499184	XP_001499234	-0.3512	0.037118
OR56A4	XM_001504516	XP_001504566	-0.51377	0.00155
OR5AN1	XM_001495188	NULL	-0.37522	0.016805
OR5P2	XM_001500473	XP_001500523	0.520624	0.039874
OR6F1	XM_001497005	XP_001497055	-0.31343	0.012326
OR7D4	XM_001492422	XP_001492472	-0.36321	0.04777
OR7G2	XM_001494401	XP_001494451	-0.31478	0.024895
OR8B3	XM_001501921	NULL	-0.67414	0.04426
OR8G2	XM_001504708	XP_001504758	0.612418	0.006317
OTUD7A	XM_001492427	XP_001492477	-0.57488	0.048103
PA2G4	XM_001504804	XP_001504854	0.180606	0.017067
PAIP1	NULL	NULL	-0.45554	0.013471
PARP12	XM_001496539	XP_001496589	0.386746	0.031737
PARP9	XM_001500274	XP_001500324	-0.30472	0.037685

Table A-12 Continued

Gene symbol	NCBI accession	RefSeq accession	Log fold change	Pvalue
PCK1	XM_001489771	XP_001489821	-0.28663	0.011703
PCP2	XM_001497385	XP_001497435	0.283109	0.042493
PDCD2	NULL	NULL	0.31781	0.00807
PDIA5	XM_001500185	XP_001500235	0.377488	0.048379
PHIP	XM_001499042	XP_001499092	0.147767	0.044369
PIGK	XM_001496963	XP_001497013	-0.44345	0.037795
PLA2G5	XM_001504348	XP_001504398	0.649197	0.04346
PLCZ1	XM_001497766	XP_001497816	0.138929	0.01243
PLD1	XM_001493497	XP_001493547	0.486716	0.030553
PON3	XM_001493457	XP_001493507	0.515501	0.03836
PPAPDC3	XM_001498987	XP_001499037	-0.23789	0.044791
PPP1R14C	XM_001494839	NULL	0.285711	0.045361
PPP1R3B	XM_001494371	XP_001494421	0.15679	0.019555
PRAME	XM_001493673	XP_001493723	-0.39663	0.021684
PRL	AY373339	NP_001075365	-0.17547	0.046162
PRPF4	XM_001488863	XP_001488913	-0.279	0.004759
PRPSAP2	XM_001488362	XP_001488412	-0.16628	0.010856
PSD4	XM_001495883	XP_001495933	-0.2094	0.04351
PTPRM	NULL	NULL	0.226717	0.037424
PXDN	XM_001503042	XP_001503092	0.116257	0.032477
RAB39	XM_001501007	XP_001501057	0.549373	0.012879
RAB39B	XM_001494307	XP_001494357	-0.10424	0.027871
RAB3GAP1	XM_001489470	XP_001489520	-0.30066	0.032446
RALGDS	XM_001499958	NULL	-0.38399	0.021835
REG3G	XM_001498156	XP_001498206	-0.26075	0.04973
RNF214	XM_001502611	XP_001502661	-0.56143	0.031646
RNF5	XM_001493452	XP_001493502	0.406873	0.034111
RPL13A	XM_001491876	XP_001491926	1.098955	0.007167
RPLP1	BM735439	XP_001495775	1.129718	0.034464
RPS3A	XM_001490864	NULL	-2.85316	0.012516
RS1	XM_001491183	XP_001491233	0.315318	0.021948
RSPO1	NM_001109680	NULL	-0.14898	0.037349
RWDD2A	XM_001503673	XP_001503723	-0.39351	0.001959
S100A2	CX598422	XP_001494717	-0.19795	0.01097
SAMHD1	XM_001499498	XP_001499548	-0.27837	0.046675
SAMM50	XM_001487978	XP_001488028	-0.40458	0.035037
SAP30	XM_001496719	NULL	-0.2628	0.042692
SCAPER	XM_001493099	XP_001493149	-0.12499	0.04387
SCARF1	XM_001502293	XP_001502343	0.20805	0.046395
SENP8	XM_001494920	XP_001494970	-0.41429	0.007808
SERF2	XM_001500420	XP_001500470	-0.36623	0.006826
SERINC5	XM_001503874	XP_001503924	0.530289	0.017862

Table A-12 Continued

Gene symbol	NCBI accession	RefSeq accession	Log fold change	Pvalue
SERPINA10	XM_001495713	XP_001495763	-0.1858	0.039105
SET	XM_001500465	XP_001500515	-0.27252	0.031999
SF3B3	XM_001500830	XP_001500880	-0.34426	0.049369
SFT2D2	XM_001490765	NULL	-0.47	0.002692
SGSM1	XM_001496176	XP_001496226	0.686988	0.034193
SH2D1A	XM_001500705	XP_001500755	0.843763	0.022965
SH3BGRL	XM_001501152	XP_001501202	-0.27699	0.017623
SIGLEC14	XM_001496296	XP_001496346	0.558058	0.023767
SLC12A3	XM_001502571	XP_001502621	-0.27738	0.007552
SLC19A1	XM_001489728	XP_001489778	-0.13466	0.019581
SLC19A2	XM_001491417	XP_001491467	-0.51867	0.001575
SLC19A3	XM_001494151	XP_001494201	-0.15146	0.02431
SLC22A10	XM_001502945	XP_001502995	-0.34629	0.045415
SLC25A1	XM_001488569	XP_001488619	0.909841	0.035852
SLC25A13	XM_001494425	XP_001494475	-0.47302	0.005013
SLC25A21	XM_001492015	XP_001492065	0.684545	0.005823
SLC35B2	XM_001497724	XP_001497774	-0.41621	0.02852
SLC38A3	XM_001493826	XP_001493876	-0.37242	0.029497
SLC5A9	XM_001493060	XP_001493110	0.348062	0.049513
SLC6A8	XM_001491633	XP_001491683	-0.64555	0.015277
SLC7A4	XM_001488939	XP_001488989	-0.44285	0.035664
SLITRK2	XM_001489935	XP_001489985	-0.14116	0.047933
SNTB2	XM_001497135	XP_001497185	-0.25643	0.045952
SPDYA	XM_001501882	XP_001501932	-0.41586	0.023565
SPHK1	XM_001491689	XP_001491739	-0.70335	0.023337
SRPR	XM_001505096	XP_001505146	-0.49765	0.043499
SSRP1	XM_001497090	XP_001497140	-0.19474	0.047947
ST6GALNAC1	XM_001491565	XP_001491615	-0.40615	0.008992
STEAP2	XM_001490032	XP_001490082	-0.44215	0.010366
STX4	XM_001500858	XP_001500908	-0.32273	0.034489
SYNE1	XM_001494275	XP_001494325	-0.26684	0.004585
TBC1D16	XM_001490266	XP_001490316	-0.54206	0.026315
TBX5	NULL	NULL	-0.52174	0.0013
TEGT	XM_001504223	XP_001504273	0.468953	0.043829
TFF1	XM_001492483	NULL	0.441392	0.032853
TFPI2	XM_001492769	XP_001492819	0.759563	0.001558
THOP1	XM_001493535	XP_001493585	-0.14155	0.049053
TIMM50	XM_001497601	XP_001497651	-0.44141	0.008628
TMEM165	XR_035951	NULL	0.669001	0.021421
TMEM16B	XM_001495269	NULL	0.927352	0.04374
TMEM34	XM_001501751	XP_001501801	-0.49327	0.005171
TMEM5	NULL	NULL	0.436213	0.029007

Table A-12 Continued

Gene symbol	NCBI accession	RefSeq accession	Log fold change	Pvalue
TMEM71	XM_001499201	XP_001499251	-0.48856	0.005713
TMEM95	XM_001503064	XP_001503114	-0.39681	0.011393
TMLHE	XM_001498280	XP_001498330	-0.33467	0.037921
TNNI2	NULL	NULL	0.139645	0.026048
TPPP	XM_001490990	NULL	-0.19321	0.004547
TRIM56	XM_001492494	XP_001492544	0.320604	0.043302
TSC22D2	XM_001490871	XP_001490921	0.195608	0.04065
TSGA13	XM_001498542	XP_001498592	-0.13727	0.029294
TTC17	XM_001489510	XP_001489560	-0.33285	0.015094
TTC25	XM_001496697	XP_001496747	0.30507	0.029763
TTLL9	XM_001498331	XP_001498381	-0.18292	0.015844
TYRP1	NM_001081840	NULL	-0.66742	0.007644
UBE2N	XM_001495374	XP_001495424	-1.74569	0.002091
UBTD2	XM_001499628	XP_001499678	0.483573	0.008712
UGT2A2	XM_001494284	XP_001494334	-0.15248	0.046386
UNC93B1	XR_035965	NULL	0.282473	0.024055
UPK2	XM_001503043	XP_001503093	-0.40456	0.002742
USF2	XM_001491920	NULL	-0.47331	0.045332
USP1	XM_001500051	XP_001500101	-0.49472	0.001116
USP38	XM_001502129	XP_001502179	-0.21656	0.004716
USP42	XM_001493859	XP_001493909	-0.19497	0.016539
USP54	XM_001503894	XP_001503944	-0.30721	0.047272
VIPR1	XM_001501612	XP_001501662	-0.28388	0.035524
VN1R4	XM_001495698	NULL	-0.57247	0.040558
VPS33B	XM_001498840	XP_001498890	-0.33929	0.034143
VSNL1	XM_001503420	XP_001503470	-0.31373	0.042909
VTCN1	XM_001496634	XP_001496684	0.783792	0.049895
WDR21A	XM_001488663	XP_001488713	-0.41757	0.028748
WDR52	XM_001501172	XP_001501222	-0.26123	0.040596
ZCCHC11	XM_001490378	NULL	0.473504	0.03041
ZDHHC19	XM_001489984	XP_001490034	-0.38606	0.018775
ZNHIT1	XM_001504461	XP_001504511	1.509699	0.015572
ZNRF2	XM_001499541	NULL	0.810946	0.049486

APPENDIX B

Table B-1: List of differentially expressed genes (pvalue <0.05 and fold change cut off of 1.2) for the allergen avoidance group at the 6-month time point compared to the baseline.

Gene symbol	NCBI accession	RefSeq accession	Log fold change	Pvalue
ABCD2	XM_001500065.1	NP_005155.1	0.543212126	0.00314231
ABLIM2	XM_001500021.1	NP_115808.3	0.677512087	0.020290061
ARPC1B	gnl|UG|Eca#S38804028	NP_005711.1	-0.376571797	0.028054279
ATAD2	XM_001497188.1	NP_054828.2	-0.354280817	0.024231517
BCDIN3D	PLT2-K07-M13.rgy.ab1	NP_859059.1	0.289543332	0.009246751
BMPER	CT020026B20C12.ab1	NP_597725.1	0.403951188	0.043768533
C11orf49	XM_001504556.1	NP_001003678.1	-0.33955333	0.020296705
C4orf20	XM_001490682.1	NP_060829.1	0.409527582	0.023476216
C9orf32	gnl|UG|Eca#S36623675	NP_054783.2	0.311728573	0.02509001
C9orf58	XM_001499384.1	NP_113614.1	0.331954857	0.025187153
CCR8	XM_001501979.1	NP_005192.1	0.613960619	0.039725657
CEACAM21	XM_001499625.1	NP_001091976.1	-0.384337534	0.027788263
CES7	XM_001493427.1	NP_659461.1	0.285658878	0.044231286
CHI3L1	XM_001496500.1	NP_001267.2	-0.272012954	0.0318671
CNR1	XM_001503748.1	NP_057167.2	0.363496686	0.036363576
COL1A1	gnl|UG|Eca#S38811517	NP_000079.2	-0.336239966	0.041266243
COL5A1	XR_036195.1	NP_000084.3	-0.498584475	0.001203738
CYP26A1	XM_001502498.1	NP_000774.2	0.580617922	0.038492287
DDIT4L	XM_001497203.1	NP_660287.1	0.620062855	0.043476285
EXDL1	XM_001503479.1	NP_689809.2	0.263419084	0.002082851
FAM55D	XM_001500547.1	NP_001071107.1	0.769514223	0.045056788
FBXO3	XM_001503169.1	NP_036307.2	0.28718879	0.003587882
GLMN	XM_001492771.1	NP_444504.1	0.331989739	0.02605657
HEG1	XM_001500006.1	NP_065784.1	-0.339816247	0.039705444
IDH2	gnl|UG|Eca#S36647263	NP_002159.2	0.501759049	0.039440607
IFNA5	XM_001497241.1	NP_002160.1	-0.308724595	0.00895384
LOC390667	XM_001497697.1	NP_001013680.1	-0.298598347	0.028592265
LOC401498	XM_001498934.1	NP_997723.2	-0.411060422	0.010703433
LOC651536	XM_001493483.1	XP_945805.1	-0.666988701	0.029417463
LOC731062	XM_001492904.1	XP_001131736.1	0.319183634	0.018260396
LRRN2	XM_001489200.1	NP_006329.2	-0.340379568	0.01728978

Table B-1 Continued

Gene symbol	NCBI accession	RefSeq accession	Log fold change	Pvalue
MICB	XM_001489019.1	NP_005922.1	-0.265053257	0.034926214
MMP16	gnl|UG|Eca#S38813088	NP_005932.2	0.559137515	0.037595674
MSH6	XM_001497961.1	NP_000170.1	0.320836095	0.02735467
NECAP1	XM_001498661.1	NP_056324.2	-0.347999738	0.01778941
NULL	PLT13-N11-M13.rgy.ab1	NULL	-0.406730322	0.031608479
NULL	PLT23-K17-M13R.ab1	NULL	-0.369398293	0.016401671
NULL	PLT28-N04-M13R.ab1	NULL	-0.366478368	0.005094035
NULL	CT020011B20C03.ab1	NULL	-0.313842563	0.026635145
NULL	PLT23-I09-M13R.ab1	NULL	-0.291604956	0.049176711
NULL	GENE:6874	NULL	-0.283947524	0.04959469
NULL	gnl|UG|Eca#S36628683	NULL	0.970314344	0.028420189
NULL	gnl|UG|Eca#S36643246	NULL	0.921816067	0.046960164
NULL	gnl|UG|Eca#S36637094	NULL	0.736564792	0.042292168
NULL	CT020015B20G04.ab1	NULL	0.475961622	0.038686166
NULL	GENE:3536	NULL	0.457990106	0.040744011
NULL	CT020026A20B09.ab1	NULL	0.377637901	0.048473522
NULL	gnl|UG|Eca#S36631924	NULL	0.376598008	0.025966309
NULL	gnl|UG|Eca#S36648412	NULL	0.373080403	0.007888671
NULL	CT02039A2G09.f1	NULL	0.360645843	0.020379178
NULL	gnl|UG|Eca#S36621081	NULL	0.357902459	0.007940736
NULL	CT020009A10C05.ab1	NULL	0.355663859	0.037079901
NULL	CT020026B20C09.ab1	NULL	0.336328697	0.043696084
NULL	gnl|UG|Eca#S36643360	NULL	0.306007238	0.020165834
NULL	CT020003B10F09.ab1	NULL	0.300084051	0.04183679
NULL	gnl|UG|Eca#S36656141	NULL	0.29112614	0.028379226
NULL	CT020019B10E05.ab1	NULL	0.286928357	0.047067626
NULL	PLT14-I23-M13.rgy.ab1	NULL	0.27483269	0.035968507
OR2G3	XM_001494102.1	NP_001001914.1	0.307988982	0.013632558
OR4D9	XM_001497973.1	NP_001004711.1	0.351569639	0.014130893
OR4F15	XM_001501753.1	NP_001001674.1	0.267059362	0.025106721
OR5B12	XM_001497597.1	NP_001004733.1	0.491741981	0.008103244
OR5K1	XM_001503633.1	NP_001004736.2	0.262952948	0.030612798
PLCD4	57.1D7.ab1	NP_116115.1	0.408784512	0.031807758
RBM39	gnl|UG|Eca#S38807635	NP_909122.1	0.273556978	0.002457149
RER1	gnl|UG|Eca#S38802589	NP_008964.3	0.29532706	0.021686433
RNF126	HL010007000_PLT_E05_37_035.ab1	NP_919442.1	0.775341424	0.015551486

Table B-1 Continued

Gene symbol	NCBI accession	RefSeq accession	Log fold change	Pvalue
SART3	gnl|UG|Eca#S36643775	NP_055521.1	0.715509095	0.00852801
SLC10A6	gnl|UG|Eca#S38816407	NP_932069.1	0.552355404	0.021698064
SLC25A1	XM_001488569.1	NP_005975.1	0.456004235	0.048270947
SLC25A20	XM_001494717.1	NP_000378.1	0.266579915	0.046006043
ST18	XM_001488723.1	NP_055497.1	0.272580956	0.047967511
TANC1	XM_001492390.1	NP_203752.1	0.290972244	0.042981327
TCP11	XM_001488694.1	NP_001087197.1	0.350016094	0.018556604
TMEM119	XM_001497020.1	NP_859075.1	-0.381115876	0.028157787
TMEM146	XM_001495780.1	NP_689997.3	0.296576744	0.046247313
TMEM20	XM_001500819.1	NP_694958.1	0.310930821	0.014345293
TMEM32	gnl|UG|Eca#S36644504	NP_775741.1	0.337175928	0.018749655
TPH1	XM_001504954.1	NP_004170.1	2.560315857	0.032021814
TXNRD3	XM_001492751.1	XP_001129642.1	0.370439929	0.027706263
UQCRB	gnl|UG|Eca#S36649002	NP_006285.1	0.643201539	0.030838074
VIM	gnl|UG|Eca#S36646726	NP_003371.2	0.29369645	0.012811472
WHSC2	XR_035785.1	NP_005654.2	0.831955918	0.033870998
ZBTB41	XM_001492621.1	NP_919290.2	0.467702871	0.009727874
#N/A	gnl|UG|Eca#S38817907 -5	#N/A	-0.320492001	0.007206627

Table B-2: List of differentially expressed genes (pvalue <0.05 and fold change cut off of 1.2) for the allergen avoidance group at the 12-month time point compared to the baseline.

Gene Symbol	NCBI accession	RefSeq accession	Log fold change	Pvalue
ABCD2	XM_001500065.1	NP_005155.1	0.40969935	0.045783307
ACVR1C	XM_001492118.1	NP_660302.2	0.291369039	0.027678903
ACVR2A	XM_001487856.1	NP_001607.1	0.290823504	0.011215241
ACY1	XM_001492838.1	NP_000657.1	0.467900827	0.038050363
ALOX5AP	gnl|UG|Eca#S36633997	NP_001620.2	-0.351566627	0.04693036
ANKS6	XM_001494967.1	NP_775822.3	-0.291347267	0.011006065
ARL6IP1	gnl|UG|Eca#S36627808	NP_055976.1	-0.394492117	0.045079062
ASPH	gnl|UG|Eca#S38812993	NP_004309.2	-0.305085935	0.028897772
ATG5	XM_001503938.1	NP_004840.1	0.402235148	0.022017641

Table B-2 Continued

Gene symbol	NCBI accession	RefSeq accession	Log fold change	Pvalue
B4GALT3	XM_001496370.1	NP_003770.1	-0.847461482	0.038340565
BTC	XM_001490427.1	NP_001720.1	-0.609231561	0.00395858
C11orf77	XM_001489899.1	NP_776172.1	-0.455146038	0.017998903
C1orf101	XM_001493885.1	NP_776168.1	0.589928364	0.030102937
C20orf112	XR_036251.1	NP_542183.1	-0.397186329	0.006774664
C20orf149	XM_001492738.1	NP_077275.1	-0.404123179	0.013764418
C5AR1	gnl|UG|Eca#S38812641	NP_001727.1	-0.457864356	0.016127144
C7orf30	gnl|UG|Eca#S38815874	NP_612455.1	-0.399516428	0.005881025
CALR	gnl|UG|Eca#S38803287	NP_004334.1	0.343841179	0.015603193
CBLB	gnl|UG|Eca#S38808556	NP_733762.2	-0.447426274	0.033829988
CD99	gnl|UG|Eca#S38802284	NP_002405.1	-0.461838978	0.033074303
CENPE	XR_036279.1	NP_001804.2	-0.294970116	0.028019544
COL5A1	XR_036195.1	NP_000084.3	0.509763626	0.028522014
COLEC10	XM_001496392.1	NP_006429.1	0.3438898	0.04355867
COX7A2L	gnl|UG|Eca#S38810038	NP_004709.2	-0.824165853	0.004657017
CYHR1	CT02037A2H11.f1.ab1	NP_116076.1	-0.307511615	0.01007686
CYP46A1	XM_001488041.1	NP_006659.1	-0.460089861	0.020815775
DDC	XM_001498321.1	NP_000781.1	-0.462577585	0.006834673
DGAT1	gnl|UG|Eca#S38802930	NP_036211.2	-0.323169318	0.018287914
EIF3CL	gnl|UG|Eca#S36653864	XP_001132506.1	-0.299479208	0.044982147
ENTPD4	XM_001492944.1	NP_004892.1	-0.421062419	0.045081081
FOXJ3	XM_001503156.1	NP_055762.3	-0.263461621	0.013186881
GABRD	XM_001495250.1	NP_000806.2	0.369108427	0.018001073
GNL1	gnl|UG|Eca#S38804347	NP_005266.2	0.354121187	0.032106865
HES7	XM_001504807.1	NP_115969.2	-0.360550084	0.043853143
HK3	XM_001498546.1	NP_002106.1	-0.311041866	0.037821183
HMGB3	gnl|UG|Eca#S38802843	NP_005333.2	-0.300867993	0.023191301
HP1BP3	gnl|UG|Eca#S38817368	NP_057371.2	0.273742855	0.048254151
IMPACT	XM_001494845.1	NP_060909.1	-0.559858234	0.041418476
ITGA9	gnl|UG|Eca#S38809311	NP_002198.2	0.678002428	0.030125014
IZUMO1	XM_001489113.1	NP_872381.1	-0.539087838	0.031990288
KCNH1	PLT27-L02-M13R.ab1	NP_758872.1	-0.591165082	0.047605705
KCNJ1	XM_001502563.1	NP_000211.1	-0.337393485	0.034155051
KIAA0922	XM_001499727.1	NP_056011.2	-0.361871265	0.047419125
LASS4	XM_001497105.1	NP_078828.1	0.395596357	0.013145545
LOC651536	XM_001492876.1	XP_945805.1	-0.632623667	0.00451103

Table B-2 Continued

Gene symbol	NCBI accession	RefSeq accession	Log fold change	Pvalue
LPXN	XM_001504694.1	NP_004802.1	0.34023857	0.032394747
LYG1	XM_001490374.1	NP_777558.1	-0.441822398	0.035412525
Magmas	SM0055-3_H03_15.ab1	NP_057153.8	-0.625081511	0.02961981
MCM2	XM_001488780.1	NP_004517.2	0.44615205	0.033032606
MMEL1	gnl|UG|Eca#S36656591	NP_258428.1	0.578569043	0.027829084
NAGK	gnl|UG|Eca#S38810098	NP_060037.2	-0.936832447	0.046628265
NFKBIZ	gnl|UG|Eca#S38808389	NP_113607.1	-0.275592895	0.041197522
NNT	gnl|UG|Eca#S38807862	NP_036475.3	-0.651475697	0.004067085
NULL	gnl|UG|Eca#S36623227	NULL	-1.360892039	0.007639309
NULL	gnl|UG|Eca#S36654383	NULL	-0.992605919	0.033239645
NULL	CT02038B2H06.f1.ab1	NULL	-0.939596001	0.04486265
NULL	gnl|UG|Eca#S36646192	NULL	-0.833187459	0.033745737
NULL	Un0130.1-277067:31850-32161:+	NULL	-0.725541772	0.028161699
NULL	CT020018B10B01.ab1	NULL	-0.680779948	0.043954501
NULL	CT020027B20F07.ab1	NULL	-0.664459257	0.01414391
NULL	gnl|UG|Eca#S36648412	NULL	-0.641702962	0.003848606
NULL	SM0050-1_A07_01.ab1	NULL	-0.641137965	0.01685251
NULL	gnl|UG|Eca#S36640829	NULL	-0.622977727	0.03555097
NULL	CT020014A10H02.ab1	NULL	-0.5866769	0.009861336
NULL	gnl|UG|Eca#S36654519	NULL	-0.585329082	0.022046166
NULL	HL02016A1E03.ab1	NULL	-0.564230003	0.038813648
NULL	gnl|UG|Eca#S36642828	NULL	-0.532377921	0.021864062
NULL	PLT19-P12-M13.rgy.ab1	NULL	-0.525777683	0.044093419
NULL	PLT21-E09-M13R.ab1	NULL	-0.512571794	0.035504693
NULL	PLT32-I04-M13R.ab1	NULL	-0.500980851	0.034005617
NULL	CT020023B20H02.ab1	NULL	-0.490294472	0.001643801
NULL	CT020008A10F11.ab1	NULL	-0.471270424	0.045189182
NULL	CT020010A10D08.ab1	NULL	-0.463108383	0.030037042
NULL	gnl|UG|Eca#S36646700	NULL	-0.443609218	0.04386729
NULL	HL02020B1F01.ab1	NULL	-0.433672813	0.02666155
NULL	CT020007B10C10.ab1	NULL	-0.420944123	0.022998606
NULL	HL02022A1F03.ab1	NULL	-0.39433484	0.033672853
NULL	gnl|UG|Eca#S36654359	NULL	-0.381586079	0.03643111
NULL	HL01015B1D11.ab1	NULL	-0.372343078	0.037761263
NULL	CT02039A2G10.f1	NULL	-0.370536944	0.028623979
NULL	gnl|UG|Eca#S36649669	NULL	-0.364902676	0.019739539

Table B-2 Continued

Gene symbol	NCBI accession	RefSeq accession	Log fold change	Pvalue
NULL	CT020021A10F04.ab1	NULL	-0.363042932	0.022901469
NULL	CT020005A10_PLT_H05_40_046.ab1	NULL	-0.356228059	0.047351836
NULL	gnl|UG|Eca#S36644977	NULL	-0.337704434	0.018890025
NULL	CT02038A2B04.f1.ab1	NULL	-0.332412978	0.018893431
NULL	SM0053-1_F09_11.ab1	NULL	-0.332407881	0.033205166
NULL	gnl|UG|Eca#S36655383	NULL	-0.329006526	0.034382763
NULL	CT020022A10D01.ab1	NULL	-0.308752861	0.049057862
NULL	PLT11-P20-M13.rgy.ab1	NULL	-0.305522448	0.021260029
NULL	gnl|UG|Eca#S36645566	NULL	-0.300543534	0.042242311
NULL	HL02020B2H10.ab1	NULL	-0.299012177	0.049686307
NULL	CT020012A20A10.ab1	NULL	-0.296980144	0.021225474
NULL	CT020020A20D04.ab1	NULL	-0.282193277	0.02041472
NULL	gnl|UG|Eca#S36653234	NULL	-0.275654193	0.048194285
NULL	gnl|UG|Eca#S36626566	NULL	-0.27136633	0.028709229
NULL	CT020003A10_PLT_H07_56_063.ab1	NULL	-0.262602224	0.026219512
NULL	gnl|UG|Eca#S36647872	NULL	0.533754875	0.0484944
NULL	PLT14-H13-M13.rgy.ab1	NULL	0.35358225	0.003500126
NULL	PLT25-P19-M13R.ab1	NULL	0.330403885	0.041989336
NULL	GENE:19132	NULL	0.275109569	0.034854859
NULL	PLT29-G23-M13R.ab1	NULL	0.274790248	0.002505995
NULL	CT020020B20D02.ab1	NULL	0.267412744	0.030670913
NULL	gnl|UG|Eca#S36646288	NULL	0.261141729	0.022576852
OLFM3	XM_001488106.1	NP_477518.1	-1.215618638	0.034524701
OR10G7	XM_001491717.1	NP_001004463.1	0.368643912	0.014457974
OR10G9	XM_001504677.1	NP_001001953.1	0.336078291	0.046647953
OR1E1	XM_001501011.1	NP_003544.2	-0.307998169	0.012266409
OR1F1	XM_001497945.1	NP_036492.1	0.393202854	0.002551987
OR2F2	XM_001503021.1	NP_001004685.1	-0.317604272	0.016481163
OR2T1	XM_001496591.1	NP_112166.1	-0.273516536	0.00483788
OR2T1	XM_001488476.1	NP_112166.1	0.294382964	0.003772257
OR2Y1	XM_001494154.1	NP_001001657.1	-0.284367365	0.021366227
OR4A15	XM_001490213.1	NP_001005275.1	-0.519685212	0.0425957
OR4P4	XM_001488616.1	NP_001004124.1	0.287336502	0.038577359
OR52A5	XM_001504149.1	NP_001005160.1	0.283370289	0.019615661
OR6C2	XM_001489614.1	NP_473446.1	-0.41802156	0.021947461
OR6N2	XM_001490459.1	NP_001005278.1	-0.284979532	0.032580901

Table B-2 Continued

Gene symbol	NCBI accession	RefSeq accession	Log fold change	Pvalue
OR7A17	XM_001494078.1	NP_112163.1	-0.343628694	0.020952282
OR8S1	XM_001490794.1	NP_001005203.2	0.288700567	0.004044799
PAPPA2	XM_001498222.1	NP_064714.2	-0.582260453	0.049565939
PES1	gnl|UG|Eca#S36631489	NP_055118.1	-0.653893375	0.014009811
PITPNB	gnl|UG|Eca#S38813557	NP_036531.1	-0.277173914	0.049711508
PNLIPRP1	XM_001497716.1	NP_006220.1	-0.331005349	0.009197281
PPM1A	gnl|UG|Eca#S38807088	NP_066283.1	-0.30480297	0.033081891
PPM1F	XM_001491065.1	NP_055449.1	-0.343607969	0.025012125
PQLC1	XM_001494788.1	NP_079354.2	-1.31338984	0.041362933
PRICKLE4	XM_001501174.1	NP_037529.3	-0.363642629	0.034920256
PROM2	CT02040B1G11.f1.ab1	NP_653308.1	-0.461571851	0.039715859
PSCD1	gnl|UG|Eca#S38812041	NP_059430.2	-0.449073598	0.048580054
PTTG1IP	gnl|UG|Eca#S36644223	NP_004330.1	-0.529919075	0.032791313
RAB38	XM_001489498.1	NP_071732.1	-0.502473944	0.048613667
RALGDS	CT02034A1D05.f1.ab1	NP_006257.1	-0.319527164	0.025028705
RASGEF1A	XM_001490265.1	NP_660356.2	-0.619346879	0.017324711
RAVER1	gnl|UG|Eca#S38803970	NP_597709.2	0.349038972	0.018726222
RPL29	gnl|UG|Eca#S36654195	NP_000983.1	-0.30938851	0.001484597
SCYL1	gnl|UG|Eca#S36644614	NP_065731.3	-0.445199637	0.012151429
SIGLEC5	XM_001497073.1	NP_003821.1	-0.404780394	0.0394426
SLC2A2	gnl|UG|Eca#S36656765	NP_000331.1	-0.486633155	0.015343175
SLC44A4	XM_001492369.1	NP_079533.2	0.464773938	0.039763669
SMCR8	XM_001488509.1	NP_658988.2	0.285088783	0.018253681
SNRPG	HL010001001_HL010_E09_69_067.ab1	NP_003087.1	-0.271854597	0.032751433
SRCAP	gnl|UG|Eca#S38810945	NP_006653.2	-0.294838444	0.04308922
TCEA1	XM_001489406.1	NP_006747.1	0.491390838	0.033216647
TCP11L1	XM_001492539.1	NP_060863.2	0.363327472	0.036354286
TMED4	XR_036138.1	NP_872353.2	-0.265628834	0.013800977
TMEM86B	XM_001489645.1	NP_776165.2	0.511078446	0.033635612
TMEM97	gnl|UG|Eca#S36645870	NP_055388.2	-0.38294	0.03388555
TNFSF4	XM_001492820.1	NP_003317.1	0.598301343	0.031701916
TRSPAP1	gnl|UG|Eca#S38817207	NP_060316.1	0.513620933	0.048994823
TTC1	gnl|UG|Eca#S38810759	NP_003305.1	-0.447531969	0.005199526
UCRC	gnl|UG|Eca#S36652606	NP_037519.2	-0.44626764	0.027284228
ULBP3	XM_001495280.1	NP_078794.1	-0.441949677	0.035434647
VAT1	XM_001496194.1	NP_006364.2	0.26822596	0.030230202

Table B-2 Continued

Gene symbol	NCBI accession	RefSeq accession	Log fold change	Pvalue
XPO7	XM_001490507.1	NP_001093632.1	1.236593078	0.041144528
ZDHHC18	XM_001500713.1	NP_115659.1	0.275813669	0.042122786
#N/A	gnl|UG|Eca#S36657275-5	#N/A	-0.560442757	0.01853162
#N/A	gnl|UG|Eca#S38809257Con	#N/A	0.374512249	0.009033948

Table B-3: List of differentially expressed genes (pvalue <0.05 and fold change cut off of 1.2) for the treatment group at the 6-month time point compared to the baseline.

Gene Symbol	NCBI accession	RefSeq accession	Log fold change	Pvalue
ACSM5	XM_001488143.1	NP_060358.2	0.739795183	0.015316929
AGXT2L2	gnl|UG|Eca#S38810526	NP_699204.1	-0.515388946	0.030155412
ALDH18A1	XR_036392.1	NP_001017423.1	-0.374921374	0.035600462
ATAD2	XM_001497188.1	NP_054828.2	-0.735905575	0.031827353
C1orf101	XM_001493885.1	NP_776168.1	-1.451517094	0.011137653
COPB2	gnl|UG|Eca#S38809205	NP_004757.1	0.454695781	0.042822909
FLJ12993	XM_001493769.1	NP_001073975.1	-0.314912101	0.049840755
ITGA9	gnl|UG|Eca#S38809311	NP_002198.2	-0.649043176	0.023983129
MC5R	XM_001490598.1	NP_005904.1	0.442723598	0.020721254
MFSD7	XM_001488157.1	NP_115595.2	-0.827526786	0.016306331
NULL	CT02042A1C04.f1.ab1	NULL	-1.520223013	0.03924965
NULL	CT020018A20F12.ab1	NULL	-0.971435263	0.040183324
NULL	gnl|UG|Eca#S36645692	NULL	-0.680466351	0.036672763
NULL	CT020010B10C07.ab1	NULL	-0.494719269	0.047457817
NULL	HL01015B2D01.ab1	NULL	-0.481382276	0.03113615
NULL	PLT13-N10-M13.rgy.ab1	NULL	-0.402842368	0.033017123
NULL	gnl|UG|Eca#S36631680	NULL	-0.349867276	0.01966565
NULL	CT02038A2G04.f1.ab1	NULL	-0.291083523	0.018663776
NULL	PLT25-P19-M13R.ab1	NULL	-0.276235302	0.039766821
NULL	gnl|UG|Eca#S36648438	NULL	0.965201075	0.028865786
NULL	SM0049-3_B09_03.ab1	NULL	0.475300715	0.020100789
OR2T4	XM_001487944.1	NP_001004696.1	-0.82464822	0.022325799
OR4A47	XM_001495702.1	NP_001005512.2	-1.066751575	0.017889806

Table B-3 Continued

Gene symbol	NCBI accession	RefSeq accession	Log fold change	Pvalue
PITPNB	gnl|UG|Eca#S38813557	NP_036531.1	0.260712929	0.023882242
RHOG	XM_001496655.1	NP_001656.2	-0.887180953	0.04005589
RUVBL2	gnl|UG|Eca#S38802810	NP_006657.1	-1.05131447	0.026372273
SCG5	gnl|UG|Eca#S38817793	NP_003011.1	-2.142916489	0.046514415
THOC4	XM_001489439.1	XP_001134346.1	-0.920545861	0.014848621
TMEM86B	XM_001489645.1	NP_776165.2	-0.418218971	0.004210093
UBE2G2	XM_001490079.1	NP_003334.2	-0.323545409	0.011366118
ZNF423	XM_001491336.1	NP_055884.2	-0.469505686	0.047100168

Table B-4: List of differentially expressed genes (pvalue <0.05 and fold change cut off of 1.2) for the treatment group at the 12-month time point compared to the baseline.

Gene Symbol	NCBI accession	RefSeq accession	Log fold change	Pvalue
ACTL7B	XM_001492641.1	NP_006677.1	0.302918202	0.01217914
APOE	XR_036412.1	NP_000032.1	0.310599988	0.036883944
ATP11A	XM_001497096.1	NP_056020.2	-0.337743215	0.026938917
ATP8A2	XM_001492094.1	NP_057613.4	0.344086701	0.016074615
BANK1	XM_001497747.1	NP_060405.3	0.494542628	0.02996333
C14orf172	gnl|UG|Eca#S38806821	NP_689520.2	0.304748	0.001728088
C16orf35	XM_001496679.1	NP_001070818.1	-0.306521565	0.008785123
C2orf66	XM_001500103.1	NP_998773.1	-0.736508874	0.039020891
C6orf136	XM_001489684.1	NP_001103408.1	0.278247739	0.036952674
C9orf58	XM_001499384.1	NP_113614.1	0.329767229	0.015163379
CASR	gnl|UG|Eca#S38808589	NP_000379.2	0.266674186	0.008222488
CLEC9A	CT02040B1A04.f1.ab1	NP_997228.1	0.786406638	0.004948974
D15Wsu75e	XM_001500344.1	NP_056519.1	-0.288245791	0.03931723
DBNDD1	XM_001488503.1	NP_001036075.1	0.309203657	0.0299733
DGAT2	gnl|UG|Eca#S38813894	NP_115953.2	-0.278654126	0.021050866
EDIL3	gnl|UG|Eca#S38810337	NP_005702.3	0.379304087	0.03414137
EPB41L5	XM_001492466.1	NP_065960.2	0.26395503	0.011585303
FAHD1	XM_001497855.1	NP_112485.1	-0.504821137	0.045547497
FAM14A	gnl|UG|Eca#S38806857	NP_114425.1	0.321211605	0.004283862
GAPDH	XR_035875.1	NP_002037.2	-0.335626721	0.027297636
IPO13	XM_001496543.1	NP_055467.2	-0.374947984	0.006946382

Table B-4 Continued

Gene symbol	NCBI accession	RefSeq accession	Log fold change	Pvalue
ITGA9	gnl|UG|Eca#S38809311	NP_002198.2	-0.616233248	0.011042576
KLRC1	XM_001494234.1	NP_002250.1	0.332014225	0.004155855
MCM4	gnl|UG|Eca#S38812968	NP_005905.2	-0.405488793	0.01305292
MCM5	gnl|UG|Eca#S38805899	NP_006730.2	0.377731922	0.033241646
MTA2	gnl|UG|Eca#S38811148	NP_004730.2	0.43431311	0.009210879
NULL	CT02034B2C11.f1.ab1	NULL	-0.435011035	0.028349656
NULL	PLT7-A17-M13.rgy.ab1	NULL	-0.352116773	0.019118938
NULL	SM0049-1_C06_06.ab1	NULL	-0.327381154	0.046064752
NULL	gnl|UG|Eca#S36623681	NULL	-0.278208242	0.024749417
NULL	gnl|UG|Eca#S36646288	NULL	-0.271386729	0.017190892
NULL	CT020007B20G07.ab1	NULL	-0.270694792	0.04095818
NULL	HL010008000_PLT_A03_17_017.ab1	NULL	1.554327386	0.017236597
NULL	CT020020B10C01.ab1	NULL	0.601976634	0.0157602
NULL	HL01019B2D08.ab1	NULL	0.522761238	0.049273337
NULL	CT020027A20A06.ab1	NULL	0.435078451	0.026515836
NULL	Un0595.1-16114:6979-10788:-	NULL	0.43309721	0.019510688
NULL	CT020020B10H03.ab1	NULL	0.418351547	0.027166219
NULL	CT020010B20B04.ab1	NULL	0.41453717	0.046928578
NULL	HL020003000_PLT_B02_10_013.ab1	NULL	0.397544208	0.006285186
NULL	CT020017B10B08.ab1	NULL	0.395252221	0.006121267
NULL	gnl|UG|Eca#S36625500	NULL	0.380809512	0.005449418
NULL	CT020026B20C09.ab1	NULL	0.378078674	0.024265649
NULL	HL02017A1B03.ab1	NULL	0.376273682	0.021739018
NULL	GENE:22350	NULL	0.343244068	0.023666006
NULL	CT02032A2E05.f1.ab1	NULL	0.336940934	0.003297009
NULL	gnl|UG|Eca#S36630542	NULL	0.311618149	0.042315911
NULL	gnl|UG|Eca#S36654519	NULL	0.305935266	0.021731965
NULL	PLT29-B21-M13R.ab1	NULL	0.282926868	0.004463238
NULL	gnl|UG|Eca#S36644914	NULL	0.28048793	0.030036968
NULL	Un0435.1-19795:12872-13609:+	NULL	0.275631338	0.009613747
NULL	CT020026A20B09.ab1	NULL	0.27500797	0.027482192
NULL	XM_001491658.1	NULL	0.272364574	0.007943113
OR10V1	XM_001492887.1	NP_001005324.1	-0.287004699	0.040998633
OR11H6	XM_001505127.1	NP_001004480.1	-0.281997553	0.04471254
OR51F2	XM_001497442.1	NP_001004753.1	-0.326967497	0.047984931

Table B-4 Continued

Gene symbol	NCBI accession	RefSeq accession	Log fold change	Pvalue
OR52D1	XM_001498223.1	NP_001005163.1	0.276158958	0.005627777
OR52J3	XM_001498056.1	NP_001001916.2	0.334842743	0.000461248
OR5B12	XM_001497640.1	NP_001004733.1	-0.458151485	0.000235412
PDYN	XM_001497665.1	NP_077722.1	0.292041589	0.022025175
PFDN1	gnl|UG|Eca#S38810689	NP_002613.2	0.317254271	0.04058558
RXRB	gnl|UG|Eca#S38808035	NP_068811.1	0.318720726	0.031988907
SCYL1	gnl|UG|Eca#S36644614	NP_065731.3	0.543979999	0.008591795
SERTAD4	XM_001493274.1	NP_062551.1	0.341799246	0.027211507
SFXN3	XM_001500003.1	NP_112233.2	-0.390777342	0.004469119
SLC38A6	XM_001492955.1	NP_722518.1	-0.410814677	0.049774426
SMYD1	XM_001497775.1	NP_938015.1	0.289853177	0.036819805
SPAG4L	XM_001498564.1	NP_542406.2	0.40535083	0.029340174
STT3A	gnl|UG|Eca#S38814116	NP_689926.1	-0.923689246	0.025379712
TBPL2	XM_001496000.1	NP_950248.1	-0.301787042	0.045153152
TNFSF4	XM_001492820.1	NP_003317.1	-0.319506354	0.041363125
TRPC5	XM_001488732.1	NP_036603.1	0.266894848	0.023625828
ZFYVE9	XM_001493830.1	NP_004790.2	-0.273565869	0.039517398
ZNF551	XM_001493785.1	NP_612356.1	0.275121901	0.031188756
#N/A	gnl|UG|Eca#S38818598-m85	#N/A	0.275618639	0.022373715

APPENDIX C

Table C-1: List of differentially expressed genes (pvalue <0.05 and fold change cut off of 1.5) between the stimulated and the un-stimulated leukocytes at Day 1.

Gene Symbol	NCBI accession	RefSeq accession	Log fold change	Pvalue
AFF4	XM_001504421	XP_001504471	0.736771554	0.001231228
ARMC8	XM_001496956	XP_001497006	0.993034946	0.000143926
ATP6V1C1	XM_001494101	XP_001494151	1.61495745	0.012828436
AZIN1	XM_001493984	XP_001494034	1.30074439	0.001350399
AZIN1	XR_035783	NULL	0.97456889	0.011838909
B3GALT4	XM_001497099	XP_001497149	0.868094259	0.0004303
B4GALT5	XM_001501176	XP_001501226	0.740378146	0.001318002
BIRC3	XM_001499875	XP_001499925	1.925939744	0.005072062
C17orf56	XM_001489994	XP_001490044	1.205522855	0.009628448
CCL20	XM_001496798	NULL	2.610358728	0.006660321
CHIC1	XM_001504969	XP_001505019	0.656790617	6.01E-05
CITED1	XM_001488044	XP_001488094	0.690298431	0.022558711
CLINT1	CX604855	NULL	1.222249813	0.018676155
CXorf21	XM_001502412	NULL	0.724386169	0.019306103
CXXC5	NULL	NULL	-0.622772728	0.017828615
DDX58	XM_001497845	XP_001497895	1.012974707	0.028022378
EDN2	AB079136	NP_001075292	0.71238449	0.025477548
FAM21C	CX603317	NULL	2.12223529	0.002892481
FAM3A	XM_001492203	XP_001492253	0.920262899	0.006131427
FLJ22662	XM_001497121	XP_001497171	-0.69439459	0.006104455
FPRL1	XM_001497411	XP_001497461	1.038335127	0.009498748
GALNT2	XM_001496209	XP_001496259	-1.29368847	0.049578246
GNAI3	XM_001494890	XP_001494940	1.152377992	0.00116789
GNB3	XM_001497120	XP_001497170	0.706700578	0.001334301
GPR109A	CD469236	NULL	0.906632573	0.032062321
GYG1	XM_001491640	XP_001491690	-0.656642951	0.027410007
HAGHL	XM_001497250	XP_001497300	0.865290302	0.000618082
HIP1R	XM_001492795	XP_001492845	0.750215372	0.000570017
HN1L	NULL	NULL	-1.234627804	0.025963621
HNRNPA1	XM_001501027	XP_001501077	-1.127468753	0.036793513
IFNA5	XM_001495486	NULL	1.112483298	0.038252084
IL1A	NM_001082500	NULL	2.413131186	0.03380699
IL1B	XM_001495926	XP_001495976	1.490260424	0.02739791
IL1RN	U92482	NP_001075994	1.876892686	0.000360812

Table C-1 Continued

Gene symbol	NCBI accession	RefSeq accession	Log fold change	Pvalue
INS-IGF2	XM_001492829	NULL	0.718615748	0.009247854
IVNS1ABP	CX604411	NULL	-0.77874227	0.006571008
KCNK2	XM_001488153	XP_001488203	0.904674402	0.032685262
KCNK7	XM_001493848	XP_001493898	-0.948840153	0.039837617
KIAA2026	DN508828	NULL	1.252853964	0.003279472
KIAA2026	NULL	NULL	0.83003415	0.006222284
KIF21A	XM_001500023	XP_001500073	0.983154746	0.042016242
KLRB1	XM_001499255	XP_001499305	0.783208614	0.039042291
LCP1	CD466266	NULL	-0.788551364	0.01608422
LILRA6	AB120413	NP_001075993	-0.712406497	0.011624887
LILRB4	XM_001489413	XP_001489463	-0.615096867	0.02846047
LMBR1L	XM_001504157	XP_001504207	0.602115766	0.018912226
MAPK14	XM_001494719	XP_001494769	-0.59840028	0.011840746
MMP13	AF034087	NP_001075273	0.628858225	0.031911612
MPP4	XM_001496932	XP_001496982	1.9042037	0.008789771
MS4A6A	XM_001493201	XP_001493251	-0.660051914	0.01734874
MTHFD2	XM_001500723	XP_001500773	1.056604193	0.016126532
NFKBIA	NULL	NULL	0.841142358	0.016476399
NLRP13	XM_001490754	XP_001490804	0.623449799	0.031212763
NUBP1	XR_035869	NULL	-0.660362741	0.042452626
NULL	NULL	NULL	3.650643824	0.001230412
NULL	BI961791	NULL	1.733094978	0.020336907
NULL	NULL	NULL	1.614431528	0.003423183
NULL	NULL	NULL	1.422963358	0.002011361
NULL	XM_001489363	NULL	1.402783642	0.005658842
NULL	NULL	NULL	1.398857319	0.010660813
NULL	DN508878	NULL	1.392061079	0.0378562
NULL	CD469517	NULL	1.383517701	0.00115628
NULL	CX604543	NULL	1.374177108	0.015431937
NULL	CD465425	NULL	1.273417274	0.000468737
NULL	DN507020	NULL	1.231137808	0.000808902
NULL	CD535494	NULL	1.150001754	0.000533264
NULL	BM414612	NULL	1.10496954	0.021648089
NULL	NULL	NULL	1.024929833	0.000965244
NULL	DN508987	NULL	0.965068028	0.018353876
NULL	NULL	NULL	0.924807265	0.017895581
NULL	NULL	NULL	0.756502529	0.027365545
NULL	XM_001503112	NULL	0.75175176	0.014359124
NULL	NULL	NULL	0.740663541	0.000707521

Table C-1 Continued

Gene symbol	NCBI accession	RefSeq accession	Log fold change	Pvalue
NULL	NULL	NULL	0.685719513	0.047748735
NULL	CX601512	NULL	0.658767096	0.047800289
NULL	NULL	NULL	0.647880706	0.012898365
NULL	NULL	NULL	0.592962906	0.000124773
NULL	CX604697	NULL	0.58437	0.047801191
NULL	XM_001497251	NULL	-1.222264504	0.022010221
NULL	XM_001497156	NULL	-1.017644465	0.04531373
NULL	DN509725	NULL	-0.940950373	0.030122187
NULL	CX605267	NULL	-0.881213651	0.047078064
NULL	CX600791	NULL	-0.846206416	0.032060274
NULL	NULL	NULL	-0.690425434	0.003427915
NULL	NULL	NULL	-0.683315393	0.003232457
NULL	NULL	NULL	-0.659463765	0.028386418
NULL	CD468881	NULL	-0.65132791	0.037279346
NULL	NULL	NULL	-0.639249664	0.031076657
NULL	XM_001499111	XP_001499161	-0.583273337	0.035671404
OLAH	XM_001498643	XP_001498693	-0.842955156	0.022441262
OLR1	XM_001493960	XP_001494010	1.654290003	0.042997441
OR2W3	XM_001498405	XP_001498455	1.280015075	7.45E-05
OR8U8	XM_001496341	NULL	-0.606710763	0.040760083
OSBPL11	XM_001501564	XP_001501614	-0.621347908	0.017476482
OXTR	XM_001491665	XP_001491715	0.639764911	0.008698872
PABPC4	XM_001503450	XP_001503500	0.822893601	0.009078976
PIK3AP1	XM_001500468	XP_001500518	1.195804752	0.004431402
PLSCR1	XM_001492309	XP_001492359	-0.768157181	0.00405952
PODXL	XM_001498373	XP_001498423	1.236325872	0.000287089
PRPF39	XM_001493416	NULL	0.944144709	0.025222003
PSMB5	XM_001494488	XP_001494538	0.640391481	0.044227039
PTAFR	XM_001503995	XP_001504045	0.684922323	0.002152635
RAB6IP1	XM_001500797	XP_001500847	0.860114154	0.00686056
RALGDS	NULL	NULL	0.581840191	0.034669024
RASGEF1B	NULL	NULL	1.308715804	0.01677066
RGS2	XM_001490543	XP_001490593	-0.998595853	0.00797569
SCUBE1	XM_001500812	XP_001500862	-0.949584788	0.041363431
SELP	CD467527	NULL	-0.613675509	0.029230938
SERPINB1	M91161	NP_001075416	-0.718289355	0.022790827
SERPINE2	XM_001495938	XP_001495988	0.866235669	0.043403297
SLC22A6	XM_001495190	XP_001495240	0.581444932	0.014295459
SMARCA4	XM_001490624	XP_001490674	0.797659347	0.000547984

Table C-1 Continued

Gene symbol	NCBI accession	RefSeq accession	Log fold change	Pvalue
SUMO2	XM_001499526	XP_001499576	-0.692012317	0.019498782
TANK	XM_001493298	XP_001493348	0.929247306	0.001159495
TCTE3	XM_001488610	XP_001488660	-0.888890706	0.017066746
TFCP2	XM_001504307	NULL	1.922040404	0.001358919
TGM2	XM_001499729	NULL	1.516040134	0.005775403
TNFAIP3	XM_001504414	XP_001504464	0.595735418	0.024467972
TRAF3	XM_001490000	XP_001490050	0.634627522	0.002496081
UBP1	XM_001489950	XP_001490000	1.157457981	0.035246983
UQCRH	CX603785	XP_001495144	0.775721189	0.040370337
USP13	XM_001496315	XP_001496365	0.639778431	0.017319985
ZNF462	XM_001493275	XP_001493325	-0.81658804	0.037827707
ZPBP2	XM_001497917	NULL	0.625513646	0.003179897

Table C-2: List of differentially expressed genes (pvalue <0.05 and fold change cut off of 1.5) between the stimulated and the un-stimulated leukocytes at Week-2.

Gene Symbol	NCBI accession	RefSeq accession	Log fold change	Pvalue
AACS	XM_001493527	XP_001493577	0.697875092	0.007947887
ALG8	XM_001492875	XP_001492925	-0.728984573	0.048304908
ALPL	XM_001504312	XP_001504362	-0.686710111	0.025516009
ATP11B	XM_001496792	XP_001496842	0.665612005	0.010133154
ATP6V1C1	XM_001494101	XP_001494151	0.975560628	0.019712683
BIRC3	XM_001499875	XP_001499925	1.615070966	7.11E-05
BTN2A1	XM_001492502	XP_001492552	1.206141566	0.018929092
C11orf49	XR_036183	NULL	0.730436448	0.027136315
C11orf49	XR_035773	NULL	0.642278149	0.000285858
C18orf22	XM_001496059	XP_001496109	0.80602411	0.003109621
C21orf91	XM_001500343	XP_001500393	0.595403623	0.020166088
CABP2	XM_001498045	NULL	0.718691313	0.045264044
CAST	XM_001503694	XP_001503744	-1.115287256	0.040730863
CCDC100	XM_001504520	XP_001504570	0.803480114	0.000671344
CLCN6	XM_001491741	XP_001491791	-0.948193616	0.035580709
CLDN14	XM_001495856	XP_001495906	0.912178907	0.040836892
CUL3	XM_001493366	XP_001493416	0.709298728	0.021485139
CXCL10	XM_001490541	XP_001490591	1.171016563	0.01448367
CXCL3	XM_001489197	XP_001489247	0.654880213	0.013169831

Table C-2 Continued

Gene symbol	NCBI accession	RefSeq accession	Log fold change	Pvalue
DDX58	XM_001497845	XP_001497895	1.353450442	0.000135334
EDN2	AB079136	NP_001075292	0.729300071	0.034286293
ELL2	XR_036497	NULL	0.766178866	0.00996606
FAM21C	CX603317	NULL	0.681328551	0.007521442
FAM89A	NULL	NULL	-1.392747977	0.015022384
GCN5L2	XM_001495089	XP_001495139	-0.778986964	0.043977187
GLB1L	XM_001493157	XP_001493207	-0.907075214	0.017892875
GPR31	XM_001489448	XP_001489498	0.75204151	0.002582712
GRB7	XM_001501037	XP_001501087	0.788591024	0.030267131
HLF	XM_001500211	XP_001500261	0.631119475	0.012749438
ICAM2	XM_001495313	XP_001495363	-0.946848255	0.034909114
ID3	XM_001504221	XP_001504271	-0.978905753	0.048206851
IL1A	NM_001082500	NULL	2.585107345	0.00267813
IL1B	XM_001495926	XP_001495976	1.117415389	0.003005676
IL1RN	U92482	NP_001075994	1.735601259	0.008432987
IMPG2	XM_001503461	XP_001503511	0.580153251	0.014373984
INDO	XM_001490681	XP_001490731	0.699291416	0.020064572
KCNA3	XM_001494050	XP_001494100	-0.781951055	0.021939954
KCNJ2	XM_001498612	XP_001498662	1.146143623	0.009018466
KIF21A	XM_001500023	XP_001500073	0.981764562	0.006683527
KLHL20	XM_001493014	XP_001493064	0.698686792	0.004861024
LIG4	XM_001493890	XP_001493940	-0.795900702	0.04039123
LMBR1L	XM_001504157	XP_001504207	0.664735066	0.00043301
LOC388630	CX592898	NULL	-0.630465559	0.046103315
LOC728772	XM_001491967	XP_001492017	0.853607511	0.032762529
LOC730422	DN507079	NP_001108413	2.084691798	0.000570065
MCM6	XM_001489698	XP_001489748	-1.193710812	0.044163362
MEF2A	CD464185	NULL	0.640787956	0.048692709
MEIS2	XM_001503626	XP_001503676	-0.612615011	0.0420056
NFKBIA	NULL	NULL	0.76992866	0.012265461
NR2F6	XM_001499719	XP_001499769	-1.301052643	0.042924624
NT5C2	XM_001499520	XP_001499570	1.018978363	0.033684678
NULL	CD470350	NULL	1.746563419	0.001395949
NULL	XM_001489363	NULL	1.665159892	5.30E-06
NULL	CD469517	NULL	1.555468456	0.000114922
NULL	DN508878	NULL	1.355154756	0.00526598
NULL	BI961791	NULL	1.226659197	0.001107059
NULL	CD469043	NULL	1.223220171	0.00356743
NULL	CD465425	NULL	1.170032197	0.006003242

Table C-2 Continued

Gene symbol	NCBI accession	RefSeq accession	Log fold change	Pvalue
NULL	BM414612	NULL	1.069382494	0.004701095
NULL	DN508987	NULL	0.948631459	0.007527228
NULL	CD465947	NULL	0.873054658	0.000692472
NULL	CX604697	NULL	0.73798422	0.009839182
NULL	CD536657	NULL	0.659792997	0.03513463
NULL	BM734930	NULL	0.629887182	0.034901723
NULL	CX602249	NULL	0.617207288	0.041069387
NULL	CX604543	NULL	0.607069351	0.02211025
NULL	CX606039	NULL	0.590691432	0.017643889
NULL	XM_001499351	NULL	-1.034739544	0.048989989
NULL	CX604033	NULL	-0.875177731	0.030203368
NULL	DN509057	NULL	-0.743127321	0.013027874
NULL	CD467035	NULL	-0.601842855	0.018924587
OR13D1	XM_001493177	XP_001493227	0.596492155	0.038405249
OR2W3	XM_001498405	XP_001498455	0.686014534	0.001182582
OR7A5	XM_001496119	NULL	-1.411614429	0.041144358
OR7E24	XM_001493162	NULL	0.799036252	0.005243035
OR8U8	XM_001496341	NULL	-1.53019112	0.004005738
PICALM	XM_001490412	XP_001490462	0.647383297	0.010620606
PIK3AP1	XM_001500468	XP_001500518	0.893155484	0.003328656
PLD5	XM_001492999	XP_001493049	-0.659744978	0.031305064
PLEK	XM_001492113	XP_001492163	1.229628257	0.02832517
PNRC2	XM_001504200	NULL	1.053665318	0.006980435
PODXL	XM_001498373	XP_001498423	0.687422164	0.002950615
PRRC1	XM_001504480	XP_001504530	-1.076634396	0.041794071
PSCDBP	XM_001491278	XP_001491328	1.272818912	0.000351192
PTAFR	XM_001503995	XP_001504045	0.822485473	0.007125783
RASGEF1B	NULL	NULL	0.848567319	0.012791089
RETN	XM_001497441	XP_001497491	0.580805519	0.030795519
RGS2	XM_001490543	XP_001490593	-0.658435263	0.004267861
RNF19A	XM_001492262	XP_001492312	0.930427638	0.001547354
RNF24	XM_001496498	NULL	1.927467483	0.048862351
RPAP2	XM_001492375	XP_001492425	-1.173849673	0.02198338
SHARPIN	XM_001495880	NULL	0.746428938	0.015341767
SLC35D2	XM_001494155	XP_001494205	-0.940151368	0.023497194
SMARCA4	XM_001490624	XP_001490674	0.96693218	0.000817632
SNX10	CD467781	NULL	0.973375468	0.046955258
SOD2	AB001693	NP_001075986	1.64600987	0.003318969
SPATA4	XM_001493009	XP_001493059	-0.740639785	0.00537563

Table C-2 Continued

Gene symbol	NCBI accession	RefSeq accession	Log fold change	Pvalue
STAMBPL1	XM_001503046	XP_001503096	0.966996845	0.035484165
TFCP2	XM_001504307	NULL	1.31403059	0.000400086
TMLHE	XM_001498280	XP_001498330	-0.667880002	0.003929976
TPR	XM_001487879	NULL	0.615968645	0.020129579
TREM1	XM_001500981	XP_001501031	0.618781248	0.013385432
UBP1	XM_001489950	XP_001490000	0.992715894	0.000908657
USP13	XM_001496315	XP_001496365	0.664360613	0.004791727
WDR51A	XR_036062	NULL	0.701553019	0.048494841
YTHDF1	XM_001492553	XP_001492603	0.788093149	0.013563092
ZNF462	XM_001493275	XP_001493325	-1.309843924	0.040337679
ZNF784	XM_001490354	XP_001490404	0.960078462	0.000240908
ZSWIM6	XM_001492480	XP_001492530	-0.635315737	0.0319159

Table C-3: List of differentially expressed genes (pvalue <0.05 and fold change cut off of 1.5) between the stimulated and the un-stimulated leukocytes at Week-4.

Gene Symbol	NCBI accession	RefSeq accession	Log fold change	Pvalue
ACTR2	XM_001494389	XP_001494439	-1.442565254	0.003314642
ADA	XM_001500443	XP_001500493	-0.875944536	0.024130993
ARHGDIB	XM_001501778	XP_001501828	-0.637499858	0.038167737
ARPC4	CD528440	NULL	-0.920637046	0.033625217
BIRC3	XM_001499875	XP_001499925	1.280228588	0.006797131
C14orf104	XM_001496267	XP_001496317	1.746290565	0.036210752
C5orf36	XM_001503712	XP_001503762	-0.603469059	0.044885869
CXCL2	AF053497	NULL	0.740888242	0.029366444
CYP26A1	XM_001502498	XP_001502548	-0.644005452	0.012248082
DDX58	XM_001497845	XP_001497895	0.849356831	0.049516409
EDEM3	XM_001490885	XP_001490935	-0.944580951	0.031360262
EDN2	AB079136	NP_001075292	0.607993768	0.025940492
EIF4A1	XM_001504774	XP_001504824	1.071830095	0.048047913
FGL2	XM_001488486	XP_001488536	-0.66421589	0.03392253
GABRB3	XM_001493048	XP_001493098	-0.587994546	0.035456941
IL1A	NM_001082500	NULL	2.572395297	0.000756361
IL1B	XM_001495926	XP_001495976	0.951317235	0.044939967
IL1RN	U92482	NP_001075994	1.729878284	0.027841748
KCNJ10	XM_001491211	XP_001491261	0.639116173	0.001835555
KCNJ2	XM_001498612	XP_001498662	0.652178111	0.015169015

Table C-3 Continued

Gene symbol	NCBI accession	RefSeq accession	Log fold change	Pvalue
KIAA1434	CD466056	NULL	-0.652669269	0.043516761
KIF21A	XM_001500023	XP_001500073	0.780286691	0.014437963
LILRB4	CD467691	NULL	0.7487236	0.002005286
LOC730796	XM_001497173	XP_001497223	-1.864425085	0.015808519
LYPLA1	NULL	NULL	-0.581273371	0.030319939
LYZL6	XM_001494897	XP_001494947	-0.730179609	0.020052288
MEF2A	CD464185	NULL	0.899356423	0.025180504
NULL	CX605267	NULL	2.025224021	0.014351557
NULL	XM_001499351	NULL	1.81497192	0.032856806
NULL	BI961791	NULL	1.594257497	0.007960216
NULL	BM414612	NULL	1.075807382	0.017516782
NULL	CD469517	NULL	0.947058826	0.002164067
NULL	CX602603	NULL	0.589551174	0.028049872
NULL	CD536079	NULL	-0.896364101	0.045862387
NULL	CD465841	NULL	-0.849233215	0.012961625
NULL	CD467057	NULL	-0.795731345	0.026775678
NULL	CD528135	NULL	-0.598270955	0.007291102
OPA3	DN509316	NULL	-1.044739656	0.03591177
OR1A1	XM_001502552	XP_001502602	0.592219414	0.007588206
PLAU	XM_001502951	XP_001503001	0.704530429	0.022173188
PLEK	XM_001492113	XP_001492163	1.102544441	0.013744419
PODXL	XM_001498373	XP_001498423	0.613394511	0.013782635
POLR1D	XM_001493249	NULL	-1.2136447	0.023244224
POLR1E	XM_001504281	XP_001504331	-0.862395043	0.025176069
PSCDBP	XM_001491278	XP_001491328	0.627090082	0.031605316
RGS2	XM_001490543	XP_001490593	-0.779635039	0.003267522
RPS25	XM_001503063	XP_001503113	-0.778312468	0.027655033
SCG5	XM_001501620	XP_001501670	-1.140674466	0.010563301
SCYL1	CX602064	NULL	-0.780474666	0.044981942
SELL	XM_001491555	XP_001491605	-0.648639128	0.023712227
TFCP2	XM_001504307	NULL	0.982984015	0.020718816
TGM2	XM_001499729	NULL	-1.223681514	0.04554654
TNNT3	XM_001492908	NULL	0.625029157	0.015217817
TREM1	XM_001500981	XP_001501031	0.69132632	0.016773534
TSC22D3	XM_001491157	XP_001491207	-0.624588592	0.01369984
TTBK2	NULL	NULL	-0.822268707	0.046272344
USP13	XM_001496315	XP_001496365	0.630416799	0.003463127
VIM	CX604176	NULL	-0.756968459	0.036629821
ZC3HAV1	XM_001499163	NULL	-0.613778865	0.038877421

Table C-3 Continued

Gene symbol	NCBI accession	RefSeq accession	Log fold change	Pvalue
ZNF211	XM_001494387	XP_001494437	-1.043226236	0.00886443
ZNF407	CX599900	NULL	-1.052235826	0.041966686
ZNF407	NULL	NULL	-0.765018041	0.020102759

Table C-4: List of differentially expressed genes (pvalue <0.05 and fold change cut off of 1.5) between the stimulated and the un-stimulated leukocytes at Week-8.

Gene Symbol	NCBI accession	RefSeq accession	Log fold change	Pvalue
AK3	DN510426	NULL	-0.661739522	0.037256069
ARMC8	XM_001496956	XP_001497006	0.846242545	0.000494223
ARRDC3	XM_001504616	XP_001504666	-0.819339052	0.024527401
BIRC3	XM_001499875	XP_001499925	2.264968369	9.56E-05
C11orf49	XM_001494248	XP_001494298	0.763452177	0.023052929
C11orf49	XR_036183	NULL	0.663628353	0.012780599
C11orf49	XR_036493	NULL	0.656792724	0.03831742
C18orf22	XM_001496059	XP_001496109	1.328615535	0.001417922
CCL20	XM_001496798	NULL	1.107191516	0.006865372
CFDP1	XM_001498771	XP_001498821	0.773997841	0.009567496
CHCHD2	XM_001499574	XP_001499624	-0.591928204	0.003264909
CSNK1G3	XM_001504513	NULL	-0.598403293	0.020198351
CUL3	XM_001493366	XP_001493416	0.979939517	0.008525381
CXCL10	XM_001490541	XP_001490591	1.575531659	0.000560746
CXCL2	AF053497	NULL	0.917729157	0.002791755
DCTN3	DN509108	XP_001503748	-0.584589224	0.040841778
DDX58	XM_001497845	XP_001497895	1.792685698	4.00E-06
EDEM3	XM_001490885	XP_001490935	-0.746385317	0.0292086
EDN2	AB079136	NP_001075292	0.870137472	0.005503041
FAM21C	CX603317	NULL	1.094500398	0.008875332
GBP1	XM_001494991	XP_001495041	1.161217967	0.021352266
GDI2	XM_001500009	XP_001500059	-0.623018754	0.043096298
GPR109A	CD469236	NULL	0.834857357	0.006961215
GPR31	XM_001489448	XP_001489498	0.717358629	0.009769871
GPR84	XM_001504570	XP_001504620	1.164376829	6.80E-05
HEXIM2	XM_001495090	XP_001495140	-1.014570409	0.021517129
HNRNPU	CD528363	NULL	-0.858937088	0.020943577
HSPE1	NULL	NULL	-1.329874116	0.010472361

Table C-4 Continued

Gene Symbol	NCBI accession	RefSeq accession	Log fold change	Pvalue
IFNA5	XM_001495486	NULL	0.645616128	0.00248139
IL1A	NM_001082500	NULL	3.829758886	1.78E-08
IL1B	XM_001495926	XP_001495976	2.162329197	0.0020009
IL1RN	U92482	NP_001075994	2.473567181	0.000714063
INDO	XM_001490681	XP_001490731	1.815170687	5.71E-05
INS-IGF2	XM_001492829	NULL	0.752345604	0.000182068
IVNS1ABP	CX604411	NULL	-0.926549023	0.002796688
KCNJ2	XM_001498612	XP_001498662	1.27988629	0.001459713
KIAA1434	CD466056	NULL	-0.79780471	0.007438089
KIF21A	XM_001500023	XP_001500073	1.268932109	0.000251705
KLRB1	XM_001499255	XP_001499305	0.611917454	0.007104291
KMO	XM_001492701	XP_001492751	0.617044902	0.005072262
LILRA6	AB120413	NP_001075993	-0.698036649	0.004198966
LILRB4	XM_001489413	XP_001489463	-0.624058776	0.014811842
LMBR1L	XM_001504157	XP_001504207	0.89806684	0.001025308
LOC730422	DN507079	NP_001108413	2.797778782	1.70E-05
LOC730803	CD471754	NULL	0.741306132	0.000501277
MPP4	XM_001496932	XP_001496982	1.169375876	0.003034343
NDUFA10	XM_001500579	XP_001500629	1.46144557	0.035064978
NFKBIA	NULL	NULL	0.909828808	0.001027568
NPBWR2	XM_001495569	NULL	0.752061566	0.000326237
NULL	CD469043	NULL	1.927062928	0.004635845
NULL	XM_001489363	NULL	1.788861079	0.000157873
NULL	DN508878	NULL	1.788274041	7.03E-07
NULL	CD470350	NULL	1.753720715	0.004053683
NULL	BI961791	NULL	1.65394905	0.006544702
NULL	CD469517	NULL	1.522912202	2.92E-05
NULL	BM414612	NULL	1.146132093	0.007689025
NULL	DN508987	NULL	1.113626273	0.00016679
NULL	CD465425	NULL	1.036822143	0.004148771
NULL	BI961659	NULL	1.018131402	0.014146126
NULL	CX604697	NULL	0.962484971	0.000347426
NULL	CD536657	NULL	0.947982933	0.010354492
NULL	DN507662	NULL	0.875493921	0.014686101
NULL	CX604543	NULL	0.867957213	0.000213978
NULL	CD467650	NULL	0.759172053	0.038807186
NULL	DN509862	NULL	0.672955815	0.030058649
NULL	CD470694	NULL	0.594570216	0.00690229
NULL	CX604033	NULL	-0.946244491	0.01018918

Table C-4 Continued

Gene Symbol	NCBI accession	RefSeq accession	Log fold change	Pvalue
NULL	CX601537	NULL	-0.740174279	0.018614933
NULL	CX599471	NULL	-0.681775599	0.034322327
NXF1	AB302133	NP_001091076	-0.611574648	0.047492306
OLR1	XM_001493960	XP_001494010	1.328882722	0.036496251
OPA3	DN509316	NULL	-0.863751882	0.005823285
PGM1	XM_001499673	XP_001499723	0.698336921	0.001334788
PIK3AP1	XM_001500468	XP_001500518	0.985168148	0.009981568
PLAU	XM_001502951	XP_001503001	0.619602346	0.013212908
PLEK	XM_001492113	XP_001492163	1.760980001	0.000304627
PODXL	XM_001498373	XP_001498423	1.099337807	0.004288463
PPFIA4	XM_001495820	XP_001495870	-0.708426479	0.048413006
PSCDBP	XM_001491278	XP_001491328	0.806746862	0.005992711
PSMB5	XM_001494488	XP_001494538	0.637221712	0.002647985
PTAFR	XM_001503995	XP_001504045	0.777576077	0.001461637
RASGEF1B	NULL	NULL	0.712141042	0.007503619
RGS2	XM_001490543	XP_001490593	-0.94991284	0.000494958
RHOG	XM_001496655	XP_001496705	0.734130137	0.01977316
RNASET2	XM_001489592	XP_001489642	-0.713822838	0.02170683
RNF19A	XM_001492262	XP_001492312	0.864644553	0.029098453
RSPH3	XM_001491976	XP_001492026	1.700046358	0.023920608
SELL	XM_001491555	XP_001491605	-0.948017951	0.015346515
SHPRH	XM_001502347	XP_001502397	-0.707018169	0.023369506
SLC15A2	XM_001500375	XP_001500425	0.644046096	0.000764652
SLC39A13	XM_001491132	XP_001491182	-0.774930279	0.029339313
SMARCA4	XM_001490624	XP_001490674	0.942879067	0.005320191
SNX10	CD467781	NULL	1.380222938	0.006243751
SOD2	AB001693	NP_001075986	1.759764413	0.009343792
TANK	XM_001493298	XP_001493348	1.109704488	0.003522222
TFCP2	XM_001504307	NULL	2.056293477	4.33E-06
TPI1	XM_001497472	XP_001497522	0.597111927	0.003084807
TRAF6	NULL	NULL	-0.726515334	0.013804121
UBP1	XM_001489950	XP_001490000	0.823570172	0.015037027
UMPS	XM_001500039	XP_001500089	0.590924746	0.010610914
USP13	XM_001496315	XP_001496365	0.589099914	0.006317992
VAPB	XM_001490076	XP_001490126	0.609593867	0.000700642
VNN1	XM_001503387	NULL	-0.957757395	0.037100202
ZNF211	XM_001494387	XP_001494437	-0.631307968	0.007563067
ZNF268	XM_001494533	XP_001494583	-0.818874188	0.010320922

Table C-4 Continued

Gene Symbol	NCBI accession	RefSeq accession	Log fold change	Pvalue
ZNF329	XM_001495088	XP_001495138	-0.652394347	0.043973111
ZNF350	XM_001495722	XP_001495772	0.984133366	0.047129427
ZNF784	XM_001490354	XP_001490404	1.061232126	0.001565597
ZNRF2	XM_001499541	NULL	-0.636871587	0.018607074

Table C-5: List of differentially expressed genes (pvalue <0.05 and fold change cut off of 1.5) between the stimulated leukocytes at week-2 compared to day 1.

Gene Symbol	NCBI accession	RefSeq accession	Log fold change	Pvalue
AADAT	XM_001498966	XP_001499016	-0.599841058	0.019685724
ACADVL	XM_001504761	XP_001504811	-1.651823215	0.017418466
AFF3	XM_001492324	XP_001492374	-1.901706459	0.011746588
ARFGEF1	XM_001494559	XP_001494609	-1.514649073	0.007706563
ARMC8	XM_001496956	XP_001497006	-0.625057636	0.007458776
ARPC3	XR_036238	NULL	-0.627643399	0.027328242
ATP6V1C1	XM_001494101	XP_001494151	-1.45038984	0.000571598
AZIN1	XM_001493984	XP_001494034	-1.004918935	0.047897784
AZIN1	XR_035783	NULL	-0.795232016	0.004857066
B3GNT2	XM_001495317	XP_001495367	-1.442155249	0.00052999
BANF2	XM_001494025	NULL	-0.859837701	0.036637416
BIRC3	XM_001499875	XP_001499925	-1.517216835	0.024332028
BTBD8	XM_001492459	XP_001492509	-1.415130725	0.009584908
C12orf35	XM_001503113	XP_001503163	0.750719425	0.032286184
C17orf56	XM_001489994	XP_001490044	-0.851436055	0.003568557
C1orf190	XM_001495298	XP_001495348	-1.378103612	0.01276244
CA12	EF397505	NP_001093230	-0.608655561	0.005510256
CBS	XM_001490849	NULL	-1.322477266	0.000607311
CCL20	XM_001496798	NULL	-2.009916209	0.00065999
CLEC4E	XM_001492794	XP_001492844	-0.601616897	0.031106152
CLINT1	CX604855	NULL	-0.855821145	0.001653176
CPT1B	XM_001490719	XP_001490769	-1.120076377	0.002317933
CRTC3	XM_001498594	XP_001498644	1.038409832	0.003098911
CXCR4	XM_001490165	XP_001490215	0.979364609	0.00165446
CYP2E1	NM_001111303	NULL	-0.63583653	0.019451826
DBN1	XM_001498360	XP_001498410	-1.006602239	0.04053832
EEF1A1	XM_001489416	XP_001489466	1.119913132	0.001026975
FAM14A	XM_001495656	XP_001495706	-0.644261163	0.008598707

Table C-5 Continued

Gene Symbol	NCBI accession	RefSeq accession	Log fold change	Pvalue
FAM21C	CX603317	NULL	-1.455950406	0.012888314
FPRL1	XM_001497411	XP_001497461	-0.692646035	0.031678634
FYB	XM_001496939	XP_001496989	-1.163563477	0.000975345
GIMAP7	NULL	NULL	0.826658955	0.018917044
GIMAP7	NULL	NULL	0.814249777	0.01133128
GNPDA1	XM_001503958	XP_001504008	-1.5737722	0.037194312
HIP1R	XM_001492795	XP_001492845	-0.611008399	0.001101656
HLA-DQB1	XM_001492617	XP_001492667	0.906897149	0.007864025
HLA-DRA	XM_001494553	XP_001494603	0.827114849	0.003035121
IFITM1	CD465069	XP_001488655	-1.310679673	0.011558093
INDO	XM_001490681	XP_001490731	1.049008421	0.02751077
KCNK2	XM_001488153	XP_001488203	-1.048962482	0.016000341
KIF2A	XM_001493976	XP_001494026	-0.864738995	0.015725822
KRT15	XM_001496858	XP_001496908	-2.008355664	0.011479337
LMOD3	XM_001498577	XP_001498627	1.96990071	0.007936875
LOC651894	CD466713	NULL	-0.832969568	0.028204696
LOC653214	XM_001496996	NULL	0.598815897	0.00648256
LOC730422	DN507079	NP_001108413	-0.885191791	0.024265709
LOC92270	XM_001503822	XP_001503872	0.628738747	0.001985344
MPP4	XM_001496932	XP_001496982	-1.312866861	0.005152038
MRPL21	CX604559	XP_001499094	-0.680057552	0.01325242
MTHFD2L	XM_001490173	XP_001490223	-0.649925322	0.033817178
NULL	CD470175	NULL	-1.357598817	0.023588974
NULL	CX604543	NULL	-1.041540848	0.003411092
NULL	CX593205	NULL	-0.794532952	0.043331451
OLFM4	XM_001493449	XP_001493499	-0.823812846	0.02530932
OR10G2	XM_001498059	XP_001498109	-0.95779856	0.010799608
OR2W3	XM_001498405	XP_001498455	-0.781737412	0.003195667
OR52D1	XM_001498223	NULL	-1.109021342	0.002134949
PGM1	XM_001499673	XP_001499723	-0.612126571	0.005268821
PIK3AP1	XM_001500468	XP_001500518	-0.758539591	0.001008768
PLA2G5	XM_001504348	XP_001504398	-1.858163792	0.003357951
RASGEF1B	NULL	NULL	-0.679248186	0.01957803
RETN	XM_001497441	XP_001497491	-0.827955159	0.002938616
RNF144B	XM_001494349	XP_001494399	-0.711980364	0.045847975
RPS25	XM_001503063	XP_001503113	0.890919203	0.044256309
RPSA	DN504853	NULL	0.749437571	0.03611253
RPSA	NULL	NULL	0.746273817	0.001529256

Table C-5 Continued

Gene Symbol	NCBI accession	RefSeq accession	Log fold change	Pvalue
S100A12	CD535886	XP_001494448	-1.532241077	0.026458394
S100A8	XM_001493589	XP_001493639	-1.417147546	0.01751323
S100A8	XM_001494358	XP_001494408	-0.982696069	0.047182232
SDCBP	XR_036510	NULL	-1.789133353	0.001510222
SDCBP	XM_001496872	XP_001496922	-1.497244159	0.03342175
SERPINB1	M91161	NP_001075416	-1.00147438	0.046329777
SYT2	XM_001495156	NULL	-1.080907123	0.001177288
TANK	XM_001493298	XP_001493348	-0.818562526	0.030943308
TFCP2	XM_001504307	NULL	-1.085022963	0.044891734
TFEC	XM_001501723	XP_001501773	-0.798728598	0.000734221
THBS1	XM_001503599	XP_001503649	0.624917399	0.024624249
TMSB4X	XM_001488854	XP_001488904	1.023105536	0.04769547
TRAK1	XM_001497614	XP_001497664	-0.964215761	0.013584595
TSPO	XM_001503143	XP_001503193	-0.822048322	0.012614901
TTBK2	AB292108	NP_001075250	1.096359411	0.047205166
TTBK2	AY237113	NULL	0.873142625	0.047749764
TUBA1A	XM_001491832	XP_001491882	0.580964062	0.004679956
ZFP14	XM_001493293	NULL	1.052025934	0.016778616

Table C-6: List of differentially expressed genes (pvalue <0.05 and fold change cut off of 1.5) between the stimulated leukocytes at week-4 compared to day 1.

Gene Symbol	NCBI accession	RefSeq accession	Log fold change	Pvalue
ABCB10	XM_001496372	XP_001496422	1.161280858	0.019254903
ABHD6	XM_001489265	XP_001489315	0.650778103	0.030679937
ABI1	XM_001494640	XP_001494690	-0.767737493	0.003962405
ACADVL	XM_001504761	XP_001504811	-1.879594703	0.014211782
AFF4	XM_001504421	XP_001504471	-0.954288105	0.002818212
ALPL	XM_001504312	XP_001504362	0.89254865	0.025561207
ANXA5	XM_001503130	XP_001503180	-0.643605893	0.006481538
ANXA7	XM_001503861	XP_001503911	-0.650895201	0.035981336
ARFGEF1	XM_001494559	XP_001494609	-1.799871891	0.003416439
ARHGAP1	XM_001489971	XP_001490021	1.463670456	0.002538143
ARHGEF3	XM_001490400	XP_001490450	1.092489183	0.023071976
ATP11B	XM_001496792	XP_001496842	-0.753303804	0.004651174
ATP13A2	XM_001488576	XP_001488626	1.524868826	0.008006548

Table C-6 Continued

Gene Symbol	NCBI accession	RefSeq accession	Log fold change	Pvalue
ATP1B3	XM_001494313	XP_001494363	-0.747397509	0.002454295
ATP6V0E1	CX602201	XP_001502972	0.702958792	0.031368646
ATP6V1C1	XM_001494101	XP_001494151	-1.89525501	0.00024631
ATXN2	XM_001491014	XP_001491064	0.964185712	0.010402414
AZIN1	XM_001493984	XP_001494034	-1.482429489	0.012098411
AZIN1	XR_035783	NULL	-0.947558216	0.005818344
BIRC3	XM_001499875	XP_001499925	-1.05168096	0.025969003
BLCAP	XM_001502351	XP_001502401	-0.665611044	0.003561071
BTBD8	XM_001492459	XP_001492509	-1.759125712	0.004509461
C10orf112	XM_001497827	XP_001497877	-1.069586233	0.006710267
C14orf104	XM_001496267	XP_001496317	1.78482992	0.005691124
C16orf78	XM_001488683	XP_001488733	1.216013897	0.028518142
C21orf66	XM_001494782	XP_001494832	0.659321985	0.008569989
CA12	EF397505	NP_001093230	-0.829216321	0.036543231
CACHD1	XM_001500703	XP_001500753	-1.123583473	0.048271085
CACNG1	XM_001499847	XP_001499897	0.741109289	0.005422058
CBLB	XM_001503354	XP_001503404	1.513523424	0.016415187
CCL20	XM_001496798	NULL	-1.31502122	0.001798704
CD47	XM_001501702	XP_001501752	-0.62802743	0.020389544
CDC2	XM_001502198	XP_001502248	-0.757883093	0.002952177
CDK3	XM_001491903	XP_001491953	-0.84103389	0.011362206
CHIC1	XM_001504969	XP_001505019	-0.586615158	0.022967356
CLCA2	XM_001496218	XP_001496268	1.467135987	0.01348303
CLIC5	XM_001502577	XP_001502627	0.794455478	0.029767639
CLINT1	CX604855	NULL	-0.910798085	0.006945032
CNP	XM_001495565	XP_001495615	-0.662740956	0.011407858
COL3A1	AF117954	NULL	0.753124137	0.021760872
CXXC5	NULL	NULL	1.237148399	0.023742178
DPM3	XM_001494606	XP_001494656	1.407031607	0.020593666
DZIP1	XM_001492095	XP_001492145	-0.784317436	0.010056089
EDN2	AB079136	NP_001075292	-0.777616848	0.035669238
EMR3	XM_001495205	XP_001495255	-0.62598915	0.036379305
ERCC3	XM_001488507	XP_001488557	1.171594418	0.032766119
EXOSC4	XR_036511	NULL	0.664744484	0.00208116
FAM21C	CX603317	NULL	-1.63507073	0.002486198
FBXO15	XM_001493325	XP_001493375	0.761524442	0.02191545
FPRL1	XM_001497411	XP_001497461	-1.229928848	0.003793493
FYB	XM_001496939	XP_001496989	-1.056103323	0.019260887
GALNT2	XM_001496209	XP_001496259	1.678343053	0.021105045

Table C-6 Continued

Gene Symbol	NCBI accession	RefSeq accession	Log fold change	Pvalue
GK	XM_001488392	XP_001488442	-0.636607299	0.014233248
GPR137	XM_001489414	XP_001489464	0.6577204	0.021086949
GPR84	XM_001504570	XP_001504620	-0.943360847	0.026265726
HSPC152	CX600330	XP_001489771	1.125263352	0.048425048
IFITM1	CD465069	XP_001488655	-1.277246242	0.009153732
IFNGR2	XR_036253	NULL	-0.654109666	0.019799342
JAK2	XM_001500499	XP_001500549	0.629148847	0.034449
KCNJ2	XM_001498612	XP_001498662	-1.260930457	0.042137556
KCNK2	XM_001488153	XP_001488203	-0.955331639	0.020296789
KCNK7	XM_001493848	XP_001493898	0.968250664	0.01938093
KIAA0460	XM_001489478	XP_001489528	-0.662138964	0.029710588
KIF2A	XM_001493976	XP_001494026	-0.964276977	0.005081501
KY	XM_001498469	XP_001498519	0.670285539	0.042327107
LHFPL1	XM_001488695	XP_001488745	0.722807015	0.010884967
LOC643596	XM_001492183	NULL	0.9263886	0.007054456
LOC651894	CD466713	NULL	-0.952000303	0.000688254
LOC730422	DN507079	NP_001108413	-1.902043561	0.003593265
LRMP	XM_001498588	XP_001498638	-0.834436784	0.029000685
LRRC23	XM_001497546	XP_001497596	1.894459	0.019468393
MAL	XM_001494547	XP_001494597	0.917596672	0.005975176
MAPK10	XM_001495324	XP_001495374	0.852832015	0.002361373
MTHFD2L	XM_001490173	XP_001490223	-0.596670218	0.032990439
NFKBIA	NULL	NULL	-0.770999382	0.019251318
NICN1	XM_001497632	XP_001497682	0.728131151	0.002068504
NT5C2	XM_001499520	XP_001499570	-0.995060761	0.021949558
NUBP1	XR_035869	NULL	1.399692908	0.023958098
NULL	CX604543	NULL	-1.483857197	0.001851788
NULL	DN508878	NULL	-1.247637922	0.009305107
NULL	CX606039	NULL	-1.023196843	0.003736644
NULL	XR_036509	NULL	-0.981207915	0.039788418
NULL	CD465425	NULL	-0.950307718	0.006110222
NULL	DN508978	NULL	-0.925169145	0.048204521
NULL	DN510428	NULL	-0.908166329	0.03181999
NULL	XR_036280	NULL	-0.903209125	0.023578169
NULL	CD469043	NULL	-0.843652508	0.038041206
NULL	CX602378	NULL	-0.810701847	0.045863924
NULL	CD528850	NULL	-0.743187436	0.014108027
NULL	CD528482	NULL	-0.727772627	0.035418894
NULL	CX601512	NULL	-0.68960818	0.001654285

Table C-6 Continued

Gene Symbol	NCBI accession	RefSeq accession	Log fold change	Pvalue
NULL	CD468881	NULL	-0.652960578	0.00062913
NULL	DN507234	NULL	-0.640263416	0.00768336
NULL	DN508304	NULL	-0.600152376	0.026311831
NULL	CX602785	NULL	-0.592140719	0.001939824
NULL	CD468898	NULL	-0.581370148	0.018228267
NULL	CD470175	NULL	2.154640616	0.007565129
NULL	CX605267	NULL	1.99496677	0.014646028
NULL	XM_001499351	NULL	1.826194049	0.011733461
NULL	XM_001497251	NULL	1.605571026	0.008928497
NULL	CX600194	NULL	1.557605331	0.014299339
NULL	XM_001498195	XP_001498245	1.492323065	0.045499211
NULL	DN509725	NULL	1.126940549	0.008703142
NULL	XM_001502325	XP_001502375	0.853830526	0.012400068
NULL	CX603299	NULL	0.768572762	0.011388289
NULL	XM_001497110	XP_001497160	0.679230586	0.036510202
NULL	CX593935	NULL	0.582608209	0.026898811
OR1J4	XM_001501393	XP_001501443	0.68007645	0.001907715
OR2S2	XM_001493425	XP_001493475	1.031860512	0.03330239
OR52B4	XM_001496909	XP_001496959	0.740666567	0.006783273
OR52D1	XM_001498223	NULL	-1.216183234	0.031932653
OR5B2	XM_001497992	XP_001498042	-0.823284405	0.002921001
OR6C68	XM_001504060	XP_001504110	-0.606378761	0.045664355
ORM2	XM_001488149	XP_001488199	-0.590570964	0.01759447
PERQ1	XM_001505064	XP_001505114	1.305957671	0.001043103
PGM1	XM_001499673	XP_001499723	-0.850064767	0.004344601
PICALM	XM_001490412	XP_001490462	-1.068610719	6.40E-05
PIK3AP1	XM_001500468	XP_001500518	-0.980084989	0.007484601
PIM1	XM_001500225	XP_001500275	1.3762541	0.045883745
PLA2G10	XM_001489049	XP_001489099	-0.660352777	0.035772003
PLA2G5	XM_001504348	XP_001504398	-1.843177878	0.004780698
PPP4R1	XR_035855	NULL	1.147376507	0.000620105
PRPF39	XM_001493416	NULL	-0.710937356	0.006095941
RAB18	XM_001494294	XP_001494344	-0.622147197	0.005824465
RAP1B	XM_001493406	XP_001493456	-0.99904749	0.01038233
RASGEF1B	NULL	NULL	-0.93326973	0.008852046
RETN	XM_001497441	XP_001497491	-0.995230551	0.014098611
RNF144A	XM_001503614	XP_001503664	1.671011302	0.015927157
RNF181	DN504657	NULL	0.846822667	0.012766161
RNF19A	XM_001492262	XP_001492312	-0.686283743	0.004148708

Table C-6 Continued

Gene Symbol	NCBI accession	RefSeq accession	Log fold change	Pvalue
RPAP2	XM_001492375	XP_001492425	1.387119963	0.024836054
RTKN	XM_001500407	XP_001500457	1.382375189	0.008040411
S100P	BM734933	XP_001501447	-1.354950417	0.029387967
SAA1	NM_001081853	NULL	-0.620685226	0.022778935
SCG5	XM_001501620	XP_001501670	-1.071491568	0.008619687
SDCBP	XR_036510	NULL	-1.907925119	0.014369212
SDCBP	XM_001496872	XP_001496922	-1.787542663	0.020917757
SELO	XM_001496075	XP_001496125	1.211623034	0.009311136
SERPINB1	M91161	NP_001075416	-1.335315655	0.017392239
SH3BGRL	XM_001501152	XP_001501202	-0.890131925	0.003219365
SLC35D2	XM_001494155	XP_001494205	1.211854003	0.003445215
SMARCA4	XM_001490624	XP_001490674	-0.702730217	0.041540223
SMC2	XM_001503998	XP_001504048	0.876809335	0.007564097
SNX3	XM_001503983	XP_001504033	-0.903569952	0.001465001
SPAG4L	XM_001498564	XP_001498614	0.665504638	0.049353951
SPINLW1	XM_001500671	NULL	-0.605375297	0.026425219
SUMF1	XM_001496576	XP_001496626	1.554337784	0.022789518
TAF4B	XM_001495354	XP_001495404	0.664136735	0.046405627
TANK	XM_001493298	XP_001493348	-0.969842651	0.045667353
TCTN3	XM_001500642	XP_001500692	-0.876988261	0.004960816
TFCP2	XM_001504307	NULL	-0.99590272	0.000813443
TFEC	XM_001501723	XP_001501773	-0.895921872	0.003425299
TLK1	XM_001498377	XP_001498427	0.930789411	0.005914872
TMEM139	XM_001489983	XP_001490033	0.854682638	0.000356726
TMLHE	XM_001498280	XP_001498330	0.791435845	0.017887668
TRAF3	XM_001490000	XP_001490050	-0.60527754	0.004209033
TREM1	XM_001500981	XP_001501031	0.734073069	0.001192172
TSPO	XM_001503143	XP_001503193	-0.968851092	0.006787871
UBL7	XM_001494059	XP_001494109	-1.135296214	0.009790008
UNC119	CX601468	XP_001504190	0.685298012	0.028585415
UNC45B	NULL	NULL	1.587404768	0.015616724
USP22	XM_001488603	XP_001488653	0.823866683	0.021871856
VPS54	XM_001493998	XP_001494048	1.61469506	0.021503377
WBP1	CX600458	NULL	-0.79674945	0.012115691
YIPF4	XM_001500250	XP_001500300	-0.785103711	0.003076969
ZCCHC4	XM_001499564	XP_001499614	0.630560054	0.01936207
ZNF423	XM_001491336	XP_001491386	0.748528672	0.02733138
ZNF462	XM_001493275	XP_001493325	1.446451666	0.015667213

Table C-7: List of differentially expressed genes (pvalue <0.05 and fold change cut off of 1.5) between the stimulated leukocytes at week-8 compared to day 1.

Gene Symbol	NCBI accession	RefSeq accession	Log fold change	Pvalue
ACADVL	XM_001504761	XP_001504811	-2.087284003	0.000847443
ARFGEF1	XM_001494559	XP_001494609	-1.610113438	0.003378656
ARRB2	XM_001502964	XP_001503014	0.606058556	0.043532194
ASNSD1	XM_001499046	XP_001499096	1.077796478	0.033549869
ATP11B	XM_001496792	XP_001496842	-0.822230159	0.016452645
ATP1B3	XM_001494313	XP_001494363	-0.648695613	0.005482556
ATP6V1C1	XM_001494101	XP_001494151	-1.202587628	0.034009971
ATRX	XM_001502685	XP_001502735	-0.616259946	0.039278326
BCL2A1	XM_001487956	XP_001488006	0.955041415	0.044290947
BTBD8	XM_001492459	XP_001492509	-0.924766866	0.038558138
C11orf58	XR_036382	NULL	0.653065607	0.023198729
C7orf34	XM_001490979	NULL	0.601862595	0.046129133
CASP4	XM_001499070	XP_001499120	0.600992949	0.046434391
CCL20	XM_001496798	NULL	-0.778462967	0.005110509
CD69	XM_001499388	XP_001499438	0.740935237	0.004646201
CDK3	XM_001491903	XP_001491953	-0.664564519	0.04827149
CLINT1	CX604855	NULL	-0.981385555	0.006492774
DEK	XM_001496593	XP_001496643	0.931423833	0.015238457
DNAJC10	XM_001498066	XP_001498116	0.77186899	0.041010184
EEF1A1	NULL	NULL	1.095967951	0.024315896
EHHADH	XM_001498736	XP_001498786	-0.766644773	0.026279904
EML3	XM_001494714	XP_001494764	0.791210587	0.019950462
EMR3	XM_001495205	XP_001495255	-0.646968248	0.030763809
FAM21C	CX603317	NULL	-1.555535197	0.048848611
FAM3A	XM_001492203	XP_001492253	-0.945540312	0.040937953
FAM45A	CX598831	NULL	0.639509616	0.033204238
FGF17	XM_001490190	XP_001490240	0.592744908	0.029997885
FOXN1	XM_001504134	XP_001504184	-0.689854717	0.027621125
FYB	XM_001496939	XP_001496989	-0.982925809	0.020545064
GIMAP7	NULL	NULL	1.04459567	0.010520798
GIMAP7	NULL	NULL	0.825287594	0.0283829
GPR84	XM_001504570	XP_001504620	-0.620613813	0.031937423
GRHL2	XM_001493287	XP_001493337	-0.821895236	0.006017268
HLA-DQB1	XM_001492617	XP_001492667	0.800585287	0.000840462
HLA-DRA	XM_001494553	XP_001494603	0.893882438	0.023371877
HLA-DRB1	XM_001495531	XP_001495581	0.68056067	0.027745738

Table C-7 Continued

Gene Symbol	NCBI accession	RefSeq accession	Log fold change	Pvalue
HOXA11	XM_001499702	NULL	0.683219088	0.039182344
HSPA8	AF411802	NULL	1.058149497	0.033203756
IFITM1	CD465069	XP_001488655	-1.11443803	0.022143739
IL7R	EF035169	NP_001075411	0.685082157	0.03278201
INDO	XM_001490681	XP_001490731	1.481234967	0.019946121
KIF2A	XM_001493976	XP_001494026	-1.306312758	0.008457702
LOC339457	XM_001495309	NULL	-0.653234193	0.022665678
LOC651894	CD466713	NULL	-0.930651515	0.02515162
LOC653214	XM_001496996	NULL	0.63790332	0.016630539
LOC730422	DN507079	NP_001108413	-1.396569217	0.005032256
MAP4K4	XM_001491720	XP_001491770	0.786029617	0.027023591
MC3R	XM_001489123	XP_001489173	0.794228461	0.035617852
MMP1	AF148882	NP_001075316	-1.383265349	0.018457835
NULL	CD528482	NULL	-1.001419634	0.036841621
NULL	CX606039	NULL	-0.950759774	0.01062028
NULL	CD466166	NULL	-0.825130352	0.036207037
NULL	CX604543	NULL	-0.749051439	0.036238202
NULL	CX602785	NULL	-0.61274206	0.0012007
NULL	CD469036	NULL	-0.612438036	0.024935751
NULL	CX593205	NULL	-0.610547975	0.02273951
NULL	CD528850	NULL	-0.604770805	0.046956995
NULL	DN508293	XP_001504999	1.64644475	0.02100169
NULL	CD465991	XP_001503681	1.258970823	0.006486919
NULL	CD465610	NULL	0.972664732	0.022041409
NULL	CD536657	NULL	0.938773528	0.039296938
NULL	CX605248	NULL	0.905460231	0.03371701
NULL	DN507426	NULL	0.772989861	0.048495289
NULL	CD469128	NULL	0.608263541	0.000200687
NULL	DN509978	NULL	0.597142053	0.040207122
OR52D1	XM_001498223	NULL	-0.6527913	0.018588612
OR5B2	XM_001497992	XP_001498042	-1.06714031	0.044328516
ORM2	CD536428	XP_001488234	0.743300485	0.049920887
OXTR	XM_001491665	XP_001491715	-0.680126049	0.047532481
PAIP1	NULL	NULL	0.665814841	0.01745315
PGM1	XM_001499673	XP_001499723	-0.737188302	0.00474333
PLA2G5	XM_001504348	XP_001504398	-1.43726865	0.015664865
PRPF39	XM_001493416	NULL	-0.846397133	0.003751746
PTPRZ1	XM_001501199	XP_001501249	-0.674121723	0.019505069
RAD50	XM_001504442	XP_001504492	-0.658976212	0.021970309

Table C-7 Continued

Gene Symbol	NCBI accession	RefSeq accession	Log fold change	Pvalue
RASSF2	BM735017	NULL	-0.586614888	0.026433264
RHOG	XM_001496655	XP_001496705	-0.877560931	0.034669375
RNF149	XM_001491820	XP_001491870	-0.633153847	0.048241295
RNF17	XM_001488530	XP_001488580	-0.613166043	0.032459796
RPL10	NULL	NULL	0.860666446	0.025198181
RPL28	CD464415	XP_001495815	0.855569252	0.023662502
RPL31	XM_001489469	XP_001489519	1.146218833	0.010572086
RPL36A	NULL	NULL	0.701082298	0.003860024
RPL37A	XM_001500265	XP_001500315	0.784064991	0.014120044
RPL7	XM_001491982	XP_001492032	1.389483366	0.030492423
RPLP1	BM735439	XP_001495775	0.791525336	0.016447705
RPS2	XR_036216	NULL	0.626066785	0.01084341
RPS25	XM_001503063	XP_001503113	1.365923741	0.028074188
RPS3A	XM_001501474	XP_001501524	1.350921423	0.044803898
RPSA	XM_001497103	XP_001497153	1.331451612	0.041836193
S100A13	CX601420	XP_001494839	0.66414564	0.037215882
S100A8	XM_001493589	XP_001493639	-1.413323341	0.015480451
S100A8	XM_001494358	XP_001494408	-0.801027911	0.016183703
SCYL1	CX602064	NULL	-0.790557375	0.046564998
SDCBP	XR_036510	NULL	-1.077260645	0.0490504
SEC61G	XM_001498680	NULL	0.759066217	0.036271045
SERPINB1	M91161	NP_001075416	-1.145077426	0.030318397
SGCE	XM_001493182	XP_001493232	-0.644246152	0.030496341
SHFM1	XM_001494095	XP_001494145	0.616331664	0.014870371
SNX3	XM_001503983	XP_001504033	-0.732013342	0.041336429
SPCS1	XM_001501306	NULL	0.589014524	0.032431208
TFCP2	XM_001504307	NULL	-0.687762496	0.034288891
TFEC	XM_001501723	XP_001501773	-0.604147246	0.016938484
TOR2A	XM_001501467	XP_001501517	1.14341584	0.016151657
TOR3A	XM_001494447	XP_001494497	-0.922058318	0.026579156
TRIM47	DN510014	NULL	-0.688295223	0.019260471
TSPO	XM_001503143	XP_001503193	-0.706198165	0.04877139
TUBA1A	XM_001491832	XP_001491882	0.865009711	0.014219178
UBL7	XM_001494059	XP_001494109	-1.243838638	0.016938105
USP48	XM_001504296	XP_001504346	-0.730407902	0.002124971
WIPI1	XM_001499325	XP_001499375	-0.689463493	0.025966418

APPENDIX D

Table D-1: Differentially expressed genes. List of differentially expressed genes for each comparison is shown in the table. Genes were considered differentially expressed with $p<0.05$ and fold change >1.5

Biological sample	Time point	Differentially expressed genes
Blood leukocytes	Birth (B-T0)	Up: 119 Down: 149
	Week-2(B-T2)	Up: 93 Down: 87
	Week-4(B-T4)	Up: 191 Down: 128
Nasal epithelial cells	Birth (N-T0)	Up: 360 Down: 141
	Week-2(N-T2)	Up: 228 Down: 348
	Week-4(N-T4)	Up: 108 Down: 159

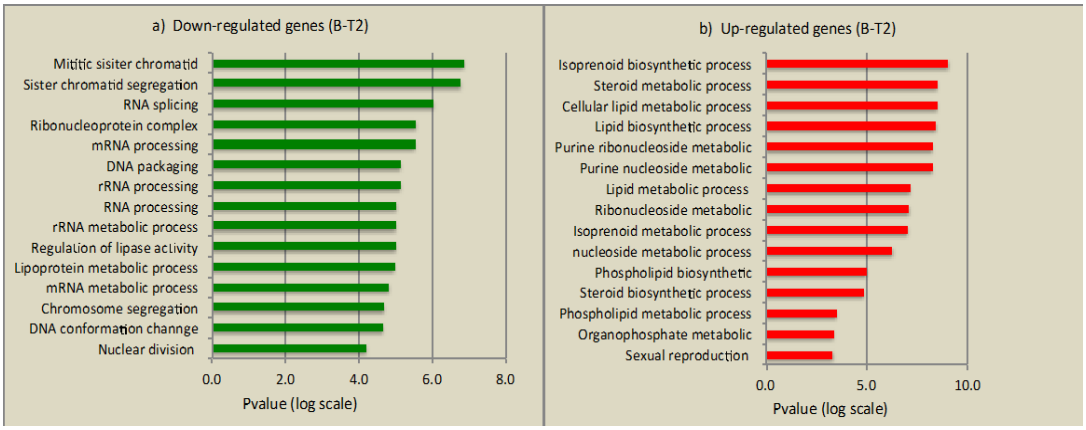

Figure D-1: Biological processes associated with DE genes in blood leukocytes at two-week time point. Graphical representation of top fifteen statistically significant processes associated with the DE genes in blood leukocytes at week-two a) represents biological processes at week-two (T2) associated with down-regulated (colored green bars) and b) up-regulated (colored red bars) genes. The Y-axis represents the biological processes and the X-axis represents the *p* value displayed as $-\log_2$ (*p* value).

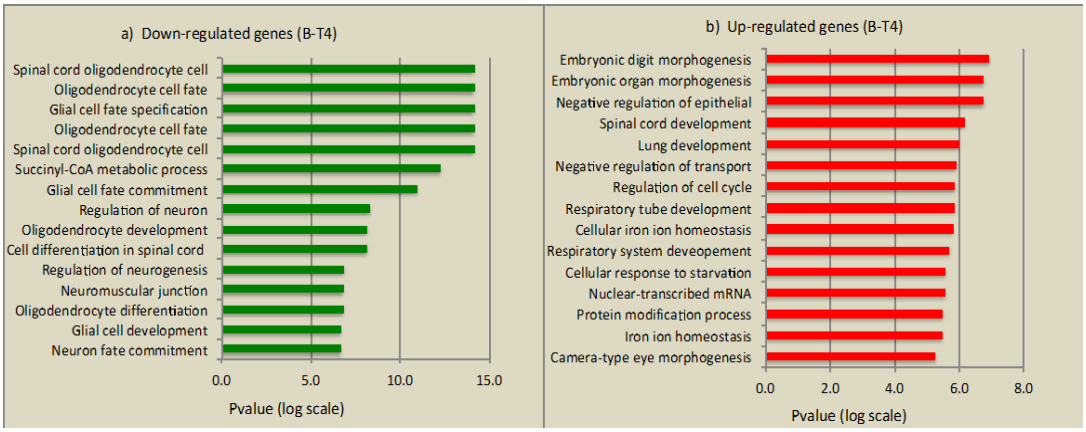

Figure D-2: Biological processes associated with DE genes in blood leukocytes at four-week time point. Graphical representation of top fifteen statistically significant processes associated with the DE genes in blood leukocytes at week-four a) represents biological processes at week-four (T4) associated with down-regulated (colored green bars) and b) up-regulated (colored red bars) genes. The Y-axis represents the biological processes and the X-axis represents the *p* value displayed as $-\log_2$ (*p* value).

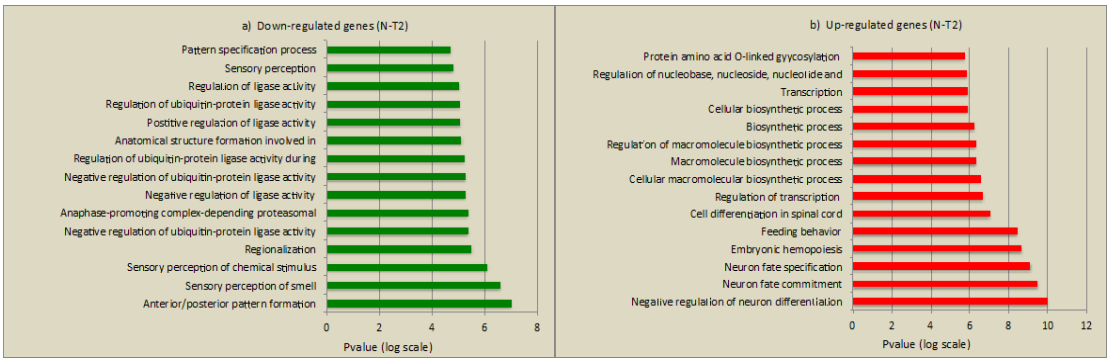

Figure D-3: Biological processes associated with DE genes in nasal epithelium at two-week time point. Graphical representation of top fifteen statistically significant processes associated with the DE genes in nasal epithelium at week-two a) represents biological processes at week-two (T2) associated with down-regulated (colored green bars) and b) up-regulated (colored red bars) genes. The Y-axis represents the biological processes and the X-axis represents the *p* value displayed as $-\log_2$ (*p* value).

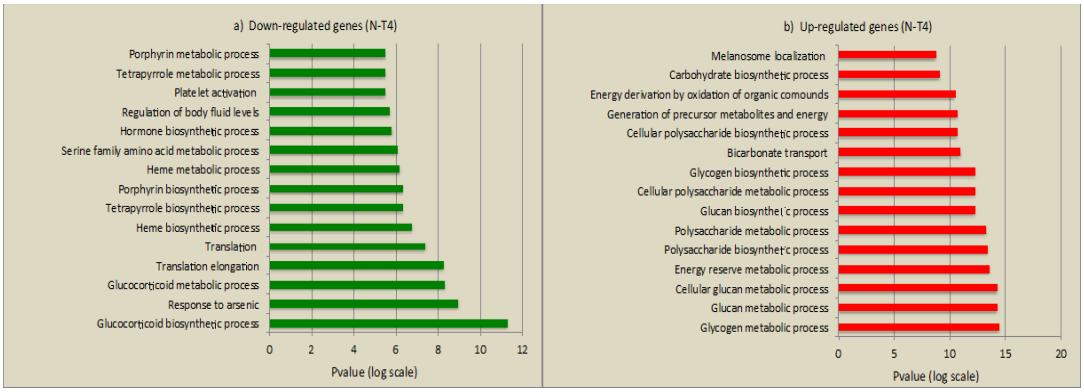

Figure D-4: Biological processes associated with DE genes in nasal epithelium at four-week time point. Graphical representation of top fifteen statistically significant processes associated with the DE genes in nasal epithelium at week-four a) represents biological processes at week-four (T4) associated with down-regulated (colored green bars) and b) up-regulated (colored red bars) genes. The Y-axis represents the biological processes and the X-axis represents the *p* value displayed as $-\log_2$ (*p* value).

Table D-2: Linear discriminant analysis of infected versus control foals at week two (blood leukocytes). The five ten one-, two-, and three-gene LDA classifiers are shown in the table below. $\varepsilon_{bolstered}$ represents the bolstered resubstitution error for the respective gene classifier and $\Delta\varepsilon_{bolstered}$ represents the decrease in error for each feature set relative to its highest ranked subset of genes.

1 feature	2 feature	3 feature	$\varepsilon_{bolstered}$	$\Delta\varepsilon_{bolstered}$
LSM10			0.1218	
PRRT2			0.1693	
GENE:21056			0.1735	
HL02022A1G02.ab1			0.1835	
gnl|UG|Eca#S36646929			0.1864	
PLEK2	HSPD1		0.0313	
LSM10	DDX47		0.0696	0.0522
PLEK2	DDX47		0.0705	
AEBP1	GENE:7122		0.0728	
CX604379	EXOSC9		0.0772	0.1092
PLEK2	DDX47	HSPD1	0.026	0.0053
EXOSC9	PRRT2	GENE:7122	0.0279	
PLEK2	ANKRD50	HSPD1	0.0329	-0.0016
GLT25D2	MXRA5	CENTA2	0.0345	
EXOSC9	PRRT2	HSPD1	0.0346	

Table D-3: Linear discriminant analysis of infected versus control foals at week four (blood leukocytes). The five ten one-, two-, and three-gene LDA classifiers are shown in the table below. $\varepsilon_{bolstered}$ represents the bolstered resubstitution error for the respective gene classifier and $\Delta\varepsilon_{bolstered}$ represents the decrease in error for each feature set relative to its highest ranked subset of genes.

1 feature	2 feature	3 feature	$\varepsilon_{bolstered}$	$\Delta\varepsilon_{bolstered}$
LOC731041			0.0463	
POLE3			0.1115	
ZNF420			0.115	
RPL10A			0.1158	
CD163			0.1222	
RPL10A			0.0315	
LOC731041	CD163		0.0316	0.0147
ZNF420	KRT4		0.0361	0.0789
SRM	LOC731041		0.0368	0.0782
ZNF420	LOC731041		0.0373	0.0777
ZNF420	KRT4	PROCR	0.0046	0.0315
RPL10A	ZNF420	PRDM4	0.0092	0.0223
ZNF420	RAB19	KRT4	0.0105	0.0256
ZNF420	LOC731041	MAP3K14	0.0119	0.0254
CEP55	ZNF420	LOC731041	0.0151	0.0222

Table D-4: Linear discriminant analysis of infected versus control foals at week two (nasal epithelial cells). The top five one-, two-, and three-gene LDA classifiers are shown in the table below. $\varepsilon_{bolstered}$ represents the bolstered resubstitution error for the respective gene classifier and $\Delta\varepsilon_{bolstered}$ represents the decrease in error for each feature set relative to its highest ranked subset of genes.

1 feature	2 feature	3 feature	$\varepsilon_{bolstered}$	$\Delta\varepsilon_{bolstered}$
YY1			0.0973	
MXRA8			0.1246	
CX605699			0.1444	
SH2B3			0.1542	
GABRB3			0.1561	
CX604514	AHSA1		0.0317	0.1477
CX601639	AHSA1		0.0339	0.1455
CT020001B10_PLT_A08_57_056.ab1	OBP2B		0.0393	
MAGEA10	MXRA8		0.0406	0.084
AHSA1	GORASP2		0.0443	0.1351
CX604514	AHSA1	GORASP2	0.013	0.0187
CX604514	AHSA1	SERPINB 2	0.0178	0.0139
CX604514	ZADH2	AHSA1	0.019	0.0127
NPPA	MAGEA10	MXRA8	0.0191	0.0215
CT020001B10_PLT_A08_57_056.ab1	CT020013A10H12.ab1	OBP2B	0.0192	0.0201

Table D-5: Linear discriminant analysis of infected versus control foals at week four (nasal epithelial cells). The top five one-, two-, and three-gene LDA classifiers are shown in the table below. $\varepsilon_{bolstered}$ represents the bolstered resubstitution error for the respective gene classifier and $\Delta\varepsilon_{bolstered}$ represents the decrease in error for each feature set relative to its highest ranked subset of genes.

1 feature	2 feature	3 feature	$\varepsilon_{bolstered}$	$\Delta\varepsilon_{bolstered}$
UQCR			0.1591	
LMBR1L			0.1729	
COX7B			0.1831	
SLC35E4			0.1851	
DN508139			0.1931	
UQCR	SCAPER		0.0565	0.1026
OR2L2	DN508139		0.0794	0.1137
COL28A1	DN508139		0.0806	0.1125
SLC35E4	MGAT4C		0.0832	0.1019
CX605849	DN508139		0.0877	0.1054
OR2L2	COL28A1	DN508139	0.0397	0.0397
KIAA1553	UQCR	SCAPER	0.0447	0.0118
OR2L2	DN508139	DN508139	0.0452	0.0342
UQCR	CLDN3	SCAPER	0.0455	0.011
UQCR	ZNF709	SCAPER	0.0463	0.0102

Section D-1

Temporal changes in blood leukocytes

Two weeks after birth the gene expression profile from the blood leukocytes suggest possible exposure to *R. equi*. At this time point the up-regulated genes were mainly involved in lipid biosynthesis and metabolic processes, processes that could play a role in disease progression.

Evidence for a role of lipid-related genes is present for *Mycobacterium tuberculosis* infection. *Mycobacterium tuberculosis* obtains nourishment from lipids as a major source of carbon (Rachman et al., 2006). Host lipids also play an important role during infection because they appear to be the primary carbon source for *M. tuberculosis in vivo* (Jain et al., 2007). A more recent study observed up-regulation of host genes associated with lipid metabolism and synthesis, causing a progression in granuloma formation (Kim et al., 2010). *R. equi* and *Mycobacterium tuberculosis* share significant genomic similarity (47% sequence homology to *Mycobacterium tuberculosis*) and this homology may be reflected in the pathogenesis (Rahman et al., 2005). We therefore propose that a similar mechanism could be involved in foal lungs due to *R. equi* stimulation of innate immunity. Targeting pathways leading to lipid biosynthesis and metabolism may therefore be of therapeutic value to control *R. equi* growth and hence pneumonia progression.

Four weeks after birth, gene expression profiles from blood leukocytes suggest that protective host immune responses are being activated due to pathogen exposure. These findings support our belief that foals have already been exposed to *R. equi*, and are therefore activating appropriate immune responses against the pathogen. Animals that are more susceptible can be expected to show differences in their profiles. In response to *R. equi*, up-regulation of genes involved in B cell differentiation and iron homeostasis are protecting against this intracellular pathogen by limiting iron requirements of the pathogen.

The hemochromatosis (HFE) and aconitase 1(ACO1) genes are involved in iron homeostasis. Hemochromatosis protein is linked to peptide presentation pathway abnormalities and functions to regulate iron absorption by regulating interaction of the transferrin receptor with transferrin (de Almeida et al., 2005). Lack of iron confers protection within macrophages to the pathogens whose virulence is dependent on iron availability (Moalem et al., 2004). Up-regulation of the HFE gene could therefore be a host defense response to limit iron availability to *R. equi*. Since the HFE gene product regulates iron homeostasis via transferrin regulation, this gene is also a good candidate to be studied for its possible role in *R. equi* pneumonia.

Section D-2

Temporal changes in nasal epithelium

At two weeks of age, the gene expression profiles of nasal epithelial cells suggest up-regulation of genes involved in wound healing, negative regulation of T-cell proliferation, and regulation of IFN-γ production. This would suggest increased protective immune responses at this time point, due to exposure to the pathogen.

CD276/B7-H3 (associated with regulation of IFN-γ production processes) is involved in controlling the immune system beyond adaptive immune responses. Epithelial cells on nasal mucosa express B7-H3 and expression is also induced on T cells, NK cells, APC like dendritic cells (DC), and macrophages (Flies and Chen, 2007). It regulates proliferation of CD4+ and CD8+ T cells, selectively stimulates IFN-γ production *in*

vitro, and has both T cell stimulatory and inhibitory roles (Yi and Chen, 2009). There is evidence that B7-H3 enhances TCR-mediated proliferation of T lymphocytes, generates cytotoxic T lymphocytes, and releases IFN-γ from CD4+ cells (Saatian et al., 2004). A B7-H3 deficiency in mice was reported to increase stimulation of T cells compared to wild type mice, and the B7-H3 deficient mice showed enhanced differentiation of T cells into Th-1 subsets (Suh et al., 2003). Another study reported no stimulatory function of B7-H3 in T cell proliferation or IFN-γ production (Steinberger et al., 2004). Based on our study its exact role in *R. equi* susceptibility is unclear, but it will be a potential candidate for future research.

From linear discriminant analysis, the three-gene classifiers, CX604515, AHSA1, and GORASP2 could discriminate *R. equi* infected foals from healthy foals at birth with the lowest misclassification error. Activator of heat shock 90 kDa protein ATPase homolog 1 (AHSA1/AHA1) activates heat shock protein 90). Heat shock proteins have immunological functions and roles in stress (Tobian et al., 2005). The golgi reassembly stacking protein 2 (GORASP2) gene-product is involved in stacking of golgi cisternae and may play a role in intracellular transport of some transmembrane proteins.

Four weeks after birth, expression profiles of nasal epithelial cells suggested that genes are being modulated (up or down) to initiate protective immune responses to restrict bacterial growth. The down-regulated genes were associated with regulation of body fluids and heme biosynthesis. Gene products associated with regulation of body fluids

include SAA1: Serum amyloid A, an equine acute phase protein that is increased during infectious and non-infectious inflammation (Hulten and Demmers, 2002). In 2005 Cohen et al. (2005b) studied SAA concentrations in serum samples. They found that concentration of this protein in foals with *R. equi* pneumonia was not a good marker for either screening or diagnosis due to variability of results. The translocator protein (TSPO) gene is associated with heme biosynthesis processes in susceptible foals. Proposed functions of TSPO include host defenses such as immunosuppression, immune cell reactivity, and apoptosis of immune cells (Veenman et al., 2007). Impaired host defense against *Mycobacterium bovis* is due to stimulation of TSPO present on macrophages/lymphocytes (Veenman et al., 2007). Since *Mycobacterium bovis* is also an intracellular bacterium, it will be interesting to further explore its role in *R. equi* related pneumonia.

Up-regulated genes at N-T4 were associated with various biological processes, of which rabGTPases signaling appeared to be of particular interest. Intracellular bacterium target Rab to colonize vacuolar compartments in cells of the host. Hence, Rab may provide a mechanism for how bacteria manipulate host cell functions to avoid destruction in lysosomes (Brumell and Scidmore, 2007).

Section D-3

Protocol for RNA extraction from nasal epithelial cells

Unless otherwise stated, all procedures are carried out at room temperature.

1. Before collecting cells, prepare one 1.5 ml microcentrifuge tube per sample with 1.5ml RNA*later*.
2. Place the brush head into the microcentrifuge tube.
3. Remove brush head from RNA*later* and gently scrap away cells from brush using a 10ul tip.
4. Spin the tubes at 5000g at 4 deg C for 5 minutes.
5. Remove the supernatant.
6. Add 1ml PBS to wash the pellet. Spin at 2000g for 5 minutes.
7. Remove supernatant and add another 1ml of PBS (Repeat step 6).
8. Add 350µl extraction buffer (RLT) supplemented with 1% (v/v) β-mercaptoethanol. (Cell lysates can be stored in RLT buffer at -80ºC for several months).
9. Disrupt the cells by homogenizing using 20gz needle on ice.
10. Centrifuge for 2 min at 14 000 rpm to homogenize.
11. Add 1 volume (usually 350 µl) of 70% ethanol to column eluate and mix well by pipetting. Do not centrifuge.
12. Apply the whole volume of the sample (up to 700 µl) to one RNeasy mini spin column sitting on a 2-ml collection tube and centrifuge for 15 sec at 14 000 rpm.
13. Perform on-column Dnase digestion step (RNeasy mini kit procedure)
14. Transfer the RNeasy column into a new 2 ml collection tube. Pipette 500 µl of buffer RPE onto RNeasy column and centrifuge for 15 sec at 14000 rpm.
15. Repeat step 9.

16. Transfer RNeasy column into a new 2-ml collection tube. Centrifuge for 2 min at 14000 rpm as (to ensure that all the ethanol is washed out from column membrane).
17. Transfer RNeasy column into a 1.5 ml collection tube and pipette 30µl of Rnase-free water directly onto the middle of the RNeasy membrane without touching it with the tip. Incubate at room temperature for 1 min then centrifuge for 1 min at 14 000 rpm.
18. After centrifugation put the tubes immediately on ice and use the samples immediately or store them at -80ºC for later usage.
19. For RNA cleanup follow RNeasy Minelute Cleanup (eluted in 14ul of water)

Table D-6a: Down-regulated genes from blood leukocytes at T0. The result for each biological process is listed in this table. For each process listed in second column the associated DE genes are presented in the third column of the table. The final column shows the p-value associated with each process.

Count	Biological process	Genes	Pvalue
1	Cartilage development	CHAD COL9A1 IHH BMP1	0.0021
2	Endosome to lysosome transport	VAMP7 SNX1	0.005
3	Regulation of tyrosine phosphorylation of Stat3 protein	JAK2 PPP2R1A	0.005
4	Tyrosine phosphorylation of Stat3 protein	JAK2 PPP2R1A	0.0058

Table D-6a Continued

Count	Biological process	Genes	Pvalue
5	Regulation of growth	TFCP2L1 CHAD CDKN2AIP UBE2E3 LTBP4 PPP2R1A LRP12	0.0277
6	Cartilage condensation	CHAD BMP1	0.0078
7	Lysosomal transport	VAMP7 SNX1	0.0111
8	Chondrocyte differentiation	COL9A1 IHH	0.0111
9	Peptide cross-linking	COL3A1 EGFLAM	1.36E-02
10	Cell activation	JAK2 VAMP7 IL27RA FGA RPL22 COL3A1 CBLB	1.42E-02

Table D-6a Continued

Count	Biological process	Genes	Pvalue
11	Cellular developemental process	DBN1 TFCP2L1 PRAME EMX1 ERCC3 NDC80 BBS10 SOHLH1 UNC45B SPATA9 LTBP4 PPP2R1A SCUBE1 IHH BMP1 JAK2 RPL22 ZNF423 COL9A1	1.46E-02
12	Negative regulation of immune response	IL27RA COL3A1	1.50E-02
13	Growth	TFCP2L1 CHAD CDKN2AIP UBE2E3 LTBP4 NUBP1 PPP2R1A LRP12	1.63E-02
14	Purine ribonucleotide metabolic process	ATP13A5 ERCC3 PRPS1 ATP13A2	1.71E-02
15	Vacuolar transport	VAMP7 SNX1	1.94E-02
16	Regulation of tyrosine phosphorylation of STAT protein	JAK2 PPP2R1A	1.94E-02

Table D-6a Continued

Count	Biological process	Genes	Pvalue
17	Ribonucleotide metabolic process	ATP13A5 ERCC3 PRPS1 ATP13A2	0.0209
18	Regulation of cellular component size	CHAD CDKN2AIP LTBP4 NEBL NUBP1 PPP2R1A	0.0219
19	Negative regulation of immune system	IL27RA COL3A1 CBLB	0.0222
20	Platelet activation	FGA COL3A1	0.0242
21	Tyrosine phosphorylation of STAT protein	JAK2 PPP2R1A	0.0259
22	Cytoskeleton organization	DBN1 NEBL KLHL20 DES TUBGCP3 FHDC1 NDC80	0.0270
23	Regulation of JAK-STAT cascade	JAK2 PPP2R1A	0.0277
24	Cell growth	CHAD CDKN2AIP LTBP4 NUBP1 PPP2R1A	0.0280

Table D-6a Continued

Count	Biological process	Genes	Pvalue
25	Cell differentiation	DBN1 TFCP2L1 PRAME EMX1 ERCC3 SOHLH1 UNC45B SPATA9 LTBP4 PPP2R1A SCUBE1 BMP1 IHH JAK2 RPL22 ZNF423 COL9A1	0.0318
26	Mitotic sister chromatid segregation	SMC2 NDC80	0.0332
27	Sister chromatid segregation	SMC2 NDC80	0.0352
28	Regulation of cell size	CHAD CDKN2AIP LTBP4 NUBP1 PPP2R1A	0.0357
29	ATP metabolic process	ATP13A5 ERCC3 ATP13A2	0.0384
30	Tissue development	TFCP2L1 CHAD ERCC3 SCUBE1 IHH BMP1 JAK2 COL9A1 COL3A1	0.0390

Table D-6a Continued

Count	Biological process	Genes	Pvalue
31	Alpha-beta T cell activation	RPL22 CBLB	0.0412
32	Blood coagulation	FGA SCUBE1 COL3A1	0.0432
33	Regulation of cell growth	CHAD CDKN2AIP LTBP4 PPP2R1A	0.0449
34	Negative regulation of DNA binding	ZNF462 JAK2	0.0455
35	Peptidyl-serine modification	GALNT2 EGFLAM	0.0455
36	Regulation of biological quality	DBN1 RXFP3 CDKN2AIP NDC80 BBS10 NUBP1 COL3A1 CHAD NEBL LTBP4 PPP2R1A SCUBE1 JAK2 FGA COL9A1 SNCAIP	0.0455
37	Coagulation	FGA SCUBE1 COL3A1	0.0449
38	Regulation of anatomical structure size	CHAD CDKN2AIP LTBP4 NEBL NUBP1 PPP2R1A	0.0479

Table D-6a Continued

Count	Biological process	Genes	Pvalue
39	Purine ribonucleoside triphosphate	ATP13A5 ERCC3 ATP13A2	0.0483
40	Ribonucleoside triphosphate metabolic	ATP13A5 ERCC3 ATP13A2	0.0496

Table D-6b: Up-regulated genes from blood leukocytes at T0. The result for each biological process is listed in this table. For each process listed in second column the associated DE genes are presented in the third column of the table. The final column shows the p-value associated with each process.

Count	Biological process	Genes	pvalue
1	Synaptic vesicle exocytosis	STX4 CPLX3 RAB3A	3.09E-05
2	Cell differentiation	HOXA7 THOC5 ACTC1 ACTG1 PMP22 ADAD1 PHOX2A KCNH1 CEBPB GSN VASP HDAC4 SLITRK4 RAB3A SPI1 TOB1 CSRP2 TSSK2	9.30E-05

Table D-6b Continued

Count	Biological process	Genes	Pvalue
3	Muscle cell differentiation	KCNH1 HDAC4 ACTC1 ACTG1 CSRP2	0.0001
4	Cell development	CEBPB KCNH1 GSN VASP HDAC4 ACTC1 ACTG1 SLITRK4 ADAD1 RAB3A PHOX2A CSRP2	0.0001
5	Cellular development process	HOXA7 THOC5 ACTC1 ACTG1 PMP22 ADAD1 PHOX2A KCNH1 CEBPB GSN VASP HDAC4 SLITRK4 RAB3A SPI1 TOB1 CSRP2 TSSK2	0.0002
6	Synaptice vesicle transport	STX4 CPLX3 RAB3A	0.0004

Table D-6b Continued

Count	Biological process	Genes	Pvalue
7	Cellular component assembly involved in morphogenesis	ACTC1 ACTG1 PMP22	0.0005
8	Neurotransmitter secretion	STX4 CPLX3 RAB3A	0.0009
9	Muscle organ development	KCNH1 HDAC4 ACTC1 ACTG1 BVES CSRP2	0.0012
10	Striated muscle tissue development	KCNH1 HDAC4 ACTC1 ACTG1 CSRP2	0.0014
11	Muscle tissue development	KCNH1 HDAC4 ACTC1 ACTG1 CSRP2	0.0017
12	Response to fungus	CARD9 S100A12	0.0018
13	Establishment of localization in cell	THOC5 ACTC1 CHML TSPO RAB3A SEC22B RAB27B STX4 CPLX3 TOB1 SRP19 STX11	0.002
14	Regulation of neurotransmitter secretion	CPLX3 RAB3A	0.0025

Table D-6b Continued

Count	Biological process	Genes	Pvalue
15	Regulation of interleukin-6 biosynthetic process	CEBPB CARD9	0.0025
16	Interleukin-6 biosynthetic process	CEBPB CARD9	0.0030
17	Exocytosis	STX4 RAB27B CPLX3 RAB3A	0.0032
18	Cellular localization	THOC5 ACTC1 CHML TSPO RAB3A SEC22B RAB27B STX4 CPLX3 TOB1 SRP19 STX11	0.0033
19	Membrane fusion	STX4 STX11 RAB3A	0.0033
20	Regulation of neurotransmitter transport	CPLX3 RAB3A	0.0034
21	Myotube differentiation	KCNH1 HDAC4	0.0034
22	Myofibril assembly	ACTC1 ACTG1	0.0039
23	Striated muscle cell development	ACTC1 ACTG1	0.0044

Table D-6b Continued

Count	Biological process	Genes	Pvalue
24	Intracellular transport	THOC5 ACTC1 CHML TSPO SEC22B STX4 SRP19 TOB1 STX11	0.0048
25	Regulation of multicellular organismal	CEBPB HOXA7 THOC5 HDAC4 CARD9 RAB3A PHOX2A SPI1 CPLX3 TOB1	0.0050
26	Regulation of neurotransmitter levels	STX4 CPLX3 RAB3A	0.0050
27	Muscle cell development	ACTC1 ACTG1	0.0055
28	Skeletal muscle fiber development	KCNH1 HDAC4 CSRP2	0.0057
29	Actomyosin structure organization	ACTC1 ACTG1	0.0060

Table D-6b Continued

Count	Biological process	Genes	Pvalue
30	Protein transport-	CHML TSPO RAB3A SEC22B RAB7L1 RAB27B STX4 SRP19 TOB1 STX11	0.0062
31	System development	HOXA7 THOC5 ACTC1 ACTG1 BVES PMP22 PHOX2A KCNH1 CEBPB GSN VASP HDAC4 NDP SLITRK4 RAB3A SPI1 TOB1 CSRP2	0.0062
32	Neurotransmitter transport	STX4 CPLX3 RAB3A	0.0063

Table D-6b Continued

Count	Biological process	Genes	Pvalue
33	Organ development	CEBPB KCNH1 HOXA7 GSN THOC5 VASP HDAC4 ACTC1 ACTG1 NDP BVES RAB3A PHOX2A SPI1 CSRP2	0.0064
34	Macromolecule localization	OSBPL2 THOC5 CHML TSPO RAB3A SEC22B RAB7L1 RAB27B STX4 TOB1 SRP19 STX11	0.0065
35	Establishment of protein localization	CHML TSPO RAB3A SEC22B RAB7L1 RAB27B STX4 SRP19 TOB1 STX11	0.0068

Table D-6b Continued

Count	Biological process	Genes	Pvalue
36	Muscle fiber development	KCNH1 HDAC4 CSRP2	0.0071
37	Tissue development	KCNH1 HOXA7 GSN VASP HDAC4 ACTC1 ACTG1 CSRP2	0.0096
38	Multicellular organismal development	HOXA7 THOC5 ACTC1 ACTG1 BVES PMP22 ADAD1 PHOX2A KCNH1 CEBPB GSN VASP HDAC4 NDP SLITRK4 RAB3A SP11 TOB1 CSRP2 TSSK2	0.0096
39	Regulation of exocytosis	RAB27B RAB3A	0.0101
40	Negative regulation of cell differentiation	HOXA7 THOC5 HDAC4 TOB1	0.0106

Table D-7a: Down-regulated genes from blood leukocytes at T2. The result for each biological process is listed in this table. For each process listed in second column the associated DE genes are presented in the third column of the table. The final column shows the p-value associated with each process.

Count	Biological process	Genes	Pvalue
1	Mitotic sister chromatid segregation	KIAA0892 NCAPG	0.0086
2	Sister chromatid segregation	KIAA0892 NCAPG	0.0091
3	RNA splicing	FRG1 PHF5A SNRPD3 LSM10	0.0152
4	Ribonucleoprotein complex biogenesis	EXOSC9 FRG1 SNRPD3	0.0212
5	mRNA processing	FRG1 PHF5A SNRPD3 LSM10	0.0217
6	DNA packaging	NCAPG SHPRH	0.0284
7	rRNA processing	EXOSC9 FRG1	0.0284
8	RNA processing	EXOSC9 FRG1 PHF5A SNRPD3 LSM10	0.0307
9	rRNA metabolic process	EXOSC9 FRG1	0.0311
10	Regulation of lipase activity	PPP2R4 HRH1	0.0311
11	Lipoprotein metabolic process	LIPG CHM	0.032
12	mRNA metabolic process	FRG1 PHF5A	0.0353

Table D-7a Continued

Count	Biological process	Genes	Pvalue
13	Chromosome segregation	KIAA0892 NCAPG	0.0387
14	DNA conformation channge	NCAPG SHPRH	0.0397
15	Nuclear division	KIAA0892 LMLN NCAPG	0.0543
16	Mitosis	KIAA0892 LMLN NCAPG	0.0543
17	Ribosome biogenesis	EXOSC9 FRG1	0.0557
18	Organelle fission	KIAA0892 LMLN NCAPG	0.0584
19	M phase of mitotic cell cycle	KIAA0892 LMLN NCAPG	0.0591
20	Response to nutrient	LIPG AACS	0.0639
21	Regulation of hydrolase activity	CHM PPP2R4 HRH1	0.0771
22	Potassium ion transport	SLC24A5 KCNJ8	0.0839
23	Cell division	KIAA0892 LMLN NCAPG	0.0895

Table D-7b: Up-regulated genes from blood leukocytes at T2. The result for each biological process is listed in this table. For each process listed in second column the associated DE genes are presented in the third column of the table. The final column shows the p-value associated with each process.

Count	Biological process	Genes	Pvalue
1	Isoprenoid biosynthetic process	DHRS9 HMGCR	0.0019
2	Steroid metabolic process	DHRS9 CYP21A2 OSBPL8 HMGCR	0.0028
3	Cellular lipid metabolic process	AGPAT5 DHRS9 CYP21A2 OSBPL8 PIGP CRYL1 HMGCR	0.0028
4	Lipid biosynthetic process	AGPAT5 DHRS9 CYP21A2 PIGP HMGCR	0.0029
5	Purine ribonucleoside metabolic process	HMGCR QTRTD1	0.0033
6	Purine nucleoside metabolic process	HMGCR QTRTD1	0.0033
7	Lipid metabolic process	AGPAT5 DHRS9 CYP21A2 OSBPL8 PIGP CRYL1 HMGCR	0.0071
8	Ribonucleoside metabolic process	HMGCR QTRTD1	0.0073
9	Isoprenoid metabolic process	DHRS9 HMGCR	0.0077
10	nucleoside metabolic process	HMGCR QTRTD1	0.0128

Table D-7b Continued

Count	Biological process	Genes	Pvalue
11	Phospholipid biosynthetic process	AGPAT5 PIGP	0.0318
12	Steroid biosynthetic process	CYP21A2 HMGCR	0.0348
13	Phospholipid metabolic process	AGPAT5 PIGP	0.0886
14	Organophosphate metabolic process	AGPAT5 PIGP	0.0986
15	Sexual reproduction	ZPBP HMGCR GDF9	0.0998

Table D-8a: Down-regulated genes from blood leukocytes at T4. The result for each biological process is listed in this table. For each process listed in second column the associated DE genes are presented in the third column of the table. The final column shows the p-value associated with each process.

Count	Biological processes	Genes	Pvalue
1	Spinal cord oligodendrocyte cell differentiation	NKX2-2 ASCL1	5.53E-05
2	Oligodendrocyte cell fate specification	NKX2-2 ASCL1	5.53E-05
3	Glial cell fate specification	NKX2-2 ASCL1	5.53E-05
4	Oligodendrocyte cell fate commitment	NKX2-2 ASCL1	5.53E-05
5	Spinal cord oligodendrocyte cell fate specification	NKX2-2 ASCL1	5.53E-05
6	Succinyl-CoA metabolic process	SUCLA2 SUCLG2	0.0002
7	Glial cell fate commitment	NKX2-2 ASCL1	0.0005
8	Regulation of neuron differentiation	LRRC4C MAG NKX2-2 ASCL1	0.0031

Table D-8a Continued

Count	Biological process	Genes	Pvalue
9	Oligodendrocyte development	NKX2-2 ASCL1	0.0035
10	Cell differentiation in spinal cord	NKX2-2 ASCL1	0.0035
11	Regulation of neurogenesis	LRRC4C MAG NKX2-2 ASCL1	0.0084
12	Neuromuscular junction development	NRD1 UTRN	0.0087
13	Oligodendrocyte differentiation	NKX2-2 ASCL1	0.0087
14	Glial cell development	NKX2-2 ASCL1	0.0096
15	Neuron fate commitment	NKX2-2 ASCL1	0.0096
16	central nervous system neuron	EPHB1 ASCL1	0.0096
17	cell development	REC8 TFCP2L1 LRRC4C ZBTB16 ASCL1 UTRN NKX2-2 MAG EPHB1 NRD1	0.0105
18	spinal cord development	NKX2-2 ASCL1	0.0106
19	tricarboxylic acid cycle	SUCLA2 SUCLG2	0.0116
20	acetyl-CoA catabolic process	SUCLA2 SUCLG2	0.0116
21	coenzyme catabolic process	SUCLA2 SUCLG2	0.0126
22	developmental maturation	REC8	0.0131

Table D-8a Continued

Count	Biological process	Genes	Pvalue
23	regulation of nervous system development	LRRC4C MAG NKX2-2 ASCL1	0.0138
24	central nervous system neuron	EPHB1 ASCL1	0.0148
25	cofactor catabolic process	SUCLA2 SUCLG2	0.0160
26	female pregnancy	HPGD TFCP2L1 SULT1E1	0.0166
27	regulation of cell development	LRRC4C MAG NKX2-2 ASCL1	0.0174
28	acetyl-CoA metabolic process	SUCLA2 SUCLG2	0.0197
29	cell fate specification	NKX2-2 ASCL1	0.0197
30	cytokinesis	BIN3 CNTROB	0.0237
31	aerobic respiration	SUCLA2 SUCLG2	0.0251
32	cell morphogenesis	TFCP2L1 BIN3 LRRC4C MAG BBS7 EPHB1	0.0260
33	protein processing	CPE C4BPA CAPN1	0.0272
34	cell fate commitment	NKX2-2 TCF3 ASCL1	0.0281
35	regulation of axonogenesis	LRRC4C MAG	0.0327
36	protein maturation	CPE	0.0350

Table D-8a Continued

Count	Biological process	Genes	Pvalue
37	cellular component morphogenesis	TFCP2L1 BIN3 LRRC4C MAG BBS7 EPHB1	0.0381
38	regulation of neuron projection	LRRC4C MAG	0.0445
39	glial cell differentiation	NKX2-2 ASCL1	0.0445
40	cell projection morphogenesis	LRRC4C MAG BBS7 EPHB1	0.0504

Table D-8b: Up-regulated genes from blood leukocytes at T4. The result for each biological process is listed in this table. For each process listed in second column the associated DE genes are presented in the third column of the table. The final column shows the p-value associated with each process.

Count	Biological process	Genes	pvalue
1	Embryonic digit morphogenesis	GNA12 GLI3	0.0083
2	Embryonic organ morphogenesis	PROX1 GLI3	0.0093
3	Negative regulation of epithelial cell proliferation	RUNX3 KRT4	0.0093
4	Spinal cord development	PROX1 GLI3	0.0141
5	Lung development	PROX1 GLI3 BMPR2	0.0158
6	Negative regulation of transport	TRAT1 GNAI2 ARL6IP5 FAF1	0.0167
7	Regulation of cell cycle	PROX1	0.0172

Table D-8b Continued

Count	Biological process	Genes	Pvalue
8	Respiratory tube development	PROX1 GLI3 BMPR2	0.0173
9	Cellular iron ion homeostasis	HFE ACO1	0.0182
10	Respiratory system development	PROX1 GLI3 BMPR2	0.0195
11	Cellular response to starvation	BMPR2 HFE	0.0211
12	Nuclear-transcribed mRNA catabolic process	PAN3 RBM8A	0.0211
13	Protein modification process	GRK5 BMPR2 PAN3 UBE2I CDKL1 PMM2 HLCS CCNT1 P4HA2 NEK2 PCNP ST8SIA1 ALG2 MAP3K14 GAD1 GNAI2 TAOK3	0.0222
14	Iron ion homeostasis	HFE ACO1	0.0227
15	Camera-type eye morphogenesis	PROX1 GLI3	0.026
16	Nuclear-transcribed mRNA catabolic	PAN3 RBM8A	0.0277
17	Odontogenesis of dentine-containing tooth	GLI3 AMBN	0.0294

Table D-8b Continued

Count	Biological process	Genes	Pvalue
18	Response to starvation	BMPR2	0.0294
19	Embryonic organ development	PROX1 GLI3	0.0330
20	Macromolecule modification	GRK5 BMPR2 PAN3 UBE2I CDKL1 PMM2 HLCS CCNT1 P4HA2 NEK2 PCNP ST8SIA1 ALG2 MAP3K14 GAD1 GNAI2 TAOK3	0.0331
21	Bone mineralization	BMPR2 AMBN	0.0349
22	Actin filament organization	PROX1 ARPC4 ARPC5L	0.0353
23	Cellular response to nutrient levels	BMPR2 HFE	0.0368
24	mRNA catabolic process	PAN3 RBM8A	0.0368
25	Tube development	PROX1 GLI3 BMPR2 BBS5	0.0380
26	Regulation of protein import into nucleus	GLI3 FAF1	0.0408
27	Regulation of cyclin-dependent protein	CDC6 CCNT1	0.0428
28	Epithelial cell differentiation	PROX1	0.0432

Table D-8b Continued

Count	Biological process	Genes	Pvalue
29	Actin filament polymerization	ARPC4 ARPC5L	0.0449
30	Epithelium development	PROX1 DMBT1 GLI3 KRT4	0.0456
31	Regulation of cellular component	PROX1 ARPC5L FAF1	0.0457
32	B cell differentiation	DCLRE1C IL2RG	0.0491
33	Antigen processing and presentation	PROCR HFE	0.0491
34	Protein amino acid phosphorylation	GRK5 BMPR2 PAN3 CCNT1 NEK2 CDKL1 MAP3K14 GNAI2 TAOK3	0.0518
35	Interspecies interaction between	DMBT1 UBE2I CCNT1 SPEN IL2RG	0.0518
36	Protein amino acid glycosylation	ALG2 ST8SIA1 PMM2	0.0533
37	Glycosylation	ALG2 ST8SIA1 PMM2	0.0533
38	Macromolecule glycosylation	ALG2 ST8SIA1 PMM2	0.0533
39	Cellular defense response	TRAT1	0.0535
40	Odontogenesis		0.0557

Table D-9: List of differentially expressed genes (pvalue <0.05 and fold change cut off of 1.5) between the affected and the unaffected foals from blood leukocytes at birth.

Gene Symbol	NCBI accession	RefSeq accession	Log fold change	Pvalue
ABCB10	XM_001496372	XP_001496422	-1.522481717	0.003156131
ACADVL	XM_001504761	XP_001504811	0.901272857	0.023283085
ACTC1	XM_001503650	XP_001503700	0.622197552	0.009610891
ACTG1	XM_001487824	XP_001487874	0.687288844	0.007623722
ADAD1	XM_001503028	XP_001503078	0.60602188	0.027378802
AKAP9	XR_036011	NULL	-0.802540398	0.023602559
AMZ1	XM_001492380	XP_001492430	-0.730530981	0.021308767
ANKRD10	XM_001496718	XP_001496768	0.807406888	0.047847196
ARF3	XM_001504136	XP_001504186	-0.684753825	0.016468376
ARHGAP1	XM_001489971	XP_001490021	-0.786564378	0.013045788
ARMC9	XM_001495098	XP_001495148	0.624324393	0.012766311
ATF4	NULL	NULL	0.727088156	0.014060121
ATP13A2	XM_001488576	XP_001488626	-1.548655689	0.00782911
ATP13A5	XM_001498779	XP_001498829	-0.637994023	0.029526287
AURKC	XM_001501997	XP_001502047	0.719072491	0.010124505
BBS10	XM_001488843	XP_001488893	-1.034576923	0.010443723
BCMO1	XM_001499593	XP_001499643	-0.779765514	0.044749297
BMP1	XM_001490465	XP_001490515	-0.777785796	0.035909583
BRI3BP	XM_001493505	XP_001493555	-0.597763284	0.042605735
BVES	XM_001503931	XP_001503981	0.649323393	0.041745944
C11orf49	CD528548	NP_001093883	0.878315891	0.01865831
C11orf49	XR_035773	NULL	0.868351106	0.03417004
C11orf49	XM_001504556	XP_001504606	0.640691012	0.024405146
C11orf49	XR_036183	NULL	0.582168227	0.029149313
C12orf57	CX604375	XP_001497722	0.818085845	0.029819354
C12orf62	XM_001504244	NULL	0.690036532	0.028337127
C14orf105	XM_001496486	XP_001496536	0.864715965	0.046449978
C14orf43	XR_035847	NULL	0.625522097	0.017656989
C15orf21	XR_035959	NULL	0.639346271	0.018260101
C16orf78	XM_001488683	XP_001488733	-1.677504406	0.010737236
C18orf19	XM_001488709	XP_001488759	-1.17282182	0.01369973
C1orf86	XM_001495164	XP_001495214	-2.030232074	0.002533635
C2orf42	XM_001492837	XP_001492887	-0.903203925	0.02092908
C5orf30	XM_001504598	XP_001504648	-0.759126552	0.014760365
C7orf31	XM_001498834	XP_001498884	-0.698931067	0.016417536
C9orf52	NULL	NULL	0.723924053	0.008753612
CARD9	XM_001496216	XP_001496266	0.705711141	0.008625631
CBLB	XM_001503354	XP_001503404	-1.370705081	0.044257806

Table D-9 Continued

Gene Symbol	NCBI accession	RefSeq accession	Log fold change	Pvalue
CC2D1A	XR_036084	NULL	-0.893623584	0.044553683
CCDC25	XM_001492881	XP_001492931	0.815060748	0.029013163
CCDC56	XM_001493268	XP_001493318	0.682068712	0.034750671
CD99L2	NULL	NULL	0.827808729	0.021303852
CDAN1	NULL	NULL	-1.272231301	0.039209144
CDK2AP2	CX594512	NULL	1.049718151	0.027878357
CDKN2AIP	XM_001491626	NULL	-1.329129282	0.001080992
CEBPB	CX605423	NULL	0.667972368	0.032229854
CHAD	NULL	NULL	-2.503411503	0.0069877
CHML	XM_001491347	XP_001491397	0.708094215	0.037483441
CLPX	XM_001498202	XP_001498252	-1.297168438	0.024119705
CNBP	XM_001504974	XP_001505024	-0.994942386	0.047939445
CNOT6	XM_001500848	XP_001500898	-0.696433103	0.006387514
COL3A1	AF117954	NULL	-0.704862657	0.021207748
COL9A1	CX605273	NULL	-0.795098338	0.025378887
CPLX1	XM_001488011	XP_001488061	-0.664168141	0.041519617
CPLX3	XM_001493846	XP_001493896	0.631167371	0.012343181
CREB3	XR_036492	NULL	-0.969029193	0.013209177
CSRP2	DN508692	XP_001489207	0.906642761	0.018317778
CST11	XM_001491723	XP_001491773	-2.731500887	0.00540897
CUEDC2	XM_001498878	XP_001498928	-0.67696995	0.012335056
CXorf36	XM_001490751	XP_001490801	0.864505838	0.013142682
CYP2B6	XM_001498423	XP_001498473	-0.907469641	0.013625083
DBN1	XM_001498360	XP_001498410	-2.012820167	0.004826148
DDT	XM_001489369	XP_001489419	0.903804782	0.046885091
DES	XM_001492002	XP_001492052	-0.600627459	0.043119663
DNTTIP2	XM_001491388	XP_001491438	0.968249056	0.005153026
EGFLAM	XM_001499382	XP_001499432	-0.610634583	0.027941388
EMR1	XM_001496454	XP_001496504	-0.631221162	0.025719867
EMX1	XM_001491947	XP_001491997	-0.897235784	0.039211738
ENPP5	XM_001502620	XP_001502670	-0.693124786	0.046822185
ERCC3	XM_001488507	XP_001488557	-1.188478791	0.013511478
FAM3C	CX603884	NULL	-0.607867065	0.012265239
FAM83C	XM_001501577	XP_001501627	0.974123457	0.031592622
FGA	BM780427	NULL	-0.665213353	0.040351304
FHDC1	XM_001501253	XP_001501303	-0.768160098	0.044649192
FILIP1	XM_001503595	XP_001503645	0.791246118	0.026489848
GALNT2	XM_001496209	XP_001496259	-1.809968873	0.007554082
GLRA2	XM_001489464	XP_001489514	-0.662502348	0.029280425

Table D-9 Continued

Gene Symbol	NCBI accession	RefSeq accession	Log fold change	Pvalue
GOLGA7	XM_001490279	XP_001490329	-0.90529579	0.041389813
GSN	U31699	NP_001075422	0.914541879	0.003675405
GSTO1	XM_001499377	XP_001499427	0.780389597	0.00693771
GZMB	AM183299	NP_001075350	0.779950329	0.029017827
HDAC4	XM_001497151	XP_001497201	0.608480982	0.012794377
HDLBP	XM_001502985	XP_001503035	-0.639252649	0.012543945
HN1L	NULL	NULL	-0.887943569	0.02023213
HOXA7	XM_001499485	XP_001499535	0.729172864	0.011052482
HTR3E	XM_001497129	XP_001497179	-0.638022949	0.009233634
IFITM1	CD465069	XP_001488655	0.711230302	0.011640268
IHH	XM_001491778	XP_001491828	-0.714841373	0.039810098
IL27RA	NULL	NULL	-0.95938214	0.019656252
ING5	XM_001497795	XP_001497845	0.629538835	0.017695541
INTS10	XM_001488562	XP_001488612	-0.614457092	0.023868351
IQCF1	XM_001492952	NULL	1.136365164	0.040843757
JAK2	XM_001500499	XP_001500549	-0.665788127	0.036663078
KCNH1	NULL	NULL	0.729327604	0.036860455
KIAA1671	XM_001496100	XP_001496150	0.584708507	0.043126379
KLHL20	XM_001493014	XP_001493064	-0.611939984	0.016770335
LAPTM5	XM_001503920	XP_001503970	0.887760158	0.032743447
LILRB4	XM_001489413	XP_001489463	0.617797169	0.024823215
LOC130074	CX603739	XP_001504975	-0.751620222	0.026871046
LOC348751	XM_001502768	XP_001502818	-0.98525902	0.044604284
LOC442388	XM_001497709	XP_001497759	-0.581122895	0.034941904
LOC651536	XM_001492588	NULL	-0.605228104	0.033234864
LRGUK	XM_001498102	XP_001498152	0.697014041	0.032402976
LRP12	XM_001494687	XP_001494737	-0.697442719	0.02669819
LRRC23	XM_001497546	XP_001497596	-2.120128088	0.000971804
LTBP4	NULL	NULL	-0.711473254	0.045515496
MAP1LC3B	XM_001493613	XP_001493663	-0.685757126	0.027611451
MET	CX603152	NULL	-0.758574781	0.03476553
MGC50722	XM_001498447	XP_001498497	-0.698113916	0.007357438
MTAP	XM_001495991	XP_001496041	0.99870131	0.003737323
NARFL	XM_001496246	XP_001496296	0.754130129	0.024830181
NDC80	XM_001492535	XP_001492585	-1.024091435	0.039873926
NDP	XM_001490351	XP_001490401	0.696997455	0.036657447
NEBL	XM_001496364	XP_001496414	-1.48846536	0.039488705
NLRP13	XM_001490754	XP_001490804	0.888155115	0.035959263
NUBP1	XR_035869	NULL	-1.684632869	0.002788328

Table D-9 Continued

Gene Symbol	NCBI accession	RefSeq accession	Log fold change	Pvalue
NULL	CX594111	NULL	1.000655406	0.013816981
NULL	CD467944	NULL	0.950169391	0.012740142
NULL	XM_001498970	NULL	0.921133159	0.013130607
NULL	DN507341	NULL	0.89610717	0.021323145
NULL	CD469043	NULL	0.749399338	0.036566827
NULL	CD528850	NULL	0.630558535	0.021685068
NULL	CX600948	NULL	0.611322518	0.014384755
NULL	CX600791	NULL	-1.35155731	0.009502707
NULL	XM_001497251	NULL	-1.112742623	0.003650484
NULL	CX600585	NULL	-1.009681056	0.015361551
NULL	XM_001499189	NULL	-0.99487445	0.033004253
NULL	XR_035972	NULL	-0.978774712	0.0089167
NULL	XM_001489861	XP_001489911	-0.934577051	0.018195029
NULL	XM_001490009	NULL	-0.73262925	0.044400263
NULL	XM_001491180	XP_001491230	-0.729432625	0.0036063
NULL	CX605044	NULL	-0.614822777	0.04981404
NULL	CX593054	NULL	-0.605222621	0.019060131
NULL	CX592395	NULL	-0.602290635	0.039202967
NULL	XM_001496183	XP_001496233	-0.591688473	0.04836191
OLAH	XM_001498643	XP_001498693	-0.674704441	0.031676262
OR4A16	XM_001490392	XP_001490442	0.653326814	0.021098789
OR4K15	XM_001502087	XP_001502137	0.941719294	0.04388778
OR51G2	XM_001498239	XP_001498289	-1.197862377	0.041200636
OR5D14	XM_001494979	XP_001495029	-0.642174291	0.041844404
OSBPL2	CX598426	NULL	0.613023914	0.046657096
PARD6A	XM_001498013	XP_001498063	0.876695706	0.040284707
PDHB	XM_001489051	XP_001489101	-0.845803576	0.007267214
PDP2	XM_001496151	XP_001496201	-0.793325814	0.024579976
PHOX2A	XM_001499157	XP_001499207	0.651382374	0.0474398
PLA2G2F	XM_001501686	XP_001501736	-0.59752463	0.030788559
PLD5	XM_001492999	XP_001493049	-0.828774696	0.027651709
PMP22	CX595068	NULL	0.654807846	0.027389336
POLD4	XM_001497352	XP_001497402	0.651250647	0.031066347
PPP1R2	XM_001491737	XP_001491787	0.618139669	0.033786061
PPP2R1A	XM_001496260	XP_001496310	-0.610448566	0.027754824
PRAME	XM_001493673	XP_001493723	-0.651626092	0.015159623
PRPF18	XM_001498739	XP_001498789	-0.767099557	0.041883146
PRPF40B	NULL	NULL	-0.710240414	0.028447653
PRPS1	XM_001496452	XP_001496502	-0.683869051	0.008400077

Table D-9 Continued

Gene Symbol	NCBI accession	RefSeq accession	Log fold change	Pvalue
PSKH2	XM_001489877	XP_001489927	-0.590348516	0.016646816
RAB27B	XM_001487851	XP_001487901	0.644456196	0.031204257
RAB38	XM_001489498	XP_001489548	-0.612629047	0.031917447
RAB3A	XM_001503228	XP_001503278	0.796919996	0.042028926
RAB7L1	XM_001490736	XP_001490786	0.813846764	0.020621332
RAPH1	XM_001497711	XP_001497761	0.842937083	0.021728695
RFXANK	XM_001503453	NULL	0.754674467	0.024953545
RG9MTD1	XR_036450	NULL	-1.118019154	0.027238049
RPAP1	XM_001503411	NULL	-0.620997182	0.036390989
RPAP2	XM_001492375	XP_001492425	-1.379780399	0.044837386
RPL22	CX605634	NULL	-0.74979204	0.014943077
RPS27A	NULL	NULL	0.82564823	0.044835487
RXFP3	XM_001498125	XP_001498175	-0.76063494	0.005603248
S100A12	CD535886	XP_001494448	0.990596593	0.021916997
S100A8	XM_001493589	XP_001493639	0.63897673	0.010271841
SCN4B	XM_001502720	XP_001502770	-0.616263269	0.04380285
SCUBE1	XM_001500812	XP_001500862	-1.414001903	0.048196995
SDPR	XM_001502303	XP_001502353	1.524486532	0.002019344
SEC22B	CX606051	XP_001501277	0.683421352	0.033324448
SERPINB1	M91161	NP_001075416	0.757844511	0.020101086
SFMBT1	XM_001492162	XP_001492212	-0.63344528	0.017762201
SLC2A4RG	XM_001492979	XP_001493029	0.742830148	0.030544217
SLC35D2	XM_001494155	XP_001494205	-0.706969785	0.016322033
SLC43A2	XM_001502290	XP_001502340	-0.984821681	0.035316119
SLC7A4	XM_001488218	XP_001488268	0.895561033	0.006688317
SLC7A4	XR_036162	NULL	0.688296445	0.049590682
SLITRK4	XM_001490209	XP_001490259	0.61196064	0.042242472
SMC2	XM_001503998	XP_001504048	-0.616404023	0.019650268
SMPX	NULL	NULL	0.631892092	0.020585721
SNCAIP	XM_001504535	XP_001504585	-0.833751075	0.004663087
SNX1	EF397509	NULL	-0.703330712	0.006209154
SOHLH1	XM_001498247	XP_001498297	-0.583529068	0.039215078
SPATA9	XM_001504610	XP_001504660	-0.683793601	0.049722137
SPI1	XM_001491380	XP_001491430	0.899636967	0.019534518
SRP19	XM_001503550	XP_001503600	0.74581405	0.017523659
SRR	XM_001504357	XP_001504407	-0.707012981	0.026784075
STX11	XM_001502432	XP_001502482	1.055050992	0.004410196
STX4	XM_001500858	XP_001500908	0.631260279	0.048415445
SULT2A1	XM_001487871	XP_001487921	-0.676260682	0.037176082

Table D-9 Continued

Gene Symbol	NCBI accession	RefSeq accession	Log fold change	Pvalue
SUMF1	XM_001496576	XP_001496626	-1.002503848	0.022002055
TCTE3	XM_001488610	XP_001488660	-1.093154066	0.018066472
TFCP2L1	XM_001498814	XP_001498864	-0.768680399	0.006497138
THOC5	XM_001499034	XP_001499084	0.812645546	0.036552415
TMEM2	XM_001489726	XP_001489776	0.69954791	0.022231162
TOB1	XM_001503158	XP_001503208	0.704725533	0.046209742
TSPO	XM_001503143	XP_001503193	0.85276228	0.023505648
TSSK2	XM_001489006	XP_001489056	0.656252757	0.019436282
TUBGCP3	XM_001497010	XP_001497060	-0.676601693	0.022195001
UBE2E3	XM_001497741	XP_001497791	-0.689896865	0.008389007
UHRF1BP1	XM_001498458	XP_001498508	0.776616759	0.016476293
UMOD	XM_001488179	XP_001488229	-0.736600076	0.040685821
UNC45B	NULL	NULL	-1.322813389	0.023183771
VAMP7	XM_001498227	XP_001498277	-0.664586098	0.01374208
VASP	NULL	NULL	0.724741729	0.007598145
ZCCHC16	XM_001488714	XP_001488764	0.688498471	0.013570475
ZNF182	XM_001501391	XP_001501441	-0.661674129	0.047936578
ZNF226	XR_036324	NULL	0.96101549	0.048960251
ZNF264	XM_001492159	XP_001492209	0.784328199	0.016232432
ZNF423	XM_001491336	XP_001491386	-0.71004126	0.022938436
ZNF462	XM_001493275	XP_001493325	-1.26585732	0.010720258

Table D-10: List of differentially expressed genes (pvalue <0.05 and fold change cut off of 1.5) between the affected and the unaffected foals from blood leukocytes at week-2.

Gene Symbol	NCBI accession	RefSeq accession	Log fold change	Pvalue
AACS	XM_001493527	XP_001493577	-0.72554489	0.030617728
ADAMDEC1	XM_001491607	XP_001491657	0.674077059	0.025630896
AEBP1	CX603424	NULL	-0.777809664	0.008218916
AGPAT5	XM_001495033	XP_001495083	0.902337995	0.018605436
AMZ1	XM_001492380	XP_001492430	-0.620366362	0.044609579
ANKRD50	XM_001502891	XP_001502941	0.731885196	0.024325397
ARHGAP11A	XM_001503656	XP_001503706	0.671819441	0.009123263
ASB5	XM_001492958	XP_001493008	-0.760489141	0.026324409
BTD	XM_001494901	XP_001494951	0.692110218	0.020796682
C13orf1	XM_001488590	XP_001488640	1.0131063	0.040576108

Table D-10 Continued

Gene Symbol	NCBI accession	RefSeq accession	Log fold change	Pvalue
C14orf140	XM_001491724	XP_001491774	0.683981542	0.038679422
C15orf44	XM_001497803	XP_001497853	-0.759673253	0.03836822
C16orf72	XM_001490783	XP_001490833	-0.861095054	0.009975494
C1orf62	XM_001493547	XP_001493597	0.668014846	0.049629074
C20orf94	XM_001495300	XP_001495350	-0.637047796	0.04356551
C21orf70	NULL	NULL	1.102323581	0.004098597
C2orf60	XM_001502779	XP_001502829	0.640462922	0.021326395
C4orf22	XM_001492815	XP_001492865	0.679215952	0.036980733
C5orf37	XM_001504673	XP_001504723	0.674457914	0.011135657
CACNB2	XM_001497017	XP_001497067	0.958617546	0.002267408
CACNG3	XM_001501201	XP_001501251	-0.879242373	0.029964138
CAMK1D	XM_001499103	XP_001499153	0.705264281	0.015947479
CENTA2	XM_001504020	XP_001504070	-0.590886198	0.027026232
CEP192	XM_001490884	NULL	-0.853455989	0.036168146
CHM	XM_001500825	XP_001500875	-0.933734768	0.032535793
CLCA2	XM_001496218	XP_001496268	-0.788624762	0.017107988
CNKSR3	XM_001493771	XP_001493821	-0.706886084	0.031665762
CRNKL1	XM_001489795	NULL	0.615174666	0.043822694
CRYL1	XM_001488972	XP_001489022	0.689884118	0.011069559
CST8	XM_001491551	XP_001491601	-0.875056149	0.039513274
CYP21A2	XM_001491922	XP_001491972	1.064524789	0.035587436
CYP2C18	XM_001502256	XP_001502306	-0.678186128	0.010695019
DDX18	NULL	NULL	-0.85162656	0.037689935
DDX47	XM_001501444	XP_001501494	0.681498892	0.012816292
DHRS9	XM_001497633	XP_001497683	0.615176779	0.018225767
DIDO1	XM_001491593	XP_001491643	-0.744185199	0.010653202
DNAH2	XM_001495846	NULL	-1.060455206	0.036124645
EHD2	XM_001503200	XP_001503250	0.754746252	0.010570599
EXOSC9	XM_001503119	XP_001503169	-0.930154126	0.038897905
FAM53C	XM_001504275	XP_001504325	-0.633062091	0.020270886
FAM55C	XM_001503412	XP_001503462	-0.601986037	0.041772985
FLJ46481	XM_001499734	XP_001499784	-0.609195651	0.048565196
FRG1	XM_001489630	XP_001489680	-0.600862611	0.038983822
GABPA	XR_036314	NULL	0.647109576	0.030150666
GBAS	XM_001493226	XP_001493276	1.68849694	0.014052715
GDF9	XM_001504427	XP_001504477	0.737468862	0.047173128
GLT25D2	XM_001489756	XP_001489806	-0.697696741	0.01147901
GMPPB	XM_001494187	XP_001494237	-0.712917959	0.026286979
GPR87	XM_001489247	XP_001489297	-0.586382239	0.014947221

Table D-10 Continued

Gene Symbol	NCBI accession	RefSeq accession	Log fold change	Pvalue
GRPEL2	XM_001503782	XP_001503832	0.848462089	0.028033358
HDHD1A	XM_001488459	XP_001488509	0.591686148	0.037073927
HEBP2	XM_001503590	XP_001503640	0.667160065	0.0342125
HIST2H2AA4	CX603409	XP_001488204	0.738002808	0.038396082
HMGCR	XM_001504678	XP_001504728	0.678907621	0.008240531
HNRPAB	XM_001499029	XP_001499079	1.033551532	0.038357121
HRH1	DQ681103	NP_001075388	-0.989025512	0.020323069
HSPD1	XM_001502665	XP_001502715	0.66368848	0.019353124
IHPK3	XM_001497932	XP_001497982	-0.802911222	0.004355956
IMPDH2	XM_001494550	XP_001494600	-0.591455282	0.024789857
KCNJ8	XM_001502229	XP_001502279	-1.035812591	0.024806367
KIAA0460	XM_001489478	XP_001489528	1.352452817	0.035612132
KIAA0892	XM_001503477	XP_001503527	-0.632646763	0.021002053
KLHL2	XM_001498031	XP_001498081	-0.62216799	0.033910232
KLK1	AY290704	NP_001075362	-0.750103253	0.046262651
KRT13	XM_001496876	XP_001496926	-0.60259676	0.028006062
KRT23	XM_001497479	XP_001497529	0.635396798	0.039521605
LGALS3	DN506570	NULL	-0.668513986	0.027895779
LIPG	XM_001499159	XP_001499209	-0.839139166	0.037984955
LMLN	XM_001499880	XP_001499930	-0.687903776	0.043202676
LOC647024	XM_001496845	NULL	0.651542448	0.037735846
LOC731848	XM_001490664	NULL	0.645230804	0.038918497
LRRC32	XM_001494868	XP_001494918	-0.670232464	0.021334099
LSM10	XM_001499047	XP_001499097	-0.85220108	0.007007341
MED29	XM_001497555	XP_001497605	-0.613728099	0.045638989
MMP7	XM_001498809	XP_001498859	-0.84269001	0.008027363
MNDA	XM_001490503	XP_001490553	-0.631020899	0.049034476
MRPL40	XM_001488462	XP_001488512	0.64823975	0.028851079
MTERFD1	XM_001490437	XP_001490487	0.756942384	0.03628174
MXRA5	XM_001500228	XP_001500278	-0.625232292	0.019498305
NCAPG	XR_036336	NULL	-0.77827476	0.016590509
NULL	CX604379	NULL	-1.098070909	0.012462016
NULL	CX601609	NULL	-1.07005894	0.00674355
NULL	XM_001503112	NULL	-0.898076939	0.041979768
NULL	CD469526	NULL	-0.769291998	0.017362102
NULL	AW260823	NULL	-0.688548257	0.044390525
NULL	XM_001498856	XP_001498906	-0.600126118	0.027026568
NULL	CX604802	NULL	-0.599349826	0.04363699
NULL	CD464486	NULL	-0.584683002	0.047939659

Table D-10 Continued

Gene Symbol	NCBI accession	RefSeq accession	Log fold change	Pvalue
NULL	DN509596	NULL	0.976336716	0.026426804
NULL	CX594703	NULL	0.910829827	0.028742552
NULL	CX600364	NULL	0.807012414	0.022943073
NULL	CD528740	NULL	0.771652352	0.02940802
NULL	CX600981	NULL	0.73574549	0.011630911
NULL	XM_001498676	XP_001498726	0.72731217	0.029067119
NULL	DN503867	NULL	0.714703071	0.011442931
NULL	CX595746	NULL	0.685704186	0.040396142
NULL	CX606013	NULL	0.672423188	0.035500837
NULL	CX600772	NULL	0.623763027	0.040570204
OR2W1	XM_001494282	XP_001494332	0.698038515	0.017990243
OR4A15	XM_001495944	NULL	-0.87414825	0.0268891
OR4F16	XM_001502069	XP_001502119	0.777416324	0.017700794
OR7A10	XM_001493265	XP_001493315	0.984070755	0.017341
OSBPL8	XM_001491827	XP_001491877	0.798807958	0.005824794
OSCAR	NULL	NULL	0.794470797	0.047685196
P4HB	XM_001489491	XP_001489541	-0.871093248	0.007967631
PDE11A	XM_001500621	XP_001500671	0.725605803	0.010807397
PHF5A	XM_001502490	XP_001502540	-0.615030668	0.040574665
PI3	BM734843	XP_001503236	0.63207267	0.035996543
PIGP	XM_001493083	NULL	0.611478941	0.023165056
PLEK2	XM_001499816	XP_001499866	-0.795496712	0.00917385
PPP2R4	XM_001499731	XP_001499781	-0.656648407	0.047238736
PRRT2	XM_001496325	XP_001496375	-0.811857158	0.016145111
QTRTD1	XM_001501053	XP_001501103	0.931189423	0.001721637
RAB39	XM_001501007	XP_001501057	0.736318608	0.018653711
RAPGEF1	XM_001499272	XP_001499322	0.885580245	0.022452879
RAPH1	XM_001497711	XP_001497761	-0.597421656	0.044153867
RASL11A	XM_001491587	XP_001491637	-0.623787216	0.031346302
RHBDD3	XM_001499400	XP_001499450	-0.816565469	0.032317308
RIOK2	XM_001504606	XP_001504656	-0.665750137	0.013661682
RY1	CX599215	XP_001490747	0.582617927	0.045381358
S100A8	XM_001493589	XP_001493639	0.626710318	0.038798705
SHPRH	XM_001502347	XP_001502397	-0.72368165	0.047278162
SLC24A5	XM_001502401	XP_001502451	-0.84992871	0.033046352
SNRPD3	DN508752	XP_001489110	-0.697387336	0.016940627
TEK	XM_001497116	XP_001497166	0.787741354	0.014292019
TFPI2	XM_001492769	XP_001492819	0.916758134	0.014108727
TMEM90A	XM_001490537	XP_001490587	0.788711016	0.015588121

Table D-10 Continued

Gene Symbol	NCBI accession	RefSeq accession	Log fold change	Pvalue
TMEM98	XM_001503985	XP_001504035	-0.614555194	0.023025361
TRAF7	XR_036252	NULL	0.865000653	0.02922601
VPS13D	XM_001490932	XP_001490982	-0.712064314	0.026703383
VSTM2A	XM_001498645	XP_001498695	-0.61881097	0.048003937
WDR16	XM_001504842	XP_001504892	-0.598652452	0.014630963
WDR90	XM_001497075	XP_001497125	-1.147768165	0.01090289
XRCC3	NULL	NULL	0.686822519	0.007897402
ZER1	XM_001500385	XP_001500435	0.680061032	0.043508235
ZFP36L2	NULL	NULL	0.664914342	0.047563354
ZNF384	XM_001492314	XP_001492364	-0.69763729	0.044935558
ZPBP	XM_001496847	XP_001496897	0.657813419	0.037813488
ZYX	CX602081	NULL	0.927692683	0.021156171

Table D-11: List of differentially expressed genes (pvalue <0.05 and fold change cut off of 1.5) between the affected and the unaffected foals from blood leukocytes at week-4.

Gene Symbol	NCBI accession	RefSeq accession	Log fold change	Pvalue
ABHD11	XM_001493693	XP_001493743	0.824432151	0.01683871
ACO1	XM_001497806	XP_001497856	1.136674395	0.027261528
ACSM1	XM_001493842	XP_001493892	-1.205818791	0.013995359
ACTRT1	XM_001500549	XP_001500599	-0.908930759	0.03487858
ALG2	NULL	NULL	0.898576415	0.033543806
AMBN	XM_001488980	XP_001489030	0.693908477	0.044976625
AMTN	XM_001488949	XP_001488999	-0.672977135	0.046689522
ANKRD44	XM_001500129	NULL	0.673019657	0.041133566
ANKRD55	XM_001493668	XP_001493718	0.646250949	0.033824786
ARHGAP1	XM_001489971	XP_001490021	-0.707295394	0.049296303
ARL6IP5	XM_001498624	XP_001498674	0.668509416	0.039764869
ARPC4	CD528440	NULL	0.835056066	0.007559072
ARPC5L	XM_001502042	XP_001502092	0.872911244	0.011008949
ASCL1	XM_001497332	NULL	-0.674414983	0.037221269
ASCL3	XM_001504908	XP_001504958	-0.603224494	0.041007398
BBS5	XM_001497722	XP_001497772	1.325015617	0.007329683
BBS7	XM_001503097	XP_001503147	-1.06064282	0.015497735
BIN3	XM_001490921	XP_001490971	-0.914487452	0.04207251
BMPR2	XM_001497300	XP_001497350	0.781985453	0.013847916
C10orf78	XM_001497644	XP_001497694	-0.730783412	0.040503406

Table D-11 Continued

Gene Symbol	NCBI accession	RefSeq accession	Log fold change	Pvalue
C11orf63	XM_001501476	XP_001501526	-0.591156139	0.044800468
C12orf40	XM_001501387	NULL	0.659184294	0.040382775
C18orf24	XM_001499477	XP_001499527	-0.757619598	0.016200898
C1orf123	CX593878	XP_001489591	0.828927528	0.035616484
C1orf89	XM_001488699	XP_001488749	0.786037797	0.01404909
C2orf44	XM_001501451	XP_001501501	0.926586862	0.033159663
C4BPA	XM_001492532	XP_001492582	-0.6757353	0.034734034
C9orf117	XM_001500138	XP_001500188	0.618962069	0.045839285
CAPN1	DN506160	NULL	-0.658404724	0.042214151
CBARA1	XM_001503797	XP_001503847	-1.13304612	0.000842687
CBX7	XM_001499938	XP_001499988	0.981449203	0.047091849
CCNT1	AF190905	NP_001075315	1.014017948	0.043345906
CD163	XM_001492693	XP_001492743	0.874794175	0.02903147
CDC6	XM_001497757	XP_001497807	0.765859809	0.020497884
CDKL1	XM_001496680	XP_001496730	0.850717165	0.028567976
CENTA2	XM_001504020	XP_001504070	0.761549991	0.045635333
CEP55	XM_001502456	XP_001502506	-1.231715977	0.049450497
CILP2	XR_036360	NULL	0.599404607	0.045188824
CLIC2	XM_001494262	XP_001494312	0.768038142	0.015996986
CNOT6	XM_001500848	XP_001500898	-0.724794156	0.015861262
CNTROB	XM_001504801	XP_001504851	-0.891468692	0.049142737
COL28A1	XM_001494969	XP_001495019	0.670835285	0.030154821
COLQ	XM_001496422	XP_001496472	-0.836694034	0.019009154
CPE	XR_036288	NULL	-0.925864549	0.024684604
CRTAC1	XM_001501238	XP_001501288	0.767143469	0.02541414
CYP2B6	XM_001498389	XP_001498439	-0.693056116	0.046602376
DACH2	XM_001500765	XP_001500815	0.635695161	0.02847851
DCDC2	XM_001495171	XP_001495221	0.653784358	0.025454344
DCI	XM_001498154	XP_001498204	-0.670046472	0.044823437
DCLRE1C	XM_001498475	XP_001498525	0.749791653	0.024574643
DDX43	XM_001497841	XP_001497891	0.900852542	0.033177947
DKFZP566E164	XM_001489668	XP_001489718	-0.701713945	0.01477661
DMBT1	XM_001488880	NULL	0.752024082	0.019218885
DPP7	XM_001492340	XP_001492390	0.869147143	0.03601938
ECGF1	NULL	NULL	1.012926327	0.014382867
EFHB	XM_001493851	XP_001493901	0.665052898	0.044798473
EPHB1	XM_001498502	XP_001498552	-0.713059954	0.01827056
FAF1	XM_001494368	XP_001494418	0.839815191	0.047701914

Table D-11 Continued

Gene Symbol	NCBI accession	RefSeq accession	Log fold change	Pvalue
FAM105A	XM_001499903	XP_001499953	-0.636009046	0.036634639
FAM139A	XM_001490518	XP_001490568	-0.78933682	0.014383001
FAT3	XM_001491911	XP_001491961	-0.91151198	0.028531857
FDFT1	XR_036232	NULL	1.175862043	0.019215251
FLJ20674	XM_001489301	XP_001489351	-0.735471225	0.031460958
FLJ25770	XM_001491036	XP_001491086	1.422616274	0.044374148
FLJ33590	XM_001495043	XP_001495093	0.75074796	0.009179796
FLJ46321	#N/A	#N/A	1.194637748	0.02635805
FOXK1	XM_001492851	XP_001492901	-0.674312971	0.044232219
FSCN1	NULL	NULL	-0.594237692	0.049900959
FXC1	XM_001499687	XP_001499737	-0.645918346	0.047874691
GAD1	XM_001498256	XP_001498306	0.765048783	0.041510819
GATA1	XM_001493845	XP_001493895	-0.892349008	0.009059292
GCSH	DN505906	NULL	0.630305503	0.030401077
GLI3	XM_001495075	XP_001495125	0.876439175	0.025513856
GNA12	XM_001492404	XP_001492454	0.717780408	0.039278073
GNAI2	XM_001496327	XP_001496377	0.879424075	0.049022977
GNGT2	XM_001502316	XP_001502366	0.634366814	0.02499616
GOLGA4	XM_001489013	XP_001489063	0.653425889	0.043649168
GOLIM4	XM_001494089	XP_001494139	0.690956125	0.037710658
GRK5	XM_001496354	XP_001496404	0.816355464	0.01386985
GZMB	AM183299	NP_001075350	0.921569337	0.020418076
HAPLN1	CX603704	NULL	0.600347281	0.029777436
HFE	XM_001505027	XP_001505077	0.784461939	0.033433178
HINT1	NULL	NULL	0.587550998	0.038438089
HIST1H2AE	XM_001495023	XP_001495073	0.743516921	0.011562785
HLCS	XM_001493178	XP_001493228	0.663388523	0.03916721
HNRNPL	CD536575	NULL	0.853732296	0.043587695
HPGD	DQ385611	NP_001075255	-0.686883502	0.019465575
HSPB1	XM_001504478	XP_001504528	0.852506892	0.015553825
HTR3E	XM_001497129	XP_001497179	-0.769744752	0.032584633
HYI	XM_001496743	XP_001496793	0.6155182	0.044043481
IL17REL	XM_001489299	XP_001489349	1.159521978	0.048756448
IL2RG	CD528508	NULL	1.115919806	0.001547772
INCA1	XM_001502893	XP_001502943	-0.788368523	0.005989588
ITGA3	XM_001502583	XP_001502633	-0.651131662	0.044016236
JMJD5	XM_001502536	XP_001502586	-0.665871511	0.044055892
JTV1	XM_001493465	NULL	1.372689206	0.019269937

Table D-11 Continued

Gene Symbol	NCBI accession	RefSeq accession	Log fold change	Pvalue
KCND3	XM_001498710	XP_001498760	0.718470634	0.031318295
KCNF1	XM_001503533	XP_001503583	1.045189101	0.010358685
KIAA0802	XM_001488953	XP_001489003	-0.789617392	0.014104903
KIAA1522	XM_001499821	XP_001499871	0.906374088	0.006776329
KRT4	XM_001504474	XP_001504524	0.758488228	0.031325828
LAMC3	XM_001499397	XP_001499447	0.66779874	0.04092658
LIN37	XM_001492756	XP_001492806	0.856195902	0.016480941
LOC253012	XM_001493648	XP_001493698	-0.778010565	0.032145741
LOC646262	XM_001501473	NULL	-0.627564117	0.041829378
LOC653604	XM_001491369	XP_001491419	0.882282461	0.041349545
LOC730415	XM_001494779	NULL	0.981775272	0.024315085
LOC731041	XM_001503445	XP_001503495	1.298620634	0.010694653
LRRC4C	XM_001488162	XP_001488212	-0.914852808	0.026656916
MAG	XM_001491638	XP_001491688	-0.799026669	0.026907538
MAP3K14	XM_001488264	XP_001488314	0.83987315	0.007262049
MAP3K7IP2	XM_001502154	XP_001502204	1.09390485	0.002437077
MEMO1	XM_001500302	NULL	0.601409126	0.036826515
MICAL2	XM_001504929	NULL	0.637072408	0.033386071
MMP2	XM_001493281	XP_001493331	-1.0253689	0.015163324
MYBL2	XM_001500357	XP_001500407	-0.857075737	0.022193169
MYH7	XM_001489572	XP_001489622	-1.402560989	0.010461775
MYOM3	XM_001501292	XP_001501342	0.728215721	0.018461048
MYPN	XM_001503598	XP_001503648	-0.65640054	0.039165919
NAGLU	NULL	NULL	-0.630091211	0.049659021
NAP1L4	XM_001496107	XP_001496157	-0.600171823	0.030755596
NEK2	XM_001489608	XP_001489658	0.850644472	0.040888305
NKRF	XM_001491762	XP_001491812	0.660887292	0.014169
NKX2-2	XM_001489173	XP_001489223	-0.584352598	0.041738966
NONO	XM_001492800	XP_001492850	-0.744486991	0.014763985
NRD1	XM_001491249	XP_001491299	-0.741767508	0.022413151
NSUN4	XM_001495067	XP_001495117	-0.748933921	0.014692122
NULL	DN508672	NULL	-1.269558684	0.032475356
NULL	CD528771	NULL	-1.0529431	0.034606894
NULL	XM_001488168	NULL	-0.867020044	0.018622789
NULL	CX602249	NULL	-0.857369732	0.023630254
NULL	CX597420	NULL	-0.848206579	0.009950008
NULL	DN504031	NULL	-0.744222424	0.014677933
NULL	DN505256	NULL	-0.732271667	0.045276634

Table D-11 Continued

Gene Symbol	NCBI accession	RefSeq accession	Log fold change	Pvalue
NULL	CD535168	NULL	-0.619713689	0.042228039
NULL	DN503870	NULL	1.079727231	0.049273076
NULL	CX604280	NULL	1.078121699	0.009844696
NULL	CX598059	NULL	0.986189189	0.025239381
NULL	DN510694	NULL	0.925682438	0.031445614
NULL	CX600400	NULL	0.819793405	0.010064804
NULL	XM_001488796	NULL	0.795635899	0.025737808
NULL	DN510044	NULL	0.758233493	0.045926298
NULL	XM_001502267	NULL	0.741574552	0.022801843
NULL	DN507862	NULL	0.739793209	0.03707351
NULL	CD465106	NULL	0.709931469	0.022586261
NULL	CX605585	NULL	0.656995272	0.037610036
NULL	CD466566	NULL	0.644238493	0.029758414
NULL	XM_001492610	XP_001492660	0.640316815	0.040630205
NULL	BI395111	NULL	0.618441602	0.043597554
NULL	CX601928	NULL	0.597679343	0.033249989
OGDH	XM_001496616	XP_001496666	-0.913042692	0.018003571
OPA3	DN509316	NULL	0.798085734	0.040692222
OR13G1	XM_001497057	XP_001497107	0.709579595	0.026301096
OR1F1	XM_001499023	XP_001499073	0.789782396	0.009673188
OR1J4	XM_001501063	XP_001501113	-0.70595534	0.036851303
OR2L2	#N/A	#N/A	-0.641878932	0.032461194
OR5AC2	XM_001502484	XP_001502534	0.731490897	0.032080733
OR6C2	XM_001490746	XP_001490796	0.671904668	0.040858071
OR6M1	XM_001501603	XP_001501653	-0.715514166	0.011801507
OR7E24	XM_001493551	XP_001493601	-0.642636316	0.024989668
P4HA2	XM_001502946	XP_001502996	1.033549394	0.044062027
PAFAH1B3	NULL	NULL	0.646462584	0.022564484
PAN3	XM_001492258	XP_001492308	0.77973085	0.005868645
PCDH17	XM_001493601	XP_001493651	0.83560144	0.031176001
PCNP	NULL	NULL	0.615589796	0.03018974
PDE7B	XM_001503536	XP_001503586	0.815677777	0.011166386
PLCXD1	XM_001492383	NULL	0.638766202	0.036536752
PMM2	XM_001492888	XP_001492938	0.629383623	0.015834635
POLE3	XM_001501741	XP_001501791	0.597046509	0.030627274
PPFIBP1	XM_001502834	XP_001502884	-0.760921186	0.028110712
PPP1R13B	XM_001492437	XP_001492487	-0.695417478	0.022822972
PRDM4	XM_001499385	XP_001499435	1.000346191	0.036545211

Table D-11 Continued

Gene Symbol	NCBI accession	RefSeq accession	Log fold change	Pvalue
PRKD1	XM_001489357	XP_001489407	-0.669132824	0.044888979
PROCR	XM_001499210	XP_001499260	0.639203304	0.021145432
PROX1	XM_001488438	NULL	0.810062595	0.009406178
PRR6	XM_001503454	XP_001503504	0.70887894	0.041039238
PSCD4	XM_001499462	XP_001499512	-0.921045731	0.010584851
PTGFR	DQ385610	NP_001075275	0.894626241	0.018569989
PTPN2	XM_001491015	XP_001491065	-0.87428708	0.047912292
PXMP2	XM_001493509	NULL	0.769523277	0.0137058
RAB19	XM_001498572	XP_001498622	0.756853978	0.017856061
RAB21	XM_001490408	XP_001490458	0.681004859	0.030582558
RANGAP1	XM_001500278	NULL	0.682166075	0.045748163
RBBP6	CX600655	NULL	-1.068891294	0.022225204
RBM26	CX605135	NULL	-0.582683787	0.034388628
RBM8A	XM_001499584	XP_001499634	0.800715532	0.033272762
RCN1	NULL	NULL	0.631689222	0.020945528
REC8	XM_001489288	XP_001489338	-0.740685088	0.01346746
RPL10	NULL	NULL	-0.679156156	0.021766591
RPL10A	DN509254	NULL	-0.761116722	0.009473794
RPL7	XM_001491982	XP_001492032	0.708588824	0.046120855
RTN4IP1	XM_001501887	XP_001501937	-0.906856973	0.013453879
RUNX3	XM_001501145	XP_001501195	0.770106513	0.046225233
S100A9	XM_001493530	XP_001493580	-0.836522783	0.014063895
SAA1	NM_001081853	NULL	-0.821241693	0.01004916
SAPS3	NM_001113235	NULL	0.609683578	0.043396702
SCN4B	XM_001502720	XP_001502770	0.743310176	0.043523389
SEC61G	XM_001498680	NULL	0.801415531	0.010060894
SERP1	DN511021	NULL	-0.867831292	0.028627955
SERTAD4	XM_001493274	XP_001493324	-0.624122725	0.041721335
SFRS15	XM_001498724	XP_001498774	0.783509317	0.034910913
SFRS2IP	NULL	NULL	0.776238743	0.035882467
SH3KBP1	XR_035923	NULL	0.622309871	0.043784292
SH3TC2	XM_001501557	XP_001501607	0.762141952	0.049308748
SLC28A3	XM_001489024	XP_001489074	-0.666797922	0.029887233
SLK	XM_001497698	XP_001497748	-0.956653955	0.035654257
SPATA20	XM_001499679	XP_001499729	0.600810343	0.042037587
SPEN	CD535806	NULL	0.754233621	0.006286923
SPINT1	XM_001501036	XP_001501086	-0.867038431	0.04471486
SRM	XM_001490359	XP_001490409	-0.710928231	0.013574664

Table D-11 Continued

Gene Symbol	NCBI accession	RefSeq accession	Log fold change	Pvalue
ST13	XM_001502270	XP_001502320	0.758904906	0.014737918
ST18	XM_001488723	XP_001488773	-0.785890475	0.01241326
ST8SIA1	XM_001502320	XP_001502370	0.897676848	0.012424287
STX8	XM_001503237	XP_001503287	1.030427866	0.046142217
SUCLA2	XM_001489977	XP_001490027	-0.819681389	0.028231525
SUCLG2	XM_001495004	XP_001495054	-0.97874017	0.041212985
SULT1E1	XM_001498087	NULL	-0.616668073	0.04154673
SYNE2	XR_036037	NULL	0.874062362	0.034937932
TAOK3	XM_001490545	NULL	0.790960579	0.010197744
TARSL2	XM_001491099	XP_001491149	-0.812502627	0.034735104
TAS2R9	XM_001496057	XP_001496107	-0.629382627	0.02285544
TBC1D22B	XM_001500276	XP_001500326	0.741567124	0.035699003
TCF3	NULL	NULL	-0.742334375	0.023431604
TFCP2L1	XM_001498204	XP_001498254	-0.653297252	0.038843455
THADA	XM_001498963	XP_001499013	-0.665159584	0.019449541
TMEM185A	XM_001499720	XP_001499770	-0.601190523	0.019957981
TOLLIP	XM_001488094	XP_001488144	-0.660499417	0.012481292
TOMM40L	XM_001503794	XP_001503844	-0.656591402	0.029678745
TPM3	NULL	NULL	0.77977646	0.01944537
TRAT1	XM_001501680	NULL	0.624713298	0.022395282
TRIM37	XM_001503728	XP_001503778	0.894801778	0.046877981
TRMU	XM_001488665	XP_001488715	0.913905861	0.022340473
UBAP2	NULL	NULL	1.172151708	0.04411146
UBC	CD470796	NULL	0.658150291	0.03181527
UBE2I	NULL	NULL	0.608852001	0.047141504
UFC1	CX601567	XP_001503885	-1.553873074	0.046275104
USP4	XM_001497962	XP_001498012	-0.852701426	0.02669579
UTRN	XR_036182	NULL	-0.748313949	0.022686422
ZBTB16	XM_001502114	XP_001502164	-0.696715068	0.041271055
ZBTB25	XM_001499182	XP_001499232	-0.652316612	0.036311795
ZNF420	XM_001497154	XP_001497204	-0.720812554	0.006799315
ZNF445	XM_001496613	XP_001496663	-0.58188432	0.046913612
ZNF7	XM_001495225	XP_001495275	-0.628032812	0.037661295
ZNF709	XM_001495842	XP_001495892	0.587432338	0.049223648
ZNF791	XM_001490211	XP_001490261	-0.654520882	0.04998415

Table D-12: List of differentially expressed genes (pvalue <0.05 and fold change cut off of 1.5) between the affected and the unaffected foals from nasal epithelium at birth.

Gene Symbol	NCBI accession	RefSeq accession	Log fold change	Pvalue
39509	XM_001487921	XP_001487971	0.793861403	0.025134599
A26C1A	XM_001497713	XP_001497763	1.075175923	0.014680301
AACS	XM_001493527	XP_001493577	0.682515573	0.04531751
ACMSD	XM_001489267	XP_001489317	-0.602542753	0.04732682
ADAM32	XM_001490591	XP_001490641	-0.916891529	0.000853704
AMPH	XM_001494195	XP_001494245	0.90161222	0.024233325
ANAPC10	XM_001501957	XP_001502007	0.728195302	0.043759224
ANP32E	XR_035813	NULL	1.083410208	0.036931548
ANXA6	XM_001503675	XP_001503725	1.162891857	0.022133563
AP4S1	XM_001489582	XP_001489632	0.860416348	0.001953339
APOA1BP	XM_001500314	XP_001500364	-0.863312078	0.039334602
AQP3	AM182511	NULL	-0.88185452	0.012152189
ARG1	XM_001503285	XP_001503335	0.615482701	0.020901431
ARHGAP18	XM_001503227	XP_001503277	0.927528868	0.033406013
ASB10	XM_001495177	XP_001495227	0.720011764	0.038442363
ASCL3	XM_001504908	XP_001504958	0.833601735	0.030677006
ATP5G3	XM_001499935	XP_001499985	-0.865052013	0.01128912
ATP6V1F	CX603584	XP_001502835	1.081723873	0.022565474
BAG3	XM_001496279	XP_001496329	1.455376368	0.033978391
BBS10	XM_001488843	XP_001488893	-0.590771318	0.032253704
BCL7C	XM_001501077	XP_001501127	0.929104434	0.018136744
BLK	XM_001497947	XP_001497997	0.830760387	0.025783394
BMP10	XM_001491616	XP_001491666	0.689692153	0.024181214
BNIP3	NULL	NULL	0.698013935	0.032062375
BOC	XM_001501187	XP_001501237	0.700781483	0.003820581
BOLA2	XM_001495385	NULL	-0.636107014	0.029490999
BRMS1	XM_001491327	XP_001491377	0.608698903	0.024557096
BTBD2	NULL	NULL	0.636264523	0.018747932
BTN1A1	XM_001492530	XP_001492580	0.941358416	0.023179345
C10orf38	XM_001498537	XP_001498587	0.735653166	0.019457784
C14orf124	XM_001488725	XP_001488775	-0.616552581	0.026921856
C14orf49	XM_001498945	XP_001498995	-0.711439248	0.045306352
C14orf73	XM_001491747	XP_001491797	0.749396125	0.033735186
C1orf125	XM_001488358	XP_001488408	-0.614871664	0.027102789
C1orf128	XM_001504214	XP_001504264	0.923585439	0.040134716
C1orf159	XM_001496587	XP_001496637	0.803968845	0.010873305
C1orf186	XM_001489497	XP_001489547	0.872783937	0.037242038
C1orf216	XM_001503671	XP_001503721	-0.588014423	0.025343041
C3orf14	XM_001490221	NULL	0.894485008	0.028271034

Table D-12 Continued

Gene Symbol	NCBI accession	RefSeq accession	Log fold change	Pvalue
C3orf23	XM_001501325	XP_001501375	-0.632233583	0.016688672
C3orf64	XM_001498735	NULL	0.698128434	0.020027336
C3orf68	CX603098	XP_001491485	1.19602234	0.038952862
C4orf36	XM_001494175	NULL	-0.842806546	0.003686987
C5orf24	XM_001504379	XP_001504429	0.818369005	0.038165009
C6orf105	XM_001495069	XP_001495119	-0.650505413	0.034698714
C6orf12	XM_001490388	NULL	-0.629339992	0.014571457
C6orf70	XM_001488580	XP_001488630	0.61352066	0.027417037
C6orf72	XM_001495513	XP_001495563	0.86109621	0.02631759
CAB39	XM_001494866	XP_001494916	0.603249606	0.041339336
CALCA	NM_001081854	NULL	1.18284334	0.021429391
CALM3	CX605038	NULL	0.730503282	0.030677938
CAMK2A	XM_001501480	XP_001501530	-0.584695813	0.013136929
CARS	XM_001492495	XP_001492545	0.662332205	0.022099055
CASP1	AF090119	NP_001075311	-0.744081199	0.010022903
CASP6	XM_001502919	XP_001502969	0.719193942	0.029022585
CCDC49	XM_001501527	XP_001501577	0.796377792	0.006251021
CCL19	XM_001492856	NULL	1.33834668	0.031616495
CCL20	XM_001496798	NULL	-0.5808208	0.014988685
CD300C	XM_001497431	XP_001497481	0.679192312	0.034974567
CD3EAP	XM_001502587	XP_001502637	1.581353089	0.027576083
CD53	XM_001498018	NULL	0.648927836	0.024650919
CD74	AB032166	NP_001093240	0.622947605	0.01476552
CDC34	XM_001488127	XP_001488177	0.851750039	0.041332086
CDH3	XM_001496960	XP_001497010	0.63364907	0.030444985
CECR5	XM_001489609	XP_001489659	1.112109527	0.035626197
CEP68	XM_001494458	XP_001494508	1.379606057	0.003140165
CES1	XM_001491526	XP_001491576	1.212305639	0.008899001
CGI-96	XM_001503030	XP_001503080	-0.66156703	0.028739111
CGNL1	XM_001500558	XP_001500608	0.836344372	0.001585353
CIB2	XM_001492446	XP_001492496	-0.609357361	0.015470955
CKAP2	XM_001488323	XP_001488373	0.817155838	0.028127283
CLCA1	AY524856	NP_001075268	0.839125726	0.046194323
CLDN3	XR_036494	NULL	0.581103035	0.027314303
CNTROB	XM_001504801	XP_001504851	-1.29769536	0.007858427
COG5	XM_001492486	XP_001492536	1.186853432	0.010629538
COL9A2	XM_001498093	XP_001498143	0.65995549	0.011054014
CORT	XM_001490564	XP_001490614	0.71180909	0.004801545
COX6A2	XM_001500332	XP_001500382	1.193135715	0.001625285

Table D-12 Continued

Gene Symbol	NCBI accession	RefSeq accession	Log fold change	Pvalue
CUGBP1	XM_001492089	XP_001492139	1.158379903	0.003947484
CYP46A1	XM_001488041	XP_001488091	-0.597130538	0.019067384
CYTL1	XM_001499643	XP_001499693	0.845872533	0.036307835
DCLRE1C	XM_001498475	XP_001498525	0.925577317	0.015199968
DCN	AF038127	NP_001075394	0.766086745	0.021892121
DCP2	XM_001503544	XP_001503594	-0.604281694	0.018552636
DEFB113	XM_001498655	NULL	0.625462234	0.028940603
DEPDC7	XM_001492566	XP_001492616	0.783027756	0.012793169
DGAT2	XM_001495302	XP_001495352	0.660882089	0.023900723
DHODH	XM_001497851	XP_001497901	1.122207249	0.000578554
DHX34	XM_001503157	XP_001503207	-0.60564385	0.031977878
DIAPH3	XM_001493869	XP_001493919	-0.645789084	0.009602191
DIXDC1	XM_001501796	XP_001501846	0.954190002	0.044568378
DKFZP564J0863	XM_001488081	XP_001488131	-0.716365868	0.027311965
DKFZP564O0823	XM_001490542	XP_001490592	0.950536437	0.040570432
DKFZP566E164	XM_001489668	XP_001489718	0.70783266	0.012755736
DNASE1L3	XM_001491051	XP_001491101	0.687040411	0.031043406
DPP6	XM_001504680	XP_001504730	0.804147805	0.014127905
DUS3L	NULL	NULL	0.61916278	0.0418401
DUSP22	XM_001489269	XP_001489319	-0.683171965	0.041313033
DYX1C1	XM_001500868	XP_001500918	0.661298556	0.004097737
EBF2	XM_001493967	XP_001494017	0.649052792	0.01600998
EBNA1BP2	BM735407	NULL	1.086986812	0.038746171
EEF1A1	NULL	NULL	-0.784274846	0.005685074
EHD2	XM_001503200	XP_001503250	-0.653983138	0.005966117
EIF3K	XM_001497212	XP_001497262	0.850467988	0.043135846
EIF4E3	XM_001494186	NULL	0.914854485	0.037685775
EIF4G3	AY484519	NP_001075231	0.831393819	0.017217161
ENO2	XM_001497578	XP_001497628	-0.619954481	0.006896585
EPB41	XM_001503955	XP_001504005	0.776419465	0.025622812
ERAS	XM_001493930	XP_001493980	0.588761915	0.047492734
ERN1	XM_001495274	XP_001495324	1.531045896	0.038320754
ESCO1	XM_001491258	XP_001491308	-0.623339599	0.017507502
EXT1	XM_001496434	XP_001496484	1.014506466	0.032669057
FAM64A	XM_001504737	XP_001504787	0.668319112	0.025847709
FANCG	XM_001498082	XP_001498132	0.664289271	0.040538804
FANCI	XM_001499443	XP_001499493	0.636264733	0.009151394
FASN	XM_001491292	XP_001491342	-0.734508103	0.043437048
FBF1	XM_001491921	XP_001491971	-0.725494056	0.009356722

Table D-12 Continued

Gene Symbol	NCBI accession	RefSeq accession	Log fold change	Pvalue
FBXO24	XM_001505057	XP_001505107	0.744713185	0.025868533
FGF14	XM_001493005	XP_001493055	-0.692184046	0.049141443
FGF6	XM_001494335	XP_001494385	0.664357496	0.047177609
FHAD1	XM_001489144	XP_001489194	0.813724168	0.015419794
FICD	XM_001501073	XP_001501123	0.693201399	0.033943236
FKBP8	XM_001503329	XP_001503379	-0.852231819	0.015395673
FLJ14154	XM_001502091	XP_001502141	0.87181905	0.042011577
FOS	XM_001491972	XP_001492022	-0.662927282	0.049851004
FRK	XM_001504096	XP_001504146	0.811793708	0.047214325
FSD1L	XM_001492739	XP_001492789	0.664435713	0.038383173
GGA2	XM_001500946	XP_001500996	0.622531176	0.048598535
GGTLA1	XM_001489252	XP_001489302	-0.593035199	0.006382838
GJA5	XM_001499011	XP_001499061	0.69622699	0.010240205
GLUL	NULL	NULL	0.928282132	0.006744328
GLUL	NULL	NULL	0.85724721	0.036213361
GNA13	XM_001494363	XP_001494413	1.498991668	0.041984327
GNB2L1	NULL	NULL	0.683718441	0.03638908
GNG12	XM_001499698	NULL	0.81094982	0.003367794
GNGT2	XM_001502316	XP_001502366	0.948897099	0.04810129
GOLGA3	XM_001493410	XP_001493460	0.765920916	0.009155926
GOT1	XM_001501044	XP_001501094	-0.605169797	0.007415579
GPATCH4	XM_001500345	XP_001500395	0.667875781	0.027379246
GSDM1	XM_001500788	XP_001500838	0.620432727	0.005087997
GSN	U31699	NP_001075422	0.664504832	0.006907027
GUCA1B	XM_001501305	XP_001501355	1.205194371	0.009654883
HAMP	BM780870	XP_001491660	0.816602516	0.003239989
HAX1	XM_001496771	XP_001496821	1.178501949	0.039053957
HDAC11	XM_001489622	XP_001489672	0.882022735	0.041259725
HDAC8	XM_001488346	XP_001488396	0.743014634	0.022832223
HEATR5B	XM_001501052	XP_001501102	0.612873919	0.049769976
HEY2	XM_001503138	XP_001503188	0.895992654	0.037743457
HLA-B	AY225157	NULL	0.783300915	0.030522313
HMOX1	XM_001498885	XP_001498935	0.760132956	0.037433476
HNRPDL	XM_001491342	XP_001491392	0.859814702	0.045230745
HOXB1	XM_001499152	XP_001499202	-0.770014369	0.025932441
HPX	XM_001504590	XP_001504640	0.739295827	0.041567623
HSPA1A	XM_001492096	XP_001492146	0.864345476	0.032784537
HSPBP1	NULL	NULL	0.92318642	0.03112715
IFIT5	XM_001491815	XP_001491865	0.607277418	0.014023483

Table D-12 Continued

Gene Symbol	NCBI accession	RefSeq accession	Log fold change	Pvalue
IFT172	XM_001502188	XP_001502238	0.601776762	0.036029254
IL13RA2	XM_001490946	XP_001490996	0.774163159	0.02389608
IL7	XM_001491850	XP_001491900	-0.883488785	0.046657251
IMPA2	XM_001491556	XP_001491606	-0.590423171	0.007567366
INMT	XM_001500503	XP_001500553	0.670653238	0.004491636
INTS1	NULL	NULL	0.959425872	0.016046688
IQCA	XM_001496502	XP_001496552	0.839771004	0.003893102
IRF2BP2	CX596722	NULL	0.603403928	0.017346397
ITGA11	XM_001495868	XP_001495918	0.664193578	0.04571672
IVL	XM_001493161	NULL	0.637947905	0.041696095
KCTD14	XM_001494397	XP_001494447	0.824586119	0.031219384
KIAA1024	XM_001503096	XP_001503146	0.684829195	0.030307156
KIAA2018	XM_001502865	XP_001502915	0.948916624	0.019335485
KLK4	XM_001497520	XP_001497570	0.932156606	0.020869561
KLRC1	XM_001494279	NULL	1.489533271	0.025309721
KLRC1	XM_001494234	NULL	0.877536075	0.030172848
KNG1	XM_001499339	XP_001499389	0.583628714	0.03192535
KPNA4	NULL	NULL	1.048286688	0.004499596
LAMA4	XR_036481	NULL	-1.244378846	0.002768756
LARS2	XM_001500836	XP_001500886	0.679129676	0.034595173
LCN2	XM_001501148	XP_001501198	0.742878665	0.008636251
LGALS3	XM_001495733	XP_001495783	1.462088497	0.001364186
LINGO2	XM_001498518	XP_001498568	0.762514347	0.01722562
LMNA	XM_001499921	XP_001499971	0.918397464	0.024484183
LOC124220	XM_001498514	XP_001498564	-0.671586964	0.007839637
LOC149478	XM_001496251	NULL	0.882018652	0.002468681
LOC389117	XM_001494114	XP_001494164	0.917831109	0.008326509
LOC401397	NULL	NULL	0.70619741	0.006328081
LOC550631	XM_001498215	XP_001498265	1.152459276	0.002409509
LOC648044	XM_001504889	XP_001504939	0.615692483	0.049381685
LOC650536	XM_001500011	XP_001500061	1.093984358	0.001635941
LOC650536	XM_001500854	XP_001500904	-0.746919459	0.018695192
LOC729059	XM_001504243	NULL	-0.601165158	0.024126868
LOC730855	AF345995	NULL	1.481132418	0.002599962
LRMP	XM_001498588	XP_001498638	0.595445618	0.032169612
LRRC45	XM_001487864	XP_001487914	-0.756284769	0.007087316
LRSAM1	XM_001501598	XP_001501648	0.603337203	0.035584322
LTBP3	NULL	NULL	1.25097694	0.002580806
LYPD2	XM_001496755	XP_001496805	1.32989038	0.014317774

Table D-12 Continued

Gene Symbol	NCBI accession	RefSeq accession	Log fold change	Pvalue
M-RIP	XM_001488526	XP_001488576	0.755652344	0.023573221
MAGIX	NULL	NULL	0.825679169	0.011044482
MAP7D1	NULL	NULL	1.207964977	0.014802669
MEST	XM_001503034	XP_001503084	0.872589204	0.036271959
MFSD1	XM_001488381	XP_001488431	1.040286886	0.010889705
MGC45438	XM_001499691	XP_001499741	0.738281231	0.038049564
MITD1	XM_001490447	XP_001490497	0.756543941	0.040994621
MMRN1	XM_001496961	XP_001497011	-0.599533727	0.038683453
MOSC2	XM_001488982	XP_001489032	0.823748577	0.011375121
MOSPD1	XM_001488097	XP_001488147	0.59655954	0.039332953
MPND	CX595878	NULL	0.599861977	0.042529829
MRLC2	XM_001494011	XP_001494061	1.213599054	0.02670087
MRPL12	XM_001488528	NULL	0.887644261	0.04475687
MRPL20	NULL	NULL	-0.592098262	0.014599042
MRPS18A	XM_001502158	XP_001502208	0.744373744	0.024622658
MSMB	XM_001493992	NULL	0.98207406	0.014584801
MTHFSD	XM_001500142	XP_001500192	0.825578675	0.007003781
MYOM2	XM_001495857	XP_001495907	0.916809813	0.016294686
MYOZ3	XM_001503704	XP_001503754	0.915143294	0.008661734
N4BP3	XM_001502111	XP_001502161	0.67760423	0.024940695
NANP	XM_001490677	XP_001490727	-0.882636891	0.047620031
NCF2	XM_001490231	XP_001490281	0.888709121	0.038261743
NCOA7	DN510980	NULL	1.18154241	0.029240481
NDUFA9	XM_001494601	XP_001494651	0.758859212	0.034616241
NEDD1	XM_001495034	XP_001495084	-0.739511338	0.043595567
NFASC	XM_001489228	XP_001489278	0.813766588	0.049797843
NKTR	NULL	NULL	0.598515139	0.032152684
NOM1	XM_001496962	XP_001497012	0.887801886	0.048238482
NOS3	XM_001504649	XP_001504699	-0.681474999	0.035505546
NPLOC4	XM_001489864	XP_001489914	-0.629539592	0.009410239
NPS	XM_001489691	NULL	0.710706637	0.016007717
NQO2	XM_001491053	XP_001491103	0.995348142	0.003501292
NULL	CD467511	NULL	1.437611457	0.02524405
NULL	CD465749	NULL	1.435496262	0.044529418
NULL	DN508302	NULL	1.116840395	0.043450202
NULL	XM_001496150	NULL	1.084021791	0.036585472
NULL	XM_001490838	XP_001490888	1.079145142	0.030242978
NULL	CX601287	NULL	0.973135161	0.010885815
NULL	CD466975	NULL	0.970526157	0.049350524

Table D-12 Continued

Gene Symbol	NCBI accession	RefSeq accession	Log fold change	Pvalue
NULL	XM_001495624	NULL	0.918857018	0.034290677
NULL	CD535881	NULL	0.918802139	0.047905361
NULL	CX604881	NULL	0.820441548	0.000764123
NULL	XM_001498667	NULL	0.785857337	0.005018975
NULL	CX604518	NULL	0.737329398	0.042693979
NULL	XR_036280	NULL	0.730224193	0.047666581
NULL	CD536744	NULL	0.70432886	0.015628323
NULL	CX594922	NULL	0.697547992	0.010821008
NULL	XM_001502801	NULL	0.688044625	0.043270306
NULL	XM_001498856	XP_001498906	0.680127909	0.015610148
NULL	CX605947	NULL	0.668737435	0.026867486
NULL	XM_001501195	XP_001501245	0.593542833	0.048546905
NULL	XM_001503948	NULL	0.589049148	0.036305871
NULL	CX601980	NULL	0.580560854	0.036525541
NULL	CD536656	NULL	-0.941443808	0.013727597
NULL	CX604893	NULL	-0.898406093	0.028844396
NULL	DN508075	NULL	-0.886875638	0.024081816
NULL	CD465327	NULL	-0.753356222	0.039195307
NULL	BI395121	NULL	-0.743151355	0.029328222
NULL	CX601278	NULL	-0.736027477	0.04764657
NULL	CD536578	NULL	-0.699730642	0.010759686
NULL	XM_001488796	NULL	-0.684030434	0.023101672
NULL	DN509542	NULL	-0.642509166	0.021201315
NULL	XM_001496183	XP_001496233	-0.641376662	0.031447975
NULL	DN510541	NULL	-0.633703324	0.014361923
NULL	DN510227	NULL	-0.627038981	0.028426111
NULL	CX601417	NULL	-0.61573787	0.024288442
NULL	XM_001493134	NULL	-0.600043106	0.022123532
NULL	XM_001495803	NULL	-0.597661713	0.009454129
NULL	CX599004	NULL	-0.586407875	0.011892391
NUP188	XM_001499796	XP_001499846	0.786697972	0.006083986
ODZ2	XM_001503295	NULL	-0.637396603	0.012974163
ODZ3	XM_001492508	NULL	-0.614633097	0.005181163
OR10J5	XM_001490887	XP_001490937	0.848465468	0.045157337
OR12D2	XM_001490772	XP_001490822	0.879570821	0.020617748
OR1F1	XM_001499014	XP_001499064	-0.884661036	0.033155361
OR1J4	XM_001501342	NULL	-1.004656597	0.012195071
OR4F16	XM_001502031	XP_001502081	-0.605456222	0.003857688
OR56B4	XM_001504553	XP_001504603	-0.807771968	0.012146897

Table D-12 Continued

Gene Symbol	NCBI accession	RefSeq accession	Log fold change	Pvalue
OR6C2	XM_001490627	XP_001490677	0.878366666	0.029304792
OR8U8	XM_001496063	XP_001496113	-0.711278124	0.047814059
ORM2	XM_001488131	XP_001488181	-0.593239239	0.039846115
OSAP	XM_001502525	XP_001502575	0.726329478	0.003915527
OSBPL10	XM_001490635	XP_001490685	0.76306215	0.023420877
OSGIN2	XM_001488667	XP_001488717	-0.876652222	0.003632846
P4HB	XM_001489491	XP_001489541	1.041391575	0.040982584
PAK4	XM_001497143	XP_001497193	0.724795018	0.011218107
PALB2	XM_001501015	XP_001501065	0.612857168	0.047154537
PARD6A	XM_001498013	XP_001498063	-1.037912625	0.044060499
PARP3	XM_001492912	XP_001492962	-0.728794027	0.032851176
PCSK1	XM_001504608	XP_001504658	0.611083241	0.035501845
PHACTR3	XM_001491669	NULL	0.982147052	0.01349672
PHF11	XM_001489978	NULL	-0.670738979	0.030489716
PIB5PA	XM_001497367	NULL	-1.297378836	0.015636553
PKIA	NULL	NULL	0.633595191	0.022771772
POGK	XM_001490105	XP_001490155	0.789127381	0.019917355
POLR2F	XM_001501259	XP_001501309	0.800020693	0.031755044
PREP	NULL	NULL	-0.624165568	0.006745959
PRKCE	XM_001499053	XP_001499103	1.107485626	0.039123203
PRND	NM_001091537	NULL	0.725009179	0.006748466
PRR15	XM_001500279	XP_001500329	0.665518938	0.026036314
PSCD4	XM_001499462	XP_001499512	1.108935856	0.010518118
PSMC1	NULL	NULL	1.063183499	0.04108997
PSMD3	XM_001500781	NULL	1.08349634	0.041542667
PTMA	XM_001498434	XP_001498484	0.914568693	0.047426787
RAB2B	XM_001505161	XP_001505211	1.093991374	0.031954427
RAD9A	XM_001491881	XP_001491931	-0.911419243	0.017405289
RAPGEF2	XM_001498831	XP_001498881	0.697129525	0.019372894
RASAL2	XM_001498432	XP_001498482	-0.650247801	0.014760315
RASD2	XM_001499945	XP_001499995	0.658440472	0.021030883
RASSF8	XM_001502654	XP_001502704	0.688682605	0.013211244
RCE1	XM_001496896	XP_001496946	-0.643550477	0.018921751
REC8	XM_001489288	XP_001489338	1.155040235	0.027187404
RENBP	XM_001491837	XP_001491887	-0.629686183	0.004747208
RGS19	XM_001495344	XP_001495394	0.581309328	0.030669808
RGS20	XM_001488849	XP_001488899	0.835246916	0.038745333
RNF167	XM_001504749	XP_001504799	0.629410096	0.032014304
ROR1	XM_001499661	XP_001499711	1.161436143	0.026477321

Table D-12 Continued

Gene Symbol	NCBI accession	RefSeq accession	Log fold change	Pvalue
RPL37	BI961238	XP_001499005	0.808632353	0.02006983
RPL4	CD467413	NULL	0.839683603	0.029757763
RPS25	XM_001503063	XP_001503113	-0.601461207	0.026748125
RPS3A	NULL	NULL	-0.693396543	0.04890535
RTKN2	XM_001502301	XP_001502351	1.009846358	0.047123126
S100A11	BI961023	XP_001493486	0.872119914	0.047026034
S100A2	CX598422	XP_001494717	-0.743181373	0.021979447
S100A5	XM_001493675	XP_001493725	0.8299638	0.037744978
S100A8	XM_001493507	XP_001493557	0.790055028	0.021918481
S100A9	XM_001493530	XP_001493580	0.884664501	0.019256606
SAP130	XM_001504933	NULL	0.826106608	0.010547452
SCN4B	XM_001502720	XP_001502770	0.753207203	0.025524634
SDC2	CX605958	NULL	-0.684257372	0.048945866
SDCCAG1	NULL	NULL	0.583550376	0.010404048
SDCCAG8	XM_001491918	XP_001491968	0.695236629	0.032847543
SDF2L1	XM_001493091	XP_001493141	0.59351772	0.039286147
SEMA6D	XM_001502470	NULL	-1.593190504	0.033031932
SETD8	XM_001492985	XP_001493035	-0.788515138	0.014593012
SF3B2	XM_001495191	XP_001495241	0.874265847	0.023223542
SGCD	XM_001503564	XP_001503614	0.590153597	0.009802713
SGPL1	XM_001502792	XP_001502842	-0.692512775	0.007172296
SIM2	XM_001493207	NULL	1.023350646	0.008149913
SIN3A	XM_001491348	XP_001491398	-0.614358146	0.015511108
SIX4	XM_001497919	XP_001497969	0.5806122	0.012577787
SLC23A1	XM_001497642	XP_001497692	0.899562588	0.029880842
SLC25A20	XM_001494717	XP_001494767	0.707175904	0.010108105
SLC35F3	XM_001493414	XP_001493464	1.179668925	0.002671981
SLC41A3	NULL	NULL	-0.594064702	0.037423476
SLC7A6OS	XM_001499093	XP_001499143	-0.644136729	0.008809386
SLCO1B3	XM_001498036	XP_001498086	-0.973073255	0.008115858
SLITRK6	XM_001490198	XP_001490248	0.622511404	0.043503366
SLMAP	XM_001489585	XP_001489635	-1.332462281	0.046019981
SMOC2	NULL	NULL	0.647352618	0.045213086
SMTNL1	XM_001497023	XP_001497073	0.681229626	0.049140476
SMYD1	XM_001497775	NULL	0.595799971	0.013001788
SNAI2	XM_001488056	XP_001488106	-0.651183949	0.017180648
SNAI3	XM_001487991	XP_001488041	0.749377969	0.02776628
SNCA	XM_001496904	XP_001496954	-0.65243193	0.032176449
SPECC1	XM_001504877	XP_001504927	0.953195401	0.031960627

Table D-12 Continued

Gene Symbol	NCBI accession	RefSeq accession	Log fold change	Pvalue
SPON2	XR_035777	NULL	0.729540402	0.006776469
SS18L2	XM_001501559	XP_001501609	1.202744658	0.044401513
TAL2	XM_001493399	XP_001493449	1.295734395	0.016481736
TBC1D9	XM_001501060	XP_001501110	0.94412618	0.02363108
TBL3	XM_001498025	XP_001498075	-0.673649982	0.011412327
TDRD7	XM_001495552	XP_001495602	0.710363783	0.02456347
TDRD9	XM_001492897	XP_001492947	0.826804023	0.017164146
TERF1	XM_001492421	XP_001492471	0.968671681	0.033068104
TFDP1	XM_001498959	XP_001499009	0.972179037	0.017469466
TIFA	XM_001503466	XP_001503516	0.774908902	0.020021701
TLK2	XR_036378	NULL	-0.654228258	0.011999707
TLN2	XM_001500242	XP_001500292	0.581905381	0.02557653
TMEM189-UBE2V1	XM_001501224	XP_001501274	0.707575887	0.00416749
TMEM29B	XM_001494608	XP_001494658	-0.581161606	0.038656476
TMEM69	XM_001495815	XP_001495865	0.737446096	0.043788024
TMOD1	XM_001504126	XP_001504176	1.35837228	0.004130751
TOMM20	CX605644	XP_001491687	0.979154088	0.038537021
TPM1	NULL	NULL	0.710815839	0.021819587
TPPP3	CX596053	XP_001496480	-0.72741117	0.039437277
TRAF3IP2	XM_001504045	XP_001504095	1.062069857	0.015251821
TRIM50	XM_001504491	XP_001504541	0.774928706	0.016373599
TRPM7	DQ329355	NULL	-0.630754677	0.013403424
TRUB1	XM_001495127	XP_001495177	0.735161042	0.010254325
TRY1	XM_001499280	NULL	0.608030767	0.018101239
TTC30B	XM_001500596	NULL	-0.664177063	0.031612473
TTC35	XM_001494974	XP_001495024	0.658176182	0.028704898
TTLL9	XM_001498331	XP_001498381	0.806528387	0.009523638
TXNDC6	XM_001496991	NULL	-0.908928625	0.000851235
UBASH3B	CD468821	NULL	-0.602108777	0.029358745
UBR5	XR_036042	NULL	0.692622189	0.044677523
UQCR	DN508330	NULL	0.738552307	0.025632613
USP4	XM_001497962	XP_001498012	-0.687467919	0.017587134
VAMP7	XM_001498227	XP_001498277	1.5621274	0.017048316
VPS37A	XM_001488521	XP_001488571	-0.617532472	0.028391898
VTCN1	NULL	NULL	0.733444514	0.048639587
VWA2	XM_001498009	XP_001498059	-1.303048746	0.003579255
WBP4	XM_001502215	NULL	0.637576061	0.046379065
WDR81	XM_001502333	XP_001502383	1.027664638	0.032012018
WWP1	XM_001488288	XP_001488338	-0.692367224	0.018650042

Table D-12 Continued

Gene Symbol	NCBI accession	RefSeq accession	Log fold change	Pvalue
XBP1	DN507369	NULL	1.05872584	0.021922233
XRN2	XM_001489295	XP_001489345	0.653526296	0.022542424
YPEL2	XM_001503736	XP_001503786	-0.833039127	0.036964088
YTHDF2	XM_001500333	XP_001500383	0.779949833	0.010022103
ZBTB32	XM_001492255	XP_001492305	0.593337827	0.03327712
ZC3H12D	XM_001495556	XP_001495606	-0.785748368	0.008716475
ZC3H7B	XM_001500311	XP_001500361	0.964421484	0.035326523
ZCCHC3	XM_001497984	XP_001498034	0.584494521	0.049137829
ZDHHC20	XM_001489587	XP_001489637	0.61651159	0.006563921
ZER1	XM_001500385	XP_001500435	0.770838104	0.020572734
ZFP3	XM_001504742	XP_001504792	1.045650043	0.014217491
ZFR	XR_036244	NULL	0.609710371	0.040616811
ZMAT3	XM_001494925	XP_001494975	-0.606974118	0.027902822
ZNF256	XM_001493473	NULL	0.898464666	0.03398908
ZNF260	XM_001494454	NULL	0.760864477	0.036507009
ZNF420	XM_001497154	XP_001497204	1.459606556	0.012555189
ZNF510	XM_001493815	XP_001493865	0.795028472	0.049739909
ZNF513	XM_001500900	XP_001500950	0.858573178	0.004841773
ZNF518B	XM_001500984	XP_001501034	0.771606816	0.033862505
ZNF543	XM_001492239	XP_001492289	0.900710034	0.048871795
ZNF554	XM_001492592	XP_001492642	0.836045963	0.038032725
ZNF662	XM_001497214	XP_001497264	0.737492596	0.017533937
ZNF709	XM_001489853	NULL	1.267656589	0.013208462
ZNF783	XM_001493065	XP_001493115	0.733980466	0.048341927

Table D-13: List of differentially expressed genes (pvalue <0.05 and fold change cut off of 1.5) between the affected and the unaffected foals from nasal epithelium at week-2.

Gene Symbol	NCBI accession	RefSeq accession	Log fold change	Pvalue
ACD	XR_036166	NULL	0.656969546	0.018694184
ADAM12	XM_001490047	XP_001490097	-0.619617799	0.022896857
AFTPH	XM_001494716	XP_001494766	0.908173221	0.04711376
AGR3	XM_001496142	XP_001496192	-1.094971903	0.02255331
AHSA1	XM_001493748	XP_001493798	0.873321819	0.000918768
AMOTL1	XM_001497365	XP_001497415	1.195381118	0.001040596
AMPD1	NULL	NULL	-0.725576546	0.04035028
ANKRD38	XM_001500075	XP_001500125	0.628376914	0.017075064

Table D-13 Continued

Gene Symbol	NCBI accession	RefSeq accession	Log fold change	Pvalue
ARHGEF16	XM_001497662	XP_001497712	0.719557642	0.035773593
ASIP	XM_001501139	XP_001501189	0.664137957	0.010371725
ATCAY	XM_001493413	XP_001493463	0.631517924	0.00796608
ATP13A2	XM_001488576	XP_001488626	0.638108153	0.039016004
B3GALNT1	XM_001493799	XP_001493849	-0.587269304	0.033200782
BAG3	XM_001496279	XP_001496329	0.782158388	0.04752626
BANK1	XM_001497747	XP_001497797	0.771094113	0.002766097
BC37295_3	XM_001491403	NULL	0.642002578	0.011480864
BCMO1	XM_001499593	XP_001499643	0.779476158	0.023487728
BPIL3	XM_001498600	XP_001498650	0.689217207	0.014628253
BSND	XM_001488199	XP_001488249	0.670074336	0.026111785
C10orf72	XM_001494453	XP_001494503	0.79770732	0.041200056
C11orf49	XR_035773	NULL	1.780417817	0.046457675
C14orf102	XM_001494144	XP_001494194	0.680739829	0.041294352
C17orf49	XM_001503003	XP_001503053	0.598204584	0.015248492
C1orf31	XM_001493392	NULL	0.721282054	0.041180889
C1orf50	XM_001497377	XP_001497427	0.874358162	0.001560545
C1orf86	XM_001495164	XP_001495214	0.746449545	0.020649018
C2orf28	XM_001502475	XP_001502525	0.63399582	0.013244341
C3orf14	XM_001490221	NULL	0.628348454	0.030751388
C6orf162	XM_001503730	XP_001503780	0.974777129	0.010378135
C9orf97	XM_001495421	XP_001495471	0.603941027	0.02294143
CAMTA1	NULL	NULL	1.168952127	0.028339629
CAMTA2	XM_001504745	XP_001504795	0.844246654	0.01884976
CAPN5	XM_001494686	XP_001494736	-0.842935825	0.032196214
CAPZA3	XM_001501974	XP_001502024	1.062774531	0.048241517
CCDC33	XM_001494109	XP_001494159	0.591554125	0.04033182
CCDC97	XM_001500237	XP_001500287	1.656412092	0.008032849
CCKBR	XM_001504583	XP_001504633	1.219772332	0.015785376
CD276	XM_001493661	XP_001493711	0.714361939	0.024061176
CDC20	XM_001498579	XP_001498629	-0.581747215	0.022992873
CDC42BPB	XM_001491699	XP_001491749	0.644675308	0.01187746
CHRDL1	XM_001489536	XP_001489586	0.793939665	0.029493466
CKM	XM_001502522	XP_001502572	0.692622098	0.016631303
CNKSR2	XM_001491941	XP_001491991	-0.760363292	0.016711729
CNN3	NULL	NULL	-0.808151628	0.004526051
CNN3	NULL	NULL	-0.673697543	0.003440911
CNTNAP5	XM_001489205	XP_001489255	0.829714632	0.027417868

Table D-13 Continued

Gene Symbol	NCBI accession	RefSeq accession	Log fold change	Pvalue
COL6A3	CX604376	NULL	-0.655606591	0.018701085
CPEB1	XM_001498253	XP_001498303	-0.581684487	0.035684408
CPN2	XM_001498855	NULL	-0.705079818	0.027046292
CUGBP1	XM_001492089	XP_001492139	0.891481366	0.025053462
DBNDD1	XM_001488503	XP_001488553	-0.78061961	0.030383164
DCUN1D1	XM_001496812	XP_001496862	1.081069094	0.037651757
DEFB4	AY170305	NP_001075356	-0.790344939	0.045741498
DGAT2	XM_001495302	XP_001495352	0.876356484	0.020391007
DHDH	XM_001489811	XP_001489861	1.506925571	0.031187588
DOK7	XM_001488918	XP_001488968	1.064184382	0.030979589
EEF1A1	NULL	NULL	-0.726116284	0.033107328
EID3	XM_001497826	XP_001497876	0.712089006	0.015418257
EPHA1	XM_001490060	XP_001490110	-0.757549202	0.044929722
EXOSC1	DN505643	XP_001501548	1.772457037	0.015509273
EXOSC5	XM_001500340	XP_001500390	0.610663343	0.007419564
F3	XM_001491449	XP_001491499	0.794775254	0.023084703
FAM120A	XM_001490989	XP_001491039	0.933395044	0.046397106
FAM120B	XM_001488467	XP_001488517	-0.817638187	0.028832059
FAM127A	XM_001487969	XP_001488019	-0.678659967	0.023849592
FAM12B	XM_001505142	NULL	-0.759241679	0.006815165
FAM149A	XM_001502897	XP_001502947	0.664592976	0.026874898
FAM82C	XM_001501075	XP_001501125	-0.738568611	0.044353096
FAM89A	NULL	NULL	0.948760061	0.012022614
FAU	BM781413	NULL	-0.599428204	0.04079038
FBRS	XR_036371	NULL	0.809134518	0.008696324
FIGF	XM_001489992	XP_001490042	0.713725285	0.012106484
FOXN4	XM_001496911	XP_001496961	0.961532416	0.041899639
GABRB3	XM_001493048	XP_001493098	1.013628019	0.000715631
GALE	XM_001504206	XP_001504256	0.791711508	0.028331814
GALNT2	XM_001496209	XP_001496259	0.667694251	0.022322351
GAPDH	XR_036361	NULL	0.763380582	0.022081426
GLG1	CX604369	NULL	0.706418368	0.034582856
GLIS2	XM_001502268	XP_001502318	0.636237359	0.028925265
GLT6D1	XM_001498210	XP_001498260	-0.824301304	0.036094321
GLUL	NULL	NULL	-0.94149975	0.039562351
GNG3	XM_001494898	XP_001494948	0.872689405	0.027141699
GNPDA1	XM_001503958	XP_001504008	-1.595394185	0.038741905
GORASP2	XM_001498298	XP_001498348	0.581179652	0.038388617

Table D-13 Continued

Gene Symbol	NCBI accession	RefSeq accession	Log fold change	Pvalue
GPATCH1	XM_001488716	XP_001488766	0.699111686	0.030861246
GTF2IRD2B	XM_001494135	XP_001494185	-0.667976574	0.035189665
GYPC	XM_001489109	NULL	0.645756885	0.009331151
HFE	XM_001497982	XP_001498032	0.870147155	0.046083861
HMGB2	NULL	NULL	-0.758829542	0.007560159
HNRNPA1	XM_001501027	XP_001501077	0.630030488	0.013386394
HNRPDL	XM_001491342	XP_001491392	0.841528649	0.010287355
HOXB1	XM_001499152	XP_001499202	-0.841899838	0.013512054
HSDL1	XM_001502194	NULL	-0.644128246	0.014358868
HTR2C	XM_001488512	XP_001488562	1.551624544	0.041571962
ID3	XM_001504221	XP_001504271	0.805536457	0.032631423
IGSF21	XM_001498665	XP_001498715	1.401863459	0.028204268
ISLR	XM_001493196	XP_001493246	0.632621359	0.012577167
ITGA5	XM_001504571	XP_001504621	0.911743274	0.010580773
KIF2C	XM_001496793	XP_001496843	0.717088291	0.003601344
KLHDC3	DN506485	NULL	-0.759397246	0.029141841
KRT33A	XM_001497042	XP_001497092	0.801589461	0.024375794
LAS1L	XM_001496190	XP_001496240	1.328026819	0.023914756
LBX1	XM_001499876	XP_001499926	0.762530574	0.018170101
LDHD	XM_001501313	XP_001501363	0.808678565	0.013161812
LDOC1L	XM_001488133	XP_001488183	-0.986694221	0.034919604
LILRA6	XM_001489385	XP_001489435	0.946966896	0.005552957
LIN54	XM_001494255	XP_001494305	0.766460653	0.031548451
LMNA	XM_001499921	XP_001499971	0.744185488	0.027439804
LOC389117	XM_001494114	XP_001494164	1.329158083	0.015971943
LOC390667	XM_001497697	XP_001497747	-2.702098418	0.016561616
LOC440829	XM_001500377	XP_001500427	1.147860523	0.007954244
LOC440956	XM_001493055	XP_001493105	0.902521159	0.012143395
LOC442461	XM_001488900	XP_001488950	1.104987082	0.026010156
LOC642592	NULL	NULL	0.911915683	0.008847904
LOC643596	XM_001492183	NULL	0.863246101	0.012415253
LOC645161	NULL	NULL	0.594646919	0.041700124
LOC730855	AF345995	NULL	1.286287529	0.000652782
LOC731062	XM_001492626	NULL	1.047785019	0.043590934
LPIN1	XM_001502170	XP_001502220	0.715966416	0.049034183
LRRC20	XM_001503727	XP_001503777	1.06487927	0.001289511
LRRTM4	XM_001498361	XP_001498411	1.021960189	0.016392528
MAEA	XR_035780	NULL	0.581087868	0.045297113

Table D-13 Continued

Gene Symbol	NCBI accession	RefSeq accession	Log fold change	Pvalue
MAGEA10	XM_001491290	XP_001491340	1.150791618	0.02594001
MED31	XM_001502782	XP_001502832	0.653167586	0.008516081
MIB1	NULL	NULL	-0.829371697	0.018482395
MPFL	XM_001497303	NULL	0.769264597	0.016968495
MRPL49	CD467563	XP_001492066	1.159126002	0.027065692
MTAP	XM_001495991	XP_001496041	0.913009578	0.014401546
MVD	XM_001488033	XP_001488083	0.613940542	0.028237542
MXRA8	NULL	NULL	0.805959487	0.002893374
MYO19	XM_001501155	NULL	0.742073563	0.035716242
NCDN	XM_001503678	XP_001503728	-0.947536281	0.028235898
NDUFB3	XM_001503625	XP_001503675	-0.698556061	0.033779904
NHSL2	XM_001487942	XP_001487992	-0.713666543	0.027646106
NKAIN3	XM_001496129	XP_001496179	-0.73922743	0.049580039
NKRF	XM_001491762	XP_001491812	0.635685834	0.031128646
NKX2-2	XM_001489173	XP_001489223	0.936666141	0.034628089
NPPA	X58563	NP_001075970	-0.630541552	0.023569862
NUBPL	XM_001490020	XP_001490070	-0.623257693	0.008816077
NUDT19	XM_001489815	NULL	0.688263013	0.017058818
NULL	CX605888	NULL	-0.953804151	0.022598933
NULL	XM_001503290	XP_001503340	-0.899785605	0.029315514
NULL	BI395121	NULL	-0.835740515	0.009234624
NULL	CD465149	NULL	-0.810753986	0.003955582
NULL	CX604514	NULL	-0.739823271	0.004129966
NULL	CX599268	NULL	-0.726975078	0.011751645
NULL	CX603838	NULL	-0.724792919	0.037720918
NULL	CX603822	NULL	-0.719007561	0.001339616
NULL	CX593567	NULL	-0.709427906	0.017311851
NULL	XM_001497660	NULL	-0.68855117	0.0119083
NULL	CD470553	NULL	-0.679422914	0.023455107
NULL	CX594584	NULL	-0.674299114	0.041954976
NULL	DN508935	NULL	-0.662010972	0.044621292
NULL	CX601639	NULL	-0.660646952	0.015321317
NULL	CX603281	NULL	-0.658146559	0.010347549
NULL	DN509644	NULL	-0.633744819	0.013981684
NULL	CX595027	NULL	-0.628233604	0.013732771
NULL	DN506649	NULL	-0.594185602	0.027833019
NULL	CX603737	NULL	-0.584074704	0.010601869
NULL	CX598905	NULL	-0.583382284	0.043177823

Table D-13 Continued

Gene Symbol	NCBI accession	RefSeq accession	Log fold change	Pvalue
NULL	XM_001497156	NULL	1.921141825	0.004280134
NULL	DN507748	NULL	1.402291407	0.020693008
NULL	XR_035772	NULL	1.349384445	0.012081833
NULL	XR_035972	NULL	0.988873844	0.048896061
NULL	CX600791	NULL	0.889209952	0.012557901
NULL	CX602835	NULL	0.888998812	0.028908699
NULL	CX595758	NULL	0.872711966	0.01510688
NULL	XM_001491549	XP_001491599	0.828461917	0.015116816
NULL	CX605699	NULL	0.822898579	0.008050584
NULL	DN507307	NULL	0.774029512	0.011063167
NULL	XM_001497251	NULL	0.704061973	0.030681865
NULL	DN509184	NULL	0.692498187	0.009988585
NULL	DN508765	NULL	0.689267067	0.036613834
NULL	DN504005	NULL	0.62871241	0.025938747
NULL	CX604280	NULL	0.620963014	0.024786153
NULL	XM_001503948	NULL	0.61980628	0.021365115
NULL	DN508760	NULL	0.602086688	0.039617624
NULL	CD465531	NULL	0.597759475	0.040196957
NULL	XM_001488352	NULL	0.594957961	0.029610242
OBP2B	XM_001502876	NULL	0.611564524	0.043319422
OPA3	DN509316	NULL	1.032244761	0.034580764
OR10H3	XM_001499453	NULL	-0.814285673	0.025020519
OR1A1	XM_001502600	XP_001502650	-0.616293085	0.008761183
OR2S2	XM_001504440	XP_001504490	-0.725505525	0.004894745
OR2T33	XM_001498999	NULL	0.609453994	0.014161985
OR52A5	XM_001498335	XP_001498385	0.642048706	0.046172995
OR52J3	XM_001498512	NULL	-2.88423699	0.03368168
OR5A1	XM_001497317	NULL	1.488559818	0.027748352
OR6C2	XM_001490665	XP_001490715	-1.434159465	0.020493842
OR9Q2	XM_001497753	XP_001497803	0.642949937	0.023980237
OTUB1	XM_001489294	XP_001489344	0.829445096	0.006281345
P4HA3	XM_001495901	XP_001495951	0.818038065	0.015979802
PAFAH1B3	NULL	NULL	-0.67690706	0.010015666
PAPPA	XM_001487931	XP_001487981	-0.597673972	0.04328644
PARD6A	XM_001498013	XP_001498063	-0.584073733	0.037715939
PBX1	XM_001493240	XP_001493290	0.59157924	0.013529476
PDE4DIP	XR_036200	NULL	0.699727199	0.006466326
PDK2	NULL	NULL	0.65478013	0.041190275

Table D-13 Continued

Gene Symbol	NCBI accession	RefSeq accession	Log fold change	Pvalue
PEX12	XM_001503933	XP_001503983	0.719585685	0.033596403
PGAM2	XM_001495636	XP_001495686	1.273323829	0.044945218
PIM1	XM_001500225	XP_001500275	0.782230297	0.047385922
PLAUR	XM_001501873	XP_001501923	0.699689215	0.028757991
PLEKHB1	XM_001496117	XP_001496167	1.087380054	0.044336809
PNMT	XM_001501154	XP_001501204	0.6539197	0.021327398
PNOC	XM_001493120	XP_001493170	0.785972633	0.013901641
PODN	XM_001493252	XP_001493302	0.840612875	0.01599106
POU4F2	XM_001501801	XP_001501851	1.426058849	0.039233121
PPP4R2	XM_001493684	XP_001493734	-0.974287137	0.024015877
PRPF8	XM_001504332	XP_001504382	0.976827755	0.038569979
PRR16	XM_001504547	XP_001504597	0.862643677	0.016402338
PRRC1	XM_001504480	XP_001504530	1.296642935	0.007066774
PSMA7	XM_001491034	XP_001491084	-0.622297366	0.049949045
PTH2	XM_001491631	XP_001491681	0.779336798	0.007113905
QDPR	NULL	NULL	-0.884611783	0.042327943
RAB19	XM_001498572	XP_001498622	0.730707392	0.010412718
RAB3IP	XM_001494486	XP_001494536	-0.611839451	0.026279794
RAB7L1	XM_001490736	XP_001490786	0.812919323	0.018331762
RAD54L2	XM_001495092	XP_001495142	0.823111858	0.017219693
RAP2C	XM_001491906	XP_001491956	0.63498104	0.019195347
RASL11B	XM_001493834	XP_001493884	-0.710382722	0.00692196
RGS22	XM_001493094	XP_001493144	-0.660077295	0.025979078
RLBP1L1	XM_001496222	XP_001496272	-0.80206447	0.003081502
RNF141	XM_001504919	XP_001504969	-1.006188034	0.034746636
RNF208	XM_001491514	XP_001491564	0.769170826	0.046097862
RPL24	DN504010	XP_001503467	-0.628381915	0.014017953
RUNX3	XM_001501145	XP_001501195	1.00710975	0.048311913
RWDD2B	XM_001499640	XP_001499690	0.773181336	0.025988073
RY1	CX599215	XP_001490747	-0.757533304	0.002943676
S100A11	BI961023	XP_001493486	0.934188482	0.007838049
SAP130	XM_001504933	NULL	1.063359722	0.029982418
SCGB1A1	XM_001487825	XP_001487875	0.748680398	0.025212101
SCUBE1	XM_001500812	XP_001500862	0.987192781	0.016081166
SCYE1	XM_001503150	XP_001503200	0.689763201	0.024351772
SECISBP2	XM_001493820	XP_001493870	0.831585086	0.024694127
SERPINB10	CD465653	NULL	0.770956657	0.022517937
SERPINB2	XM_001491808	NULL	0.779884618	0.004768348

Table D-13 Continued

Gene Symbol	NCBI accession	RefSeq accession	Log fold change	Pvalue
SEZ6L2	XM_001496356	XP_001496406	0.652943258	0.023510909
SH2B3	XM_001491066	XP_001491116	0.600097682	0.031979584
SH3BGR	XM_001491925	NULL	-0.581664834	0.020954076
SHB	XM_001496517	XP_001496567	-0.822715528	0.049587963
SLC31A2	XM_001488681	XP_001488731	-0.586337278	0.049270301
SLC6A12	XM_001490499	XP_001490549	-1.732852539	0.018632826
SMARCA5	XM_001502026	XP_001502076	0.818034782	0.040482641
SNTA1	XM_001498897	XP_001498947	0.8294296	0.028040237
SPCS1	XM_001501306	NULL	0.680129218	0.027177819
STAT3	XM_001494631	XP_001494681	0.887247365	0.000743008
SVOPL	XM_001496950	XP_001497000	0.669968544	0.039739242
TANC1	XM_001492390	XP_001492440	0.65394972	0.020851928
TAP1	XM_001496035	XP_001496085	0.739352332	0.019165206
TATDN2	XM_001493683	XP_001493733	-0.640102262	0.031234213
TCF7L1	XM_001497480	XP_001497530	0.655375069	0.02066466
TCTA	XM_001497739	NULL	0.897418245	0.038317218
TIGD3	XM_001492759	XP_001492809	0.662665139	0.017670498
TIMM17B	CX602842	XP_001494391	0.71519637	0.02189663
TMEM16B	XM_001495269	NULL	0.820285481	0.039293569
TMEM183A	XM_001495801	XP_001495851	-0.720554342	0.027557868
TMEM82	XM_001489391	XP_001489441	0.675173017	0.015266721
TMOD1	XM_001504126	XP_001504176	1.350824501	0.00053532
TPD52L3	XM_001492482	XP_001492532	-0.846619691	0.03142352
TREH	XM_001500995	XP_001501045	0.608711692	0.018626315
TRIM55	XM_001494869	XP_001494919	0.601147667	0.042591963
TSGA13	XM_001498542	XP_001498592	0.684163704	0.041572459
TSR1	XM_001504361	XP_001504411	0.673223149	0.028278009
UBA7	XM_001497081	XP_001497131	0.798680323	0.0310785
VKORC1	DN507704	XP_001500839	-0.803460257	0.01789172
VPREB1	XM_001502296	XP_001502346	0.787349107	0.044326592
WDR36	XM_001503571	XP_001503621	-1.227377559	0.016543822
WDR45	XM_001495045	XP_001495095	-0.608004918	0.047830193
WFIKKN2	XM_001499780	XP_001499830	0.68420186	0.029953197
YARS	XM_001499806	XP_001499856	0.649987292	0.033156852
YY1	NULL	NULL	-0.797186972	0.004030764
ZADH2	XM_001493715	XP_001493765	0.957242907	0.007660384
ZDHHC1	XM_001496451	XP_001496501	0.788722704	0.024037043
ZNF280C	XM_001491635	XP_001491685	0.902762058	0.002149491

Table D-13 Continued

Gene Symbol	NCBI accession	RefSeq accession	Log fold change	Pvalue
ZNF518B	XM_001500984	XP_001501034	0.763095013	0.00740351
ZNF613	XM_001495866	XP_001495916	0.858922683	0.029197421
ZNF709	XM_001496676	NULL	0.604876427	0.030614397
ZNF768	XM_001496047	XP_001496097	1.029166026	0.038296502
ZNF793	XM_001493662	XP_001493712	0.887183716	0.027163284
ZSCAN21	XM_001498385	XP_001498435	1.338258736	0.038262999

Table D-14: List of differentially expressed genes (pvalue <0.05 and fold change cut off of 1.5) between the affected and the unaffected foals from nasal epithelium at week-4.

Gene Symbol	NCBI accession	RefSeq accession	Log fold change	Pvalue
A1CF	XM_001501691	XP_001501741	0.832646485	0.008475736
ABT1	XM_001505089	XP_001505139	-1.340956152	0.028058504
ACAA1	XM_001488559	XP_001488609	-0.599259628	0.021954768
ADAMTSL3	XM_001497774	XP_001497824	0.673192244	0.020793411
ALLC	XM_001502861	XP_001502911	-0.629860172	0.0399707
ANKRD24	XM_001494451	NULL	-0.766840939	0.042867721
APOL6	XM_001499112	XP_001499162	0.927984486	0.021667634
ARFRP1	XM_001494418	NULL	-0.675858211	0.024028676
ARL13A	XM_001492492	XP_001492542	-0.758983522	0.029237818
ARL6IP1	CD468299	NULL	0.732932792	0.036965874
ATP1A1	NM_001114532	NULL	-0.716243753	0.046996329
ATP6V1E2	XM_001498882	XP_001498932	-0.639625905	0.038221582
AUP1	XR_036315	NULL	-0.677871977	0.036884568
BARHL2	XM_001493713	XP_001493763	-0.707829186	0.010255616
C11orf17	XM_001504906	XP_001504956	0.703475678	0.020682066
C11orf52	NULL	NULL	-0.865026707	0.005671981
C12orf4	NULL	NULL	0.619639222	0.026739291
C13orf33	XM_001495031	XP_001495081	0.687821247	0.024792286
C17orf83	XM_001503077	XP_001503127	-0.610318513	0.047004149
C1orf121	XM_001493908	XP_001493958	0.67561054	0.024732358
C1orf35	XM_001493264	NULL	-0.649411995	0.015091344
C21orf91	XM_001500343	XP_001500393	0.582694424	0.028265653
C5orf15	DN510151	NULL	-1.042525299	0.033545177
C5orf40	XM_001503539	XP_001503589	0.616200431	0.02263458
C6orf221	XM_001498118	XP_001498168	0.815726782	0.003178694

Table D-14 Continued

Gene Symbol	NCBI accession	RefSeq accession	Log fold change	Pvalue
C7orf28A	XM_001493987	XP_001494037	-0.874362548	0.032756702
C9orf85	XM_001489559	XP_001489609	0.725317641	0.00690778
CALM3	XM_001493222	NULL	0.770740595	0.009438996
CAPN1	DN506160	NULL	-0.94158798	0.007713713
CCNG1	XM_001488405	XP_001488455	0.67734665	0.048421213
CCNG2	XM_001491674	XP_001491724	-1.241657362	0.018497741
CD33	XM_001496873	XP_001496923	-0.648887819	0.010507107
CD3G	XM_001502838	XP_001502888	1.730160072	0.027925442
CHST6	XM_001498821	XP_001498871	1.374623399	0.00164069
CLCA1	AY524856	NP_001075268	-1.045824705	0.029654985
CLDN3	XR_036494	NULL	-0.645549497	0.048170879
CMBL	XM_001501583	XP_001501633	-0.728143213	0.012008076
COL28A1	XM_001494969	XP_001495019	-0.753460679	0.003954833
COX7A1	XM_001492779	XP_001492829	0.596383149	0.03175034
COX7B	CX594711	NULL	-0.953208059	0.01077352
CYB561D2	XM_001495830	XP_001495880	0.651061822	0.049786506
CYB5A	CX594722	XP_001493485	-1.037358425	0.010087741
CYP11B2	XM_001505011	NULL	-0.900442413	0.023597412
CYP2C19	XM_001502162	XP_001502212	0.723343608	0.034332803
CYP2F1	XM_001498170	XP_001498220	-0.647047136	0.045941176
DALRD3	XM_001498501	XP_001498551	-0.885722486	0.046784999
DCK	XM_001489225	XP_001489275	0.594122721	0.030622224
DGCR2	NULL	NULL	0.998980412	0.011496334
DHDH	XM_001489811	XP_001489861	-0.912698794	0.002607083
DMGDH	XM_001503911	XP_001503961	-0.58124661	0.012318285
DPP6	XM_001504680	XP_001504730	0.639589149	0.038518855
DRG1	XM_001496885	NULL	-0.790989946	0.012829095
EBF2	XM_001493967	XP_001494017	0.680123254	0.030277644
EGFL6	XM_001489342	XP_001489392	-0.71057822	0.027662423
ENDOGL1	XM_001488144	XP_001488194	-1.096294216	0.032538391
ENO1	XM_001494862	XP_001494912	-0.665318417	0.021811995
ENPP1	CX604920	NULL	0.837131364	0.017560686
EPHA2	XM_001488739	XP_001488789	-0.5850366	0.048357932
EPM2A	XM_001496670	XP_001496720	0.619608961	0.021463107
ERC1	XM_001491831	XP_001491881	-0.886302539	0.013715135
EXT1	XM_001496434	XP_001496484	-1.075444222	0.013044512
FAIM	XM_001495529	XP_001495579	-0.661017724	0.017062522
FAM13C1	XM_001503399	XP_001503449	0.591687363	0.033483098

Table D-14 Continued

Gene Symbol	NCBI accession	RefSeq accession	Log fold change	Pvalue
FAM21C	CX603317	NULL	0.602254898	0.035258997
FAM54B	XM_001504118	XP_001504168	-0.606508088	0.019025016
FASTKD1	XM_001494348	XP_001494398	-0.969695295	0.02545841
FLJ20160	XM_001501990	XP_001502040	-0.892536429	0.013064446
FOXP1	DN503968	NULL	-0.624439992	0.011483
FRYL	NULL	NULL	-0.957623249	0.047714411
GAPDH	XM_001502360	XP_001502410	-0.823217483	0.020257953
GNAT3	XM_001487934	XP_001487984	-0.847804659	0.047339394
GNB2L1	NULL	NULL	0.981080011	0.0030302
GRAMD1C	XM_001501094	XP_001501144	0.805227311	0.010062435
GSTA1	XM_001503053	XP_001503103	-0.853867865	0.026818494
GSTM4	CX601710	NULL	1.282766019	0.019971397
GYS1	XM_001489239	XP_001489289	0.623847039	0.021310691
H1F0	XM_001501126	XP_001501176	-0.62813259	0.043011576
HCCS	XM_001488423	XP_001488473	1.264818868	0.030002828
HCRTR2	XM_001503207	XP_001503257	-0.642392375	0.006776825
HEY2	XM_001503138	XP_001503188	-0.926509745	0.009572611
HIST1H4J	XM_001501708	XP_001501758	-0.826688278	0.042242517
HSP90AB1	AY383484	NP_001075407	-0.622090752	0.042959672
HTR1E	XM_001503723	XP_001503773	0.700853188	0.013648808
IFITM3	CX605459	XP_001488671	-0.798407606	0.024211354
IMPDH2	XM_001494550	XP_001494600	-0.737341281	0.029862585
INPP5A	XM_001488022	XP_001488072	0.755185322	0.048649758
INPP5F	XM_001496265	XP_001496315	0.674966522	0.034717242
KCNN3	XM_001497582	XP_001497632	-0.828428635	0.010968736
KCNRG	XM_001488550	XP_001488600	0.704151051	0.048556785
KIAA1553	XM_001503954	XP_001504004	-1.195143719	0.044609018
KIF2C	XM_001496793	XP_001496843	-0.948292019	0.008586719
LBXCOR1	XM_001498728	NULL	-0.661626455	0.009408176
LENG1	XM_001488396	XP_001488446	-0.626107991	0.03914387
LIMCH1	XM_001494623	XP_001494673	-1.349227692	0.005874797
LIN28B	XM_001503925	XP_001503975	-1.776635547	0.037298043
LMBR1L	XM_001504157	XP_001504207	-0.593052611	0.042595949
LMO7	XM_001488279	XP_001488329	0.583802808	0.045353481
LOC124446	XM_001501754	XP_001501804	-0.866724706	0.041451409
LOC728780	XM_001504674	XP_001504724	-0.757158723	0.039061296
LOC729085	XR_036379	NULL	0.678461784	0.035907053
LRRC15	XM_001500569	XP_001500619	0.689693763	0.048339409

Table D-14 Continued

Gene Symbol	NCBI accession	RefSeq accession	Log fold change	Pvalue
LYRM4	CX605171	NULL	0.655867417	0.036665488
LYSMD4	XR_035862	NULL	-0.733594726	0.044530761
MAGEB16	XM_001488696	XP_001488746	-0.622695779	0.0381295
MAP2K1	XM_001496420	XP_001496470	0.787575065	0.045455961
MESP2	XM_001499242	NULL	-0.623735646	0.045830675
MGAT4C	XM_001495737	XP_001495787	0.860979516	0.004608274
MKI67	XM_001489412	XP_001489462	1.01169943	0.044068579
MRPL21	CX604559	XP_001499094	-1.034579234	0.010308367
MXI1	XM_001496951	XP_001497001	-0.738855714	0.033110951
NANOS3	XM_001494819	XP_001494869	-0.614937874	0.040185863
NBPF6	XM_001497337	NULL	0.608487406	0.037123347
NOL8	XM_001489687	XP_001489737	-1.543571813	0.014143301
NONO	XM_001492800	XP_001492850	-0.616463186	0.027019073
NULL	XM_001503112	NULL	-1.174740052	0.036027527
NULL	CD465327	NULL	-1.159813556	0.012179574
NULL	DN508036	NULL	-1.054096365	0.034266373
NULL	CX599420	NULL	-0.981846219	0.02626958
NULL	CD470845	NULL	-0.977777737	0.00619198
NULL	CX604338	NULL	-0.922961234	0.008579522
NULL	CX593230	NULL	-0.850991777	0.031489335
NULL	CX601522	NULL	-0.846585201	0.027092655
NULL	BM414703	NULL	-0.775474009	0.016410087
NULL	DN508295	NULL	-0.724062199	0.012467506
NULL	CX601641	NULL	-0.711086963	0.019963884
NULL	CX605199	NULL	-0.673486932	0.005752077
NULL	CX605849	NULL	-0.672146284	0.012038211
NULL	XR_036258	NULL	-0.658216857	0.045318492
NULL	XM_001496363	XP_001496413	-0.650827063	0.016304912
NULL	XM_001502325	XP_001502375	-0.624090671	0.028234523
NULL	DN504949	NULL	-0.584613984	0.014224809
NULL	DN508139	NULL	0.814218578	0.007929484
NULL	CX592100	NULL	0.682515155	0.039915205
NULL	XM_001488836	NULL	0.631965438	0.022524357
NULL	CX600577	NULL	0.618601028	0.023004272
NULL	BI960932	NULL	0.587600399	0.049318147
NULL	CX595091	NULL	0.584213972	0.013822649
NUP43	XM_001495468	XP_001495518	0.693637301	0.013764025
OR13C3	XM_001493767	XP_001493817	0.8532832	0.033569935

Table D-14 Continued

Gene Symbol	NCBI accession	RefSeq accession	Log fold change	Pvalue
OR2L2	XM_001491169	NULL	-0.880001026	0.03980507
OR2T33	XM_001491604	NULL	0.638186115	0.038510702
OR52A5	XM_001498335	XP_001498385	-0.91904009	0.005454211
PATZ1	XM_001496979	XP_001497029	1.012064056	0.022763939
PDCD2	XR_035769	NULL	-0.8718239	0.009651637
PGBD2	XM_001489628	XP_001489678	-0.712424507	0.018875561
PHKG1	XM_001493353	XP_001493403	0.593849525	0.025875054
PIM3	XM_001489277	XP_001489327	0.760014044	0.021386153
PIP3-E	XM_001493835	XP_001493885	-0.907827901	0.044234612
PNLIPRP3	XM_001497755	XP_001497805	0.764672641	0.016280741
PPIF	XM_001503133	XP_001503183	-1.1290225	0.026632136
PPM1L	NULL	NULL	-0.751893498	0.031957557
PTGIR	XM_001500857	XP_001500907	0.735222145	0.010329417
PTH2R	XM_001499116	XP_001499166	-0.662387891	0.036334377
PTPLB	XM_001500147	XP_001500197	0.822906174	0.00341293
QDPR	XM_001498522	XP_001498572	0.664223696	0.034470498
RAB8A	CX593996	NULL	-1.225994858	0.003683153
RABAC1	CX605896	NULL	-0.583006162	0.031789253
RABGAP1	XM_001502284	XP_001502334	-1.053200274	0.044050016
RABGAP1L	CX604606	NULL	0.646938991	0.045842495
RALGDS	XM_001494159	NULL	-0.628124826	0.034664569
RASA1	XM_001503763	XP_001503813	-0.648346323	0.038766202
RFESD	XM_001504611	XP_001504661	-0.698905074	0.008368325
RHBDL3	XM_001501624	XP_001501674	-0.811082785	0.048977433
RNF125	XM_001495353	XP_001495403	-0.664859632	0.023065159
RPL10	NULL	NULL	-0.671277767	0.012879941
RPL13	XM_001488825	XP_001488875	-0.760386076	0.021152271
RPL28	CD464415	XP_001495815	-0.657473936	0.009462253
RPL3L	XM_001497904	XP_001497954	-0.851485046	0.016568967
RPL7A	CD535100	NULL	-0.972501046	0.005000503
RPS18	NULL	NULL	-1.006931347	0.003186254
RPS2	CD536630	NULL	-0.673069241	0.014418029
S100A11	BI961023	XP_001493486	-0.805591769	0.040404051
SAA1	BM780732	NULL	-0.745340627	0.030636949
SAMD8	XM_001503968	XP_001504018	0.722574858	0.02194306
SCAPER	XM_001493099	XP_001493149	0.63637674	0.032201637
SELENBP1	NULL	NULL	-1.444713323	0.006144535
SHB	XM_001496517	XP_001496567	-1.327035275	0.041358482

Table D-14 Continued

Gene Symbol	NCBI accession	RefSeq accession	Log fold change	Pvalue
SIGLEC5	XM_001496694	XP_001496744	0.702159421	0.023251966
SKP1	XM_001504404	XP_001504454	0.671973889	0.034570903
SLC26A9	XM_001490825	XP_001490875	0.628557108	0.045214646
SLC35E4	XM_001497797	XP_001497847	0.86116699	0.003975234
SLC4A11	XM_001496863	XP_001496913	0.991168621	0.004650469
SLC9A10	XM_001501303	XP_001501353	-0.825198351	0.005202031
SMARCA5	XM_001502026	XP_001502076	1.576157971	0.045398111
SMOX	XM_001495369	XP_001495419	1.040094617	0.008716366
SNAI2	XM_001488056	XP_001488106	0.604557377	0.036071761
SPACA5B	XM_001493471	XP_001493521	0.65972288	0.049159818
SPRED1	XM_001503617	XP_001503667	0.901968423	0.030022338
SRR	XM_001504357	XP_001504407	-0.958727	0.014125923
STAMBP	XR_035758	NULL	0.583755129	0.025867117
SUCLG2	XM_001495004	XP_001495054	1.034716329	0.030225375
SYNPO2	XM_001503239	XP_001503289	-0.718121452	0.046501452
SYVN1	XM_001492161	XP_001492211	-1.69912096	0.030607827
TBC1D21	XM_001493579	XP_001493629	0.840322793	0.01302098
TDRD9	XM_001492897	XP_001492947	-0.729460062	0.023965311
TEX13A	XM_001493678	NULL	-1.598003933	0.026460985
TFE3	XM_001494896	XP_001494946	-1.014575441	0.00674404
TGM3	CD469900	NULL	-0.78195184	0.041442648
TM4SF5	XM_001502944	XP_001502994	-0.724263111	0.003839672
TMEM60	XM_001488320	XP_001488370	0.602420509	0.026684834
TMEM86A	XM_001504973	XP_001505023	0.989725936	0.045763512
TMPRSS6	XM_001499386	XP_001499436	-0.793618707	0.010138285
TNFRSF11B	XR_036157	NULL	-1.003769927	0.045532736
TRAPPC6A	XM_001502472	NULL	0.701696566	0.029711442
TSPO	XM_001503143	XP_001503193	-0.685253525	0.045634441
U2AF2	XM_001496109	XP_001496159	-1.014113889	0.03850713
UBC	XM_001499082	XP_001499132	-1.029557409	0.004146667
UBP1	XM_001489950	XP_001490000	0.690667964	0.008448361
UQCR	DN508330	NULL	-0.71106548	0.008736253
UROS	XM_001490158	XP_001490208	-1.278854565	0.008720487
UTP6	XM_001504028	XP_001504078	0.767721739	0.010602056
VPS33B	XM_001498840	XP_001498890	1.016084454	0.006130397
VTN	XM_001504123	XP_001504173	-0.76527476	0.016391353
VWF	NULL	NULL	-0.736158608	0.015957781
WDR76	CX602330	NULL	-1.190662663	0.035751286

Table D-14 Continued

Gene Symbol	NCBI accession	RefSeq accession	Log fold change	Pvalue
WNT11	XM_001495163	XP_001495213	0.908741195	0.002654203
ZC3H11A	XM_001488552	XP_001488602	0.671539747	0.027301477
ZCCHC10	XM_001504415	NULL	-0.669967344	0.027040513
ZNF2	XM_001493971	XP_001494021	0.805254836	0.022108275
ZNF266	XM_001491960	XP_001492010	0.853414065	0.001243353
ZNF295	XM_001492957	XP_001493007	-0.611785979	0.042952336
ZNF709	XM_001489853	NULL	0.727714625	0.017516736
ZNF92	XM_001494628	NULL	-1.076826878	0.036612228

VITA

Name: Priyanka Kachroo

Address: Department of Veterinary Integrative Biosciences
College of Veterinary Medicine
Texas A&M University
College Station, Texas 77843-4458

Email Address: decipher.priyanka@gmail.com

Education: B.E., Biotechnology, PES Institute of Technology, India, 2006
Ph.D., Biomedical Sciences, Texas A&M University, USA, 2012

Awards and Honors: CVM-Graduate Student Association Symposium, Best poster presentation award, 2011
CVM-Graduate Student Research Grant $5000, 2011
USDA-NRSP8 Horse Genome Travel Award, 2009

Publications: Kachroo P, Ivanov I, Davidson LA, Chowdhary BP, Lupton JR, Chpakin RS, Classification of Diet-Modulated Gene Signatures at the Colon Cancer Initiation and Progression Stages. *Dig Dis Sci.* 2011 Mar 16

Raudsepp T, Durkin K, Lear TL, Das PJ, Avila F, Kachroo P, Chowdhary BP. Molecular Heterogeneity of XY Sex Reversal in Horses. *Anim Genet*. 2010 Dec